Cranfield

ASTOVL COMBAT AIRCRAFT DESIGN SYNTHESIS AND OPTIMIZATION

N.Kehayas

College of Aeronautics
Cranfield Institute of Technology
Cranfield, Bedford MK43 0AL. England

Cranfield

ASTOVL COMBAT AIRCRAFT DESIGN SYNTHESIS AND OPTIMIZATION

N.Kehayas

College of Aeronautics
Cranfield Institute of Technology
Cranfield, Bedford MK43 0AL. England

CRANFIELD INSTITUTE OF TECHNOLOGY

COLLEGE OF AERONAUTICS

DEPARTMENT OF AEROSPACE TECHNOLOGY

COLLEGE OF AERONAUTICS REPORT NO 9201

JANUARY 1992

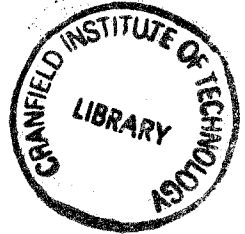ASTOVL COMBAT AIRCRAFT DESIGN SYNTHESIS
AND OPTIMIZATION

N.KEHAYAS

Acknowledgments

ABSTRACT

This report presents the development of a Baseline
Configuration for an Advanced Short Take-Off and Vertical
Landing (ASTOVL) Combat Aircraft, the Design Synthesis
and coding of this Baseline Congiguration (Code VERTI),
the interfacing of the Design Synthesis Code VERTI with
the Optimizer code RQPMIN and the optimization of the
Baseline Configuration.

The background and the objectives of this Research
Programme are initially examined. The evaluation of the
ASTOVL Combat Aircraft Baseline Configuration is then
described, including all the problems, assumptions,
choices and compromises that led to the specific
configuration.

The development of the Design Synthesis and the Code
VERTI then follow, where the methodology used, the
techniques adopted and the code operation are explained.
A full description of the Design Synthesis is included as
an appendix.

Finally, the interfacing of Code VERTI with the optimizer
RQPMIN and the optimization of the Baseline Configuration
are presented. The problems and difficulties of the
RQPMIN operation are thoroughly discussed. The RQPMIN-
VERTI code is used to optimize the initial Baseline
Configuration and an optimization example is provided in
appendix form. The optimized Baseline Configuration is
partly validated against two ASTOVL combat aircraft
designs. In addition to the optimization with the
aircraft empty mass as objective function, a search for a
better objective function is attempted.

NOTATION

AR	Aspect ratio
b	Flying surface span
Cl	Lift coefficient
d	Diameter
KN	Interference factor due to aircraft body
KW(B)	Interference factor due to the interaction of the body with the wing
KB(W)	Interference factor due to the interaction of the wing with the body
L	Lift
S	Flying surface area
V_∞	Freestream velocity
w	Velocity induced by the wing
x_T	Distance between wing and tailplane quarter-chords
α	Angle of incidence
β	Angle formed between wing vortex element and tailplane surface element
ϵ	Downwash angle

Subscripts

a/c	Aircraft
b	Body
fb	Forebody
n	Net
t	Tail

FIGURES

TABLES

CONTENTS

1. INTRODUCTION

The present work covers the evaluation of a Baseline Configuration for an ASTOVL Combat Aircraft, the Design Synthesis of the Baseline Configuration, the coding of the Design Synthesis, the interfacing of the Design Synthesis code VERTI with the optimizer code RQPMIN and the optimization of the Baseline Configuration using RQPMIN-VERTI.

The ASTOVL Combat Aircraft Baseline Configuration evaluated is an advanced technology, supersonic, short take-off and vertical landing combat aircraft with an internal weapon bay. It is powered by a modern military turbofan with a remote lift system for landing.

The Baseline Configuration was described in the Design Synthesis in terms of geometry, mass and aerodynamics. Using as input general design, aerodynamic, engine performance and sortie data the aircraft was synthesized and its performance was estimated.

The optimization of the Baseline Configuration was achieved by interfacing the optimizer code RQPMIN with the Design Synthesis code VERTI.

Finally, a brief investigation on the most suitable objective function for the optimization was performed.

1.1. Background

The optimization of aircraft designs has a long history and a lot of effort has been spent due to the very substantive benefits resulting. Originally partial optimization was attempted, structural optimization being the best example, but the overall aircraft design optimization came soon afterwards. Aircraft design optimization schemes tend to use simple semi-empirical design approaches (Refs 12, 43, 69 and 77), as the actual optimization demands thousands of iterations for an optimum, but recently attemps are being made to consider the assembly of big finite-element type of optimizers for structures, aerodynamics and other areas into one (Ref.24).

Research on the optimization of aircraft designs has been undertaken at the Royal Aerospace Establishment (RAE) since the late sixties. This field of research, under the name Multivariate Optimization (MVO), initially directed to civil designs but later including military, is pursued along two lines. The development of better techniques for the design synthesis of various aircraft types and and the development of more efficient optimization codes.

The College of Aeronautics, Cranfield Institute of Technology, has been involved in MVO research since 1975 with a canard-delta fighter design.

1.2.   Objectives

This research programme was sponsored by the RAE and the objectives set-out in the research agreement were :

a.   The evaluation of the aircraft Baseline Configuration

b.   The Design Synthesis of the Baseline Configuration

c.   The coding of the Design Synthesis.

d.   The interfacing of the Design Synthesis code VERTI with the optimizer code RQPMIN.

e.   The optimization of the Baseline Configuration using RQPMIN-VERTI.

2.   BASELINE CONFIGURATION

2.1.   Introduction

The Baseline Configuration of the aircraft was mainly
based on RAE requirements and Refs 23 and 39, but some
flexibility was allowed if it was deemed necessary.

The RAE requirements specified the following :

Aircraft

- Single-seat, single-engine, supersonic combat aircraft
- ASTOVL with a hot remote front duct (Remote Lift
  System) and swivelling exhaust ducts either side of the
  engine
- Maximum Mach number 1.6
- Thrust-to-weight ratio of 1.15 dry and 1.4 reheat with
  reference to landing and combat mass respectivelly.
- Mid to high trapezoidal wing with high lift devices
- Tricycle undercarriage, if not possible, bicycle
- One wheel main undercarriage

Engine

- Mixed flow
- Fixed geometry side intakes
- Axisymmetric nozzles
- Side ducts used only for landing - stowed in fuselage
  during take-off and landing
- Front and side duct inlets located after the turbine
  exit position

Weapons

- Internal bay
- Four medium and two short range air-to-air missiles
- Internal gun

2.2.   Description

The Baseline Configuration that has evolved after several
exploratory configurations is shown in Fig.1.

The wing is of fixed geometry, medium-to-high position, swept back and trapezoidal in planform. It has low taper and aspect ratio and is based on a thin aerofoil section of constant thickness-to-chord ratio along the span. The wing dihedral and twist were considered to be zero. The tail is conventional and placed low. The aerofoil section type of the fin and the tailplane are identical to that of the wing.

The engine is a modern military reheated turbofan of the split-flow type when operating in the landing mode. A system of three ducts, used in landing to provide thrust in the front part of the aircraft, starts just after the turbine exit position and ends in a nozzle at the undersurface of the aircraft after the nose undercarriage bay. It is a hot system without any reheat at the nozzle. It is therefore a simply Remote Lift System (RLS) without any augmentation. The three ducts, one bigger in the middle and two smaller either side (Fig.A7), recombine at the nozzle. At landing the thrust in the rear part of the aircraft is not provided by vectoring the engine nozzle, but by a pair of swivelling ducts situated either side after the engine position. These two side ducts are positioned vertically during landing and stowed horizontally in the fuselage during take-off and forward flight. The system of front ducts and the side ducts are used only for landing. The engine has a conventional variable geometry rear nozzle for forward flight.

Two S shaped intake diffusers with rectangular intakes are used. The intakes have fixed geometry since the aircraft is specified not to exceed 1.6 Mach. The cross-section of the intake diffusers slowly changes, especially after they meet, to become circular and meet the engine face. The cross-sectional area of the intake diffusers gradually increases to reduce the flow speed to around Mach 0.4 at the engine (gas generator) inlet, to be appropriate for the proper working of the compressor. Due to the operation of the RLS nozzle in the front part of the aircraft during landing the inlets of the diffusers are placed well ahead, in front of the eye position of the cockpit.

The nose undercarriage bay is located after the radome. It is off-set to allow movement of the RLS nozzle if needed. The main undercarriage bay lies flat under the engine (gas generator).

The weapons of the aircraft comprising four medium and two short range air-to-air missiles or a number of bombs,

are carried internally in a bay, placed between the RLS
nozzle and the engine axially and between the two intake
diffusers laterally. They are jettisoned by means of
ejectors situated on the top of the bay. An internal gun
is located in a bay on the left side of the weapons bay.

In addition to the wing fuel tanks, three fuselage tanks
have been specified. A central fuel tank located above
the internal weapons bay, ahead of the engine and between
the intake diffusers and two side tanks in either side of
the engine gas generator. The side tanks have the same
height as the engine at that position and blend with the
side ducts that follow them.

The initial Baseline Configuration defines an aircraft of
around 20 metres in length and with a 13 metre wing span.
The wing surface area is nearly 40 square metres, the
mass almost 19 tons and the engine maximum gross thrust
at sea level conditions 185 k Newtons.

Figures 6,7 and 8 show some of the configurations
considered during the Baseline Configuration development.
Configurations 1 and 2 of Fig.6 represent early attempts.
The engine is very small and the RLS rather crude.
The third configuration of Fig.6 includes a realistic
engine size and an augmented RLS (RALS), and the fourth
configuration of Fig.6 returns to a RLS but positioned
further ahead. In Fig.7 various engine and RLS
arrangements are presented. The choice of RLS is
established but the delivery of the rear part of the
thrust at landing is not yet decided. In the first
configuration of Fig.8 the engine side ducts are
introduced. The second configuration of Fig.8 illustrates
the problem with the enormous RLS front duct.
Configurations 3 and 4 of Fig.8 indicate a change in of
RLS front duct inlet position. The Baseline Configuration
reached is shown in Fig.1.

3. DESIGN SYNTHESIS

3.1. Introduction

The Design Synthesis describes the aircraft Baseline Configuration in mathematical form, by means of semi-empirical and sometimes analytical design relationships.

Initially, using design input data , the sizing of the aircraft fixed items is performed. Fixed items are all the "standard" parts of the aircraft such as the radome, the cockpit, the undercarriage, the internal weapons bay, the internal gun bay, the intake diffusers, the engine, the remote lift system, the basic wing and the empennage. These parts are determined by input design data, and in this sense are considered fixed items within the Design Synthesis. In the optimization, as it will be discussed in Chapter 6.3., many of these fixed items may vary.

Next the geometry of the aircraft is evaluated, again with the use of input design data, taking into consideration the related fixed items so that the aircraft can contain all the specified fixed items. The fuselage geometry is evaluated at several stations along the fuselage with the help of a fairing curve, in order to define an acceptable aerodynamic shape and area rule if required.

From the fixed items and the geometry, the mass and the centre of gravity are calculated. The aerodynamics follow based on the geometry and input aerodynamic data.

At the end, having all the aircraft characteristics, the aircraft sortie and point performance are estimated.

The Design Synthesis is fully described in Appendix A. It follows closely the approach of Lovell (Ref.43) applied to the ASTOVL configuration although in a number of cases alterations and additions have been made.

3.2. Fixed Items Sizing

The fixed items are the basic parts of the aircraft and they are contained within the fuselage. Their size is estimated from the Baseline Configuration and in turn from the fixed items size detailed fuselage and aircraft dimensions are derived.

3.2.1. Radome

The radome cone is defined by the radar dish diameter. In addition a linear variation of cone cross-sectional area with axial distance is assumed.

3.2.2. Cockpit

The geometry of a single-seat combat aircraft cockpit is defined in Ref.43. The cockpit dimensions are calculated using input data related to the cockpit type specifications.

3.2.3. Undercarriage Bays

The geometry of the nose and main undercarriage bays is derived from a number of correlations with a landing reference mass. The reference mass is obtained by removing from the aircraft take-off mass the mass of all external stores and a proportion of the fuel mass and then adding a reference mass (reference load for definition of stressing masses).

The total leg length of both undercarriages is first calculated using a correlation with the reference landing mass and from that using the ratio of the nose to main undercarriage leg length, each leg length is deduced.

The undercarriage bays are evaluated as the sum of the leg and tyre volumes. The leg length is used to define the leg volume and the tyre diameter and width the tyre volume.

3.2.4. Engine

The engine sizing module was provided by the RAE (F). It defines a datum military reheat turbofan engine which can be scaled up or down by a scale factor. Within the fixed

items module the engine dimensions are scaled while the engine performance is scaled by the same factor in the engine performance module (Appendix A).

3.2.5.   Intake Diffusers and Boundary Layer Diverters

The intake diffusers are assumed to have a given fixed area ratio with reference to the inlet area of the engine. The intake diffuser(s) rectangular inlet is then calculated using a given aspect ratio (ratio of height to width). A minimum length for the intake diffusers is then described, which is a function of their width or height.

The boundary layer diverters are assumed to have the same height with the intake diffusers and a width which is proportional to its distance from the aircraft nose.

3.2.6.   Internal Weapon Bay

The internal weapons bay contains four medium and two short range air-to-air missiles.The medium range missiles form two rows, of two missiles each, the one above the other. The smaller short range missiles are located either side of the first row of the medium range ones.

Folding fins for the missiles have not been assumed. The missiles are lowered below the aircraft to be fired by means of a system of ejectors. The ejectors system is situated in the upper part of the bay.

The bay lies in the lower section of the fuselage below the central fuselage fuel tank and between the front RLS system of ducts nozzle and the engine. It is partially covered from both sides by the intake diffusers.

3.2.7.   Internal Gun Bay

The internal gun bay is considered in three parts; the gun mechanism, the gun barrel and the ammunition drum. The gun represented is a typical 25 mm calibre with 150 rounds of ammunition.

The gun mechanism and ammunition drum are located on the left side of the internal weapons bay, while the barrel

protrudes forward to exit near the nose undercarriage bay.

3.2.8. Remote Lift System

The remote lift system delivers the necessary thrust for vertical landing.

For the forward part of the thrust a system of three ducts travels the aircraft upper fuselage from the engine after turbine position up to a position behind the cockpit. From there it descends at an angle to the vertical to reach the undersurface of the fuselage just ahead of the internal weapons bay. The three duct system of one bigger and two smaller circular ducts, forms a semi-circular cross-section combination that fits better in the constrained space of the upper fuselage, than the case would have been with one enormous circular duct. The tree ducts have separate inlets but combine at the fuselage undersurface to form a nozzle.

The rear part of the thrust is delivered through two side ducts, located in either side of the engine, with inlets at the after turbine position. These side ducts which can swivel about a lateral axis, are positioned vertically when in use, and horizontally, stowed in the fuselage, when not.

3.3. Geometry

3.3.1. Fuselage Stations

Before any geometry calculations are performed, a number of fuselage main stations and sub-stations are defined. Critical, for the geometry definition, positions along the fuselage serve as main stations. The fuselage length between the main stations is divided into sub-stations. Any geometrical calculation for the fuselage or the aircraft as a whole is performed at these stations.

The total number of stations is 50 ; the main stations are 11 and they are situated at : The radar dish, the intake diffuser inlet, the cockpit eye position, the start of the internal weapons bay, the face of the engine (gas generator), the turbine exit, the engine RLS section centre, the engine RLS section exit, the afterburner exit

and the nozzle exit. The distance between main stations is arbitrary but the distance between successive sub-stations is constant.

3.3.2. Fairing Curve

A fairing curve is defined that provides a good aerodynamic shape for the fuselage and an area-ruled fuselage if required (Appendix A). This fairing curve determines the nett longitudinal cross-sectional area distribution of the fuselage or the whole aircraft if area-rule is applied. The nett cross-sectional area referred is the actual cross-sectional area minus the cross-sectional area of the streamtube of the intake diffuser or the engine.

In mathematical form the fairing curve is described by two cubics, for the forward and the rear part respectively (Ref.43). The fairing curve is divided in six segments, the length of each being possible to be altered by a set of Independent Variables. By adjusting these six Independent Variables a fairing curve of the desired shape is obtained.

3.3.3. Flying Surfaces

The wing geometry is evaluated from input design data for the wing area, the aspect ratio, the taper ratio, the quarter chord sweep angle and the chordwise thickness distribution of the aerofoil. From these the span, the chord at different spanwise positions and the leading, the mid-chord and the trailing sweep angles are estimated.

Following these gross wing calculations and using a first estimate of the fuselage width at the wing position, the nett wing geometry is derived. This includes the wing box, the wing fuel tanks, the ailerons, the flaps and the leading and trailing edge sections.

The geometrical characteristics of the fin and tailplane are determined similarly to the wing ones but volume coefficients are used instead. The input data provided are the nett aspect ratio, the nett taper ratio, the sweep angles of leading and trailing edges and the thickness-to-chord ratios. The distance between wing quarter-chord and fin and tailplane quarter-chord are

given as a fraction of the fuselage length. Hence, the nett surface areas of fin and tailplane are estimated.

3.3.4. Lateral Cross-Sectional Area of the Flying Surfaces

If area-rule is to be available, it is necessary to be able to calculate the lateral cross-sectional area of the flying surfaces - wing, the fin and the tailplane. The lateral cross-sectional area is the subtracted from the nett cross-sectional area defined by the fairing curve, to give the nett cross-sectional area of the area-ruled fuselage.

The lateral cross-sectional area of a flying surface is obtained by integrating across the semi-span the chordwise distribution of the thickness of the aerofoil of the flying surface for a number of axial positions corresponding to the defined fuselage stations.

3.3.5. Geometry of Main Fuselage Stations

The geometry of the eleven main fuselage stations is determined by the principle that the cross-sections of the stations must contain the fixed items present there.

In simple cases, such as the radome or the engine nozzle exit station for example, the geometry is a circle defined by the radar dish diameter plus clearances and the nozzle exit diameter. In the rest a more complicated procedure is needed whose outline is presented below.

First the nett cross-sectional area of the fuselage for that station is obtained from the fairing curve. If area-rule is applied the corresponding flying surface lateral cross-sectional area is subtracted. Then the cross-sectional area of the stations is evaluated in general terms. In this evaluation, utilization factors to account for corners and the dimensions of the contained fixed items are used. The ratio of the fairing curve nett cross-sectional area to the cross-sectional area evaluated in general terms is next defined as a scaling factor. One dimension of the cross-section of the station, height or width, depending which is better defined by the dimensions of the contained fixed items, is assumed as a minimum dimension. Using the scaling

factor, the other dimension is found and thus the cross-sectional area of the station is calculated.

3.3.6. Fuselage Cross-Sectional Area

The definition of the fuselage cross-sectional area, is the actual fuselage cross-sectional area in contrast to the nett fuselage cross-sectional area provided by the fairing curve (If area-rule is applied, the nett fuselage cross-sectional area is the one determined by the fairing curve minus the corresponding lateral cross-sectional area of the flying surfaces).

Therefore, to find the fuselage cross-sectional area relative to the cross-sectional area defined by the fairing curve (minus the lateral cross-sectional area of the flying surfaces if area rule is required), the corresponding intake diffusers and engine streamtube cross-sectional area must be added.

The fuselage cross-sectional area, as with all geometrical calculations of the fuselage, is evaluated at the 50 specified fuselage stations.

3.3.7. Fuselage Perimeter

A relationship between fuselage cross-sectional area and perimeter is assumed (Ref.43). This relationship applies to combat aircraft designs similar to our Baseline Configuration. In practice, two relationships are used, one for the fuselage up to the intake diffuser inlet and the other for the rest of the fuselage.

As before, the perimeter is evaluated at the 50 specified fuselage stations.

3.3.8. Fuselage Volume and Surface Area

The fuselage volume is derived by integrating the fuselage cross-sectional area over the length of the fuselage and by means of a numerical integration.

The main fuselage stations are positioned arbitrarily to suit conditions for a better definition of the fuselage.

Therefore, the numerical integration is performed separately for each fuselage part defined by successive main stations and as the intermediate sub-stations are placed at equal intervals, the necessary prerequisite for the application of a simple Simpson's rule type of numerical integration is satisfied.

For the fuselage surface area, the same procedure is followed replacing the fuselage cross-sectional area by the fuselage perimeter.

3.4.   Mass and Centre of Gravity (cg)

3.4.1.   Mass

The mass prediction was mainly based on Ref.43 with some additional information, especially for the RLS from Refs 28, 50, 60 and 63.

The mass of the fixed items is estimated within the fixed items modules, while the masses of the fuel tanks, the fuselage, the flying surfaces and the various systems are estimated separately.

For the radar, the associated electronics and the rest electronic equipment, the mass is given in the form of input data.

The cockpit mass is included in the fuselage mass and the crew mass is given as input data.

The undercarriage mass, in terms of nose undercarriage, main undercarriage and associated hydraulics, is calculated in relation to the reference landing mass.

The engine mass, made of the gas generator, the RLS section, the afterburner, the nozzle, the thrust reverser and the installation mass, are estimated in the RAE engine module. The RLS side duct mass is considered to be a part of the total engine mass while the RLS front system of ducts is estimated separately.

The intake diffuser and the boundary layer diverter mass are included in the fuselage mass.

The internal gun bay mass is made of the gun mass given as input data and the ammunition mass which is estimated from the number of ammunition rounds carried.

The mass of the RLS front system of ducts is derived in relation to its length and input data of mass per unit length. It includes insulation as well as structural mass.

The fuel tank mass is directly related to the volume of the fuel tanks and the fuel density.

Elaborate methods (Ref.43) are used for the mass estimation of the fuselage and the flying surfaces mass (Appendix A).

The fuselage mass includes shell and internal structure, windscreen, canopy, intakes and various minor structural items.

The wing mass is made of the wing-box, the leading edge, the trailing edge, the flap, the flaptrack and the aileron mass.

Separately is estimated the air services, the fuel system, the flight controls, the ASTOVL reaction control, the electrical services and the paint mass.

3.4.2.   Centre of Gravity

Parallel to the above mass estimation of the parts and components of the aircraft, respective moment arms from the aircraft nose are evaluated. The moment arms are derived from the distance of the item or component from the aircraft nose and the position of its centre of gravity. For the majority of aircraft parts or components the approach of Ref.43 was adopted and for the rest that were particular to the ASTOVL Baseline Configuration or a change was thought necessary, appropriate expressions were evaluated.

These moment arms are used in the prediction of the aircraft centre of gravity limits. As the aircraft requirements do not include stores and external fuel tanks and the internal weapon bay is regarded as an integral part of the aircraft, only two cases were considered ; full and empty fuel tanks.

3.5.   Aerodynamics

Substantial calculations determine the aircraft
aerodynamics using the fuselage and the flying surfaces
geometry. As a result the total and the zero-lift drag
coefficient and the lift-curve slope of the aircraft are
evaluated over the specified Mach number range.

The aerodynamics do not contain any flight stability
calculations as they were considered beyond the scope of
this work and a subject that should be treated on its own
right. However, tail volume coefficients were used to
give first-order layouts.

3.5.1.   Lift-Curve slope

Initially, the lift-curve slope was evaluated for two
Mach number regimes

For the subsonic Mach number regime, Mach $\leq$ 0.8, the
lift-curve slope was derived from the aerofoil lift-curve
slope that was suitably developed to provide a finite
wing lift-curve slope.

For the supersonic Mach number regime, defined by a
critical Mach number above which the leading edge flow is
supersonic, linear theory provided the lift curve-slope.

Then the two lift-curve expressions were matched by a
cubic variation of the lift-curve slope with respect to
the Mach number.

To the lift-curve slope interference effects were added.
Interference of the body, the wing-body interaction and
the tail were considered. The interference effects due to
the body and the wing-body interaction were estimated
according to a DATCOM method (Ref.3). For the tail
interference a simplified expression was derived based on
finite wing theory. The lift-curve slope evaluation with
reference to interference is presented in Appendix C.

3.5.2.   Drag

The total aircraft drag is calculated by establishing the
contributions of the zero-lift, the wave, the spillage

and the lift-dependent drag. The methodology of Ref.43 is followed with the appropriate adjustments (Appendix A).

3.5.2.1.   Zero-Lift Drag

The zero-lift drag in the subsonic Mach number regime, $M \leq 0.8$, is made of contributions from the fuselage, the flying surfaces, the canopy and boundary layer diverter. To this a fuselage afterbody term and a 15% of the total fuselage drag interference term are added. The total subsonic zero-lift drag is then scaled as a function of Mach number to give the zero-lift drag at higher Mach numbers.

3.5.2.2. Wave Drag

At first the drag-rise Mach number is estimated and then the wave drag of the aircraft is calculated, comprising wing, fin, tailplane, fuselage and canopy wave drag.

The wave drag is evaluated at Mach numbers 1.0 and 1.3. Between the drag-rise Mach and Mach 1.0 a drag variation with Mach number is assumed. Between Mach 1.0 and 1.3 an empirical relation is used and above Mach 1.3 the drag is considered constant.

3.5.2.3.   Spillage Drag

The drag at zero-lift due to spillage around the intake and the separation drag are estimated using empirical methods. The spillage is assumed to be proportional to the pre-entry drag.

3.5.2.4.   Lift-Dependent Drag

The lift-dependent drag is a function of the lift coefficient (CL). Two regions are considered : For $CL \leq CLC-0.01$ and for $CL \geq CLC+0.01$ where CLC is the critical lift coefficient and is given as input data. Between these two regions a cubic variation of the lift-dependent drag with the lift coefficient is accepted. The variation is a function of the lift-dependent drag parameters K1 and K2. K1 is estimated by a long method of curve fits to experimental data. After the K1 estimation the difference

between K1 and K2 DK2, given as input data, is providing K2.

3.6. Performance

3.6.1. Engine performance

The engine performance is given as input data in table form (Appendix B - Fig.B4). The engine performance data comprise engine power setting, thrust, air mass flow, fuel mass flow and nozzle exit area for a range of altitudes and Mach numbers.For any altitude and Mach number specified, three modules evaluate the corresponding power setting, thrust, air mass flow fuel mass flow and nozzle exit area. The data evaluation works in two modes ; either the power setting or the thrust is specified in addition to the already specified altitude and Mach number.

The evaluation is based on a three point interpolation. The input data table is read and three sets of data before, after and some distance away from the specified altitude and Mach number, in turn, are located . Subsequently these sets of data are interpolated to find the desired data corresponding to the specified altitude and Mach number.

Provision is made if the specified altitude and Mach number coincide with table data to be read directly.

3.6.2. Sortie Performance

The objective of the sortie performance is the calculation of the fuel consumed by the aircraft in a specified sortie.

The sortie is defined as a number of legs. Each leg is assumed to be flown at constant altitude, Mach number and normal load factor (Table 1). The legs involving climb, descent, longitudinal acceleration and other manoeuvres are approximated by adjusting the leg length and the normal load factor to account for them. The error involved has been found to be relatively small and this approach represents to an acceptable degree the real sortie. For landing and take-off separate estimation are used. The mass changes during the sortie (weapons,

stores) are taken into consideration by specifying the relevant masses at each leg.

Three iterations perform the sortie calculations. The first estimates the maximum sustained aircraft incidence and lift coefficient with full engine power setting.

The results obtained become the input of the second iteration for the estimation of the maximum sustained load factor mid-way the sortie leg. Structural and human limits constrain the resulting values.

The third iteration calculates the incidence, lift coefficient, leg duration, gross thrust and consequently the fuel consumed and the aircraft mass at the end of the leg and the whole sortie.

3.6.3.   Point Performance

The point performance calculations comprise the following :

Sustained turn rate
Attained turn rate
Specific excess power
Maximum Mach number
Acceleration time through a Mach number increment
Ride quality factor

3.6.3.1. Sustained Turn Rate

The sustained turn rate is a measure of the continuous turn rate capability of the aircraft.

The aircraft lift coefficient and incidence that can be sustained at the altitude, Mach number and engine power setting are first determined by an iterative approach similar to the one in the sortie calculations (first sortie iteration). From the obtained lift coefficient and incidence the maximum normal load factor and subsequently the sustained turn rate are derived.

3.6.3.2. Attained Turn Rate

Attained turn rate is the maximum turn rate that can be achieved by the aircraft.

The maximum normal load factor is estimated using the maximum lift coefficient for the Mach number specified provided as input data. The obtained maximum load factor determines in turn the attained turn rate.

3.6.3.3. Specific Excess Power

Specific excess power is the excess power available, that is the nett thrust minus the total drag, per unit aircraft weight. Specific excess power is calculated for specified altitude, Mach number amd engine power setting for 1 g flight.

3.6.3.4. Maximum Mach Number

The maximum Mach number that can be attained in 1 g flight at a specified altitude and engine power setting, is estimated by an iterative process during which the nett propulsive force is varied until it reaches a specified minimum. The corresponding Mach number is the maximum Mach number.

3.6.3.5. Acceleration Time Through a Mach Number Increment

It is the time needed by the aircraft to accelerate from a given Mach number through a specified Mach number increment at a specified altitude and engine power setting in a 1 g flight. The acceleration time is estimated by considering the nett propulsive force per unit mass.

The Mach number unit increment of 0.1 was found to provide an acceptable accuracy of the calculated acceleration time. Consequently the acceleration time is derived by myltiplying the the acceleration time for the unit Mach number increment by the ratio of the specified to the unit Mach number increment.

3.6.3.6. Ride Quality Factor

The ride quality factor of the aircraft, as a measure of its response to gusts, can be shown to be proportional to the speed, wing area, and lift-curve slope and inversely proportional to the mass of the aircraft.

3.6.3.7. Take-Off Performance

The take-off distance is estimated using the empirical methods of Ref.43. The total take-off distance is the sum of the ground roll distance and the airborne distance to clear a height of 15 metres. Both distances are functions of the thrust-to-weight ratio, the available thrust, the wing loading and the take-off lift.

3.7. Design Synthesis Code VERTI

3.7.1. Introduction

The ASTOVL Design Synthesis was suitably coded to take the form of a computer program ; code VERTI.

Code VERTI was written in FORTRAN 77 and is around 6500 instructions long. It consists of around 1500 variables and 50 subroutines. It uses five input files covering general design, aerodynamic, sortie performance, engine performance and point performance data.

Code VERTI performs the entire Design Synthesis calculations in approximately eight CPU seconds on a VAX 11/750 computer. After an execution an output file is created. This output file contains information about the geometry and the mass of the aircraft and its components, as well as the details of the sortie performance and the point performance of the aircraft.

Code VERTI is itself a subroutine of the optimization code RQPMIN whose operation is described in Chapter 4. As a subroutine of the optimization code RQPMIN, VERTI has three types of variables. External Variables (EVs) that are input variables, Independent Variables (IVs) that are given an initial value and then are varied by RQPMIN, and Dependent Variables (DVs) that represent the majority of the variables and depend on EVs and IVs.

However, code VERTI can be operated on its own in a manual mode. In such a mode only EVs and DVs exist. The operator using his experience, judgement and the results produced varies some or all the EVs after each execution, until an optimum configuration is established according to the requirements - performance or otherwise - specified.

3.7.2.   Code Development

Code VERTI was developed on the computers of the College of Aeronautics.

It was decided right from the start to adopt a flexible approach in its making. An approach that would produce a code easy to follow and amenable to alterations and extensions. As a consequence the code is highly modular comprising a relatively large number of subroutines. The subroutine size depends on the task tackled and it was tried to have one subroutine for each distinct item of the Design Synthesis. Consequently, the subroutines differ in length but none is very long, longer than say 250 instructions.

The subroutines were developed gradually and after they have been tested separately were added to the already finished ones. When a number of subroutines came to cover a significant part of the Design Synthesis, they were tested as a whole in order to establish their proper operation in relation to each other.

3.7.3.   Code Architecture

The operation of code VERTI is shown in the simplified flowchart of Fig.4.

VERTI contains a main segment that reads the input data files, controls the order of execution of subroutines via common blocks, performs some major calculations and produces two output files with the starting point and the final results respectively (when combined with the optimizer) . All the variables used in a given subroutine are grouped in a single common block with the same name as the subroutine. The variables used in the main segment calculations are grouped in separate common blocks.

In the subroutines, initially, the fixed item geometry is estimated. Then the various fuselage stations, chosen appropriately in order to effectively define the fuselage, are established and the fairing curve providing the nett fuselage - or aircraft, if area rule is applied - cross-sectional area is evaluated.Using the fixed item geometry and the fairing curve the fuselage station geometry is estimated. Next the geometry and the lateral cross-sectional area of the flying are calculated.With the fuselage and the flying surface geometry available, the aerodynamics and the mass and centre of gravity (cg) of the aircraft are evaluated. Finally, using the aerodynamics, the mass and the engine performance, the sortie performance and point performance are estimated.

The calculations performed by the main segment involve the final stages of the integration to find the volume and surface area of the fuselage and the estimation of the mass and the centre of gravity of the aircraft.

3.7.3.1.   Subroutines

Each subroutine performs a specific task and is given a name that identifies with the task for easier code use. The common block of the subroutine together with the common blocks of the subroutines that are being called and the common blocks of the main segment if needed are listed in the start of the subroutine. Individual subroutines do not process output statements as all output is handled by the main segment.

All the VERTI subroutines are listed below with a short description of their function.

Sizing of the fixed items

RADOME	:	Radome geometry
COCKPG	:	Cockpit geometry
UNDCB	:	Undercarriage bay geometry
ENGSIZ	:	Engine sizing
INTAKD	:	Intake diffuser geometry
BLDIV	:	Boundary layer diverter geometry
IWEPB	:	Internal weapon bay geometry
IGUNB	:	Internal gun bay geometry
RLS	:	Remote Lift System
STATION	:	Fuselage station definition

Fairing curve

FAIRCUR1   : Fairing curve coefficient definition

FAIRCUR2   : Fairing curve cross-sectional area
               evaluation

Flying surface geometry

WING   : Wing geometry
EMPENN   : Empennage geometry

FLATCROSS   : Lateral cross-sectional area of flying
               surfaces

Fuselage geometry

FUSSTNA   : Fuselage geometry at station A
FUSSTNB   : Fuselage geometry at station B
FUSSTNC   : Fuselage geometry at station C
FUSSTND   : Fuselage geometry at station D
FUSSTNE   : Fuselage geometry at station E
FUSSTNF   : Fuselage geometry at station F
FUSSTNG   : Fuselage geometry at station G
FUSSTNH   : Fuselage geometry at station H
FUSSTNJ   : Fuselage geometry at station J
FUSSTNI   : Fuselage geometry at station I
FUSCRA   : Evaluation of the actual cross-sectional
               area of the fuselage
PERIM   : Evaluation of the perimeter of the fuselage

Mass and centre of gravity (cg)

MASSEFULT   : Fuel tank mass estimation
MASSEFUS   : Fuselage mass estimation
MASSEFLS   : Flying surface mass estimation
MASSEVAR   : Mass estimation of various aircraft systems
               and components
CEGRAV   : Moment arm evaluation

Aerodynamics

LIFT   : Lift-curve slope evaluation
LIFTCO   : Critical lift coefficient, lift-dependent
               factor DK2 and maximum lift coefficient
               evaluation
DRAG   : Drag coefficient estimation

Performance

ENGPER   : Engine performance evaluation
ENGRE   : Engine performance input data reading
INTER   : Engine performance data interpolation
SORTIE   : Sortie performance evaluation
SSTR   : Sustained turn rate estimation
SATR   : Attained turn rate estimation
SSEP   : Specific excess power estimation
SMML   : Maximum Mach number estimation

SACA   : Estimation of acceleration time through a
                  Mach number increment
RIDE   : Ride quality factor estimation
TAKEOFF   : Take-off performance evaluation

Various

ATMOS   : Evaluation of atmospheric properties
INTEGRA   : Numerical Integration
BLEND   : Blending two functions
(FUNCTION)

3.7.3.2.   Input and Output Files

The input files and their contents are as follows :

VERTI.DAT   : General design data. Geometry, mass and
                  and aerodynamic design data. Some
                  constraint data.

AERO.DAT   : Critical lift coefficient, lift-dependent
                  drag DK2 factor and maximum lift
                  coefficient against Mach number data
                  in table form.

CITENG.DAT   : Engine performance table data. Engine
                  power setting, thrust, air mass flow, fuel
                  mass flow and nozzle exit area against
                  Mach number and altitude.

PERF.DAT   : Sortie performance data. Leg length,
                  altitude, Mach number, normal load factor,
                  jettisoned mass and initial estimate of
                  thrust for the leg.

POINTP.DAT   : Point performance data. Sustained turn
                  rate ; altitude, Mach number, engine
                  power setting and constraints.
                  Attained turn rate ; altitude, Mach
                  number, engine power setting and
                  constraints.
                  Specific excess power ; altitude, Mach
                  number, engine power setting and
                  constraints.
                  Maximum Mach number, altitude, initial
                  speed estimate, engine power setting and
                  constraints.
                  Acceleration time through a Mach
                  increment ; altitude, Mach number, engine
                  power setting and constraints.
                  Ride quality factor ; altitude, Mach

number, engine power setting and
constraints.

The output files for the starting point and the final
results, and their contents are as follows :

VERTI.RES   : Take-off mass, fuel fraction, wing
                  loading, thrust-to-weight ratio.
                  Fuselage length and engine scale factor.
                  Geometry ; wing, fuselage, engine,
                  empennage.
                  Aircraft cg position and limits.
                  Mass ; fuselage, wing, empennage,
                  engine, undercarriage, fixed role
                  equipment, systems, fuel, payload and
                  aircraft total, empty and landing.
                  Sortie performance ; altitude, Mach
                  number, range, normal load factor, end
                  mass, duration, mid-mass lift coefficient,
                  total drag coefficient, engine power
                  setting, thrust, fuel flow, air flow and
                  fuel used for each leg. Take-off and
                  landing fuel used.
                  Point performance. Achieved and constraint
                  value, altitude, Mach number and engine
                  power setting for : acceleration time
                  through a 0.6 Mach increment, maximum Mach
                  number, sustained turn rate, attained turn
                  rate, specific excess power and ride
                  quality factor. Achieved and constraint
                  value for take-off distance.

4.   OPTIMIZATION

4.1.   Introduction

The optimization of the ASTOVL Combat Aircraft Design
Synthesis was carried out with the use of the
optimization code RQPMIN, supplied by the RAE.

RQPMIN is a general numerical multivariate optimization
code. It is designed to solve the constrained
optimization problem, that is to minimize (or maximize) a
function, subject to a number of constraints and upper
and lower bounds imposed on designated variables.

The operation of RQPMIN is based on the Lagrange-Newton
optimization. A stationary point of the Langrangian
function is calculated by Newton's method. RQPMIN differs
from similar codes in that it does not use a penalty or a
criterion function to force global convergence. Instead
the concept of pseudo-feasibility is applied. A trial
point is rejected if the square root of the sum of the
squares of the constraints is greater than the radius of
pseudo-feasibility.

RQPMIN involves in its operation Independent
Variables (IVs), External Variables (EVs) and Dependent
Variables (DVs) as described in chapter 3.7.1, an
Objective Function (OF), Equality Constraints (ECs) and
Inequality Constraints (ICs). The variables are the
variables of the Design Synthesis code VERTI. The
Objective Function and the Constraints are specially
specified for RQPMIN. External and Dependent Variables
have been defined in the VERTI description ; for the rest
we have :

An Independent Variable is a variable of the Design
Synthesis code VERTI that can be varied by RQPMIN.

An Objective Function is a VERTI function chosen to be
optimized by RQPMIN.

An Equality Constraint is a specified equality involving
VERTI variables that must be satisfied by the end of the
optimization.

An Inequality Constraint is similar to an Equality one
with the difference that involves an inequality and
becomes active only if this inequality is not satisfied.

RQPMIN can sustain up to 50 IVs and a total of 75 ECs and ICs. It requires that all functions involved are continuously differentiable. It is written in FORTRAN 77 and has a modular structure. A full description of RQPMIN is given by Skrobanski (Ref.68).

4.2.   RQPMIN Operation

The OF, the IVs,the ECs and the ICs are selected by the user and incorporated in the user-created subroutine USERF. A second subroutine, USERD, is created by the user that provides analytical derivatives of the VERTI functions, if they exist. Therefore, RQPMIN operates using the Design Synthesis code VERTI, USERF and USERD as subroutines. In addition, RQPMIN uses an input data file RQPMIN.DAT with all the information required for its operation (Fig.5).

Initially, RQPMIN checks the three subroutines and the input data file mentioned above, and if errors are not found, errors in USERF, USERD and RQPMIN.DAT, as VERTI has been checked before for its proper functioning, proceeds with the optimization.

During the optimization initialization, RQPMIN calls a few times VERTI and USERF and evaluates the OF and the ECs and ICs using the initial values of the IVs. Then, a number of feasibility steps start, during which the IVs are varied in order to find a feasible path, subject to the constraints, along which the optimization of the OF is attempted.

If a feasible path cannot be found, RQPMIN stops and prompts a message to that effect. New initial values for the IVs have then to be set. When a feasible path has been located, a series of minimization steps begins until the OF and ECs and ICs reach an optimum within a prescribed tolerance and a convergence is detected.Three types of convergence ; A, B and C can be obtained.

Convergence A occurs when RQPMIN has located a point where the distances to the minimum OF and to the minimum of the sum of the squares of the ECs and ICs are smaller than the specified tolerance.

Convergence B occurs when RQPMIN has located a point where the distances to the minimum of the sum of the squares of the ECs and ICs is smaller than the specified tolerance and a smaller value for the OF cannot be reached.

Convergence C occurs when the RQPMIN has located a point at which the estimated distance to the minimum of the sum of the squares of the constraint functions is less than the prescribed tolerance and no independent variables exist.

4.3.   RQPMIN interfacing with VERTI

Before any interfacing of RQPMIN with VERTI, the user-created subroutines USERF and USERD were prepared according to the RQPMIN User-Guide (Ref.67).

The USERF subroutine contains a listing of the IVs, the OF, the ECs and the ICs.

The RQPMIN input data file, RQPMIN.DAT, contains the upper and lower limits and the scale factors of the IVs, the OF, the ECs and the ICs. At the end of RQPMIN.DAT a number of assignement keywords and optimization tolerances follow. The scale factors serve to keep values during the optimization around one.

The selection of IVs, the variables that could be varied by RQPMIN, was largely based on their influence on the overall aircraft configuration. The following 19 variables were selected as the most appropriate IVs :

1   Wing area
2   Wing aspect ratio
3   Wing taper ratio
4   Wing quarter-chord sweep
5   Wing thickness to chord ratio
6   Position of front spar
7   Position of rear spar
8   Position of wing
9   Fin quarter-chord
10 Tailplane quarter-chord
11 Engine scale factor
12 Fuselage length
13 First fairing curve definition parameter
14 Second fairing curve definition parameter
15 Third fairing curve definition parameter

16 Fourth fairing curve definition parameter
17 Fifth fairing curve definition parameter
18 Side fuel tank width
19 Side fuel tank moment arm

As OF the empty mass of the aircraft was chosen. A number of OFs were tested to examine the possibility of a better OF as described in Chapter 5. In addition, two ECs and 22 ICs were selected. They are as follows (OF, ECs and ICs share common numbering sequence) :

ECs

2   The total fuel carried by the aircraft must equal the fuel consumed plus reserves.
3   The dry thrust at landing must equal 1.15 times the weight of the aircraft at landing -1.22 including RCS

ICs

4   The loaded aircraft moment arm must be less than the after cg limit.
5   The zero-fuel aircraft moment arm must be greater than the forward cg limit.
6   The length of the aircraft must be bigger than the sum of the lengths of the radome, nose undercarriage, RLS front nozzle (diameter), internal weapon bay, intake diffuser bent and engine.
7   The intake diffuser length must be bigger than a minimum intake diffuser length.
8   The nose undercarriage width must be smaller than the fuselage width at the same position.
9   At fuselage station E the actual cross-sectional area must be greater than the corresponding engine cross-sectional area.
10 At fuselage station J the actual cross-sectional area must be greater than the corresponding engine cross-sectional area.
11 The sustained turn rate at a specified altitude, Mach number and engine power setting must be greater than a specified minimum value (first sustained turn rate constraint).
12 The sustained turn rate at a specified altitude, Mach number and engine power setting must be greater than a specified minimum value (second sustained turn rate constraint).
13 The sustained turn rate at a specified altitude, Mach number and engine power setting must be greater than a specified minimum value (third sustained turn rate constraint).
14 The attained turn rate at a specified altitude, Mach number and engine power setting must be greater than a specified minimum value.

15 The specific excess power at a specified altitude,
    Mach number and engine power setting must be greater
    than a specified minimum value (first specific excess
    power constraint).
16 The specific excess power at a specified altitude,
    Mach number and engine power setting must be greater
    than a specified minimum value (second specific
    excess power constraint).
17 The maximum Mach number at a specified altitude,
    initial speed and engine power setting must be
    greater than a specified minimum value (first
    maximum Mach number constraint).
18 The maximum Mach number at a specified altitude,
    initial speed and engine power setting must be
    greater than a specified minimum value (second
    maximum Mach number constraint).
19 The acceleration time through a Mach number increment
    of 0.6 at a specified altitude, Mach number and
    engine power setting must be smaller than a specified
    maximum value.
20 The ride quality factor at a specified altitude, Mach
    number and engine power setting must be smaller than
    a specified maximum value.
21 The take-off distance must be smaller than a
    specified maximum value.
22 The fuselage volume must be smaller than a specified
    maximum value.
23 Constraint on the combinations of wing aspect ratio
    and wing sweep (quarter-chord sweep to the power of
    0.8 times aspect ratio must be smaller than 3.2).
24 The side fuel tank moment arm must be smaller than
    the fuselage length minus the total engine length
    plus half the gas generator length.
25 The side fuel tank moment arm must be greater than
    the fuselage length minus the total engine length.

The example presented in Appendix B, in which a
convergence is achieved, does not include IV 19 and the
related ICs 24 and 25.

Since analytical expressions for VERTI functions did not
exist, USERD subroutine is void.

The RQPMIN results file, RQPMIN.RES, contains information
on the IVs, the OF, the ECs and the ICs and various
constraint, convergence and code operation parameters. It
specifies which constraints have been satisfied and if
convergence has been achieved.

The interfacing of RQPMIN with VERTI was gradual. A part
of VERTI was at first interfaced with RQPMIN and after a
successful combined operation additional VERTI parts were
added until the whole VERTI was interfaced.

Equally gradual was the introduction of constraints.
Initially, the easier constraints were considered.
Especially the thrust-to-weight constraint at landing and
the multiple point performance constraints were left to
the end.

The choice of assignement keywords posed a few problems
as the RQPMIN User-Guide (Ref.67) provides very little
information. The same was true for the scale factor
choice, both for the IVs and the ECs and ICs. Many runs
were tried in order to establish the best values of these
parameters and to find suitable solutions.

In total, more than 250 runs were performed. Six versions
of the RQPMIN-VERTI combination were tried ; each one of
increased complexity in terms of constraints. The run
times on the VAX 11/750 varied widely. In general,
versions with relatively relaxed constraints tend to take
longer, as the optimization code RQPMIN has the freedom
to move and the optimization is considerable. Usually,
with the smallest change in RQPMIN input either in the
IVs, the ECs, the ICs, the OF or the scale factors, the
convergence is lost.

For the tuning of a RQPMIN-VERTI version, in order to run
successfully and a convergence to be reached, more than
30 trial runs were needed.

5.   OPTIMIZATION OBJECTIVE FUNCTION DEVELOPMENT

Although it was suggested in Refs 43 and 67 that the
aircraft take-off mass or the aircraft empty mass is the
best OF, a number of other OFs were tried.

It was thought that as this type of aircraft is "built
around the engine" the engine mass might be a better OF.
This approach was followed in two ways ; one with the
engine mass and the other with the engine scaling factor
as OF. Both in essence failed as the objective of a
better optimization, a greater reduction in aircraft
mass, was achieved but only nominally. The aircraft mass
reduction was better by the amount of around 80 kg (Table
2 - Columns 7,8).

To exhaust this line of thought several versions of the
engine mass OF were run with various combinations of
initial conditions, scale factors and convergence
tolerances. Again, no breakthrough was observed and the
results remained marginally better and not allways (Table
2 - Columns 3-7).

Finally, two other OFs were tested ; the wing area and
the fuel mass. The first showed marginally better and the
second worse results (Table 2 - Columns 9,11).

NOSE UNDERCARRIAGE BAY

INTAKE DIFFUSER

INTERNAL GUN BAY

INTERNAL WEAPONS BAY

AFTERBURNER SECTION

SIDE DUCTS

ENGINE (GAS GENERATOR)

MAIN UNDERCARRIAGE BAY

REMOTE LIFT SYSTEM DUCT
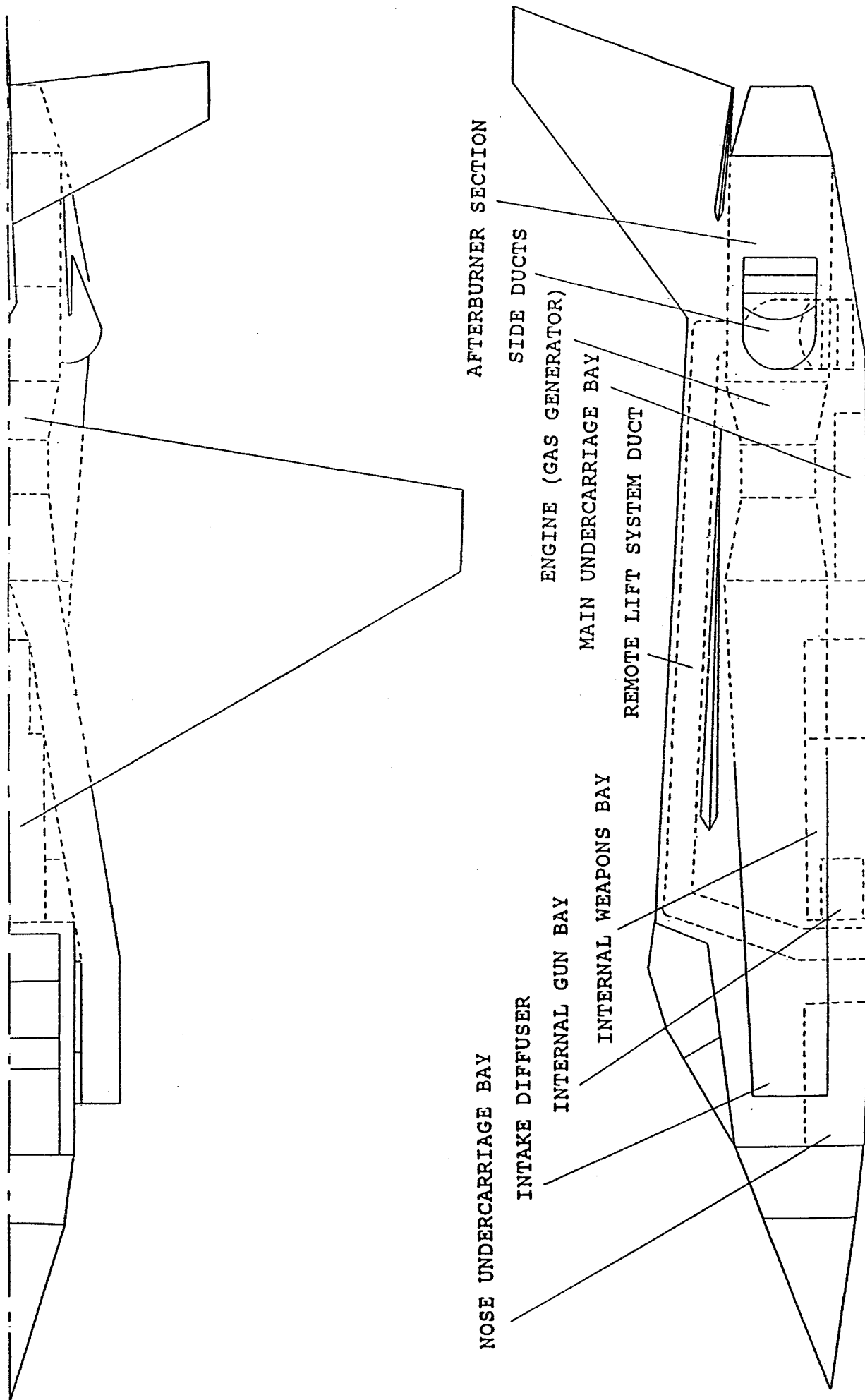
FIG. 1 AIRCRAFT BASELINE CONFIGURATION

FIG. 2 FUSELAGE STATIONS WITH CORRESPONDING SECTIONS
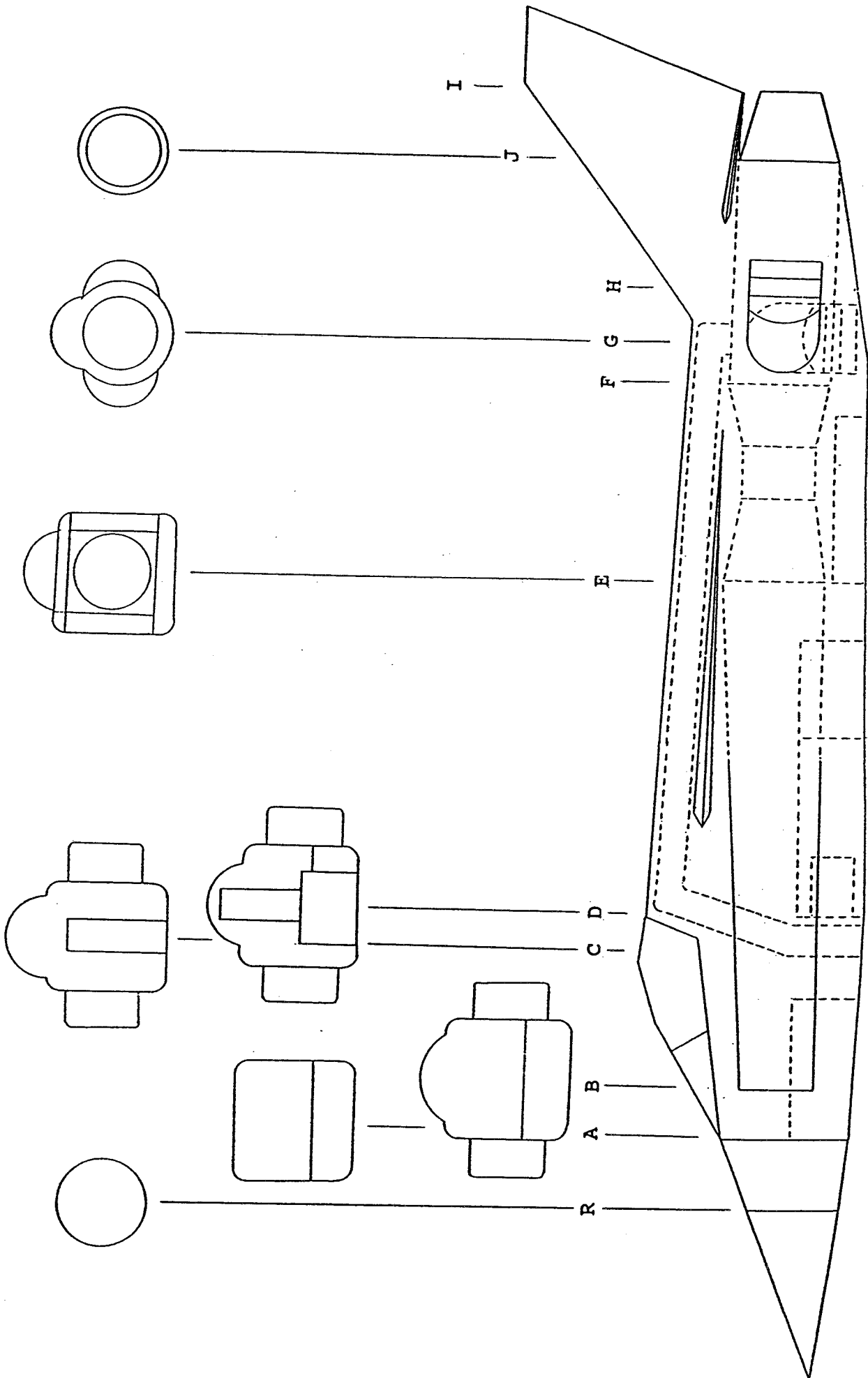
SIDE FUSELAGE FUEL TANK

CENTRAL FUSELAGE FUEL TANK
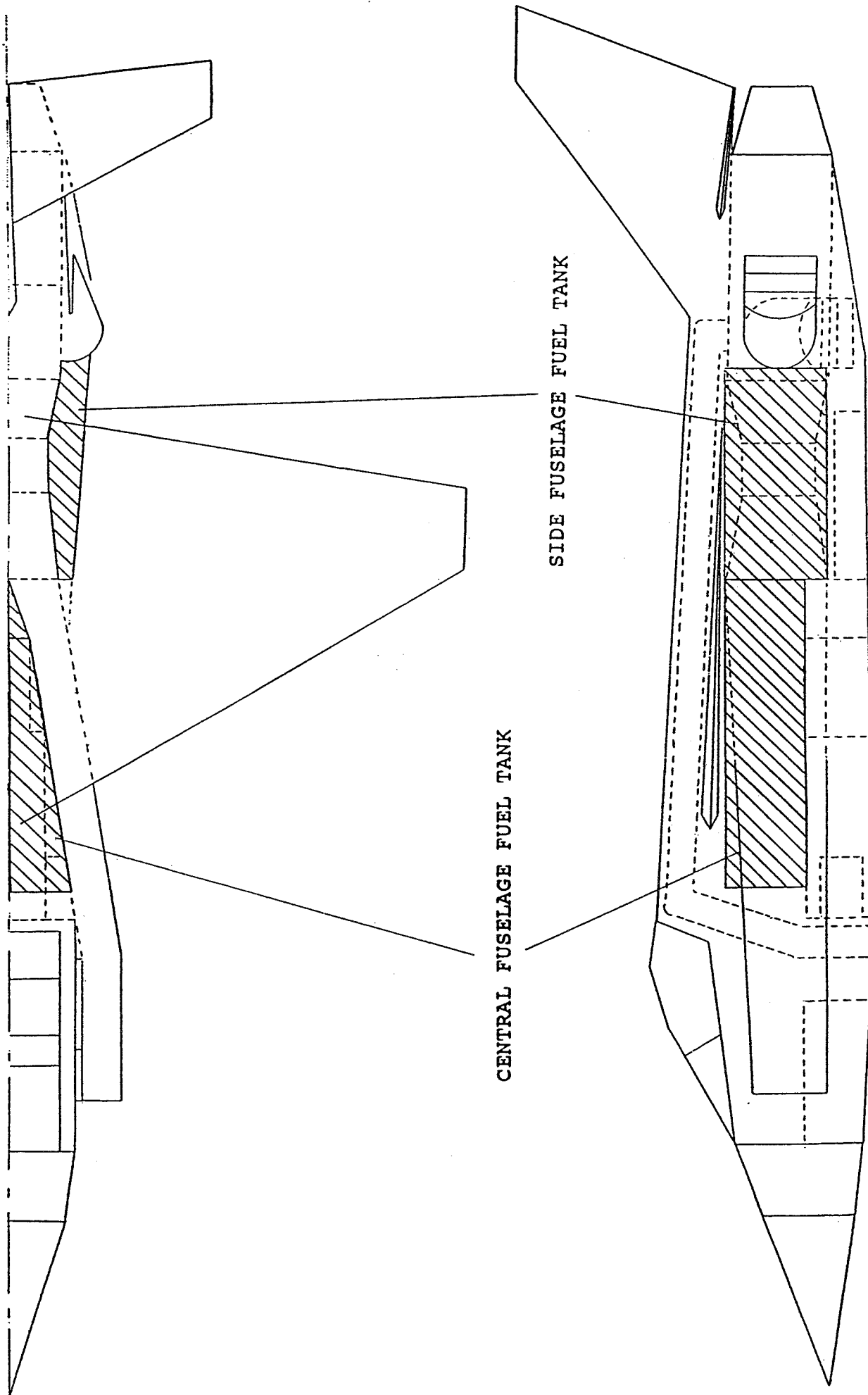
FIG. 3   FUSELAGE FUEL TANK ARRANGEMENT

36
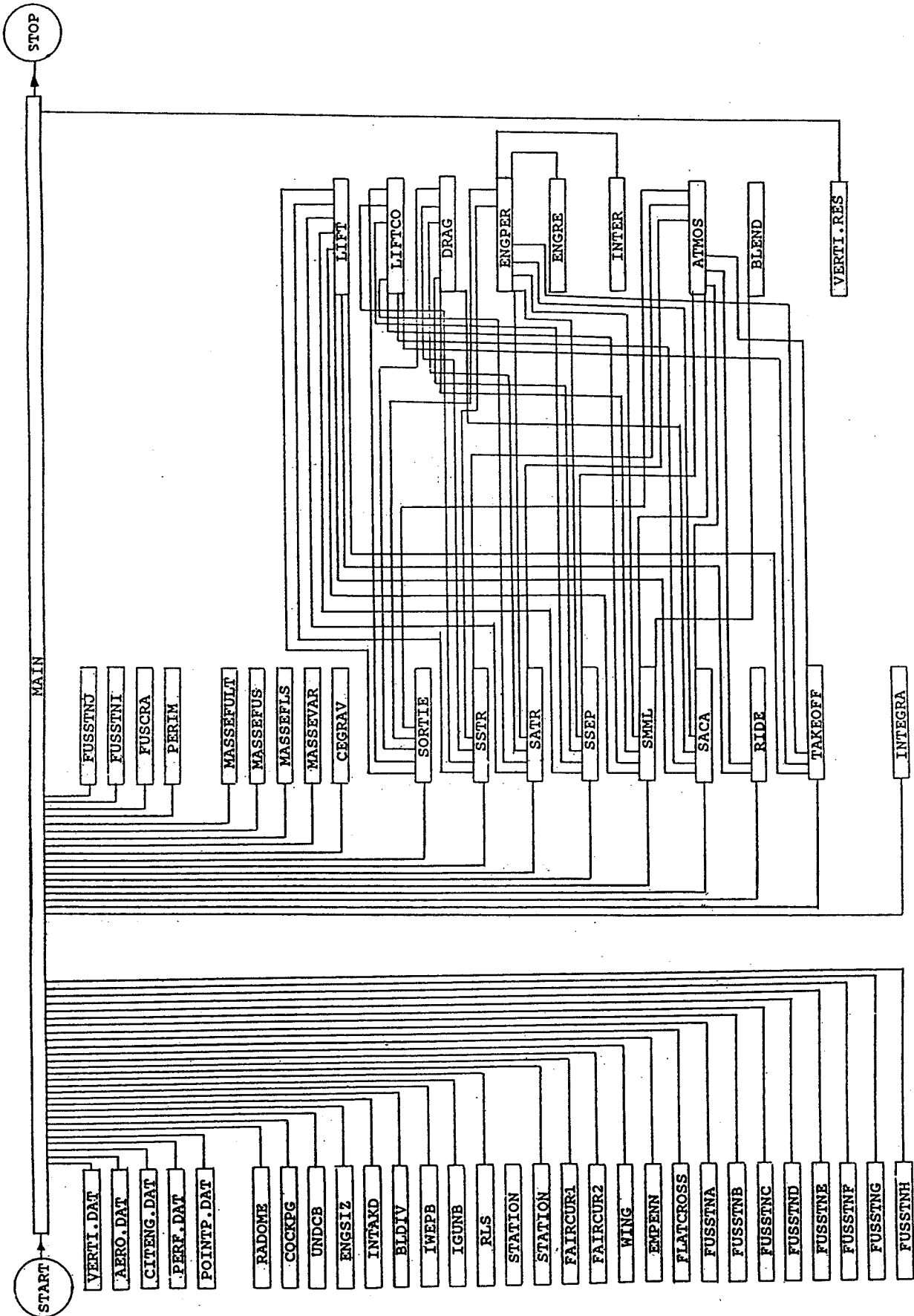
FIG. 4   SIMPLIFIED FLOWCHART FOR CODE VERTI
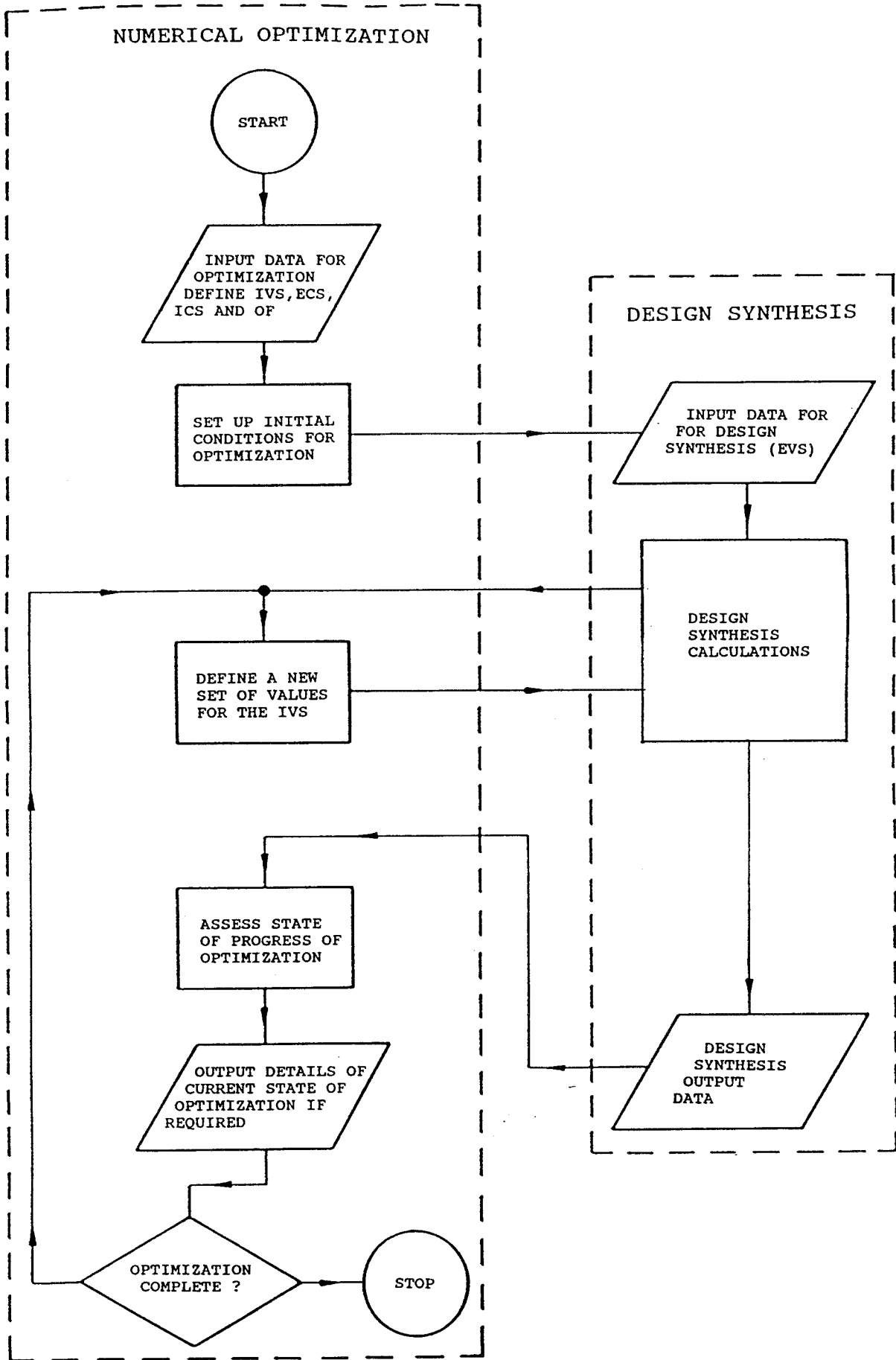
FIG.5   SIMPLIFIED FLOWCHART FOR CODE RQPMIN-VERTI
          (REF.43)
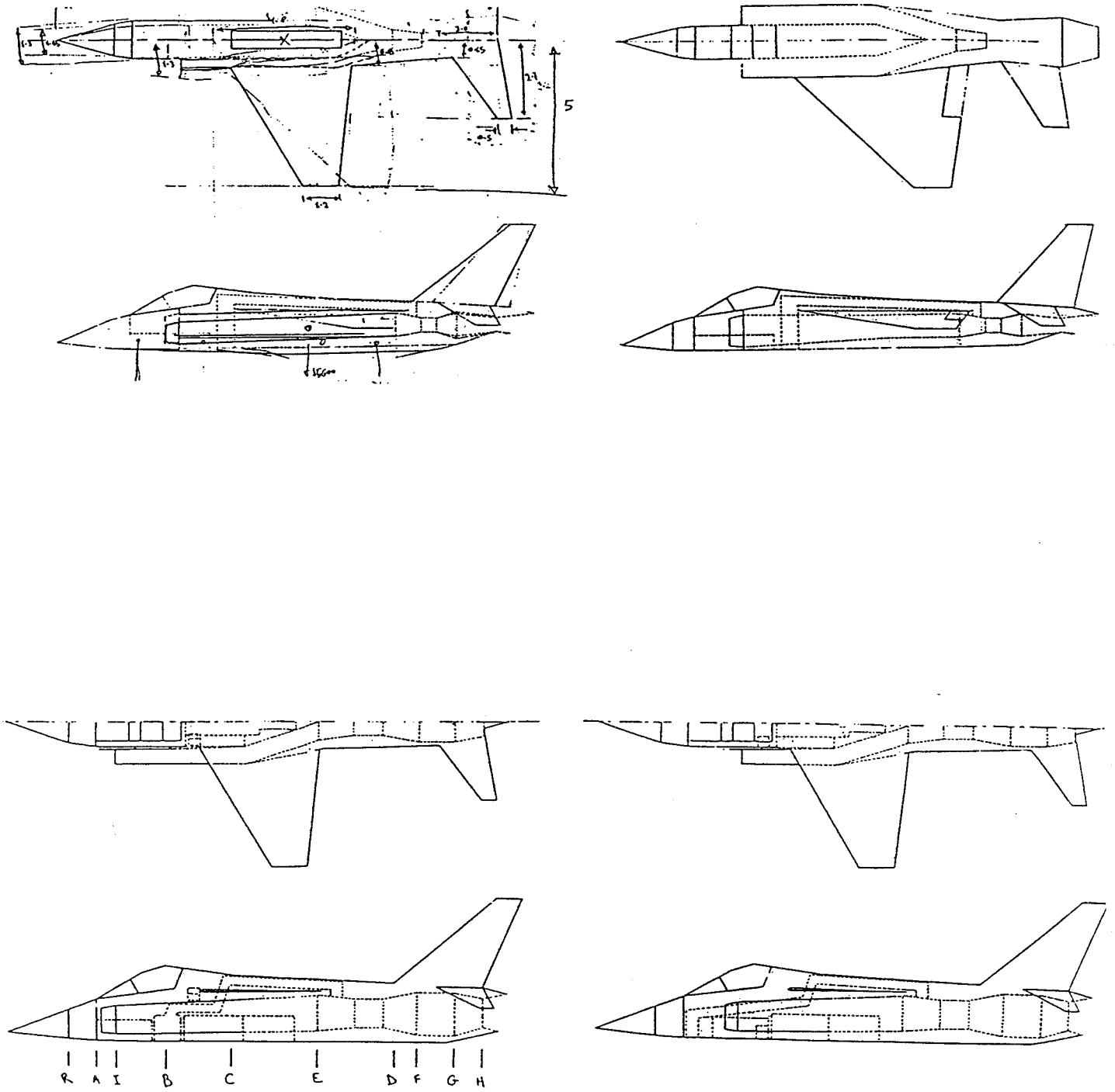
FIG.6   ASTOVL DEVELOPMENT CONFIGURATIONS
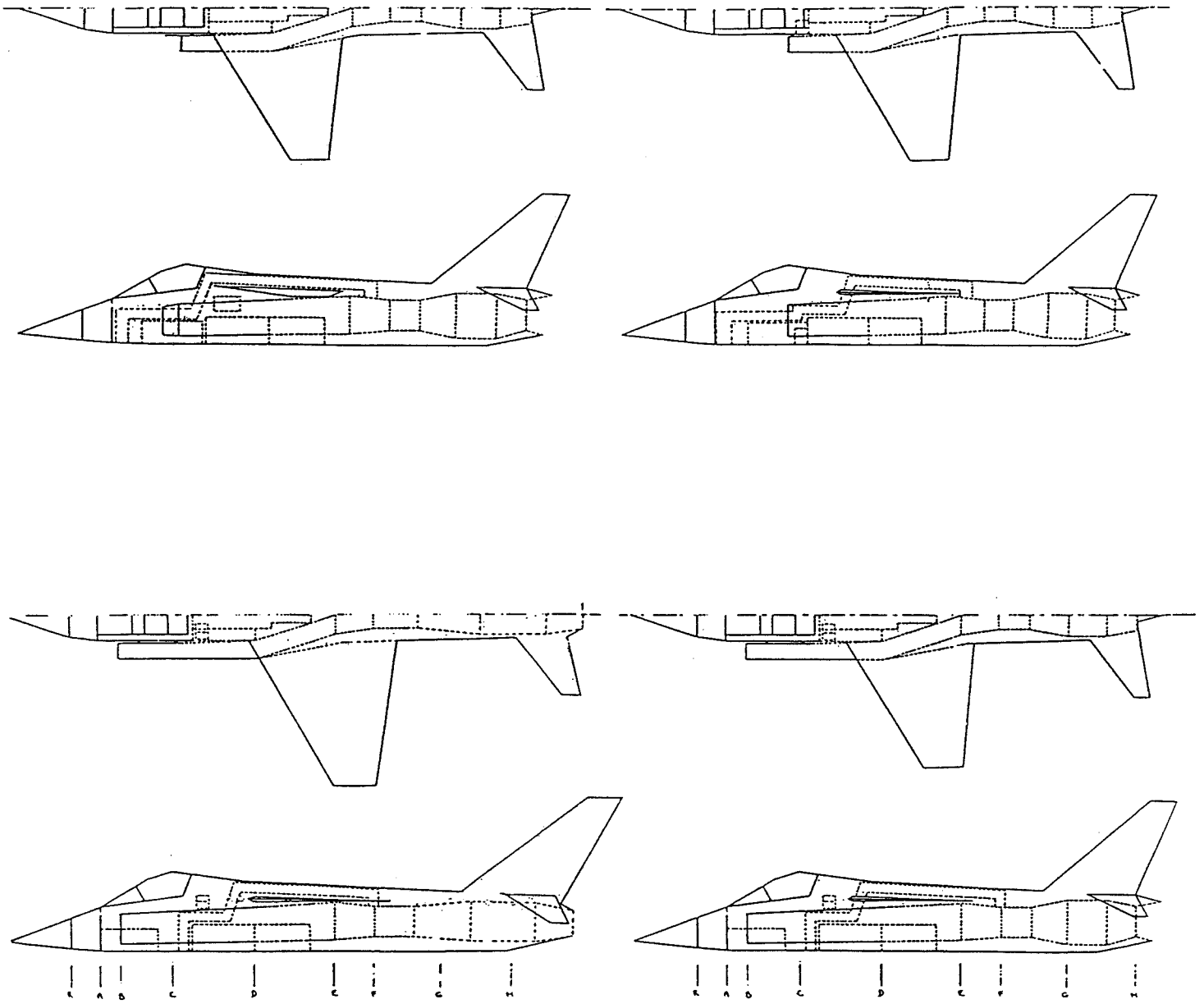
FIG.7   ASTOVL DEVELOPMENT CONFIGURATIONS
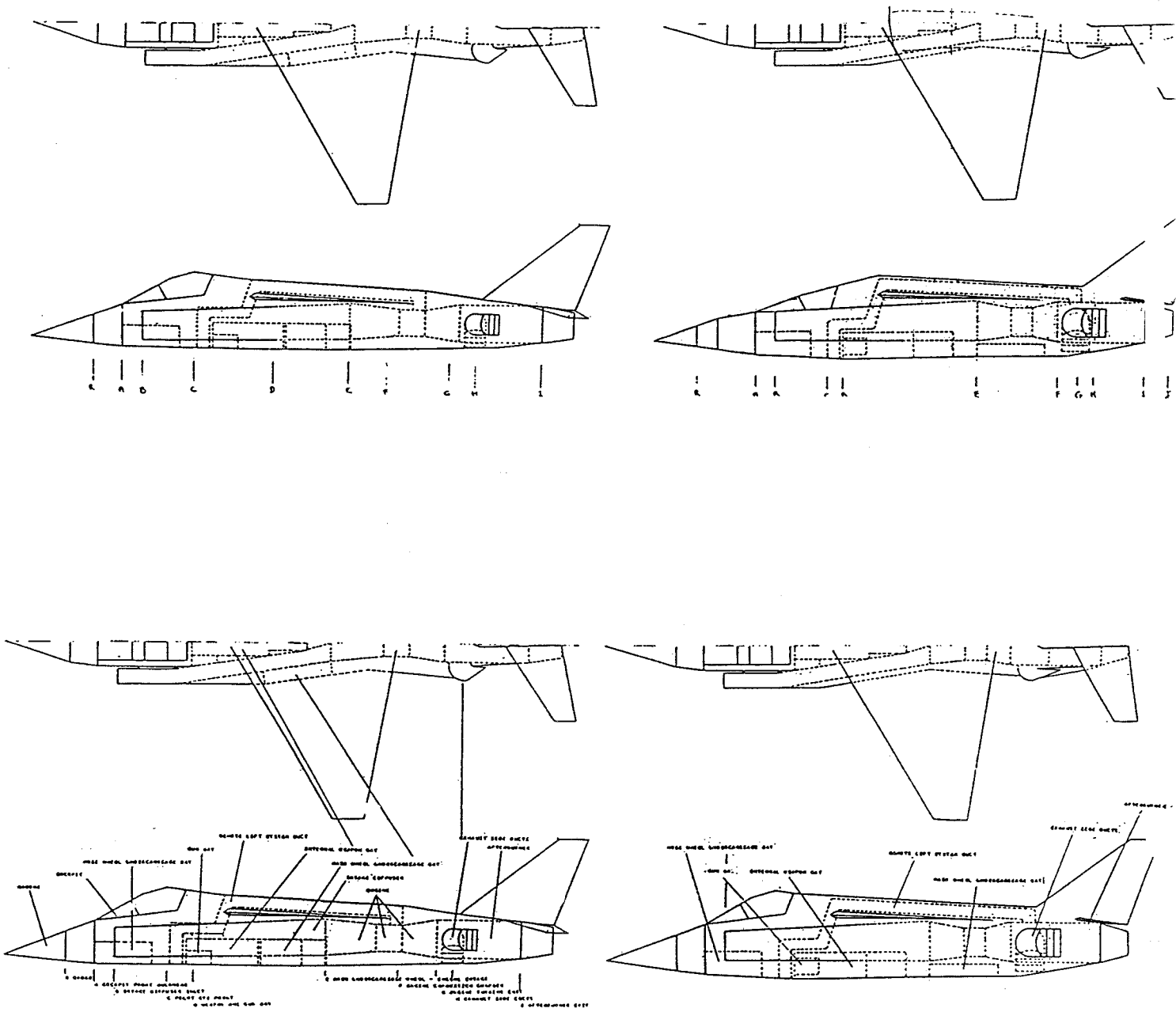
FIG.8   ASTOVL DEVELOPMENT   CONFIGURATIONS

SORTIE
LEG

\-   START-UP, TAXI, SHORT TAKE-OFF (30 sec).
        CLIMB TO CRUISE ALTITUDE AND MACH NO.

1   CRUISE AT 10000 m, 0.7 M FOR 400 km AT 1.0 g.

2   CRUISE AT 9000 m, 0.6 M FOR 45 mins AT 1.1 g.
        FIRE 2 AMRAAMS.

3   COMBAT AT 9000 M, 1.4 M, 1.0 TURNS AT 3.0 g.
        FIRE 2 AMRAAMS.

4   COMBAT AT 1000 m, 0.8 M, 2.0 TURNS AT 8.0 g.
        FIRE 2 ASRAAMS, ALL AMMO.
        CLIMB TO CRUISE ALTITUDE AND MACH NO.

5   CRUISE AT 10000 m, 0.7 M FOR 400 km AT 1.0 g.

\-   HOVER FOR 30 sec OUT OF GROUND EFFECT.
        VERTICAL LANDING WITH 5 % OF INTERNAL FUEL
        REMAINING AT ENTRY TO HOVER.

TABLE 1   EXAMPLE SORTIE PROFILE

COLUMN	1	2	3	4	5	6	7	8	9	10	11
OBJ FUNCT	INIT CONF	A/C M	ENG M	ENG M	ENG M	ENG M	ENG M	RTP	SW	MWC	MTGFI
ENGINE M	3570.4	2599.7	2598.0	2640.1	2603.3	2602.2	2597.6	2597.5	2609.4	2638.0	2759.3
FUEL M	4570.0	3094.1	3033.1	3058.6	3027.0	3029.8	3016.3	3015.7	2948.4	3160.4	2906.7
FUSELAGE M	2735.0	2192.6	2195.8	2244.5	2211.8	2191.6	2191.0	2190.0	2191.4	2324.6	2330.8
WING M	2286.4	999.6	1055.3	1164.0	1064.8	1026.5	1019.5	1019.6	1094.7	1008.9	1607.1
EMP TAIL M	476.0	199.2	199.8	206.0	200.5	198.4	196.5	196.5	195.6	206.1	209.7
EMP FIN M	1812.1	628.4	641.3	656.1	643.4	628.7	619.6	619.9	608.0	627.0	586.4
SUM ABOVE	15449.5	9713.6	9723.3	9969.3	9750.8	9674.6	9640.5	9638.6	9647.5	9965.0	10400.0
AIRCRAFT M	19301.3	13559.3	13569.0	13852.1	13596.5	13520.1	13486.1	13484.6	13492.7	13810.9	14246.0
ENG SCALE F	1.50000	1.02348	1.02267	1.04300	1.02520	1.02485	1.02248	1.02239	1.02813	1.04193	1.10076
A/C LENGTH	17.8000	14.9264	14.9239	14.9871	14.9318	14.9306	14.9233	14.9230	14.9409	14.9691	15.1633
WING AREA	35.0000	23.2766	23.3737	23.8597	23.4466	23.1786	23.1150	23.1103	23.0502	23.8663	24.1958
CONVER	-	B	B	MX ITER	A	NO F PR	A	A	B	NO F PR	B
ITER NO	-	7700	5700	8000	16000	5100	6600	8800	8500	6700	5500
NOTES	-	XTOLV, XTOLU 0.001	CONST 5 NOT REL IN COND	CHANGED CONST 5 IN COND NOT REL	CONST 5 NOT REL	XTOLV, XTOLU 0.00001 CHANGED IN COND	XTOLV, XTOLU 0.001	XTOLV, XTOLU 0.001	XTOLV, XTOLU 0.001	XTOLV, XTOLU 0.001	XTOLV, XTOLU 0.001

TABLE 2   OPTIMIZATION OBJECTIVE FUNCTION
DEVELOPMENT RESULTS

6.   DISCUSSION

6.1.   Baseline Configuration

The design of V/STOVL aircraft is a controversial issue
where a number of schools of thought propose markedly
different approaches.

In this work, extensive literature searches have been
performed with the objectives of acquiring an
understanding of V/STOVL combat aircraft design and to be
informed of the latest developments in this field.

The first objective has been accomplished and numerous
useful references have been found (Refs 5, 6, 8, 11, 17,
19, 33, 40, 41, 66, 71 and 74). A particularly useful
background was written by Fozard (Ref.21), giving briefly
the full history of V/STOVL, with an emphasis on vectored
thrust !. Kohlman (Ref.36) provided a good introduction
on V/STOVL, Wilson and Eskey (Ref.82) helpful comparisons
between CTOL and V/STOVL and Sweetman (Ref.75) one of the
best accounts of recent state of affairs on ASTOVL.
Ref. 39 (Levine and Inglis) on the US/UK ASTOVL Program,
formed the basis, in conjuction with the RAE requirements
and the ASTOVL Concept Evaluation Model (Ref.23), of the
Baseline Configuration evaluation.

Nikolai and Stinton (Refs 54 and 72) provided any basic
aircraft design information such as tail sizing,
Heinemann and Huenecke (Refs 25 and 30) a review of
combat aircraft design and Hitch and Lee (Refs 26 and 38)
some aspects of computerized aircraft design. Mangold
(Ref. 45) gave a few indications for combat aircraft
aerodynamics trends and Patel and Dixit (Ref. 56) an
interesting approach to reverse design. Ref.76 was used
for comparisons with other recent fighter designs for
sizing purposes.

The second objective was not achieved, mainly because
most of the recent material is classified. Nevertheless,
a few publications gave some hints into certain areas.
Fowler (Ref.20) on ducting, Lumnus (Ref.44), Nelms
(Ref.50) Nelms, Durston and Lumnus (Refs 51 and 52),
Brown (Ref.7), Stoll and Koening (Ref.73) and Burns
(Ref.9) on STOVL aerodynamics, McNally and Brown (Ref.47)
and Schrage and Meyer (Ref.61) on operational aspects and
Sheridan (Refs 65 and 66), Scott (Ref.63) and Willis

(Refs 79 and 80) on engine and remote lift concepts. Ref.4 provided considerable detail on control matters.

The Baseline Configuration that was attempted, that of an advanced supersonic STOVL combat aircraft with a Remote Lift System (RLS) without a burning front nozzle (that is a hot RLS) and an internal weapon bay, is an extremely complicated one. Such a configuration has never been proposed before, at least openly, as indicated in the literature search.

The above mentioned complications were to be added to the many that exist in the STOVL field. STOVL configurations are broadly divided into vectored thrust and split-flow concepts (Refs 21, 36 and 39). Some mixed, to a certain degree, concepts exist in the sense that split-flow can be vectored. Vectored thrust concepts are straightforward. The engine thrust is vectored for landing and sometimes for take-off and in forward flight. The split-flow concepts encompass a variety of schemes (Refs 21 and 36). From separate engines for landing (and take-off), perhaps a category on its own, to various arrangements for remote lift, either plain or augmented. Remote refers to lift provided by ducts to a remote, in relation to the engine, position (Fig.1).

It was very interesting to find so many views on the subject. The views are not only numerous but equally strong. The opinions are divided between the vectored thrust and the split-flow approaches, with some prominent members of the vectored thrust group (Ref.21) insisting that split-flow concepts are not feasible.In addition to these main groups, there are many in-between and far-away, including positions such as that the only realistic solution is the propeller ! (Ref.61).

From the engine point of view, vectored thrust is favored. Ward and Lewis (Ref.78) suggest that a vectored thrust scheme is much more efficient and offers a better performance than a split-flow one. However, for supersonic STOVL combat aircraft, as in our case, vectored thrust is not allways the right choice. Vectored thrust requires the engine to be placed near the centre of gravity of the aircraft and this requirement results in aircraft with big fuselages in the middle ; a situation in contrast to the area-ruling needed in supersonic aircraft.

Additional problems, to the usual ASTOVL configuration problems, were faced. The requirements of a high thrust-to-weight ratio necessary for vertical landing (giving a long engine) and an internal weapon bay with a very long medium range missile, are conflicting. Several attempts to place the internal weapon bay in such a way as not to have the length of it added to the engine length and consequently a very long aircraft, have failed. The internal weapon bay was considered in different locations overlapped by the engine or split in two parts in the aircraft sides. All these schemes proved unrealistic and could not be justified. As a consequence the weapon bay remained ahead and in line with the engine.

Another major problem was the size of the RLS front duct. With a configuration that dictated a thrust split between the front duct and the side ducts of the RLS of around 50 percent, a RLS front duct of enormous size - cross-section - became necessary.

It was evident that a RLS front duct of this size could not be accommodated in the aircraft fuselage. The resulting fuselage was of unacceptable height. In addition an extremely inefficient use of the upper fuselage, where a substantial part of the RLS front duct was located, was made.

Many alternatives were considered which fall in two categories ; the first to have two distinct RLS front ducts running the sides or the lower part of the fuselage and joining at the front nozzle and the second to have a RLS front duct with a non-circular cross-section that could better fit in the upper fuselage.

For the first category a realistic solution could not be found as the internal weapon bay and the large engine posed too many problems ; consequently a solution within the second was sought. Many cross-sectional shapes were put into consideration and their advantages and disadvantages were accounted for. Cross-sectional shapes, like the semi-circular, that offered fuselage volume efficiency suffered from substantial pressure losses (Refs 1 and 27). Hence it was decided to have a RLS front duct composed of three circular ducts, one bigger in the middle and two smaller one in either side. Together they formed a semi-circular system of ducts that was much smaller in height than a circular one of the same cross-sectional area (Fig.A7). A penalty was paid in terms of frictional losses but that was much less than the pressure losses of the other cross-sectional shapes.

Finally, the well known V/STOVL combat aircraft problem
of engine hot gas ingestion while hovering, was very
briefly investigated with reference to the intake
diffuser inlet position (Refs 37 and 46). Positioning of
the inlet further back from the RLS front nozzle location
was impossible because the length of the intake diffuser
would become too small for a smooth flow or the length of
the already long fuselage too long (Fig.1). Thus the only
alternative was to place the inlet very much ahead of the
RLS front nozzle position. A satisfactory distance
between inlet and nozzle was hence guaranteed but at the
expense of the pilot's good visibility ; the intake
diffusers extended up to nearly the cockpit front
bulkhead (Fig.1). Fixed intakes were chosen, in view of
the 1.6 M maximum speed of the aircraft (Ref.62).

To reach the final Baseline Configuration some tens of
cofigurations were put down to paper in the form of
scketches. Just a dozen of them in Figures 6, 7 and 8
show how the configuration evolved. These configuration
attempts indicate some of the steps taken, the problems
and the alterations considered, and the compromises
accepted to reach the final Baseline Configuration of
Fig.1.

The final Baseline Configuration characteristics could
not be validated against operational ASTOVL supersonic
combat aircraft, simply because they do not exist. Very
recently, a Soviet ASTOVL combat aircraft design, code-
named YAK-141, was unveilled. It is in the development
phase with two prototypes engaged in flight testing. Very
little information is available for the moment and the
best source that has been found is Ref.2. However, it
does not have the same engine configuration being a
"lift/cruise plus lift" type. A similar type as a study
and in some detail was found in Ref.14 by Cox and
Roskam.

Therefore, a table was constructed to compare our
Baseline Configuration with the above mentioned two
(Table 3). The poor data for the YAK are not more than
rough estimates derived from the information presented in
Ref.2. Since the payload and the mission profile is very
much the same - an assumption for the YAK - we can note
the following by their comparison (Table 3) :

The take-off mass of our configuration (Column 1) at

18.9 tons is nearly identical to the YAK's (Column 4).
Cox and Roskam's is much lighter at 14.2, a tendency
found in all "paper" designs. The maximum sea level
thrust of the engine of our configuration (Column 1) is
something like 70 percent greater than the other two -
the other two have almost the same thrust. The reason is
obvious as they use a dedicated lift engine (the YAK two)
for landing and their cruise/lift engine is not driven by
the landing thrust-to-weight condition. Consequently, the
cruise/lift engine mass of Cox and Roskam is less than
half our configuration's (Column 1) engine mass (data for
the YAK not available). The fact that the Cox and Roskam
and the YAK have nearly the same thrust for different
landing mass is because the YAK uses reheat at landing.

Last but most important, is the mass comparison of the
dedicated lift engine mass of Cox and Roskam to the mass
of the RLS front system of ducts and nozzle of our
configuration (Column 1); the dedicated lift engine mass
is nearly the same - actually Cox and Roskam's is
slightly lower (data for the YAK not available). Even if
this dedicated lift engine is scaled-up to account for
the difference in landing mass between the two
configurations (Column 3 [2]), it is only 67 kg heavier
without taking into account that the volume occupied by
the RLS system results in increased fuselage mass. This
comparison is made with a very optimistic estimation for
the mass of the RLS front duct and nozzle (Column 1 [4]).
A second estimation (Column 1 [5]) gives a 42 kg higher
mass compared to the scaled dedicated lift engine mass.

All the above observations are based on the convergence
example of Appendix B. As it will be discussed later in
Chapter 6.3.2., without convergence the aircraft mass
reduction is much better. Column 2 shows such a case and
is evident that the trends described above apply to a
much larger extent.

6.2.   Design Synthesis

6.2.1.   Introduction

Although the approach of Lovell (Ref.43) was in general
followed, in many instances changes have been made. A few
of the changes were due to what was believed to be an
imbalance in the approach as some parts of the design
synthesis were evaluated in great detail and others not.

The rest were differences in the techniques used and additions related to the specific ASTOVL configuration.

6.2.2.   Fixed Items

The undercarriage dimensions and mass estimation of Ref.43 was at first thought to be rather simple. Various possibilities were considered (Ref.15) but all tended to be at the other extreme ; very complicated. Thus it was decided to follow Lovell disregarding any reservations.

In the internal weapon bay the missile ejectors posed problems. Again very little information could be found for their dimensions and configuration (Refs 10,58). As a consequence the ejectors and their mechanisms were represented by a box occupying the upper part of the internal weapon bay.

The engine dry thrust to weight ratio at landing was put to 1.15 excluding bleed air for the Reaction Control System (RCS). To this a 7 % (from Ref.14) was added for the RCS to bring the total to 1.22. This is a low value and the literature (Refs 14, 17 and 59) suggests something between 1.25 and 1.30. However, as it was requested by the RAE it was left to 1.22. However, it should be pointed that very substantial variations exist for the various thrust losses ; a good example is the suckdown losses given as 13 % in Ref.14 and 3 % in Ref. 59. To this a 3 % thrust due to the RLS was added, based on RAE information.

The Remote Lift System (RLS) presented many difficulties. Estimates for its mass - mass per unit length - had to be made to account not only for its structural but for its insulation mass as well. The structural mass calculation was based on comparisons with RALS (Remote Augmented Lift Systems) concepts (Refs 60 and 63). Ref.81 (Willis) particularly, although dealing with ejector RALS systems, contained substantial information on sizes and masses of ducts and nozzles. Ref.16 was also consulted for nozzle information but without success. The insulation mass, being a hot RLS duct with nothing similar in the literature, was a problem. Detail investigation of the RLS front duct insulation was beyond the scope of this work. Therefore, a rough estimate was the only solution.

The position of the RLS front duct nozzle was examined in relation to the engine front/rear thrust split. As very

little room for nozzle movement was available due to the configuration (internal weapon bay), a 50 : 50 % thrust split was decided that assured a nozzle position between the cockpit front bulkhead and the internal weapon bay (Figs 1 and 2).

6.2.3.   Geometry

A lot of emphasis was placed on the fairing curve definition. It was very well defined as the nett cross-sectional area of the fuselage, or the aircraft if area rule is applied, in order to avoid any confusion with the actual cross-sectional area.

The fairing curve evaluation in Ref.43 presents a problem at the rear end of the fuselage. The problem appears if the fin and tailplane surfaces extend beyond the end of the fuselage and only in the case where area rule is applied. With area rule the fairing curve includes the flying surfaces lateral cross-sectional area (Ref.53), hence in the fairing curve evaluation with area rule the fifth fairing curve definition parameter that indicates the cross-sectional area of the fuselage at the end of the fuselage - at the nozzle exit - must include the related flying surface lateral cross-sectional area.

In the fin and tailplane calculations, volume ratios are used. The mean quarter-chord distance between wing and fin in the volume definition of fin, was not estimated by the iterative process of Ref.43 but given as EV (or IV in combination with RQPMIN); the reason being difficulties with convergence. The tailplane was treated similarly.

The equation of the lateral cross-sectional area of the flying surfaces of Ref.43 was re-evaluated from the chordwise thickness distribution of the wing and the resulted equation was found to be different from the one of Ref.43. Serghides (Ref.64) does not include area rule in his design synthesis to make a comparison, therefore the RAE was contacted and after consultation a final third version was adopted.

The fuselage geometry was evaluated with due care for the definitions of the cross-sectional areas in question. A greater number of fuselage stations than in Ref.43 was considered mainly due to the complicated rear fuselage

(RLS side ducts) and the use of area utilization factors has not been extensive.

6.2.4.   Mass and Centre of Gravity

In general, densities are not used in mass calculations as in Ref.43. Instead the actual mass values for items such as electronics are preferred. It was felt that for items far away from the aircraft cg an improved accuracy was necessary this being particularly important on STOVL aircraft.

The internal fuel tank solution of Ref.43 was not followed. The evaluation of the internal fuel volume capacity of the fuselage by subtracting the fixed items volume from the fuselage volume has some drawbacks. The reason is that many parts of the fuselage are not suitable for fuel storage. Instead, three fuselage fuel tanks (described in Chapter 2.2.) were chosen, their location dictated by safety, reliability, aircraft centre of gravity and complexity considerations.

6.2.5.   Aerodynamics

Only very minor details have been altered in the drag aerodynamics of Ref.43. They related to the afterbody drag estimation when VERTI operates in conjuction with RQPMIN. A limit was placed on the equivalent afterbody length which sometimes during a feasible path search by RQPMIN would reach a length several times that of the whole fuselage.

The lift-curve slope estimation of Ref.43 was enhanced with interference effects. Preliminary calculations showed these effects to amount to around 10 %. For body and wing-body interaction interference, the methods of DATCOM (Ref.3) were used transformed into analytical form. For the tail interference again Ref.3 was used with the difference that as the downwash term needed considerable information from graphs and charts for its evaluation, a situation unsuitable for a code, an analytical expression was derived for it and is presented, with the rest of the interference evaluation, in Appendix C. This analytical expression was derived from first principles using finite wing theory and assuming that the tailplane is situated at the same height with the wing (Ref.28).

Stability considerations were not among the requirements
for this work. However, some literature was reviwed (Refs
32, 37 and 44) with the purpose to establish if anything
referring to stability heavily influences the
configuration. Nothing was found.

6.2.6.   Performance

The engine performance, provided by the RAE, was in the
form of input data table. It has been noted that the fuel
consumption, and the reheat thrust in relation to dry
thrust, were rather high compared to other modern
military turbofans but no further action was taken.

The suitability of the engine performance in the form of
an input data table, as opposed to a set of formulae
descibing the engine performance - a practice of Refs 43
and 64, has been questioned. The subroutines needed to
evaluate the engine performance from the input data table
run to nearly 700 instructions in length. This represent
around 10 percent of the whole VERTI code where a formula
approach would need 100 to 200 instructions. In addition,
although every effort has been made to ensure flexible
engine performance subroutines, a universal system of
data input is impossible. Consequently, a change in the
input data table format would involve re-writing of the
engine performance subroutines. The table form, being a
RAE requirement, was kept.

The sortie performance evaluation suffers from
convergence problems ; a situation that occurs, to a
lesser extent, in some point performance estimations as
well. These convergence problems were faced by adding
relaxation if convergence is not achieved after a
specified number of iterations. If that failed, a trap
was activated giving an end to the iteration process with
a value that is the average of the two previous ones.

In the attained turn rate estimation the values obtained
are lower than expected. This must be due to the the
input aerodynamic data for maximum lift coefficient.
Clearly the data used from Ref.43 are not appropriate.
The maximum Mach number results seem rather erratic. The
method used in their estimation is sound in principle but
its application and perhaps the relaxation applied
require further investigation.

6.3.   Optimization

6.3.1.   Background

The optimization code RQPMIN used in this work, has been developed by Skrobanski (Ref.68). It is, as described in Chapter 4.1., a general optimization code, the last of a series of optimization codes along the lines of the Multivariate Optimization (MVO) research carried-out by the RAE.

MVO reserch started in the late sixties and a number of reports on the subject have been published since then. Peckham (Ref.57) is one of the first reports describing a relatively simple design synthesis of a civil transport aircraft that is then optimized for minimum operating cost. Kirkpatrick and Collingbourne (Ref.35) concentrate on the problem of flap chord selection encountered in the previous publication. Kirkpatrick and Peckham (Ref.34) investigated the effects of parameters such as the aerofoil section, the engine performance, new materials and structural savings on the design of a short range transport. Collingbourne's (Ref.12) is the latest and fullest report on transport aircraft.

MVO work was then continued with military aircraft, with Lovell (Ref.42) examining its application on the preliminary design of a combat aircraft and Mothershill (Ref.49) on a twin-engine version. Lovell (Ref.43) provided the latest developments in combat aircraft design synthesis. Serghides (Ref.64) considered a canard-delta combat aircraft configuration.

At the same time, comparable research has been under way elsewhere. In the USA notable work has been done by Vanderplaats (Ref.77) with the development of the code CONMIN. CONMIN is a code for the solution of linear or non-linear constrained optimization problems, very similar to the RAE's MVO techniques. Other work in the USA is that of Sliwa (Ref.69) on the constrained optimization of a medium range transport aircraft with reference to the application of new technologies. A relatively early work is by Hague and Glatt (Ref.22) on multivariate search techniques.

Recent reports include Ref.48 of ONERA which describes an optimization technique based on a generalized projected

gradient, Ref.13 of Cousin and Metcalfe on the British
Aerospace (Commercial Aircraft) Sunthesis and
Optimization Program and Smith and Lee (Ref.70) giving an
overview of the combat aircraft MVO work.

Cousin and Metcalfe's report is very interesting ; it
does not only deal with the developments that culminated
in the BAe design synthesis and optimization code TASOP,
but discusses many of the problems of the MVO approach.
According to this report attention is focused on modular
design, clear structure and grouping of data, well
defined logical path, disciplined order to the aircraft
evaluation, flexibility to use alternative sub-models and
a top-down structured design of the code. All these areas
have been pointed-out in the present work before the
publication of Ref.13, and appropriate solutions were
found and incorporated in VERTI.

On another level, Sobieski (Ref.24) must be mentioned.
His efforts relate to large scale optimization ; that is
the combination of finite element type of optimization
codes for aerodynamics and structures to produce a single
super-code. The difficulties associated with the task are
obvious. From the computing time side, if a design
synthesis using simple empirical design relationships
when interfaced with an optimization code needs a few
hours for a run, one can imagine what finite-element
codes would need.

6.3.2.   RQPMIN Operation

In the RQPMIN interfacing with VERTI and the RQPMIN-VERTI
operation substantial problems were encountered. The
information available in the RQPMIN User-Guide (Ref.67)
was sparse. Although it provides guidelines for the set-
up of the IVs, the OF, the ECs, the ICs and their scale
factors in the user-created subroutine USERF and the
input data file RQPMIN.DAT, it does not indicate how the
code operates. Equally, very little is given on
assignment keywords in RQPMIN.DAT. Where the User-Guide
is very informative, is in the diagnostics of the code. A
very comprehensive list of warning, error and stop
messages is included.

Initially, some exploratory runs were performed to
determine the proper values of the scale factors and the
assignment keywords. The RQPMIN User-Guide (Ref.67)
suggests scale factor values that keep the corresponding
parameters -IVs, OF, ECs and ICs - around one during the

optimization. This is an impossible condition because, even if the initial values are around one, as some paremeters change considerably during the optimization, the condition is lost. In addition, many times initial parameter values other than one were necessary for a successful optimization.

For the assignement keywords, the main difficulty was that the function of most of them was unknown, but this is not reported in the RQPMIN User-Guide (Ref.67). For the ones the function is known, such as EC and IC tolerance limits, they are given unsuitable range of values. RQPMIN was designed for mathematical applications and these tolerance limits, that guide as to whether the constraints have been satisfied or convergence achieved, are too small. Even their upper (maximum) value of 0.001 is inappropriate for engineering purposes. Numerous runs with a substantial reduction in the OF, ended unsuccessfully because these tolerances could not be satisfied.

The RQPMIN User-Guide (Ref.67) refers to three types of convergence but indicates that even if a convergence is reached is not guaranteed that RQPMIN has found a valid solution. Nor does the "no further progress possible" message necessarily means that the run has failed. As the "no further progress possible" message appears in almost every unsuccessful run, it is very difficult to make a decision on what the results of the run represent. The great majority of convergent runs were of type B ; rarely A and never C.

It should be mentioned that in addition to the "no further progress" message, in over 200 unsuccessful runs only six times other messages appeared. The warning, error and stop messages listed in the RQPMIN User-Guide (Ref.67) number around 130.

The convergence and the "no further progress possible" are not the only situations arising in RQPMIN operation. Cases where the code infinitely iterates or does not work at all, appear as well. Furthermore, the "no further progress possible" message can be found with and without the constraints having been satisfied. In one case we had the unusual situation in reaching convergence without the constraints having been satisfied.

Another important point is that the smallest change in the input RQPMIN.DAT or the USERF file can have

tremendous consequences. A convergence can be lost by just changing the scale factor of one IV, EC or IC. The only difference can be a small change in the initial (normalized) value of the OF this allways remaining within the RQPMIN User-Guide (Ref.67) recommendations to have a value of around one. The same applies for the IVs, ECs and ICs.

RQPMIN varies during its feasibility steps, the IVs in every direction until it finds a feasible path. When very tight constraints were specified (discussed in the following chapter), only four IVs showed considerable variation during the optimization. They were the engine scale factor, the wing quarter-chord position and and the front and rear spar positions. The engine scale factor carries the most of the aircraft mass reduction and the wing quarter-chord position the cg balance.

Other important IVs remain roughly the same. The fuselage length because the aircraft does not have any free space in the axial direction, the wing area because is needed for the point performance constraints and the size and moment arm of the side tanks for no apparent reason.

A unexplainable tendency of RQPMIN operation was observed, with regard to the wing front and rear spar positions ; RQPMIN brings the two spars close together. The reason could not be found ; a guess might be that it is a way to reduce wing fuel tank volume for cg purposes. However, the question is why RQPMIN chooses the wing fuel tanks and not the fuselage fuel tanks and especially why not the fuselage side tanks as they are much more suitable for cg balance. To ease the situation, the fixed moment arm of the side fuel tanks, was changed to an IV that can be varied by RQPMIN but with no effect ; the size and moment arm of the side fuel tanks remained almost constant.

This trend appeared in earlier versions of RQPMIN-VERTI with light constraints. The difference is that in those earlier versions it was a temporary trend and the spars returned, in the end of the optimization, near to their original positions. In the last RQPMIN-VERTI version where we have very tight constraints this does not happen and as a consequence the wing mass is very much increased.

A very important point with reference to the results obtained - optimization of OF - is that RQPMIN can give

much better optimization - reduction in aircraft empty
mass - when convergence is not achieved. This occurs with
the constraints being satisfied.

6.3.3.   Constraints

The final point performance constraints are shown in
Table 4 and all the constaints have been described in
Chapter 3.7.3.1.

The constraint driving the configuration is the one for
the thrust-to-weight ratio at landing. As a result we
have a very large engine and, due to the configuration, a
large RLS front duct system. Both add substantially to
the aircraft mass. Another significant constraint
deriving from the configuration is the in-line
positioning of the internal weapon bay and the engine.
Again this adds to the aircraft mass due to a longer
fuselage.

From the performance point of view, the important
constraints are those for the sustained turn rate, the
specific excess power and the maximum Mach number. The
second sustained turn rate constraint proved impossible
to achieve. The closest to the constraint value of 9.5
degrees per second at 9000 metres, Mach 0.9 and full
engine power that could be achieved, was around 4.

In general, these sets of constraints make a convergence
very difficult. It seems that RQPMIN needs some freedom
in order to converge. To do so the second sustained turn
rate constraint had to be put at 2 degrees per second.
Although the results given for the second sustained turn
rate were between 3 and 4 degrees per second, if these
values were considered as constraints instead of the
value of 2, convergence could not be achieved. The
problem of the tight constraints is reflected on the
aircraft empty mass optimization. The reduction in
aircraft empty mass is of the order of 1 % where in
Lovell's (Ref.43) example it is around 16 %.

It is rather evident that some of the performance
constraints contradict each other. Information on how
sustained turn rate, specific excess power and maximum
Mach number vary with altitude, Mach number and engine
power setting - the first sustained turn rate constraint

is at maximum dry power - should have been consulted, in order to locate the problem, but such information was unavailable.

The rest of the constraints either due to the configuration or the performance were, in most of the cases, all satisfied.

From the purely optimizational point of view, the most difficult constraints are the ECs and this is because the tolerance problem discussed earlier, is much more accute than in the ICs. The reason is that an equality is approached from both sides ; an inequality from one. A way to by-pass this difficulty might be to replace every EC with two ICs, thus allowing whatever tolerance is considered appropriate. It is a problem connected with RQPMIN operation. RQPMIN, in its attempts to find a feasible path to an optimization, cannot accommodate the specified constraints.

6.4.   Optimization Objective Function (OF)
        Development

When the OF was changed from the aircraft empty mass to the engine mass (Table 2 - Column 3), the obtained optimized aircraft mass was nearly the same (a 10 kg increase). A reduction in computing time was noticed, from 7700 to 5700 iterations, but that was not the purpose of the exercise.

Therefore, different initial conditions were tried and the maximum number of iterations was reached without a result (Table 2 - Column 4). The maximum number of iterations was raised to 16000 and a type A convergence was reached with worse results - aircraft mass increase by 37 kg (Table 2 - Column 5). Again, initial conditions were altered and smaller tolerances set and a "no further progress possible" message was given (Table 2 - Column 6). Finally, with another set of tolerances, convergence and a better result - aircraft mass decreased by around 80 kg - was achieved.

As this last result was rather disappointing the engine scale factor and the wing area were tried as OFs. The results remained essentially the same, better but to an insignificant degree (Table 2 - Columns 8 and 9). Since a wing mass increase was observed during all these trials,

next the wing mass was put as OF but the aircraft mass
increased (Table 2 - Column 10). The last attempt was
with fuel mass but again failed (Table 2 - Column 11).

Although the matter requires further investigation, it
was decided that most probably the aircraft empty mass or
the engine mass is the best choice for OF ; the engine
mass giving typically better results and reduced
computing time.

A noticeable feature of this investigation is the engine
scale factor variation. It never falls below the value of
one. This may be just a coincidence, but perhaps there is
a reason for this behaviour, a reason that could not be
identified.

COLUMN	1 CoA ASTOVL CONVERGED (APPEND.B)	2 CoA ASTOVL NOT CONVERGED	3 COX AND ROSKAM (REF.14)	4 YAK-141 (REF.2) [1]
TAKE-OFF MASS kg	18900	17630	14240	19000
LANDING MASS kg	15870	14380	11100	15700
S.L. THRUST kN				
CRUISE/LIFT ENGINE				
REHEAT	272	250	159	152
AT LANDING				122
DRY	195	176	88	88
DEDICATED LIFT ENG	-	-	54	78
MASS kg				
CRUISE/LIFT ENGINE	3500	3260	1620	?
DEDICATED LIFT ENG	-	-	220 (296) [2] (267) [3]	?
RLS FRONT DUCT AND NOZZLE	229 [4] (338) [5]	225 [4] (332) [5]	-	-

[1] ESTIMATED
[2] SCALED TO THE CoA ASTOVL (CONVERGED) LANDING MASS
[3] SCALED TO THE CoA ASTOVL (NOT CONVERGED) LANDING MASS
[4] FIRST ESTIMATION - RLS FRONT DUCT MASS 17 kg/m, FRONT NOZZLE MASS 50 kg
[5] SECOND ESTIMATION - RLS FRONT DUCT MASS 25 kg/m, FRONT NOZZLE MASS 75 kg

TABLE 3   ASTOVL COMBAT AIRCRAFT COMPARISON

	CONSTRAINT
0.6 M ACCELERATION FROM M=0.8 AT 9000 m, MAX POWER	$\leq$ 60 s
MAX MACH NO AT SEA LEVEL, AT MAX POWER	$\geq$ 1.1
MAX MACH NO AT 1000 m, AT MAX POWER	$\geq$ 1.6
SPECIFIC EXCESS POWER AT M=0.9, AT SEA LEVEL, AT MAX POWER	$\geq$ 300 m/s
SPECIFIC EXCESS POWER AT M=0.9, AT 9000 m, AT MAX POWER	$\geq$ 150 m/s
SUSTAINED TURN RATE AT M=0.9, AT SEA LEVEL, AT MAX DRY POWER	$\geq$ 12 deg/s
SUSTAINED TURN RATE AT M=0.9, AT 9000 m, AT MAX POWER	$\geq$ 9.5 deg/s
SUSTAINED TURN RATE AT M=1.4, AT 9000 m, AT MAX POWER	$\geq$ 6 deg/s
ATTAINED TURN RATE AT M=1.4, AT 9000 m, AT MAX POWER	$\geq$ 11 deg/s
RIDE QUALITY FACTOR AT 1000 m, AT MAX POWER	$\leq$ 5.0

TABLE 4   POINT PERFORMANCE CONSTRAINTS

7.   CONCLUSIONS

7.1.   Baseline Configuration

An ASTOVL Combat Aircraft configuration with a RLS and an internal weapon bay was evaluated based on RAE requirements.

The Baseline Configuration, evolved realisticly, represents an ASTOVL Combat Aircraft along the current trends for this type of aircraft.

The use of a RLS was a requirement but some questions about its suitability remain. A "cruise/lift plus lift" configuration with a dedicated lift engine might be a better solution.

7.2.   Design Synthesis

The Baseline Configuration was used to develop the Design Synthesis code VERTI, applicable to ASTOVL Combat Aircraft with a RLS and an internal weapon bay.

Code VERTI provides a fast computation of the aircraft geometry, mass, aerodynamics and performance.

It is modular in form and can be easily modified to incorporate different methods and techniques and to account for other configurations.

It is compatible with the RAE optimization code RQPMIN, but equally it can operate on its own, for preliminary design, technology evaluation and configuration selection studies.

Every effort has been made to strike a good balance between the various parts of the code in terms of the detail in the techniques used, but further consideration is needed.

7.3.   Optimization

The interfacing of the code VERTI with the RAE
optimization code RQPMIN, and the optimization of the
initial configuration, were successfully achieved.

The optimization code RQPMIN had considerable functional
problems for which further attention is required. RQPMIN
operates successfully only under certain conditions that
are not known.

The constraints specified were very tight and the second
sustained turn rate could not be satisfied.

The best Objective Function for the optimization was
found to be either the aircraft empty mass or the engine
mass.

8. RECOMMENDATIONS FOR FURTHER WORK

For the configuration it is highly recommended to evaluate a "cruise/lift plus lift" version, develop a design synthesis based on it, interface it with RQPMIN and compare its performnce with the present RLS configuration.

Another area of further configuration work is to examine, if for "RLS" and "cruise/lift plus lift" configurations that are otherwise identical, the RLS front duct and nozzle are heavier than the dedicated lift engine.

For the design synthesis a sensitivity study to balance in terms of detail the various parts of the code is proposed. Additionally, the iteration process involved should be re-examined to ensure better convergence.

The main recommendations for further work on the optimization concern code RQPMIN. For a start RQPMIN must be fully documentated. An investigation under what conditions is properly functioning should be undertaken. Furthermore, an adaption of RQPMIN to engineering purposes, in relation to convergence and constraint tolerances, could be very useful. As an intermediate step the replacement of the ECs with ICs could be tried.

Finally, in connection with the optimization of the specific configuration of this work, information should be found on some point performance parameters in order to evaluate appropriate constraints.

9. REFERENCES

1	ANONYMOUS	ESDU, Fluid Mechanics, Internal Flow, Volumes 1 and 2.
2	ANONYMOUS	Jane's Defence Weekly, 22 June 1991.
3	ANONYMOUS	USAF Stability and Control, McDonnell Douglas Corporation, 1975.
4	ANONYMOUS	V/STOL Propulsion Control Analysis, General Electric Co., NASA CR-165523, 1983.
5	BERG D.F., ELLIOT D.W. and SIMMONS J.R.	Comparison Study of Supersonic STOVL Propulsion Systems, AIAA Paper 88-2808, 1988.
6	BROWN D.M.	Supersonic STOVL Conceptual Design of a Fighter Attack Aircraft, AIAA Paper 89-2112, 1989.
7	BROWN S.H.	Study of Aerodynamic Technology For VSTOL Fighter/Attack Aircraft, Horizontal Attitude Concept, Final Report, Northtrop Corp., NASA CR-152130, 1978.
8	BUCKNELL R.L.	STOVL Engine/Airframe Integration, AIAA Paper 87-1711,1987.
9	BURNS B.R.A.	Advanced Aerodynamic Design For Future Combat Aircraft, ICAS Paper 1.1.2., 1982.
10	CHANT C.	Modern Air Weapons, IMP Publishing Services, 1980.
11	COEN P.G. and FOSS W.E.	Computer Sizing of Fighter Aircraft, Journal of Aircraft, Vol. 23, No. 5, 1986.

12 COLLINGBOURNE J.   Multivariate Optimization
                            Applied to the Initial Design
                            Of Transport Aircraft, RAE
                            Technical Report 84044, 1984.

13 COUSIN J. and   The BAe (Commercial Aircraft)
    METCALFE M.   Ltd Transport Aircraft Synthesis
                            and Optimization Program, AIAA
                            Paper 90-3295, 1990.

14 COX B. and   Preliminary Design of a
    ROSKAM J.   Supersonic Short Takeoff and
                            Vertical Landing (STOVL) Fighter
                            Aircraft, AIAA Paper 90-3231,
                            1990.

15 CURREY N.S.   Undercarriage Design Handbook,
                            Lockheed-Georgia, 1982.

16 DUSA D.J.,   Multi-Functional Nozzle for
    SPEIR D.W. and   Advanced Weapon Systems, SAE
    DUNBAR D.K.   Paper 831426, SP-555, October 1983.

17 ELLIOT D.W. and   Impact of Engine Technology on
    SIMMONS J.R.   Supersonic STOVL, AIAA Paper
                            87-1709, 1987.

18 FISHBACH L.H. and   A Remote Augmentor Lift System with
    FRANCISCUS L.C.   a Turbine Bypass Engine, NASA
                            TM-82932, 1982.

19 FLETCHER D. and   Supersonic Combat Aircraft Design,
    BURNS B.R.A.   Aeronautical Journal, December
                            1979.

20 FOWLER H.S.   The Design of Powerplant Ducting,
                            National Research Council of
                            Canada, Mechanical Engineering
                            Report 208, 1954.

21 FOZARD J.W.   Tactical Jet V/STOL - Its Future in
                            A CTOL World, SAE Paper 861637,
                            SP-680, October 1986.

22 HAGUE D.S. and   An Introduction to Multivariate
    GLATT C.R.   Search Techniques for Parameter
                            Optimization, NASA CR-73200, April
                            1968.

23 HARTLAND A.J.   Disperse Base Combat Aircraft,
                            Ph.D. Thesis, Cranfield Institute
                            of Technology, 1989.

24	HAFTKA R.T., KAO P.J., GROSSMAN B., POLEN D. and SOBIESZCZANSKI-SOBIESKI J.	Integrated Structural Aerodynamic Design Optimization, ICAS, 1.10 R, 1988.
25	HEINEMANN E., RAUSA R. and VAN EVERY K.	Aircraft Design, The Nautical & Aviation Publishing Co. of America Inc., 1985.
26	HITCH H.P.Y.	Computer Aided Aircraft Project Design, Aeronautical Journal, February 1977.
27	HOERNER S.F.	Fluid-Dynamic Drag, Published by the author, 1965.
28	HOERNER S.F.and BORST H.V.	Fluid-Dynamic Lift, Published by the author, 1975.
29	HOWE D. and FIELDING J.P.	Aerospace Vehicle Design, M.Sc. Course notes, CoA, Cranfield Institute of Technology, 1985.
30	HUENECKE K.	Modern Combat Aircraft Design, Airlife Publishing Ltd., 1987.
31	HUNTCHISON R.A., SUSSMAN M.B., MAINQUIST R. and PAULSON J.W.	STOL Wind Tunnel Test Results for A Tactical Supercruiser, AIAA Paper 83-1224, 1983.
32	KELLY J.R. and GARREN J.F.	Study of Optimum Values of Several Parameters Affecting Longitudinal Handling Qualities of VTOL Aircraft, NASA TN D-4624, July 1968.
33	KIDWELL G.H. and LAMPKIN B.A.	An Evaluation of Supersonic STOVL Technology, AIAA Paper 83-2493, 1987.
34	KIRKPATRICK D.L.I. and PECKHAM D.H.	Multivariate Analysis Applied to Aircraft Optimization - Some Effects of Research Advances on the Design of Future Subsonic Transport Aircraft, RAE Technical Memorandum AERO 1448, September 1972.

35 KIRKPATRICK D.L.I. and COLLINGBOURNE J.   Multivariate Analysis Applied to Aircraft Optimization - A Second Progress Report, RAE Technical Memorandum AERO 1553, November 1973.

36 KOHLMAN D.L.   Introduction to V/STOL Airplanes, Iowa State University Press, 1981.

37 LAVI R., HALL G.R. and STARK W.W.   Full Scale Ground Proximity Investigation of a VTOL Fighter Model Aircraft, NASA CR-1098, 1968.

38 LEE V.A.   Computerized Aircraft Synthesis, Journal of Aircraft, Vol. 4, No. 5, 1967.

39 LEVINE J. and INGLIS M.   US/UK Advanced Short Take-Off and Vertical Landing Program (ASTOVL), AIAA Paper 89-2039, 1989.

40 LEWIS W.J. and PALFREYMAN D.   Supersonic V/STOL ready for Technology Push, Aerospace America Vol. 22, October 1984.

41 LIND G.W. and TAMPLIN G.   V/STOL Technology Requirements for Future Fighter Aircraft, AIAA Paper 81-1360, 1981.

42 LOVELL D.A.   Some Experiences with Numerical Optimization in Aircraft Specification and Preliminary Design Studies, RAE Technical Memorandum AERO 1850, May 1980.

43 LOVELL D.A.   The Application of Multivariate Optimization to Combat Aircraft Design, RAE Technical Report 88003, January 1988.

44 LUMMUS J.R.   Aerodynamics Characteristics of two VSTOL Fighter Configurations, AIAA Paper 81-1292, 1981.

45 MANGOLD P.   Some Aerodynamic Aspects of the Design of Future Combat Aircraft, ICAS Paper 1.1.3., 1982.

46 MCLEMORE H.C. and SMITH C.C.   Hot Gas Ingestion Investigation of Large - Scale Jet VTOL Fighter Type Models, NASA TN D-4609, 1968.

47 MCNALLY D.J. and   Requirements for Future RALS/STOVL
    BROWN D.M.   Operating Concepts, SAE Paper
                             851840, October 1985.

48 MICHAUT C.,   Preliminary Design of Civil
    CAVALLI D.,   Transport Aircraft, AIAA Paper
    HUYNH H-T. and   89-2152, 1989.
    LE THUY H.

49 MOTHERSILL R.J.   A Twin-Engine Version of the
                             Combat Aircraft Multivariate
                             Optimization Program, RAE
                             Technical Memorandum AERO 1902,
                             November 1981.

50 NELMS W.P.   Studies of Aerodynamic Technology
                             For VSTOL Fighter/Attack Aircraft,
                             AIAA Paper 78-1511, 1978.

51 NELMS W.P.,   Experimental Aerodynamic
    DURSTON D.A. and   Characteristics of two V/STOL
    LUMMUS J.R.   Fighter/Attack Aircraft
                             Configurations at Mach Numbers
                             From 0.4 to 1.4, NASA TM-81234,
                             1981.

52 NELMS W.P. ,   Experimental Aerodynamic
    DURSTON D.A. and   Characteristics of two V/STOL
    LUMMUS J.R.   Fighter/Attack Aircraft
                             Configurations at Mach Numbers
                             From 1.6 to 2.0, NASA TM-81286,
                             1981.

53 NELSON R.L. and   Some Examples of the Application
    WELSH C.J.   Of the Transonic and Supersonic
                             Area Rules to the Prediction of
                             Wave Drag, NASA TN-D446, September
                             1960.

54 NIKOLAI L.M.   Fundamentals of Aircraft Design,
                             METS Inc., 1975.

55 O'LONE R.G.   STOVL Wind Tunnel Tests Demonstrate
                             Ejector Viability, Aviation Week
                             And Space Technology, January 8,
                             1990.

56 PATEL T.S. and   Optimum Selection of Main
    DIXIT C.S.   Parameters for the Reverse Design
                             Of a Supersonic Military Aircraft,
                             Canadian Aeronautics and Space
                             Journal, Vol. 26, No. 3, 1980.

57 PECKHAM D.H.   Multivariate Analysis Applied to
                           Aircraft Optimization - A First
                           Progress Report, RAE Technical
                           Memorandum AERO 1352, September
                           1971.

58 PRETTY R.T. (ED)   Jane's Weapon Systems 1984-1985,
                           Jane's Information Group, 1984.

59 RAYMER D.P.   The Impact of VTOL on the
                           Conceptual Design Process, AIAA
                           Paper 88-44798, 1988.

60 SAMMUELS J.J. and   A Parametric Approach to Hover
    HAHN A.S.   Balance Analysis of Two STOVL
                           Fighter Concepts, SAE Paper 861631,
                           SP-680, October 1986.

61 SCHRAGE D.P. and   VTOL Operational Considerations and
    MEYER S.A.   their Impact on Future Military
                           Design Requirements, AIAA Paper
                           86-2649, 1986.

62 SEDDON J. and   Intake Aerodynamics, Collings,
    GOLDSMITH E.L.   1985.

63 SCOTT M.L.   S80 Roll Control and Remote
                           Augmented Lift Systems, Cranfield
                           Institute of Technology M.Sc.
                           Thesis, 1981.

64 SERGHIDES V.C.   Design Synthesis for Canard-Delta
                           Combat Aircraft, Ph.D. Thesis,
                           Cranfield Institute of Technology,
                           1988.

65 SHERIDAN A.E.   The Application of Turbine Bypass
                           Engines to High Performance V/STOL
                           Aircraft, AIAA Paper 83-2512, 1983.

66 SHERIDAN A.E.   Study of Turbine Bypass Remote
                           Augmentator Lift System for V/STOL
                           Aircraft, AIAA Paper 85-3086, 1985.

67 SKROBANSKI J.J.   User Guide for RQPMIN, RAE
                           Technical Memorandum AERO 2059,
                           January 1986.

68 SKROBANSKI J.J.   Optimization subject to Non-Linear
                           Constraints, Ph.D. Thesis, London
                           University, 1986.

69 SLIWA S.M.   Use of Constrained Optimization
                        in the Conceptual Design of a
                        Medium-Range Subsonic Transport,
                        NASA TP 1762, 1980.

70 SMITH J. and   The RAE Combat Aircraft Multi-
    LEE C.   Variate Optimization, AIAA Paper
                        89-2080, 1989.

71 SMITH H.W. and   The Outside has to be bigger than
    BURNHAM R.   the Inside, Journal of Aircraft,
                        June 1981.

72 STINTON D.   The Anatomy of the Aeroplane,
                        Granada, 1980.

73 STOLL F. and   Large Scale Wind-Tunnel Tests of
    KOENING D.G.   A Sting -Supported V/STOL Fighter
                        Model at High Angles of Attack,
                        AIAA Paper No.81-2621, 1981.

74 SWEETMAN B.   From AV-8B to the ASTOVL,
                        Interavia Vol. 39, December 1984.

75 SWEETMAN B.   ASTOVL Requirements begin to take
                        Shape, Interavia Vol. 43, March
                        1988.

76 TAYLOR J. (ED)   Jane's All the World's Aircraft
                        1988-1989, Jane's Information
                        Group, 1988.

77 VANDERPLAATS G.N.   CONMIN A FORTRAN Program for
                        Constrained Function Optimization.
                        User's Manual, NASA TM X-62282,
                        1973.

78 WARD B.D. and   Advantages of Thrust Vectoring
    LEWIS W.J.   For STOVL, AIAA Paper 87-1708,
                        1987.

79 WILLIS W.S.   The Effects of Turbine Inlet
                        Temperature and Engine Complexity
                        On VCE/RALS Powered Supersonic
                        V/STOL Aircraft, AIAA Paper
                        80-1853, 1980.

80 WILLIS W.S.   Advanced Technology Engine Studies
                        / ATES / A Status Report, AIAA
                        Paper 81-1502, 1981.

81 WILLIS W.S.,   Conceptual Design, Evaluation and
    KONARSKI M. and   Research Identification for Remote
    SUTHERLAND M.V.   Augmented Propulsive Lift Systems
                            (RALS) with Ejectors for VTOL
                            Aircraft, NASA CR-167906, 1983.

82 WILSON S.B. and   CTOL, STOVL and VTOL Fighter
    ESKEY M.A.   Design Comparisons, AIAA Paper
                            85-0210, 1985.

→

APPENDIX A

ASTOVL COMBAT AIRCRAFT DESIGN SYNTHESIS CODE VERTI
DESCRIPTION

73

CONTENTS

1.   INTRODUCTION

This appendix is a simple guide for the ASTOVL Combat Aircraft Design Synthesis Code VERTI.

It provides the mathematical formulation for the Design Synthesis of the aircraft Baseline Configuration which forms the basis of the code VERTI.

In addition, all the reasoning and the methodology that leads to the development of the code is explained.

In general, the approach of Lovell (Ref.43) is followed, but in many cases considerable changes have been made and additions included.

The version of Code VERTI described here, is the fully interfaced RQPMIN subroutine (subroutine VERTI5).

The baseline configuration of the aircraft is shown in Fig.A1.

A simplified flowchart for code VERTI is shown in Fig.A15.

2.   MAIN SEGMENT OF THE CODE

2. 1.   INPUT OF DATA

The following five files provide the input data.

VERTI2.DAT contains the general design data.

AERO5.DAT, the aerodynamic data file, contains
the critical lift coefficient, the factor DK1 in the
lift-dependent drag estimation and the maximum lift
coefficient versus Mach numbers that cover the flight
envelope.

CITENG5.DAT, the engine performance file, contains the
nett and gross thrust, the fuel flow rate, the nozzle
exit area and the air flow rate of the engine for a
number of altitudes, Mach numbers and engine power
settings.

PERF5.DAT, contains all the initial sortie performance
data - leg distance, altitude, Mach number, normal load
factor, discarded mass (missiles, tanks), flap angle and
an estimate of the gross thrust.

POINTP5.DAT, the point performance data file, includes
altitude, Mach number, power setting and constraint
values for all point performance evaluations -
sustained turn rate, attained turn rate, specific excess
performance, maximum Mach number, acceleration through a
Mach number increment and ride quality factor..

These files are opened, their contents read and stored as
variables and then they are closed not to be read again.

2. 2.   SUBROUTINE CALLS

Initially the fixed items subroutines are called to
calculate the fixed items geometry (Fig.A15). Next is
subroutine STATION to define the various fuselage
stations and subroutines and FAIRCUR1-2 to define the
nett cross-sectional area of the fuselage. Then the
subroutines for the flying surfaces (WING, EMPENN)
including subroutine FLATCROSS if area-rule is required.

Having all the basic geometrical characteristics of the
aircraft the station sections subroutines estimate the
dimensions of the different aircraft sections along
the fuselage (FUSSTNA-I). The cross-sectional area and
perimeter subroutines FUSCRA and PERIM conclude the

calculations for the aircraft geometry and then fuselage volume and surface area are estimated.

Having the aircraft geometry, mass and centre of gravity are then estimated - subroutines MASSEFULT, MASSEFUS, MASSEFLS, MASSEVAR and CEGRAV.

With the geometry calculated, the aerodynamic characteristics can be estimated - subroutines DRAG and LIFT.

Finally, with mass and aerodynamic characteristics available and engine performance read from input file CITENG5.DAT the sortie and point performance of the aircraft are evaluated - subroutines SORTIE, SSTR, SATR, SSEP, SMML, SACA, RIDE and TAKEOFF.

The results include detailed aircraft geometry and mass, the sortie performance and the point performance in conjuction with the constraints (Appendix B - Figs B6 and B7).

3.   SIZING OF FIXED ITEMS

The mathematical formulation of the design synthesis
starts with the sizing of the fixed items of the
aircraft.

Fixed items of the aircraft are its basic parts that are
given in standard form.

Using design data and taking into consideration the
specifications that have been provided, the dimensions
and mass of the fixed items are estimated and
subsequently incorporated in the mathematical formulation
of the whole aircraft.

The fixed items include the radome, the cockpit, the
undercarriage, the gross wing, the engine, the intake
diffuser and the remote lift system.

3.1.   RADOME (SUBROUTINE RADOME)

The nose diameter is defined from a specified radar dish
diameter,DAR, and an increment, EDAR, to allow for
clearance. A linear variation of cross-sectional area
with axial distance, gradient GOFI is assumed.

The cross-sectional area of the fuselage at the radar
dish position (Fig.A2, station R), OFI, is :

$$OFI= \frac{\pi}{4} (DAR + EDAR)^2 \qquad (A1)$$

and the radome length is :

$$XFR = \frac{OFI}{GOFI} \qquad (A2)$$

The volume and the wetted area of the radome, VFR and
WFR, assuming a parabolic shape are :

$$VFR = 0.5\ GOFI\ XFR^2 \qquad (A3)$$

$$WFR = \frac{4}{3} XFR \; (\pi \; OFI)^{\frac{1}{2}} \left(1 + \frac{GOFI}{4 \; \pi \; XFR} \right) - \frac{GOFI^2}{6 \; \pi}$$

(A4)

Behind the radar dish a fuselage length LAR is allowed for related avionics of mass MAR.

Following these there is a second bay of length LAX1 containing further avionics of mass MAX1.

The front bulkhead of the cockpit is situated at the rear of this bay. Its distance from the aircraft nose XA is :

$$XA = XFR + LAR + LAX1 \qquad (A5)$$

3.2.   COCKPIT (SUBROUTINE COCKPG)

The arrangement of the cockpit is shown in Fig.A4 and is based on military specifications. The dimensions HC1, HC2, HC3, HC4, HCSEAT, LCFOOT, QCSEAT, QCEYE and EHC5 are specified input design data appropriate for the type of cockpit selected. From these the following are derived :

$$QCFOOT = \sin^{-1} \left(\frac{HC3 \; \sin \; QCSEAT + HCSEAT \; \cos \; QCSEAT}{HC2} \right)$$

(A6)

$$HCEYE = HC1 \; \cos \; QCSEAT + HC3 \; \sin \; QCSEAT +$$

$$HCSEAT \; \cos \; QCSEAT \qquad (A7)$$

$$LCEYE = HC1 \; \sin \; QCSEAT + HC2 \; \cos \; QCFOOT + LCFOOT$$

(A8)

$$LCFL = HC2 \; \cos \; QCFOOT + LCFOOT + HC3 \; \cos \; QCSEAT -$$

$$HCSEAT \; \sin \; QCSEAT + \frac{EHC5}{\cos \; QCSEAT} \qquad (A9)$$

$$HC5 = HCEYE - LCEYE \; \tan \; QCEYE \qquad (A10)$$

Hence the distance of the eye position from the nose of the aircraft is :

$$XB = XA + LCEYE \qquad (A11)$$

The mass of the cockpit structure is included in the fuselage mass evaluated later, and in addition to this a mass, MCI, is allowed for the instruments oxygen system, pyrotechnics, furnishings and armour and a mass, MCP, for the crew.

3.3. UNDERCARRIAGE (SUBROUTINE UNDCB)

The geometry of the main and nose undercarriages is derived from a number of correlations with a landing reference mass, MTLR. This is obtained by removing the load of external stores, ammunition and expendable weapons (bombs,missiles) from the take-off mass, MTT, adding a reference load, MTPR, to form a take-off reference mass, MTTR, and then removing a fixed proportion of the internal fuel. The reference mass at take-off is

$$MTTR = MTT - MXT - MXTF - MGA - MB - MXP - MSWBI$$
$$+ MTPR \qquad (A12)$$

and the reference landing mass is

$$MTLR + MTTR - (1 - RMTLIF) \; MTGFI \qquad (A13)$$

where RMTLIF is the proportion of the remaining fuel.

To find an expression for the mass of the nose and main undercarriages and their associated hydraulics, these were correlated with the landing reference mass to obtain the linear relations

$$MUM = FMUMK \; MTLR + MUMK \qquad (A14)$$

$$MUN = FMUNK \; MTLR + MUNK \qquad (A15)$$

$$MUH = FMUHK \; MTLR + MUHK \qquad (A16)$$

By examining the variation of the sum of the total undercarriage lengths with the reference landing mass the following correlation was found

$$LULG = \left(\frac{MTLR}{LULG1K} \right)^{LULG2K} \tag{A17}$$

The ratio of the length of the nose leg to the length of one main undercarriage leg, RLUNM, enables the length of the nose length to be found

$$LUNS = \frac{LULG \ RLUNM}{(\ RLUNM \ + \ 2)} \tag{A18}$$

and the length of each main leg

$$LUMN = 0.5 \ (LULG \ - \ LUNS) \tag{A19}$$

For the accuracy required in this synthesis, linear correlations of wheel dimensions with the landing reference mass are considered adequate, assuming a fixed requirement for ground hardness. Hence the main wheel diameter is given by

$$DUMW = FDUMWK \ MTLR \ + \ DUMWK \tag{A20}$$

and the width

$$BUMW = FBUMWK \ MTLR \ + \ BUMWK \tag{A21}$$

Nose wheel diameter is given by

$$DUNW = FDUNWK \ MTLR \ + \ DUNWK \tag{A22}$$

and the nose wheel width, BUNW, is asumed constant.

The volume required in the fuselage for the retracted undercarriage is considered in two parts, one related to the wheels and the other to the legs. The volume needed for the wheel of each main undercarriage is given by

$$VUMWB = DUMW^2 \ BUMW \ FDUMW \ FBUMW \qquad (A23)$$

where FDUMW and FBUMW are clearance factors. The volume needed for the wheel of the nose undercarriage is

$$VUNWB = DUNW^2 \ BUNW \ FDUNW \ FBUNW \qquad (A24)$$

The volume needed for the leg of each main undercarriage is provided by a correlation of leg length and landing reference mass, valid for a number of combat aircraft. The relation is

$$VUMLB = FVUMLK \ LUMN \ MTLR + VUMLBK \qquad (A25)$$

where FVUMLK and VUMLBK are constants. The volume needed for the nose leg is estimated using the above correlation with the volume factored by the ratio of the masses of nose and main undercarriages

$$VUNLB = \frac{2 \ MUN}{MUM} \ (FVUMLK \ LUNS \ MTLR + VUMLBK) \qquad (A26)$$

The length of the undercarriage bays is given by

$$LUMB = 0.5 \ DUMW + LUMN \qquad (A27)$$

$$LUNB = 0.5 \ DUNW + LUNS \qquad (A28)$$

The cross-sectional area of the wheel bays

$$OUMWB = DUMW \ BUMW \ FDUMW \ FBUMW \qquad (A29)$$

$$OUNWB = DUNW \ BUNW \ FDUNW \ FBUNW \qquad (A30)$$

and the cross-sectional area of the leg bays

$$OUMLB = \frac{VUMLB}{(LUMN - 0.5 \ DUMW)} \qquad (A31)$$

$$OUNLB = \frac{VUNLB}{(LUNS - 0.5\ DUNW)} \qquad (A32)$$

3.4.   ENGINE SIZING (SUBROUTINE ENGSIZ)

The engine geometry is scaled from a datum military turbofan engine, whose simplified geometry is shown in Fig.A5, using a scaling factor, RTP. The following scaling relations are used :

For the length we have

$$LP12 = LP12R\ RTP^{FLP1K} \qquad (A33)$$

$$LP23 = LP23R\ RTP^{FLP2K} \qquad (A34)$$

$$LP34 = LP34R\ RTP^{FLP2K} \qquad (A35)$$

$$LP45 = LP45R\ RTP^{FLP2K} \qquad (A36)$$

$$LP56 = LP56R\ RTP^{FLP3K} \qquad (A37)$$

$$LP24 = LP23 + LP34 \qquad (A38)$$

and the overall length is   (A39)

$$LPG = LP12 + LP23 + LP34 + LP45 + LP56 \qquad (A40)$$

For the diameter

$$DP1 = DP1R\ RTP^{\frac{1}{2}} \qquad (A41)$$

$$DP2 = DP2R\ RTP^{\frac{1}{2}} \qquad (A42)$$

$$DP3 = DP3R\ RTP^{\frac{1}{2}} \qquad (A43)$$

$$DP4 = DP4R\ RTP^{\frac{1}{2}} \qquad (A44)$$

$$DP5 = DP5R\ RTP^{\frac{1}{2}} \qquad (A45)$$

$$DP6 = DP6R\ RTP^{\frac{1}{2}} \qquad (A46)$$

The geometry of the engine bay is defined by adding vertical and horizontal clearances to the scaled values of the engine diametre. The clearances are defined as the differences in diameter at the particular position between the engine and the fuselage. The clearances are accepted to be linear functions of the engine diameter, but are limited to a range between specified minimum and maximum values. Therefore we have

$$EHP1 = FHP1K \; DP1 \qquad \text{for} \quad EHP1S \leq EHP1 \leq EHP1H \qquad (A47)$$

$$EBP1 = \frac{FBP1K \; DP1}{NENG} \qquad \text{for} \quad EBP1S \leq EBP1 \leq EBP1H \qquad (A48)$$

$$EHP2 = FHP2K \; DP2 \qquad \text{for} \quad EHP2S \leq EHP2 \leq EHP2H \qquad (A49)$$

$$EBP2 = \frac{FBP2K \; DP2}{NENG} \qquad \text{for} \quad EBP2S \leq EBP2 \leq EBP2H \qquad (A50)$$

$$EHP3 = FHP3K \; DP3 \qquad \text{for} \quad EHP3S \leq EHP3 \leq EHP3H \qquad (A51)$$

$$EBP3 = \frac{FBP3K \; DP3}{NENG} \qquad \text{for} \quad EBP3S \leq EBP3 \leq EBP3H \qquad (A52)$$

$$EHP4 = FHP4K \; DP4 \qquad \text{for} \quad EHP4S \leq EHP4 \leq EHP4H \qquad (A53)$$

$$EBP4 = \frac{FBP4K \; DP4}{NENG} \qquad \text{for} \quad EBP4S \leq EBP4 \leq EBP4H \qquad (A54)$$

$$EHP5 = FHP5K \; DP5 \qquad \text{for} \quad EHP5S \leq EHP5 \leq EHP5H \qquad (A55)$$

$$EBP5 = \frac{FBP5K \; DP5}{NENG} \qquad \text{for} \quad EBP5S \leq EBP5 \leq EBP5H \qquad (A56)$$

$$EHP6 = FHP6K \; DP6 \qquad \text{for} \quad EHP6S \leq EHP6 \leq EHP6H \qquad (A57)$$

$$EBP6 = \frac{FBP6K \; DP6}{NENG} \quad \text{for} \quad EBP6S \leq EBP6 \leq EBP6H \quad (A58)$$

The clearances at engine station 6, the nozzle exit, are usually null.

For the purpose of this synthesis the cross-sections of the engine bay are assumed to be ellipses. They are given by

$$OP1B = NENG \; \frac{\pi}{4} \; (DP1 + EHP1) \; (DP1 + EBP1) \quad (A59)$$

$$OP2B = NENG \; \frac{\pi}{4} \; (DP2 + EHP2) \; (DP2 + EBP2) \quad (A60)$$

$$OP3B = NENG \; \frac{\pi}{4} \; (DP3 + EHP3) \; (DP3 + EBP3) \quad (A61)$$

$$OP4B = NENG \; \frac{\pi}{4} \; (DP4 + EHP4) \; (DP4 + EBP4) \quad (A62)$$

$$OP5B = NENG \; \frac{\pi}{4} \; (DP5 + EHP5) \; (DP5 + EBP5) \quad (A63)$$

and for the nozzle exit area

$$OPN = NENG \; \frac{\pi}{4} \; DP6^2 \quad (A64)$$

The volume of the engine bay is estimated by assuming a linear variation of bay height and width between the engine stations. Therefore we have

$$VP12B = \frac{LP12}{3} \{ OP1B + OP2B + NENG - \frac{\pi}{8} [(DP1 + EHP1)$$

$$(DP2 + EBP2) + (DP2 + EHP2) (DP1 + EBP1)] \}$$

$$\text{(A65)}$$

$$VP23B = \frac{LP23}{3} \{ OP2B + OP3B + NENG - \frac{\pi}{8} [(DP2 + EHP2)$$

$$(DP3 + EBP3) + (DP3 + EHP3) (DP2 + EBP2)] \}$$

$$\text{(A66)}$$

$$VP34B = \frac{LP34}{3} \{ OP3B + OP4B + NENG - \frac{\pi}{8} [(DP3 + EHP3)$$

$$(DP4 + EBP4) + (DP4 + EHP4) (DP3 + EBP3)] \}$$

$$\text{(A67)}$$

$$VP45B = \frac{LP45}{3} \{ OP4B + OP5B + NENG - \frac{\pi}{8} [(DP4 + EHP4)$$

$$(DP5 + EBP5) + (DP5 + EHP5) (DP4 + EBP4)] \}$$

$$\text{(A68)}$$

$$VP56B = \frac{LP56}{3} \{ OP5B + OP6B + NENG - \frac{\pi}{8} [(DP5 + EHP5)$$

$$(DP6 + EBP6) + (DP6 + EHP6) (DP5 + EBP5)] \}$$

$$\text{(A69)}$$

$$VPB = VP12B + VP23B + VP34B + VP45B + VP56B \qquad \text{(A70)}$$

The mass of the engine is considered in four parts. For the gas generator

$$MPB = NENG (FMPBK\ RTP + 1 - FMPBK) \qquad \text{(A71)}$$

For the RLS (Remote Lift System) section

$$MPL = NENG \ MPLR \ RTP^{FMPRK} \tag{A72}$$

For the reheat system

$$MPR = NENG \ MPRR \ RTP^{FMPRK} \tag{A73}$$

For the nozzle

$$MPN = NENG \ MPNR \ RTP^{FMPRK} \tag{A74}$$

For the thrust reverser

$$MPT = NENG \ MPTR \ RTP \tag{A75}$$

For the engine installation mass

$$MPI = FMPIK \ (MPB + MPL + MPR + MPN + MPT) \tag{A76}$$

Thus the total mass for the engine is

$$MPG = MPB + MPL + MPR + MPN + MPT + MPI \tag{A77}$$

The fuselage stations corresponding to the engine bay are defined as follows :

$$XE = XFN - LPG \tag{A78}$$

$$XF = XE + LP12 \tag{A79}$$

$$XG = XF + LP23 \tag{A80}$$

$$XH = XG + LP34 \tag{A81}$$

$$XJ = XH + LP45 \tag{A82}$$

$$XI = XJ + LP56 \tag{A83}$$

where XFN is the fuselage length.

3.5.   INTAKE DIFFUSER (SUBROUTINE INTAKD)

The geometry of the intake diffuser is shown in Fig.A6.
The intake inlet is situated forward of the pilot due to
the RLS nozzle. The distance of the intake inlet, XII,
from the aircraft nose is

$$XII = XA + FLII \tag{A84}$$

where FLII is its distance from the cockpit front
bulkhead and for the distance of the exit

$$XIE = XFN - LPG \tag{A85}$$

Thus the diffuser has a length, LIDG, that is

$$LIDG = XIE - XII \tag{A86}$$

The exit area of the diffuser is the same as the engine
inlet area

$$OIE = NENG \; \frac{\pi}{4} \; DP1^2 \tag{A87}$$

and the diffuser is assumed to have a a fixed area ratio
ROIEI

$$ROIEI = \frac{OIE}{OII} \tag{A88}$$

and an aspect ratio, AII, for each intake is given by

$$AII = \frac{HII}{BII} \tag{A89}$$

where HII and BII are the dimensions of the rectangular
intake. Hence

$$HII \ BII = \frac{OII}{2} \tag{A90}$$

$$HII = \left(\frac{AII \ OII}{2} \right)^{\frac{1}{2}} \tag{A91}$$

$$HII = \left(\frac{AII \ OIE}{2 \ ROIEI} \right)^{\frac{1}{2}} \tag{A92}$$

$$BII = \left(\frac{OII}{2 \ HII \ ROIEI} \right) \tag{A93}$$

From this inlet area an equivalent inlet width, DII, is defined

$$DII = \left(\frac{OIE}{ROIEI \ NENG \ \pi} \right)^{\frac{1}{2}} \tag{A94}$$

In order to ensure a satisfactory entry flow at the engine compressor a minimum length, LIDS, for each diffuser is defined in terms of DII

$$LIDS = FLIDVK \ DII \tag{A95}$$

A linear variation of diffuser cross sectional area with axial distance is assumed so that the volume of the diffuser is given by

$$VIDG = \frac{LIDG}{2} \ (OII + OIE) \tag{A96}$$

3.6.   BOUNDARY LAYER DIVERTER (SUBROUTINE BLDIV)

Between the intakes and the fuselage sides boundary layer diverters are situated of width BVI on each side (Fig.A6). Their intake plane is the same as the intake diffuser plane hence

$$XVI = XII \qquad\qquad (A97)$$

Their width is considered to be a linear function of the distance from the nose

$$BVI = FBVIK \ XVI \qquad\qquad (A98)$$

The total diverter cross-sectional area is

$$OVI = 2 \ BVI \ HII \qquad\qquad (A99)$$

and the length

$$LVG = FLVK \ HII \qquad\qquad (A100)$$

The mean position of the exit, XVE, wich extends over a length of 0.5 LVG is given by

$$XVE = XVI + LVG \qquad\qquad (A101)$$

3.7.   INTERNAL WEAPON BAY (SUBROUTINE IWEPB)

The internal weapon bay is located in the lower part of the fuselage, after the nose undercarriage bay and the RLS front nozzle as shown in Fig.A1. Its geometry is derived from the weapons specifications and is relatively flexible within the limits of the usual combinations of missiles - or bombs - for a combat fighter. The general layout is for one or two rows one above the other as indicated in Fig.A7. The missiles are launched by means of ejectors. The usual requirements are for four medium range and two short range air-to-air missiles.

For the length we have

$$LSWBI = LMRM + LSWBIK \qquad\qquad (A102)$$

where LMRM is the length of the longer missile (usually the medium range) and LSWBIK the length clearance.

For the width

$$BSWBI = 2 (DMRM + DSRM) + BSWBIK \qquad (A103)$$

where DMRM and DSRM are the diameters of the medium and short range missiles respectively and BSWBIK is the width clearance.

For the height if we have one row (in our design synthesis taking into consideration the general configuration of the aircraft more than two medium range missiles require two rows)

$$HSWBI = DMRM + HSWBIK \qquad (A104)$$

and if we have two rows

$$HSWBI = 2 DMRM + HSWBIK \qquad (A105)$$

where HSWBIK is the height clearance.

The cross-sectional area, volume and mass are given by

$$OSWBI = BSWBI (HSWBI + EHSWBI) \qquad (A106)$$

$$VSWBI = OSWBI \; LSWBI \qquad (A107)$$

$$MSWBI = (NMRM \; MMRM) + (NSRM \; MSRM) \qquad (A108)$$

where EHSWBI is the height of the top part of the bay occupied by the ejector mechanism, NMRM and NSRM are the numbers of the medium and short range missiles and MMRM and MSRM the mass of each respectively.

3.8.   INTERNAL GUN BAY (SUBROUTINE IGUNB)

The internal gun bay is situated in the lower part of the fuselage, under the cockpit, as shown in Fig.A1, and its geometry is derived from the gun specifications. The bay is considered to be made of three parts the gun mechanism, the gun barrel and the ammunition container.

For the gun mechanism dimensions length, width and height we have

$$LGMBI = LGM + LGMK \qquad (A109)$$

$$BGMBI = BGM + BGMK \qquad (A110)$$

$$HGMBI = HGM + HGMK \qquad (A111)$$

where LGM, BGM and HGM are the dimensions of the gun mechanism and LGMK, BGMK and HGMK the clearances required.

The cross-sectional area, the volume and the mass are given by

$$OGMBI = BGMBI \ HGMBI \qquad (A112)$$

$$VGMBI = LGMBI \ OGMBI \qquad (A113)$$

$$MGMBI = MGM \ FMGM \qquad (A114)$$

where MGM is the gun mechanism mass and FMGM is a mass installation factor.

For the gun barrel dimensions, cross-sectional area, volume and mass we have

$$LGBBI = LGB + LGBK \qquad (A115)$$

$$OGBBI = \frac{\pi}{4} \ (DGB + DGBK)^2 \qquad (A116)$$

$$VGBBI = OGBBI \ LGBBI \qquad (A117)$$

$$MGBBI = MGB + FMGB \qquad (A118)$$

where LGB is the barrel length, LGBK is the length clearance, DGB is the barrel external diameter and DGBK the associated clearance, MGB the barrel mass and MGBK an installation factor.

For the ammunition container dimensions a rectangular or nearly rectangular shape, depending on the number of

rounds specified, is defined. The dimensions of the container are

$$LGABI = LGA + LGAK \tag{A119}$$

$$BGABI = BGAK \ (DGA + DGAK) \tag{A120}$$

$$HGABI = HGAK \ (DGA + DGAK) \tag{A121}$$

where LGA is the round length, LGAK is the length clearance, DGA is the round maximun external diameter - not the calibre - , DGAK is the diameter clearance, BGAK is the the number of columns of rounds and HGAK is the number of rows of rounds as they are packed in the container.

For the cross-sectional area, volume and mass of the ammunition

$$OGABI = BGABI \ HGABI \tag{A122}$$

$$VGABI = OGABI \ LGABI \tag{A123}$$

$$MGABI = NGAK \ MGA \ FMGA \tag{A124}$$

where NGAK is the total number of rounds, MGA is the mass of one round and FMGA is a factor for installation and for the actual container mass.

3.9.   RLS (REMOTE LIFT SYSTEM) (SUBROUTINE RLS)

The RLS includes two side ducts located after the engine turbine exit, which form part of the engine, and a system of three front ducts having an intake after the turbine exit and leading to and combining to a front nozzle. The nozzle is situated in the undersurface of the fuselage side-by-side or behind the nose undercarriage bay (Fig.A1). The cross-sectional shapes of the RLS three front ducts form a semi-circle (Fig.A7). The RLS configuration is considered in very simple terms in order to have some dimension and mass estimates.

For the calculation of the internal diameter, DRDI, of the RLS system of front ducts the engine nozzle exit area is used, as it is assumed that the RLS system of ducts has half the cross-sectional area of the nozzle exit area. Relating the circular engine exhaust area to the cross-sectional area of the three RLS ducts (Fig.A7), the

internal diameter of the semi-sircular RLS system of ducts is given by

$$DRDI = 2 \left(\frac{4}{3 \pi} OPN \right)^{1/2} \tag{A125}$$

and specifying a insulation thickness WIRD we have for the external diameter DRDE

$$DRDE = DRDI + (2 \ WIRD) \tag{A126}$$

For the length of the RLS system of ducts since the exhaust nozzle cannot be located further after due to the internal weapon bay or much further in front for lack of space, the following rough estimate, derived from Fig.A1, is provided

$$LRDG = XFN - (LP34 + LP45 + LP56) - XD + HFD \tag{A127}$$

Therefore for the external cross-sectional are and the external volume of the RLS system of ducts we have

$$ORDE = \frac{\pi}{8} \ DRDE^2 \tag{A128}$$

$$VRDE = ORDE \ LRDG \tag{A129}$$

The mass is estimated in two parts, from engine to the turning point and from there to the exhaust nozzle

$$MRLD1 = (LRDG - HFD) \ RMLRD \tag{A130}$$

$$MRLD2 = HFD \ RMLRD \tag{A131}$$

where RMLRD is a design factor of mass per unit length. To this a mass MRLD3 for the nozzle is added. Thus the total mass MRLD is

$$MRLD = MRLD1 + MRLD2 + MRLD3 \tag{A132}$$

In this module the fuselage station D is defined

$$XD = XFN - LPG - (0.15 \; LIDG) - LSWBI \qquad (A133)$$

the 0.15 LIDG term being the distance needed for the intake diffusers to turn and merge between the internal weapon bay and the engine face.

4.   DEFINITION OF FUSELAGE STATIONS (SUBROUTINE
      STATION)

This module uses the definitions of the specified main
fuselage stations XA, XB, XC, XD, XE, XF, XG, XH, XJ and
XI and the specified number of subdivisions between main
fuselage stations to calculate the positions of all
fuselage stations (Fig.A2)

For each segment between main fuselage stations a
different number of sub-stations is specified according
to the need of stations for calculation purposes in that
particular segment.

5.1.   LONGITUDINAL DISTRIBUTION OF NETT CROSS-
        SECTIONAL AREA - PART I (SUBROUTINE FAIRCUR1)

The fixed items described above are fitted into the
aircraft fuselage. Consequently the fuselage must be able
to contain all these items and in addition to have an
acceptable aerodynamic shape.

To achieve both these ends a fairing curve is used to
define the longitudinal cross-sectional area of the
fuselage, or of the whole aircraft if area rule is to be
applied. In the latter case the contributions of the
wing, tailplane and fin to the cross-sectional area at a
given station are subtracted from the cross-sectional
area defined by the fairing curve to determine the
fuselage cross-sectional area distribution. It must be
emphasized that the cross-sectional area in question is
the nett cross-sectional area not the actual cross-
sectional area which is dealt in subroutine FUSCRA.
Therefore, any reference to fairing curve cross-sectional
area implies nett cross-sectional area.

As shown in Fig.A8 six independent variables and a number
of fixed item variables define the fairing curve. The six
independent variables are given below.

XFN   is the overall fuselage length from nose to
         nozzle exit.
RLTMFN   is the ratio of the length of the forward
         fairing to the ovarall fuselage length minus the
         length of the radome.
RLTFFN   is the ratio of the length from the end of the
         radome to the point at which the cross-sectional
         area is half of its maximum value.
RLTCFN   is the ratio of the length of the centre -
         constant cross-sectional area - section to the

length of the fuselage after of the forward fairing.

RLTAFN   is the ratio of the length from the end of the centre section to the point at which the cross-sectional area is half its maximum value, to the length of the after fairing.

FOT6N   is the increment in cross-sectional area, at the nozzle exit, above the datum value.

From the above the following are derived as indicated in Fig.A8

$$X1 = XFR \qquad\qquad (A134)$$

$$X3 = XFR + RLTMFN \ (XFN - XFR) \qquad (A135)$$

$$X2 = XFR + RLTFFN \ (X3 - XFR) \qquad (A136)$$

$$X4 = X3 + RLTCFN \ (XFN - X3) \qquad (A137)$$

$$X5 = X4 + RLTAFN \ (XFN - X4) \qquad (A138)$$

$$X6 = XFN \qquad\qquad (A139)$$

The next step in the definition of the fairing curve is the assumption of a cubic variation of (nett) cross-sectional area OTXN with axial distance (length), X. For the forward fairing we have

$$OTXN = OTF1K + OTF2K \ (X3 - X) + OTF3K \ (X3 - X)^2 +$$

$$OTF4K \ (X3 - X)^3 \qquad (A140)$$

with the following boundary conditions, as shown in Fig.A8

$$\text{at } X = X1 \ : \ OTXN = OF1, \quad \frac{d \ (OTXN)}{d(X3 - X)} = - \ GOG1 \qquad (A141)$$

$$\text{at } X = X2 \ : \ OTXN = \frac{OTM}{2} \qquad\qquad (A142)$$

$$\text{at } X = X3 \ : \ OTXN = OTM, \quad \frac{d \ (OTXN)}{d(X3 - X)} = 0 \qquad (A143)$$

As X1, X2, X3, OF1 and GOF1 are known we have five
conditions to determine the four constants OTF1K, OTF2K,
OTF3K and OTF4K and the maximum cross-sectional area OTM.

What can be found is

$$
OTF4K = \frac{- \{ 2\ OF1\ (X3 - X1) + GOF1\ [\ (X3 - X1)^2 - 2}{(X3 - X1)\ [\ (X3 - X1) - 2\ (X3 - X2)\ ]}
$$

$$
\frac{(X3 - X2)^2\ ]\ \}}{\{\ (X3 - X2)\ [\ (X3 - X1) - 2\ (X3 - X2)\ ]}
$$

$$
+ (X3 - X1)\ [\ (X3 - X1) + (X3 - X2)\ ]\ \}
$$

(A144)

$$
OTF3K = -1.5\ (X3 - X1)\ OTF4K - \frac{GOF1}{2\ (X3 - X1)} \tag{A145}
$$

$$
OTF2K = 0 \tag{A146}
$$

$$
OTF1K = -2\ (X3 - X2)^2\ [OTF3K + OTF4K\ (X3 - X2)
$$

(A147)

and hence for X = X3

$$
OTM = OTF1K \tag{A148}
$$

The use of the cubic limits the allowable range of values
for RLTFFN to 0 < RLTFFN < 0.5 in order for OTF4K to be
finite.

For the after fairing curve a similar cubic variation of
cross-sectional area is assumed

$$
OTXN = OTA1K + OTA2K\ (X - X4) + OTA3K\ (X - X4)^2 +
$$

$$
OTA4K\ (X - X4)^3 \tag{A149}
$$

with the conditions

$$\text{at } X = X4 \; : \; OTXN = OTM, \quad \frac{d \; (OTXN)}{dX} = 0 \qquad (A150)$$

$$\text{at } X = X5 \; : \; OTXN = \frac{OTM}{2} \qquad (A151)$$

$$\text{at } X = X6 \; : \; OTXN = FOT6N \qquad (A152)$$

As X4, X5 and X6 are known and OTM has been determined from the forward fairing we have four conditions to find the four coefficients. It can be found that

$$OTA4K = \frac{1}{(X6 - X5)} \; [\; \frac{(FOT6N - OTM)}{(X6 - X4)^2} + \frac{OTM}{2 \; (X5 - X4)^2} \;]$$

$$(A153)$$

$$OTA3K = - \; \frac{OTM}{2 \; (X5 - X4)^2} - OTA4K \; (X5 - X4) \qquad (A154)$$

$$OTA2K = 0 \qquad (A155)$$

$$OTA1K = OTM \qquad (A156)$$

From this cubic we have the restriction for RLTAFN to 0.5 < RLTAFN < 1 in order to keep OTXN above OTM.

5.2. LONGITUDINAL DISTRIBUTION OF NETT CROSS-SECTIONAL AREA - PART II (SUBROUTINE FAIRCUR2)

In this module all the coefficients found in the previous module are replaced in the forward and after fairing cubic and then the nett cross-sectional area is calculated for the stations that have been specified - module STATION.

In addition, the maximum nett cross-sectional area and maximum afterbody nett cross-sectional area, and the stations at which are found, are evaluated.

6.   FLYING SURFACES

6.1.   WING (SUBROUTINE WING)

Following the wing planform shown in Fig.A9, we have

$$BW = (AW \; SW)^{\frac{1}{2}} \tag{A157}$$

where BW is the gross span, AW is the gross wing aspect ratio and SW is the gross wing surface area.

$$CWCC = \frac{2 \; SW}{BW \; (1 + UW)} \tag{A158}$$

where CWCC is the centre-line chord of the gross wing and UW is the taper ratio of the gross wing

$$CWMG = 0.5 \; CWCC \; (1 + UW) \tag{A159}$$

$$CWMA = \frac{2}{3} \; CWCC \; [\; UW + \frac{1}{(1 + UW)} \;] \tag{A160}$$

$$CWCT = UW \; CWCC \tag{A161}$$

where CWMG is the geometric mean chord, CWMA is the aerodynamic mean chord and CWCT is the tip chord

$$QWL = \tan^{-1} [\; \tan (QW4) + \frac{CWCC}{2 \; BW} \; (1 - UW) \;] \tag{A162}$$

$$QW2 = \tan^{-1} \left[\tan(QW4) - \frac{CWCC}{2\ BW} (1 - UW) \right] \qquad (A163)$$

where QW4 is the quarter chord sweep, QW2 is the mid-chord sweep and QWL is the leading edge sweep

$$BWBB = BFE \qquad (A164)$$

$$BWN = BW - BWBB \qquad (A165)$$

$$CWCB = CWCC \left[1 - \frac{BWBB}{BW} (1 - UW) \right] \qquad (A166)$$

$$UWCB = \frac{CWCT}{CWCB} \qquad (A167)$$

$$CWMN = 0.5\ (CWCB + CWCT) \qquad (A168)$$

$$SWN = CWMN\ BWN \qquad (A169)$$

$$AWN = \frac{BWN}{CWMN} \qquad (A170)$$

where BFE is an initial estimate of the fuselage width at the position of the centre section of the wing box, BWBB is the width of the centre section of the wing box, BWN is the span of the nett wing, CWCB is the root chord of the nett wing, UWCB is the taper ratio of the nett wing, CWMN is the mean chord of the nett wing, SWN is the area of the nett wing and AWN is the aspect ratio of the nett wing.

The structural box of the two nett wing halves is defined by forward and rear spars at fixed fractions of the chord and these two halves are joined by an unswept box of constant section shape through the fuselage (Fig.A9). The associated variables are :

$$CWBB = CWCB\ (FCWR - FCWD) \qquad (A171)$$

$$CWBT = CWCT\ (FCWR - FCWD) \qquad (A172)$$

where CWBB and CWBT are the chord of the wing box at the body side and at the tip respectively and FCWD and FCWR are the front and rear spar fractions.

$$QWB = \tan^{-1} [\tan (QWL) - \frac{CWCC}{BW} (FCWR - FCWD)$$

$$(1 - UW)] \qquad\qquad (A173)$$

$$UWB = \frac{CWBT}{CWBB} \qquad\qquad (A174)$$

$$SWB = \frac{CWBB}{2} (BW + BWBB + UWB\ BWN) \qquad (A175)$$

$$AWB = \frac{BW^2}{SWB} \qquad\qquad (A176)$$

$$HWBB = RTW\ CWCB \qquad\qquad (A177)$$

where QWB is sweep of the centre-line , UWB is the taper ratio, SWB is the planform area and AWB is the aspect ratio of the wing box. HWBB is the maximum depth of the centre section of the wing box.

The arrangement of the wing control surfaces and high-lift devices are shown in Fig.A9. The associated variables are :

For the spoilers

$$BWS = FBWS\ BW \qquad\qquad (A178)$$

$$CWS = \frac{BWS}{NWS\ AWS} \qquad\qquad (A179)$$

$$SWS = BWS\ CWS \qquad\qquad (A180)$$

$$AWSG = \frac{2\ AWS}{NWS} \tag{A181}$$

where BWS is the gross span of the spoilers, CWS the mean chord, AWSG the gross aspect ratio and SWS the area. NWS is the number of spoilers and AWS the aspect ratio of each spoiler.

For the ailerons

$$BWA = FBWA\ BW \tag{A182}$$

$$CWA = \frac{BWA}{2\ AWA} \tag{A183}$$

$$SWA = CWA\ BWA \tag{A184}$$

$$CWCA2 = CWCC\ [UW + 0.5\ FBWA\ (1 - UW)] \tag{A185}$$

$$QWA = \tan^{-1}\ [\ \tan(QWL) - \frac{2\ CWCC}{BW\ CWCA2}\ (CWCA2 - CWA)$$

$$(1 - UW)\ ] \tag{A186}$$

where BWA is the gross span of the ailerons, CWA the mean chord and and SWA the area. CWCA2 is the wing chord at the mid-span of each aileron and QWA is the sweep of the leading edge of the aileron.

For the high-lift devices we have for the one on the leading edge, the area of the fixed section of the leading edge, SWLF, is

$$SWLF = FCWLFT\ SWN \tag{A187}$$

the planform area of the leading edge device when retracted, SWLH, is

$$SWLH = (FCWD - FCWLHT)\ SWN \tag{A188}$$

and the total area of the leading-edge section of the wing is

$$SWL = FCWD\ SWN \qquad (A189)$$

where FCWLFT is chord of fixed leading edge forward of front spar as a fraction of the local chord and FCWLHT is distance of the trailing edge of the leading edge high lift device, forward of the front spar as a fraction of the local wing chord.

For the high-lift device on the trailing edge of the wing, the gross span, BWF, including the body width, is

$$BWF = FBWF\ BW \qquad (A190)$$

and the chord of the wing at the outboard end of the flap, CWCCT, is

$$CWCCT = CWCC\ [1 - FBWF\ (1 - UW)] \qquad (A191)$$

The mean chord of the flap, CWFM, is

$$CWFM = 0.5\ (CWCB + CWCCT)\ (1 - FCWR - FCWTHL) \qquad (A192)$$

The area of the flap, SWF, is

$$SWF = CWFM\ (BWF - BWBB) \qquad (A193)$$

The area of the fixed part of the trailing edge after of the rear spar is, SWTF,

$$SWTF = 0.5\ FCWTFT\ (CWCB + CWCCT)\ (BWF - BWBB) - SWA +$$
$$0.5\ (BW - BWF)\ (CWCT + CWCCT)\ (1 - FCWR) \qquad (A193)$$

The gross area of the wing trailing edge after of the rear spar, SWTG, is

$$SWTG = SWN \ (1 - FCWR) \tag{A194}$$

The chordwise distribution of the thickness of the aerofoil of the wing, HWX, is given by

$$HWX = \frac{3 \ 3^{\frac{1}{2}}}{2} \ RTW \ (CWY - X) \left(1 - \frac{X}{CWY} \right) \tag{A195}$$

The cross-sectional area of the centre section of the wing box, OWBB, is derived by integrating the aerofoil thickness between the front and rear spar positions.

$$OWBB = 0.3464 \ HWBB \ CWCB \ [\ 5 \ (FCWR^{1.5} - FCWD^{1.5}) -$$

$$3 \ (FCWR^{2.5} - FCWD^{2.5}) \ ] \tag{A196}$$

The volume of the centre section of the box, VWBB, and the volume of the corresponding fuel tank VWBCF, are :

$$VWBB = BWBB \ OWBB \tag{A197}$$

$$VWBCF = VWBB \ UWBCF \tag{A198}$$

where UWBCF is a utilization factor.

The span of the fuel tank in the wing box external to the fuselage, BWNF, is

$$BWNF = FBWNF \ BWN \tag{A199}$$

The taper ratio of the tank, UWCNF, is

$$UWCNF = 1 - \frac{BWNF}{BWN} \ (1 - UWCN) \tag{A200}$$

The volume of the wing box available for fuel tanks,VWBEF, is

$$VWBEF = UWBEF \ OWBB \ \frac{BWNF}{3} \ (1 + UWCNF + UWCNF^2) \tag{A201}$$

where UWBEF is the utilization factor of the wing box external to the fuselage.

5.2.   FLYING SURFACES EMPENNAGE (SUBROUTINE EMPENN)

5.2.1.   TAILPLANE

A number of external variables define the geometry of the tailplane. These external variables are :

AETN   the aspect ratio of the nett tailplane external
            to the fuselage
UETN   the taper ratio of the nett tailplane
QETL   the sweep angle of the leading edge of the
            tailplane
QETT   the sweep angle of the trailing edge of the
            tailplane
RTET   the thickness to chord ratio for the tailplane
RETSW   the tailplane volume ratio

$$\left(= \frac{SETN\ LTCQM}{SW\ CWMG} \right) \tag{A202}$$

The tail moment arm, LTCQM, is defined as the distance between the quarter chord points of the wing and the tailplane. As two independent variables, RXWCQM and RXTCQM, determine the position of the wing and the tailplane quarter chords respectively in terms of the fuselage length, we have

$$XWCQM = RXWCQM\ XFN \tag{A203}$$

$$XTCQM = RXTCQM\ XFN \tag{A204}$$

therefore

$$LTCQM = XTCQM - XWCQM \tag{A205}$$

From the above the nett area, SETN, and the nett span, BETN, of the tailplane are

$$SETN = \frac{RETSW\ SW\ CWMG}{LTCQM} \tag{A206}$$

$$BETN = (SETN\ AETN)^{\frac{1}{2}} \qquad (A207)$$

and the cord of the tailplane at the body side, CETB

$$CETB = \frac{2\ BETN}{AETN\ (1 + UETN)} \qquad (A208)$$

5.2.2.   FIN

A number of external variables define the geometry of the fin. These external variables are :

AEFN   the aspect ratio of the nett fin external to the fuselage

UEFN   the taper ratio of the nett fin

QEFL   the sweep angle of the leading edge of the fin

QEFT   the sweep angle of the trailing edge of the fin

RTEF   the thickness to chord ratio for the fin

REFFC   the tailplane volume ratio

$$[\ = \frac{SEFN\ LFCQM}{0.5\ XWCQM\ BFC2}\ ] \qquad (A209)$$

The fin moment arm, LFCQM, is defined as the distance between the quarter chord points of the wing and the fin. As RXFCQM, determines the position of the fin quarter chord in terms of the fuselage length, we have

$$XFCQM = RXFCQM\ XFN \qquad (A210)$$

therefore

$$LFCQM = XFCQM - XWCQM \qquad (A211)$$

From the above the nett area, SETN, and the nett span, BETN, of the fin are

$$SEFN = \frac{REFFC\ 0.5\ XWCQM\ BFC^2}{LFCQM}$$ (A212)

$$BEFN = (SEFN\ AEFN)^{\frac{1}{2}}$$ (A213)

and the cord of the fin at the body side, CEFB

$$CETB = \frac{2\ BEFN}{AEFN\ (1 + UEFN)}$$ (A214)

7.   LATERAL CROSS-SECTIONAL AREA OF THE FLYING
       SURFACES (SUBROUTINE FLATCROSS)

This subroutine estimates the lateral cross-sectional
area of the flying surfaces that is to be subtracted from
the nett cross-sectional area, defined by the fairing
curve, in order to area rule the aircraft.

The (wing) thickness distribution equation, found in the
WING subroutine, is integrated across the semi-span to
give for an X axial position (station) the lateral cross-
sectional area of the flying surface, OX

$$OX = \frac{3\ 3^{\frac{1}{2}}\ TC\ B2}{2\ C\ (1 - U)} \left\{ \frac{1}{2} \left[\frac{C}{B2}\ (1 - U)\ \tan QL \right]^{\frac{1}{2}} \right.$$

$$\left[\frac{X\ (1 - U) - B2\ \tan QL}{2\ (1 - U)\ \tan QL} \right]^2 \left[\frac{C}{B2}\ (1 - U) + 3 \right.$$

$$\left. \tan QL \right] \left[\log \mid \sec \theta + \tan \theta \mid - \tan \theta \sec \theta \right]_{\theta_L}^{\theta_U}$$

$$+ 2 \left[\left(C \left(1 - (1 - U)\ \frac{Y}{B2} \right) \right)^{\frac{1}{2}} (X - Y\ \tan QL) 1.5 \right]_{Y_L}^{Y_U} \right\}$$

(A214)

where

$$\cos \theta = \frac{B2 - X (1 - U) \cot QL}{[X (1 - U) \cot QL + B2 - 2Y (1 - U)} \qquad (A215)$$

The equation and its variables apply to a general flying surface - half wing, half tailplane, fin - provided the thickness distribution remains the same. They are

TC   thickness to chord ratio
C   root chord
B2   span of single surface
U   taper ratio
QL   leading edge sweep angle
X   distance from the apex of the nett flying surface

The lower Y limit, YL, may occur on the root chord (YL = 0) or the trailing edge if it is swept backward

$$\left[YL = \frac{X - C}{\tan QL - \dfrac{C}{B2} (1 - U)} \right] \qquad (A216)$$

The upper Y limit may occur on the leading edge (YU = X cot QL), the tip chord (YU = B2) or the trailing edge if it is swept forward

$$\left[YU = \frac{X - C}{\tan QL - \dfrac{C}{B2} (1 - U)} \right] \qquad (A217)$$

In this subroutine the above equations are applied to all three flying surfaces wing, tailplane and fin and their lateral cross-sectional area is calculated for all the stations and their subdivisions specified·in the subroutine STATION that have a common lateral plane (Fig.A2).

8.   FUSELAGE STATIONS

Along the fuselage a number of fuselage stations are defined in order to ensure that there is adequate cross-sectional area within the fuselage to accomodate the

specified fixed items. At each station the section shape
is described in terms of some geometric parameters,
taking into consideration the configuration and the whole
layout of the aircraft, and a minimum allowable cross-
sectional area is calculated.

8.1.   FUSELAGE STATION A (SUBROUTINE FUSSTNA)

Station A - station number 7 - is located at the front
bulkhead of the cockpit (Fig.A2). It is specified as a
rectangle section with elliptic corners of a fixed
proportion RFCNRA (Fig.A10). The ratio of the rectangle
sides, RAHB, is taken to be the same as the eccentricity
of an ellipse. Thus

$$HFA = BFA\ RAHB \qquad\qquad (A218)$$

$$HFACNR = HFA\ RFCNRA \qquad\qquad (A219)$$

$$BFACNR = BFA\ RFCNRA \qquad\qquad (A220)$$

where HFA and BFA are the height and width of the section
and HFACNR and BFACNR the heigh and width of the corners
of the section.

The cross-sectional area, OFA, is that of the fairing
curve and enables BFA and HFA to be estimated. The cross-
sectional area in terms of the section dimensions is the
product of the width by the height minus the squares of
the four corners plus the elliptic parts of the four
corners.

$$OFA = OTXN(7) \qquad\qquad (A221)$$

$$OFA = HFA\ BFA - 4\ HFACNR\ BFACNR + \pi\ HFACNR\ BFACNR$$

$$(A222)$$

$$= HFA\ BFA\ [\ 1 - \frac{HFACNR}{HFA}\ \frac{BFCNRA}{BFA}\ (4 - \pi)\ ] \qquad (A223)$$

$$= RAHB\ BFA^2\ [\ 1 - \frac{HFACNR}{HFA}\ \frac{BFACNR}{BFA}\ (4 - \pi)\ ]$$

$$(A224)$$

$$BFA = \left\{ \frac{OFA}{RAHB \left[1 - \dfrac{HFACNR}{HFA} - \dfrac{BFACNR}{BFA} (4 - \pi) \right]} \right\}^{\frac{1}{2}}$$

(A225)

The underfloor height, HFA1, is

$$HFA1 = HFA - HC5 \tag{A226}$$

The cross-sectional area of the underfloor, OFAUF, depends on the relation between underfloor height and corner height. If HFA1 ≤ HFACNR then

$$OFAUF = HFACNR \ BFACNR \ (QFA - \sin QFA \cos QFA + HFA1$$

$$(BFA - 2 \ BFACNR) \tag{A227}$$

where

$$\cos QFA = \frac{(HFACNR - HFA1)}{HFACNR} \tag{A228}$$

If HFACNR < HFA1 ≤ HFA - HFACNR then

$$OFAUF = HFACNR \ BFACNR \ \frac{\pi}{2} + HFACNR \ (BFA - 2 \ BFACNR) +$$

$$BFA \ (HFA1 - HFACNR) \tag{A229}$$

If HFA - HFACNR < HFA1 then

$$OFAUF = OFA - HFACNR \ BFACNR \ (QFA - \sin QFA \cos QFA) -$$

$$(HFA - HFA1) \ (BFA - 2 \ BFACNR) \tag{A230}$$

where

$$\cos\ QFA\ =\ \frac{(HFA1\ -\ HFA\ +\ HFACNR)}{HFACNR} \tag{A231}$$

This underfloor area must be able to contain the nose undercarriage bay. Hence a minimum underfloor cross-sectional area, OFAUFS, is defined as

$$OFAUFS\ =\ \frac{OUNWB}{UOFAUF} \tag{A232}$$

where OUNWB is the cross-sectional area of the nose undercarriage bay and UOFAUF is a utilization factor for the nose underfloor.

8.2. FUSELAGE STATION B (SUBROUTINE FUSSTNB)

Station B - station number 9-10 - is located at the entry of the intake diffuser as shown in Fig.A2, between the cockpit front bulkhead (Station A) and the position of the pilot's eye point as defined in Fig.A4. The fuselage at station B contains the cockpit, the nose undercarriage bay and the intake diffuser(s). The fuselage section at station B is a rectangle with rounded corners and a semi-circular canopy (front part of the canopy) plus the two rectangles of the inlets of the engine intake (Fig.A10).

A minimum cockpit width BCH is given as part of the cockpit specification and consequently the minimum width at station B (without the intakes), BFBS, is set as the greater of the width at station A, BFA, or BCH.

The minimum cross-sectional area at station B, OFBS, is

$$OFBS\ =\ \frac{\pi}{2}\ RCCANB^2\ +\ BFBS\ FOFB1K\ (HC4\ +\ HCEYE\ -\ RCCANB)$$

$$+\ HFA1\ BFBS\ FOFB2K\ +\ 2\ HII\ (BII\ +\ BVI) \tag{A233}$$

where RCCANB is the radius of the cockpit canopy at station B and FOFB1K, FOFB2K are utilization factors.

To determine the actual dimensions at station B, a scaling factor, ROFBNS, is defined as the ratio of the nett cross-sectional area without the canopy section to the corresponding minimum nett cross-sectional area (without the canopy). Again the nett cross-sectional area is provided by the fairing curve. If OFB is the actual cross-sectional area

$$OFB = OTXN(9) + 2 \; HII \; (BII + BVI) \qquad (A234)$$

$$ROFBNS = \frac{OFB - 0.5 \; \pi \; RCCANB^2 - 2 \; HII \; (BII + BVI)}{OFBS - 0.5 \; \pi \; RCCANB^2 - 2 \; HII \; (BII + BVI)}$$

$$(A235)$$

Then

$$BFB = BFBS \; ROFBNS^{\frac{1}{2}} \qquad (A236)$$

and substituting HFB1 for HFA1

$$HFB1 = \frac{OFB - 0.5 \; \pi \; RCCANB^2}{BFB \; FOFB2K} -$$

$$\frac{BFB \; FOFB1K \; (HC4 + HCEYE - RCCANB)}{BFB \; FOFB2K} \qquad (A237)$$

The cross-sectional area of the underfloor, OFBUF, is

$$OFBUF = HFB1 \; BFB \; FOFB2K \qquad (A238)$$

8.3. FUSSELAGE STATION C (SUBROUTINE FUSSTNC)

Station C - station number 14 - is located at the pilot's eye position as shown in Fig.A2. The fuselage at station C contains the cockpit, some of the vertical part of the RLS front duct and the intake diffuser(s).The fuselage section at station C is a rectangle plus a semi-circular canopy and two rectangular intake diffuser sections

(Fig.A10). As a minimum width, BFCS, the width at station C, BFB, is chosen. The height of the underfloor is the same as in station B. Thus the minimum actual cross-sectional area, OFCS, is

$$BFCS = BFB \qquad\qquad\qquad (A239)$$

$$OFCS = 0.5 \ \pi \ RCCANC^2 + FOFC1K \ BFCS \ (HC4 + HCEYE - $$

$$RCCANC) + FOFC2K \ BFCS \ HFB1$$

$$+ \frac{(OIE - OII) \ (FX(14) - XII)}{LIDG} + OII \qquad (A240)$$

where FOFC1K, FOFC2K are area utilization factors and FX(14) is the distance of the station from the aircraft nose. The last term above represents the cross-sectional area of the intake diffuser, which is changing along the intake diffuser length in order to produce appropriate flow conditions at the engine intake (Mach number near 0.4).

To determine the fuselage dimensions at station C a scaling factor, ROFCNS, is defined as the ratio of the nett cross-sectional area without the canopy section to the corresponding minimum nett cross-sectional area. The nett cross-sectional area is provided by the fairing curve. The actual cross-sectional area, OFC, is

$$OFC = OTXN(14) + \frac{(OIE - OII) \ (FX(14) - XII)}{LIDG} + OII$$

$$(A241)$$

therefore

$$ROFCNS = \frac{OFC - \left[\dfrac{(OIE - OII) \ (FX(14) - XII)}{LIDG} + OII \right]}{OFCS - \left[\dfrac{(OIE - OII) \ (FX(14) - XII)}{LIDG} + OII \right]}$$

$$\frac{- 0.5 \ \pi \ RCCANC^2}{- 0.5 \ \pi \ RCCANC^2} \tag{A242}$$

Hence for width and underfloor height

$$BFC = BFCS \ ROFCNS^{\frac{1}{2}} \tag{A243}$$

$$HFC1 = \frac{OFC - [\ \dfrac{(OIE - OII) \ (FX(14) - XII)}{LIDG} + OII \ ]}{FOFC2K \ BFC}$$

$$\frac{- 0.5 \ \pi \ RCCANC^2 - FOFC1K \ BFC}{FOFC2K \ BFC}$$

$$\frac{(HC4 + HCEYE - RCCANC)}{FOFC2K \ BFC} \tag{A244}$$

$$OFCUF = FOFC2K \ HFC1 \ BFC \tag{A245}$$

where OFCUF is the underfloor cross-sectional area.

8.4.·   FUSELAGE STATION D (SUBROUTINE FUSSTND)

Station D - station number 18 - is located at the front face of the internal weapon bay as shown in Fig.A2. The fuselage at station D contains the RLS front duct, the internal weapon bay, the gun bay and the intake diffuser(s). The fuselage section at station D is a rectangle plus a semi-circular spine section and two rectangular intake diffuser sections (Fig.A11). As a minimum height, HFDS, the greater of the height of the

weapons bay plus the height of the eye position or the height of the gun bay plus the height of the eye position is chosen .

$$HFDS = HSWBI + HCEYE \text{ or} \qquad \text{(A246a)}$$

$$HFDS = HHGABI + HCEYE \qquad \text{(A246b)}$$

The semi-circular spine houses the RLS front duct system which is is made of three circular ducts that form together an externally semi-circular duct. Therefore the radius of the semi-circular spine is the same to that of the RLS front duct system.

$$RCCAND = \frac{DRDE}{2} \qquad \text{(A247)}$$

Thus the minimum actual cross-sectional area, OFDS, is

$$OFDS = 0.5 \; \pi \; RCCAND^2 + FOFDK \; HFDS \; (2 \; (BGMBI + BGABI) +$$

$$BSWBI) + \frac{(OIE - OII) \; (FX(18) - XII)}{LIDG} + OII$$

$$\text{(A248)}$$

where FOFDK is an area utilization factor and FX(18) the distance of the station from the aircraft nose.

To determine the fuselage dimensions at station D a scaling factor, ROFDNS, is defined as the ratio of the nett cross-sectional area without the spine section to the corresponding minimum nett cross-sectional area. The nett cross-sectional area is provided by the fairing curve. The actual cross-sectional area, OFD, is

$$OFD = OTXN(18) + [\; \frac{(OIE - OII) \; (FX(18) - XII)}{LIDG} + OII \;]$$

$$\text{(A249)}$$

Hence

$$\text{ROFDNS} = \cfrac{\text{OFD} - \left[\cfrac{(\text{OIE} - \text{OII})\ (\text{FX}(18) - \text{XII})}{\text{LIDG}} + \text{OII} \right]}{\text{OFDS} - \left[\cfrac{(\text{OIE} - \text{OII})\ (\text{FX}(18) - \text{XII})}{\text{LIDG}} + \text{OII} \right]}$$

$$\cfrac{-\ 0.5\ \pi\ \text{RCCAND}^2}{-\ 0.5\ \pi\ \text{RCCAND}^2} \qquad\qquad (\text{A}250)$$

and for height and width

$$\text{HFD} = \text{HFDS}\ \text{ROFDNS}^{\frac{1}{2}} \qquad\qquad (\text{A}251)$$

$$\text{BFD} = [2\ (\text{BGMBI} + \text{BGABI}) + \text{BSWBI}]\ \text{ROFDNS}^{\frac{1}{2}} \qquad (\text{A}252)$$

8.5.   FUSSELAGE STATION E (SUBROUTINE FUSSTNE)

Station E - station number 30 - is located at the engine intake (compressor intake) as shown in Fig.A2. The fuselage at station E includes the engine, the RLS front duct, the wing box and the main undercarriage. The fuselage section at station E is a rectangle plus a semi-circular spine section (Fig.A11). The semi-circular spine is of the same size as in the previous station (RCCANE = RCCAND). The minimum width, BFES, is the greater of the width of the main undercarriage (DUMWB) or the width of the engine (DP1 + EBP1). Hence the minimum actual cross-sectional area, OFES, is

$$\text{OFES} = \text{FOFEK}\ \text{BFES}\ (\text{BUMWB} + \text{DP1} + \text{EHP1} + \text{HWBB}) +$$

$$0.5\ \pi\ \text{RCCANE}^2 \qquad\qquad (\text{A}253)$$

where FOFEK ia an utilization factor. It should be noted that the width and height definitions for the main undercarriage bay are here opposite the ones adopted in subroutine UNDCB due to the non-standard orientation of the wheels in the bay.

To determine the fuselage dimensions at station E a scaling factor, ROFENS, is defined as the ratio of the

nett cross-sectional area without the spine section to the corresponding minimum nett cross-sectional area. The nett cross-sectional is provided by the fairing curve. The actual cross-sectional area, OFE, is

$$OFE = OTXN(30) - OXW2(30) + 0.25 \ \pi \ DP1^2 \qquad (A254)$$

OXW2(38) is the lateral cross-sectional area of the wing at station E (30), and if the aircraft is area ruled, it must be deduced from the total nett cross-sectional area given by the fairing curve. If the aircraft is not area ruled OXW2 is zero.

Thus

$$ROFENS = \frac{OFE - 0.25 \ \pi \ DP1^2 - 0.5 \ \pi \ RCCANE^2}{OFES - 0.25 \ \pi \ DP1^2 - 0.5 \ \pi \ RCCANE^2} \qquad (A255)$$

Consequently for width and height we have

$$BFE = BFES \ ROFENS^{\frac{1}{2}} \qquad (A256)$$

$$HFE = (BUMWB + DP1 + EHP1 + HWBB) \ ROFENS^{\frac{1}{2}} \qquad (A257)$$

8.6.   FUSSELAGE STATION F (SUBROUTINE FUSSTNF)

Station F - station number 38 - is located at the turbine exit as shown in Fig.A2. The fuselage at station F includes the engine, the RLS front duct and the side fuel tanks. The fuselage section at station F is a rectangle plus a semi-circular spine section and two rectangular sections on the sides (Fig.A11). The semi-circular spine is of the same size as in the previous station (RCCANF = RCCANE). The minimum wheight, HFFS, is the greater of the height of the engine (DP2 + EHP2) or the height of the side fuel tanks (HRD). Hence the minimum actual cross-sectional area, OFFS, is

$$OFFS = FOFFK \ HFFS \ (2 \ BRD + DP2 + EBP2) + 0.5 \ \pi \ RCCANF^2$$

$$(A258)$$

where FOFFK is an area utilization factor and BRD the width of each side fuel tank.

To determine the fuselage dimensions at station F a scaling factor, ROFFNS, is defined as the ratio of the nett cross-sectional area without the spine section to the corresponding minimum nett cross-sectional area. The nett cross-sectional area is provided by the fairing curve. The actual cross-sectional area, OFF, is

$$OFF = OTXN(38) - OXET2(38) - OXEF(38) + 0.25 \, \pi \, DP2^2$$

$$(A259)$$

OXET2(38) and OXEF(38) are the lateral cross-sectional areas of the tailplane and fin - if they exist - at station F (38).

$$ROFFNS = \frac{OFF - 0.25 \, \pi \, DP2^2 - 0.5 \, \pi \, RCCANF^2}{OFFS - 0.25 \, \pi \, DP2^2 - 0.5 \, \pi \, RCCANF^2} \qquad (A260)$$

Hence for the height and the width

$$HFF = HFFS \, ROFFNS^{\frac{1}{2}} \qquad\qquad (A261)$$

$$BFF = (BRD + DP2 + EBP2) \, ROFFNS^{\frac{1}{2}} \qquad (A262)$$

8.7.   FUSSELAGE STATION G (SUBROUTINE FUSSTNG)

Station G - station number 40 - is located at the RLS intake as shown in Fig.A2. The fuselage at station G includes the engine (RLS section), the RLS front duct and the side ducts that have the same nearly rectangular section as the side fuel tanks . The fuselage section at station G is a rectangle plus a semi-circular spine section and two nearly rectangular sections on the sides (Fig.A13). The semi-circular spine is of the same size as in the previous station (RCCANG = RCCANF). The minimum wheight, HFGS, is the greater of the height of the engine (DP3 + EHP3) or the height of the side ducts (HRD). Hence the minimum actual cross-sectional area, OFGS, is

$$OFGS = FOFGK \, HFGS \, (2 \, BRD + DP3 + EBP3) + 0.5 \, \pi \, RCCANG^2$$

$$(A263)$$

where FOFGK is an area utilization factor and BRD the width of each side duct.

To determine the fuselage dimensions at station G a scaling factor, ROFGNS, is defined as the ratio of the nett cross-sectional area without the spine section to the corresponding minimum nett cross-sectional area. The nett cross-sectional is provided by the fairing curve. The actual cross-sectional area, OFG, is

$$OFG = OTXN(40) - OXET2(40) - OXEF(40) + 0.25 \pi DP3^2$$

(A264)

OXET2(40) and OXEF(40) are the lateral cross-sectional areas of the tailplane and fin - if they exist - at station G (40).

$$ROFGNS = \frac{OFG - 0.25 \pi DP3^2 - 0.5 \pi RCCANG^2}{OFGS - 0.25 \pi DP3^2 - 0.5 \pi RCCANG^2}$$

(A265)

Hence for the height and the width

$$HFG = HFGS \ ROFGNS^{\frac{1}{2}}$$

(A266)

$$BFG = (BRD + DP3 + EBP3) \ ROFGNS^{\frac{1}{2}}$$

(A267)

8.8.   FUSSELAGE STATION H (SUBROUTINE FUSSTNH)

Station H - station number 42 - is located at the exit of the RLS section of the engine as shown in Fig.A2. The fuselage at station H includes the engine (RLS section), the side ducts and the end of the spine that until the previous station contained the RLS front duct. The fuselage section at station H is a rectangle plus a semi-circular spine (the end of the spine) section and two nearly rectangular sections on the sides (Fig.A12). The semi-circular spine is of the same size as in the previous station (RCCANH = RCCANG). The minimum height, HFHS, is the greater of the height of the engine (DP4 + EHP4) or the height of the side ducts (HRD). Hence the minimum actual cross-sectional area, OFGS, is

$$OFHS = FOFHK \ HFHS \ (2 \ BRD + DP4 + EBP4) + 0.5 \pi RCCANH^2$$

(A268)

where FOFHK is an area utilization factor and BRD the width of each side duct.

To determine the fuselage dimensions at station G a scaling factor, ROFHNS, is defined as the ratio of the nett cross-sectional area without the spine section to the corresponding minimum nett cross-sectional area. The nett cross-sectional is provided by the fairing curve. The actual cross-sectional area, OFH, is

$$OFH = OTXN(42) - OXET2(42) - OXEF(42) + 0.25 \, \pi \, DP4^2$$

$$(A269)$$

OXET2(42) and OXEF(42) are the lateral cross-sectional areas of the tailplane and fin - if they exist - at station H (40).

$$ROFHNS = \frac{OFH - 0.25 \, \pi \, DP4^2 - 0.5 \, \pi \, RCCANH^2}{OFHS - 0.25 \, \pi \, DP4^2 - 0.5 \, \pi \, RCCANH^2} \qquad (A270)$$

Hence for the height and the width

$$HFH = HFHS \, ROFHNS^{\frac{1}{2}} \qquad\qquad (A271a)$$

$$BFH = (BRD + DP4 + EBP4) \, ROFHNS^{\frac{1}{2}} \qquad (A271b)$$

8.9.　　FUSSELAGE STATION J (SUBROUTINE FUSSTNJ)

Station J - station number 46 - is located at the exit of the afterburner of the engine as shown in Fig.A2. The fuselage at station J includes only the engine . The fuselage section at station J is almost circular (Fig.A13). The height, HFJ, at station J (46) is

$$HFJ = (DP5 + EHP5) \qquad\qquad (A272)$$

and the width, BFJ, is

$$BFJ = (DP5 + EHP5) \qquad\qquad (A273)$$

From these dimensions we have for this almost circular cross-sectional area, OFJ

$$OFJ = 0.25 \ \pi \ HFJ \ BFJ \qquad\qquad (A274)$$

8.10.   FUSSELAGE STATION I (SUBROUTINE FUSSTNI)

Station I - station number 50 - is located at the nozzle exit as shown in Fig.A2. The fuselage at station I includes only the engine (nozzle). The fuselage section at station I is circular (Fig.A13). The height, HFJ, at station I (50) is

$$HFI = (DP6 + EHP6) \qquad\qquad (A275)$$

and the width, BFI, is

$$BFI = (DP6 + EHP6) \qquad\qquad (A276)$$

From these dimensions we have for this circular cross-sectional area, OFI

$$OFI = 0.25 \ \pi \ HFI \ BFI \qquad\qquad (A277)$$

9.   ACTUAL FUSELAGE CROSS-SECTIONAL AREA (SUBROUTINE FUSCRA)

This subroutine evaluates the actual cross-sectional area of the fuselage. The actual cross-sectional area of the fuselage is made of the nett cross-sectional area plus the flow-through cross-sectional areas, that is the ones of the intake diffuser and the engine.

The nett cross-sectional area is given by the fairing curve (subroutines FAIRCUR1 and FAIRCUR2).

For the fuselage stations up to the intake diffuser inlet (station 9-10), the actual cross-sectional area, OFX, is equal to the nett cross-sectional area provided by the fairing curve.

$$OFX = OTXN \qquad\qquad\qquad\qquad (A278)$$

From the intake diffuser inlet to the engine inlet, the actual cross-sectional area equals the nett cross-sectional area plus the cross-sectional area of the intake diffuser.

$$OFX = OTXN + OIX \qquad\qquad\qquad (A279)$$

where

$$OIX = \frac{FX - XII}{LIDG}\ (OIE - OII) + OII \qquad (A280)$$

From the engine inlet to the nozzle exit, the actual cross-sectional area equals the nett cross-sectional area provided by the fairing curve plus the cross-sectional area of the engine.

$$OFX = OTXN + OPX \qquad\qquad\qquad (A281)$$

where OPX is estimated for the various engine sections

For station 31 to 37

$$OPX(I) = OPX(38) + \left[\frac{FX(I) - FX(30)}{LP12} \right] [OPX(38) -$$

$$OPX(30)\ ] \qquad\qquad\qquad\qquad (A282)$$

The other engine cross-sections are evaluated similarly.

Between stations 14 and 37 the lateral cross-sectional area of the wing OXW2 is deduced from the nett cross-sectional area if the aircraft is area ruled. The same applies for stations 37 to 50 where the tailplane, OXET2, and the fin, OXEF, lateral cross-sectional areas are deduced.

In this subroutine the maximum fuselage actual cross-sectional area, OFXH and the maximum afterbody actual

cross-sectional area, OFXTH and their positions, XFOH
and XFOTH, are evaluated.

10.   FUSELAGE PERIMETER (SUBROUTINE PERIM)

This subroutine evaluates the perimeter, PFX, of the
fuselage.

For this purpose the actual cross-sectional area of the
fuselage, OFX, from subroutine FUSCRA is used. In
addition a shape factor RPFX is defined as the ratio of
the perimeter of a cross section to the perimeter of a
circle having the same cross-sectional area. Thus

$$PFX = RPFX \; 2 \; (\pi \; OFX)^{\frac{1}{2}} \tag{A283}$$

The variation of the shape factor RPFX with axial
distance along the fuselage for combat aircraft could be
approximated by

$$RPFX = (RPFX1K - 1) \left[\frac{FX}{XII} \right]^2 + 1 \tag{A284}$$

for fuselage stations up to the intake diffuser inlet and
by

$$RPFX = \left[\left(\frac{XFN - FX}{XFN - XII} \right) - RPFX4K \right]^2 (RPFX2K - RPFX3K)$$

$$+ \; RPFX3K \tag{A285}$$

where RPFX1K, RPFX2K, RPFX3K and RPFX4K are constants.
For a fuselage containing a single engine RPFX4K = 0

11.   NUMERICAL INTEGRATION (SUBROUTINE INTEGRA)

This subroutine is a general numerical integration module
that is being called from other parts of the code when an
integration is needed.

The numerical integration method is based on Simpson's
rule and the variables used are defined as follows :

```
NNUMI      is the number of function values
F(I)       is the function to be integrated
ALF        is the lower limit of integration
BET        is the upper limit of integration
IFUN       is the integrated function
```

12.   MASS ESTIMATION

12.1.   FUEL TANK MASS ESTIMATION (SUBROUTINE MASSEFULT)

This subroutine estimates the mass of the central and side fuel tanks. The wing fuel tank mass estimation was included in subroutine WING.

12.1.1. CENTRAL FUEL TANK MASS ESTIMATION

The central fuel tank has the shape of a wedge as shown in Fig.A3. It is located over the internal weapon bay, between the two intake diffuser ducts. Its base width is equal to the internal weapon bay width, BSWBI, and its height is what remains from the fuselage height, HFD, after the wing box and the internal weapon height are deduced. Thus the volume of the central tank, VCTF, is

$$VCTF = (XFN - XD - LPG) \; \frac{BSWBI}{2} \; (HFD - RTW \; CWCC - HSWBI)$$

$$(A286)$$

and the mass of the full tank, MCTF,

$$MCTF = VCTF \; RFUL \qquad\qquad (A287)$$

where RFUL is the fuel density.

12.1.2. SIDE FUEL TANK MASS ESTIMATION

The side fuel tanks are of nearly rectangular cross-section and are situated on both sides of the engine. They run the whole length of the engine and blend with the side ducts as shown in Fig. A3. The volume of each side tank, VESTF, is

$$VESTF = BRD \; DP2 \; LP12 \qquad\qquad (A288)$$

and the mass of the full tank, MESTF, is

$$MESTF = VESTF \; RFUL \qquad\qquad (A289)$$

12.2.   FUSELAGE MASS ESTIMATION (SUBROUTINE MASSEFUS)

The mass of the fuselage is considered as the sum of the masses of the fuselage shell, the internal structure, the cockpit windscreen and canopy and various other items such as airbrakes and variable intake ramps, if they exist. The mass of the fuselage shell, MFX, is given by

$$MFX = FMF2 \ (WFG1 + WFG2 - WCWSC - WCCAN) \ [\ 0.07232$$

$$(VD - 180)^{0.9} + \frac{0.0000002602 \ XFN \ ULTN \ TPGD^{0.8}}{(BFCDH + HFCDH)} +$$

$$+ \ 3.7 \ ] \hspace{6cm} (A290)$$

where

VD   is the design maximum speed
ULTN   is the ultimate load factor
TPGD   is the maximum, sea level, static thrust of the
        engine with reheat
WCWSC   is the surface of the cockpit windscreen
WCCAN   is the surface of the cockpit canopy
BFCDH   is the greatest fuselage width, obtained as the
        greater of the widths at sections C and D.
HFCDH   is the greatest fuselage height as above
FMF2   is a materials mass factor (for aluminium
        alloy = 1)

The mass of the fuselage internal structure, MFW, is given by

$$MFW = FMF2 \ VFXT \ [\ 0.000005906 \ (VD \ AMMX)^2 + 13 +$$

$$\frac{0.018575 \ ULTN \ XFN}{CWBB^2} + \frac{0.01002 \ ULTN}{HFCDH}$$

$$(1000 \ VFGF)^{0.6} \ ] \hspace{5cm} (A291)$$

where

VFXT   is the total fuselage volume
AMMX   is the design maximum Mach number for the
        structure
VFGF   is the total volume of fuel in the fuselage

The mass of the cockpit windscreen, MCW, is given by

$$MCW = WCWSC\ (0.0011475\ VD^2\ sin2\ QCWSC + 5.83) \qquad (A292)$$

where QCWSC is the angle of the windscreen to the
horizontal.

The mass of the cockpit canopy is given by

$$MCC = WCCAN\ (0.00011818\ VD^2 + 10.74) \qquad (A293)$$

The mass of various items was considered to be around
15 % of the total. Hence for the total mass of the
fuselage, MFG, we have

$$MFG = 1.15\ (MFX + MFW + MCW + MCC) \qquad (A294)$$

12.3.   FLYING SURFACES MASS ESTIMATION (SUBROUTINE MASSEFLS)

The method of the wing mass estimation is applicable to a
wide variety of wing planforms under many different
loading conditions. In addition to the restrictions in
wing geometry introduced in subroutine WING, some more
assumptions have been made to simplify the mass
calculations. The most extreme loading case is assumed to
occur when the fuel in the fuselage is unused and no fuel
remains in the wing. No relief loads are assumed to be
present on the wing.

12.3.1.   WING BOX MASS ESTIMATION

The mass per unit area of the wing box structure is split
into eight terms defined as follows :

$$TERM1B = \frac{0.000089\ BMS}{CWBB\ DE1\ cos^2\ QWB} \qquad (A295)$$

where the bending moment, BMS, is given by

$$
BMS = 0.25 \text{ YCPX BWN MTCR ULTN} \left\{ 1 - 0.5 \frac{BWBB}{BW} \left[1.28 - \right. \right.
$$

$$
6.35 \text{ (YCPG} - 0.425) + 1.28 \left(1 - \frac{BWBB2}{BW^2} \right)^{\frac{1}{2}} +
$$

$$
(14.13 \frac{BWBB}{BW} - 6.35) \text{ (YPCG} - 0.425) \left. \left. \right] \right\} \qquad (A296)
$$

and DE1 is defined as the lesser of the maximum depth of the wing at the body side (RTW CWCB) and an equivalent depth of the wing box at the body side {RTW CWCB [1.25 - 0.462 (FCWD + FCWR)]}.

The spanwise position of the centre of pressure of the nett wing, YCPX, is given by

$$
YCPX = 0.42 + 0.001 \text{ AWN } [(4.4 + UWCN) \tan QW4 + 10.4
$$

$$
UWCN^{\frac{1}{2}} - 6.7] \qquad (A297)
$$

and for the gross wing, YCPG, is given by

$$
YCPG = 0.42 + 0.001 \text{ AW } [(4.4 + UW) \tan QW4 + 10.4 \text{ } UW^{\frac{1}{2}}
$$

$$
- 6.7] \qquad (A298)
$$

MTCR is the stressing mass for the wing and is obtained by subtracting the mass of fuel in the exposed wing and the reference load from the reference take-off mass

$$
MTCR = MTTR - MWBEF - MTPR \qquad (A299)
$$

For the other terms we have

$$
TERM2B = 0.82 \left(\frac{AWB}{AW \cos QWB} \right)^2 FK^{\frac{1}{4}} \qquad (A300)
$$

where FK is defined as the greater of 1 and the expression

$$\frac{BMS}{59500 \ CWBB \ DE1 \ \cos \ QWB} \tag{A301}$$

$$TERM3B = \frac{6.82 \ (1 - UWB)^2}{\cos 2 \ QWB \ \ FK^{\frac{1}{4}}} \tag{A302}$$

$$TERM4B = 0.00007063 \left(\frac{AWB}{AW} \right)^{\frac{1}{2}} VD^2 \cos^2 QWB \tag{A303}$$

$$TERM5B = 25.98 \ [\ 0.5 \ (DE1 + DE6) \ ]^{1.5} \ \sec^2 QWB \tag{A304}$$

where DE6 is defined as the lesser of the maximum depth of the wing at the tip (RTW CWCT) and an equivalent depth of the wing box at the tip [RTW CWCT (1.25 - 0.462 (FCWD + FCWR)]

$$TERM6B = 0.522 \ AMMX^2 \tag{A305}$$

$$TERM7B = \frac{8.2 \ FBWCF \ SWBF}{SWB \ FK} \tag{A306}$$

where

$$FBWCF = \frac{(BWNF + BWBB)}{BW} \tag{A307}$$

$$TERM8B = 0.00002785 \ VD^2 \left(\frac{NWP}{FK} \right)^{\frac{1}{4}} \tag{A308}$$

The total mass of the wing box, MWB, is given by

$$MWB = FMWB \; SWB \; FMWBH \; (TERM1B + TERM2B + TERM3B +$$
$$TERM4B + TERM5B + TERM6B + TERM7B + TERM8B)$$

$$(A309)$$

where FMWB is a materials mass factor (for aluminium alloys FMWB = 1).

FMWBH is a correction factor for estimates of wing box mass for thin wings of moderate to high aspect ratio. Up to an aspect ratio of AWR given by

$$AWR = 14.29 \; (RTW - 0.033)^{\frac{1}{2}} + 2 \qquad (A310a)$$

or

$$AWR = 1 \qquad (A310b)$$

if RTW < 0.033

then

$$FMWBH = 1 \qquad (A311)$$

Above these values of aspect ratio

$$FMWBH = 1 + 0.3 \left(\frac{AW}{AWR} - 1 \right)^{1.2} \qquad (A312)$$

12.3.2. WING LEADING EDGE MASS ESTIMATION

The mass per unit area of the leading edge of the wing, including fixed and moving parts, is split into four terms

$$TERM1L = 0.522 \; \frac{ULTN}{SW} \; MTCR \left(\frac{SWL \; RTW}{BWN} \right)^2 \qquad (A313)$$

$$TERM2L = 0.00007285 \; \frac{ULTN \; MTCR}{SW \; RTW} \left(\frac{SWL}{BWN} \right)^{0.125} \qquad (A314)$$

$$TERM3L = 0.000056 \ VD^2 \qquad\qquad (A315)$$

$$TERM4L = 1.536 \ BWN^{0.75} \qquad\qquad (A316)$$

Thus the total mass of the wing leading edge, MWL, is

$$MWL = FMWL \ (SWLF + SWLH) \ (TERM1L + TERM2L + TERM3L$$
$$+ \ TERM4L) \qquad\qquad (A317)$$

where FMWL is a materials mass factor (for aluminium alloys FMWL = 1)

12.3.3. WING TRAILING EDGE MASS ESTIMATION

The mass per unit area of the fixed section of the trailing edge is made of three terms

$$TERM1T = 1.482 \ \left(\frac{ULTN \ MTCR}{SW} \right)^{\frac{1}{4}} \left(\frac{SWTG}{BWN} \right)^{\frac{1}{2}} \qquad (A318)$$

$$TERM2T = \frac{0.0030223 \ ULTN \ MTCR \ SWTG}{SW \ BWN \ DTE^{\frac{1}{2}}} \left[\frac{SWTG}{BWN} - \right.$$

$$\left. \frac{(SWA + SWF)}{(BWA + BWF - BWBB)} \right]^2 \qquad\qquad (A319)$$

where DTE is the average depth of the rear spar and is given by

$$DTE = 1.54 \ \frac{SWTG \ RTW}{BWN} \qquad\qquad (A320)$$

$$TERM3T = 0.646 \ \left(\frac{SWTG}{SWTF} \right)^2 DTE^{\frac{1}{2}} \qquad\qquad (A321)$$

Thus the total mass of the fixed part of the wing trailing edge, MWT, is

$$MWT = FMWT\ SWTF\ (TERM1T + TERM2T + TERM3T) \qquad (A322)$$

where FMWT is a materials mass factor (for aluminium alloys FMWT = 1)

12.3.4. WING TRAILING EDGE FLAPS MASS ESTIMATION

The mass per unit area of the trailing edge flaps is made of two parts

$$TERM1F = 0.151\ \frac{MTCR}{SW}\ \sin^2 EQWFH\ DF^{0.5}\ SWF^{0.125} \qquad (A323)$$

where

$$DF = 1.54\ RTW\ CWFM \qquad (A324)$$

and EQWFH is the maximum deflection of the flap.

$$TERM2F = 0.384\ CWFN\ \frac{SWF^{\frac{1}{2}}}{DF} \qquad (A325)$$

Thus for the total mass of the flaps, MWF, we have

$$MWF = FMWT\ SWF\ (TERM1F + TERM2F) \qquad (A326)$$

The mass of the flap tracks, MWFK, is given by

$$MWFK = NWFK\ (0.000323\ ULTN\ MTCR\ \frac{SWF}{SW}\ LWFK^2\ CWFM^2 +$$

$$0.91) \qquad (A327)$$

where NWFK is the number of flap tracks and LWFK is the length of the flap tracks as a fraction of the wing chord.

12.3.5. WING (AILERONS, SPOILERS AND VARIOUS ATTACHEMENTS) MASS ESTIMATION

The mass of the ailerons is given by

$$MWA = FMWT \ SWA \left[\frac{0.00009795 \ VD^2}{AWA^{0.125}} + \frac{14.14 \ CWA \ \cos^2 QWA}{CWCA2^{0.5}} \right]$$

(A328)

and the mass of the spoiler, MWS, by

$$MWS = FMWT \ SWS \left(\frac{34.322 \ NWS^{0.125}}{AWSG^{0.5}} + 4.653 \right)$$ (A329)

The mass of various attachements, MWCX, is given by

$$MWCX = 0.0235 \ (MWB + MWL + MWT + MWF + MWA + MWS)$$

$$+ 18.14$$ (A330)

and the mass of various fairings, MWXF, by

$$MWXF = 0.488 \ SWN$$ (A331)

Therefore the total mass of the wing, MWC, is

$$MWC = MWB + MWL + MWT + MWF + MWA + MWS + MWFK +$$

$$MWCX + MWXF$$ (A332)

12.3.6. EMPENNAGE MASS ESTIMATION

The mass of the tailplane, MET, is given by

$$MET = FMET \ \frac{MET1K \ SETN \ VD^{MET2K}}{\left(\dfrac{LTCQM}{CWMG} \right)^{MET3K}} \tag{A333}$$

where

FMET   is a materials mass factor
MET1K   is a constant factor
MET2K   is a constant factor
MET3K   is a constant factor

The mass of the fin, MEF, is given by

$$MEF = FMEF \ \frac{MEF1K \ SEFN^{MEF2K} \ VD^{MEF3K}}{\left(\dfrac{LFCQM}{XFN} \right)^{MEF4K}} \tag{A334}$$

where

FMEF   is a materials mass factor
MEF1K   is a constant factor
MEF2K   is a constant factor
MEF3K   is a constant factor
MEF4K   is a constant factor.

12.4.   MASS ESTIMATION OF VARIOUS COMPONENTS (SUBROUTINE MASSEVAR)

The mass of the fuel system, MFS, is given by

$$MFS = 0.02 \ MTT \tag{A335}$$

The mass of the flying controls, MSC, is given by

$$MSC = MSCK + FMSCK \ MTTR \tag{A336}$$

where MSCK and FMSCK are constant factors.

The mass of the electrical systems, MSE, is given by

$$MSE = MSEK + FMSEK \ MTTR \qquad (A337)$$

where MSEK and FMSEK are constant factors.

The mass of air conditioning, MSA, is given by

$$MSA = MSAK + FMSAK \ MTTR \qquad (A338)$$

where MSAK and FMSAK are constant factors.

The mass of the aircraft paint, MPNT, is given by

$$MPNT = 0.5 \ SW \qquad (A339)$$

The mass of the hover control system, MDI, is given by

$$MDI = MHDG \ (XFN + BW) \qquad (A340)$$

where MHDG is a factor of mass per unit length.

13.   CENTRE OF GRAVITY (CG) (SUBROUTINE CEGRAV)

In this subroutine the moment arms of the aircraft components are estimated. The moment arms are measured from the aircraft nose.

13.1.   CG OF UNDERCARRIAGE

The gross mass of the nose undercarriage, including a proportion of the undercarriage hydraulics, MUNG, is given by

$$MUNG = MUN \left(1 + \frac{MUH}{(MUN + MUM)} \right) \qquad (A341)$$

and this mass is assumed to act at the mid-point of the length of the undercarriage bay. Thus the moment arm, XUNCG, is

$$XUNCG = XA + 0.5 \ LUNB \qquad\qquad (A342)$$

From the definition of MUNG the gross mass of the main undercarriage, MUMG, is given by

$$MUMG = MUN + MUM + MUH - MUNG \qquad (A343)$$

and this mass is assumed to act at a fraction RLPCW of the mean aerodynamic chord behind the quarter chord point of the wing. The moment arm, XUMCG, is

$$XUMCG = XWCQM + RLPCW \ CWMA \qquad (A344)$$

13.2.   CG OF FUSELAGE

The structural mass of the fuselage is assumed to act midway between the position of the centre of surface of the fuselage, XFXM, and the centre of volume of the fuselage, XFWM, in order to reflect the contributions of the shell and the internal structure respectively. Hence the moment arm of the structural mass of the fuselage, XFCG, is given by

$$XFCG = 0.5 \ (XFXM + XFWM) \qquad (A345)$$

To determine the centre of surface of the fuselage, XFXM, the fuselage is considered as a series of frustra of cones of height EXF(I), having radii derived from the local perimeter of the fuselage PFX(I). To determine the centre of volume, XFWM, the same procedure is followed but with radii derived from the local actual cross-sectional area of the fuselage OFX(I).

$$XFXM = \frac{\displaystyle\sum_{I=2}^{50} 0.5 \ [FX(I) - FX(I - 1)] \ EFX(I)}{\displaystyle\sum_{I=2}^{50} EFX(I)} \qquad (A346)$$

where

$$EFX(I) = 0.5 \ [\ PFX(I) + PFX(I-1) \ ] \ \left\{ \ \frac{1}{4\ \pi^2} \ [\ PFX(I) \right.$$

$$\left. - \ PFX(I-1) \ ]2 \ + \ EXF(I)2 \ \right\}^{\frac{1}{2}} \tag{A347}$$

and

$$XFWM = \frac{\displaystyle\sum_{I=2}^{50} \ 0.5 \ [\ FX(I) - FX(I-1) \ ] \ EFW(I)}{\displaystyle\sum_{I=2}^{50} \ EFW(I)} \tag{A348}$$

where

$$EFW(I) = \frac{EFX(I)}{3} \ \{ \ OFX(I) + OFX(I-1) + \{ \ OFX(I)$$

$$OFX(I-1)^{\frac{1}{2}} \ \} \tag{A349}$$

13.3.   WING CG

The mass of the structure of the wing is assumed to act at the centre of volume of the wing. The centre of volume is defined as a distance, RLWCC, after the mean quarter chord point of the wing, as a fraction of the mean aerodynamic chord. Using the wing thickness distribution the distance RLWCC can be shown to be

$$RLWCC = \frac{1}{56} \ \left\{ \ 13 - \frac{[\ 27 \ UW^2 + 1.75 \ AW \ (1 - UW^2)}{(1 + UW + UW^2)^2} \right.$$

$$\left. \frac{(1 + 4 \ UW + UW^2) \ \tan \ QWL}{(1 + UW + UW^2)^2} \ \right\} \tag{A350}$$

Hence the moment arm, XWCG, is

$$XWCG = XWCQM + RLWCC \ CWMA \tag{A351}$$

13.4.   EMPENNAGE CG

The structural masses of the fin and tailplane are assumed to act at the centre of volume of their nett surfaces. However, as these masses are smaller than the mass of the wing a simple approximation of the distance of the centre of volume behind the mean quarter point is considered adequate.

Thus for the tailplane moment arm, XETCG, we have

$$XETCG = XWCQM + LTCQM + \frac{CETB\ (1 + UETN + UETN^2)}{15\ (1 + UETN)} \tag{A352}$$

and for the fin moment arm, XEFCG

$$XEFCG = XWCQM + LFCQM + \frac{CEFB\ (1 + UEFN + UEFN^2)}{15\ (1 + UEFN)}$$

$$\tag{A353}$$

13.5.   INTERNAL WEAPON BAY CG

The internal weapon bay moment arm XWBCG is given by

$$XWBCG = XD + \frac{1}{2\ (MMRM + MSRM)}\ (\ LMRM\ MMRM +$$

$$LSRN\ MSRM) \tag{A354}$$

13.6.   REMOTE LIFT SYSTEM FRONT DUCT CG

The RLS system of front ducts is considered in two parts. The first is the horizontal one from the engine to the position behind the cockpit and the second the vertical

from the position behind the cockpit to the underface of
the fuselage.

For the first the moment arm, XRCG1, is

$$XRCG1 = XA + LCFL + \left(\frac{LRDG - XD}{2} \right) \qquad \text{(A355)}$$

For the second the moment arm, XRCG2, is

$$XRCG2 = XA + LCFL + \left(\frac{DRDE}{2} \right) \qquad \text{(A356a)}$$

and the arm of the RLS front duct nozzle is

$$XRCG3 = XRCG2 \qquad \text{(A356b)}$$

13.7.   FUEL TANKS CG

The centre wing fuel tank is rectangular in planform and
its CG lies at the centre of its volume. By integrating
the moment of the wing thickness distribution between the
front and the rear spars the distance of the CG of the
fuel tank in terms of body side chord, RWBC2, is found
to be

$$RWBC2 = \frac{3}{7} \left\{ \frac{7 \; (FCWR^{2.5} - FCWD^{2.5}) - 5 \; (FCWR^{3.5} - }{5 \; (FCWR^{1.5} - FCWD^{1.5}) - 3 \; (FCWR^{2.5} - } \right.$$

$$\left. \frac{FCWD^{3.5})}{FCWD^{2.5})} \right\} \qquad \text{(A357)}$$

Hence the moment arm of the central wing fuel tank,
XFWCG, is

$$XFWCG = XWLB + RWBC2 \; CWCB \qquad \text{(A358)}$$

where XWLB is the distance of the wing leading edge

from the aircraft nose at the body side.

The exposed wing fuel tank is of tapered planform. The distance of its centre of volume from the wing leading edge, LWBEF, is given by

$$
LWBEF = \frac{[\ 3\ CWCB\ RWBC^2\ (1\ +\ UWCNF)\ (1\ +\ UWCNF^2)}{4\ (1\ +\ UWCNF\ +\ UWCNF^2)}
$$

$$
\frac{+\ 0.5\ BWNF\ \tan\ QWL\ (1\ +\ 2\ UWCNF\ +\ 3\ UWCNF^2\ )\ ]}{4\ (1\ +\ UWCNF\ +\ UWCNF2)}
$$

(A359)

Thus the moment arm of the exposed wing fuel tank, XFECG, is

$$
XFECG\ =\ XWLB\ +\ LWBEF \tag{A360}
$$

For the central (fuselage) fuel tank, as it is wedge shaped, its centre of volume lies at one third of its length from the base. Hence the moment arm, XFCCG, is given by

$$
XFCCG\ =\ XD\ +\ \frac{1}{3}\ (XFN\ -\ XD\ -\ LPG) \tag{A361}
$$

The moment arm of the side fuel tanks, XFSCG, is given as input data.

14.   SORTIE PERFORMANCE (SUBROUTINE SORTIE)

Subroutine SORTIE estimates the fuel used by the aircraft flying a specified sortie.

A sortie is defined as comprising a number of legs. Each leg is assumed to be flown at constant height, Mach number and normal acceleration. Climbing and longitudinal acceleration are not considered as separate legs and their effects in fuel consumption are accounted by changing the range or the normal acceleration of relevant legs. Following are the steps taken in SORTIE.

Before the actual sortie, we have the estimation of the take-off fuel, MTTF. The take-off altitude and Mach number are given as well as the thrust setting of the engine. Subroutine ENGPER that provides the engine performance is called (subroutine ENGPER is described later) and the fuel consuption for take-off, MPFC, is established. Having as an external variable TTTF the run time for take-off the take-off fuel is given by

$$MTTF = TTTF\ MPFC \qquad\qquad (A362)$$

Following, there is the overall sortie iteration that goes through the same routine for each leg, for the estimation of the fuel spent. This overall sortie iteration comprises three iterations, namely the iteration for the estimation of the maximum sustained incidence and lift coefficient, the iteration for estimating the maximum sustained normal acceleration halfway along the leg in terms of used fuel and the iteration for the estimation of the actual , lift coefficient, incidence, thrust and fuel spent.

The overall sortie iteration starts with the reading of the external variables used in each leg. These are :

SLEG   is the leg range (km)
HTLEG   is the leg altitude (m)
MNLEG   is the leg Mach number
GNLEG   is the leg normal acceleration (g)
MLEG   is the mass that is lost during the leg
          (missiles, bombs, fuel tanks) (kg)
EQWFLG   is the flap setting of the leg (if flaps are
          used) (degrees)
TPG1   is an initial estimate of the thrust required
          in the leg. (N)

The iteration steps for the estimation of the maximum
incidence, ALH, and lift coefficient, CL2, that may
be sustained by the aircraft under full thrust, are
described below.

Step 1

$$ALH = \frac{CL1}{GCLA} \qquad (A363)$$

where CL1 is an initial estimate of the lift coefficient
and GCLA is the lift-curve slope of the aircraft
(provided by subroutine LIFT).

Step 2

$$CDV = \frac{(TPGC\ \cos\ ALH\ -\ V\ MPAC)}{Q\ SW} - CDOT \qquad (A364)$$

where

CDV	is the lift dependent-drag
TPGC	is the maximum gross thrust
MPAC	is the maximum air mass flow
V	is the air speed
Q	is the dynamic pressure
CDOT	is the total zero-lift drag coefficient

CDOT is provided by subrouine DRAG, TPGC and MPAC by
subroutine ENGPER and V and Q by subroutine ATMOS.

Step 3

$$CL2 = function\ (CDV) \qquad (A365)$$

As the lift-dependent drag is a function of drag we
use the inverse function to determine the lift
coefficient from the lift-dependent drag coefficient
that was estimated in step 2. The relation between the
lift coefficient and the lift-dependent drag coefficient
is found in subroutine DRAG.

Step 4

If CL2 is greater than the maximum CL or

$$\text{if} \qquad \left| ALH - \frac{CL2}{GCLA} \right| \leq 0.001 \text{ degrees} \qquad (A366)$$

then the iteration is complete.

Otherwise

$$CL1 = CL1 + 0.93 \ (CL2 - CL1) \tag{A367}$$

and the iteration is resumed.

A relaxation factor value 0.93 was found appropriate.

The second iteration for the estimation of the maximum normal acceleration, GNH, that the aircraft can sustain, when half of the fuel needed in the leg is consumed, is described below.

Step 1

$$GNH = \frac{(\ Q \ SW \ CL2 + TPGC \ \sin ALH \ )}{G \ (MASS - 0.5 \ MPFB1)} \tag{A368}$$

where

MASS   is the total mass of the aircraft
        at the start of the leg
MPFB1   is an initial estimate of the fuel
        needed for the leg
G   is the acceleration due to gravity
        (subroutine ATMOS).

Step 2

$$RT1 = \frac{SLEG \ 1000}{V} \tag{A369}$$

where RT1 is the duration of the leg.

Step 3

$$MPFB2 = \frac{MPFC \ RT1}{(GNH^2 - 1)} \tag{A370}$$

where MPFC is the maximum fuel mass flow (subroutine
ENGPER) and MPFB2 the fuel spent in the leg.

If GNH ≤ 1 or if |MPFB1 - MPFB2| ≤ 0.01 the
iteration is complete.

Otherwise

$$MPFB1 = MPFB1 + 0.96 \ (MPFB2 - MPFB1) \qquad (A371)$$

and the iteration is resumed.

A relaxation factor value of 0.96 was found appropriate.

The last iteration is for the estimation of the actual
lift coefficient, incidence, thrust and fuel spent is
described below.

Step 1

$$MPFB2 = \frac{SLEG \ 1000}{V} \ MPF \qquad (A372)$$

where MPF is the fuel mass flow obtained from the
subroutine ENGPER and corresponds to the initial value
for thrust, TPG1, that was usd as input to the
subroutine call.

Step 2

$$CL = \frac{GN \ G \ (MASS - 0.5 \ MPFB2) - TPG1 \ \sin AL}{Q \ SW} \qquad (A373)$$

where

GN is the specified normal acceleration for the leg
and AL an initial estimate for the incidence.

Step 3

$$AL = \frac{CL}{GCLA} \qquad (A374)$$

Step 4

$$TPG2 = \frac{V \; MPA \; + \; SW \; CDTOT}{\cos \; AL} \qquad \text{(A375)}$$

where

CDTOT is the total aircraft drag coefficient provided
by subroutine DRAG.

If $|MPFB1 - MPFB2| \leq 1$ or $|TPG1 - TPG2| \leq 10$
the iteration is complete.

Otherwise

$$MPFB1 = MPFB2 \qquad \text{(A376)}$$

$$TPG1 = TPG1 + RTK \; (TPG2 - TPG1) \qquad \text{(A377)}$$

and the iteration is resumed.

The value of the relaxation factor RTK depends on the
input data. An initial value of 0.6 is used and if
convergence is not reached after 25 iterations this
value is reduced to 0.1.

Due to often convergence problems in this third
iteration, a limit of 50 iterations was set and then
the average of the two last values is assumed
for the fuel consumed in the leg.

After the overall sortie iteration the total fuel
mass, MPFB2T, consumed in the sortie is calculated
and to this the take-off, MTTF, and landing, MTLF,
fuel masses are added. The landing fuel mass being
estimated as a percentage, FMTLF, of total fuel mass.

According to the specifications provided, an aircraft
mass for the point performance calculations, MTTPP, is
estimated. Usually, this mass does not include take-off
fuel mass and any fuel spent in any legs prior to the
manoeuvre legs specified.

15.   ATMOSPHERIC PROPERTIES (SUBROUTINE ATMOS)

This subroutine calculates standard atmospheric properties and acceleration due to gravity for any altitude .

16.   ENGINE PERFORMANCE

The engine performance is given in table form. The data provided include net thrust, gross thrust fuel mass flow, exit nozzle area and air mass flow for a range of altitudes, Mach numbers and power settings. The method used in establishing the required values is a three point interpolation.

The three subroutines used are :

ENGPER which is the main one, calls the other two and does all the intermediate stages of the evaluation.
ENGRE which is reading all the input data in table form and establishes the points of interpolation.
INTER which performs the actual interpolation.

16.1.   ENGINE PERFORMANCE EVALUATION (SUBROUTINE ENGPER)

Two ways of engine performance evaluation are available (ways should not be confused with modes). In the first the altitude, Mach number and power setting are known and the thrust, air and fuel mass flows and nozzle exit area are sought. In the second the altitude, the Mach number and the thrust are known and the power setting, the air and mass flows and the nozzle exit area are sought.

Two modes of engine performance evaluation are available, MODE = 1 and MODE = 3. In MODE = 3 maximum thrust is requested. All other conditions fall under MODE = 1.

The method of communicating the engine performance requirements from any part of the code to subroutine ENGPER, the following four variables are used :

HTEN   the altitude
MNEN   the Mach number
MODE   defined above
XV   the input variable for either power setting
          or thrust (as described above)

In return ENGPER provides the following :

R1   the output variable for either thrust or
             power setting (as described above)
MPF   fuel mass flow
MPA   air mass flow
OPJ   nozzle exit area.

As the input data are altitude and Mach number - the
power setting (or the thrust) is ignored because it has a
standard number of values for each Mach number value of
each altitude value - we have four cases of input data :

In the first case both altitude and Mach number input
values exist in the available data. There is no need
for interpolation, ENGPER just reads the data. In the
second case the Mach number input value exists in
the available data but not the altitude input value.
ENGPER interpolates only in respect to altitude.
The third case is identical with the second with the
difference that altitude data exists while Mach number
data not.The fourth, and most common case, is when both
altitude and Mach number input values do not exist in the
available data. ENGPER interpolates for altitude and Mach
number.The above four cases are managed in ENGPER by the
control numbers NNN1 and NNN2.

Examining closely the fourth case we have the
following procedure. ENGPER calls ENGRE to read the
engine performance data file. Then ENGRE reads the
values for altitude and all the corresponding other
variables - thrust for example - nearest and above and
below to the required input value (HTEN) for altitude. A
third set is obtained by considering the zero altitude
or any other suitable if the input value is near zero.
These values are read for three Mach number values,
which in turn are taken nearest and above and below the
required input value for Mach number (MNEN) and the
third usually zero. These sets are interpolated by
ENGPER and INTER to provide the required thrust
corresponding to the input altitude and Mach number
values. In all these interpolations the altitude and
Mach number variables are the independent variables
and thrust, fuel mass flow, air mass flow and nozzle exit
area the dependent.

To illustrate the procedure with a simple example,
assume that the available data exist for altitude
values every one thousand meters and Mach numbers
every two. That is altitude values of 0, 1000, 2000,
3000, 4000, 5000 metres and for each altitude Mach
number values of 0, 2, 4, 6, 8, 10. Assume the input
data is 2500 metres and 5 Mach number. An interpolation
between the values of thrust for example, corresponding
to altitude 0, 2000 and 3000 for Mach number 0 will
take place to give a value for thrust for an altitude

take place to give a value for thrust for an altitude
of 2500 and Mach number 0. With the same procedure we
have values for thrust for an altitude of 2500 m and
Mach number 4 and an altitude of 2500 and Mach number
6. Finally these three values are interpolated to give
one value for thrust for an altitude of 2500 and Mach
number 5.

Having ten power settings the interpolation is not
for single values but for sets of ten values. At the
end we have, for the altitude and Mach number specified,
sets of values of ten for thrust, fuel mass flow, air
mass flow and nozzle exit area corresponding to the ten
power settings. Depending on whether the power setting
or the thrust is the independent - the input - variable
the appropriate three values out of the ten are selected
and the final interpolation takes place.

16.2.   ENGINE PERFORMANCE DATA READING (SUBROUTINE
         ENGRE)

This subroutine reads the engine performance data given
in table form. Subsequently, it finds the three points
of interpolation corresponding to each input value
provided by ENGPER. Control numbers NED1 - NED32
define the position of all interpolation values.

16.3.   INTERPOLATION (SUBROUTINE INTER)

This subroutine performs the interpolation. It
receives from ENGPER sets of three values for the
independent (XX1, XX2, XX3) and dependent (YY1, YY2,
YY3) variables plus the input value for the independent
variable (XINT) and returns the interpolated value for
the dependent variable (YINT).

17.   LIFT-CURVE SLOPE (SUBROUTINE LIFT)

This subroutine evaluates the lift-curve slope over
the Mach number regime of the aircraft.

The variation of lift coefficient with incidence is
assumed to be linear over the range of incidence for
which it is necessary to calculate aircraft performance.

For Mach numbers ≤ 0.8 the lift-curve slope, GCLWD, for
the aerofoil section is given by

$$GCLWD = FREEF\ [\ 2\ \pi\ +\ 4.7\ RTW\ (1\ +\ 0.215\ FQWTI\ RTW)\ ]$$

$$(A378)$$

where FREEF is a Reynolds effects factor and FQWTI
is a factor, for a particular family of airfoils,
that relates the trailing edge included angle to the
thickness to chord ratio, RTW, of the section.

The lift-curve slope for the wing, GCLA, is the given
by

$$GCLA = \frac{GCLWD}{\left[\ \dfrac{GCLWD}{\pi\ AW\ (1\ +\ FWLD)}\ +\ (GCLK4\ +\ 1\ -\ MN^2)\ \right]}$$

$$(A379)$$

where FWLD is a factor for a non-elliptical lift
distribution and

$$GCLK4 = (\ \frac{GCLWD}{\pi\ AW}\ )^2\ +\ \tan^2\ QW2 \qquad (A380)$$

A critical Mach number, MCR, is defined above which the
leading edge flow becomes supersonic

$$MCR = \frac{1}{\cos\ QWL} \qquad (A381)$$

For Mach numbers $\geq$ MCR linear theory is used for the
wing lift-curve slope, GCLA

$$GCLA = \frac{4}{(MN^2\ -\ 1)^{\frac{1}{2}}} \qquad (A382)$$

The value of four in the above lift-curve slope relation
most closely follows the characteristics of the wing
in question.

For Mach numbers between 0.8 and MCR a cubic variation
of GCLA with Mach number, MN, is assumed with the
gradient and value of GCLA matched at MN = 0.8 and
MN = MCR to the values obtained from the two previous
expressions.

Thus

$$GCLA = GCLK0 + GCLK1 \ (MN - 0.8) + GCLK2 \ (MN - 0.8)^2$$

$$+ \ GCLK3 \ (MN - 0.8)^3 \qquad \text{(A383)}$$

where

$$GCLK0 = \frac{GCLWD}{\left[\dfrac{GCLWD}{\pi \ AW} + (GCLK4 + 1 - 0.64)^{\frac{1}{2}} \right]} \qquad \text{(A384)}$$

$$GCLK1 = \frac{0.8 \ GCLK0^2}{GCLWD \ (GCLK4 + 1 - 0.64)^{\frac{1}{2}}} \qquad \text{(A385)}$$

$$GCLK2 = \frac{1}{(MCR - 0.8)} \left[\frac{3 \ (4 \ \cot \ QWL - GCLK0)}{(MCR - 0.8)} - \right.$$

$$\left. 2 \ GCLK1 + \frac{4 \ \cot^2 \ QWL}{\sin \ QWL} \right] \qquad \text{(A386)}$$

$$GCLK3 = \frac{1}{(MCR - 0.8)} \left[GCLK1 - \frac{4 \ \cot^2 \ QWL}{\sin \ QWL} - \right.$$

$$\left. \frac{2 \ (4 \ \cot \ QWL - GCLK0)}{(MCR - 0.8)} \right] \qquad \text{(A387)}$$

For the lift-curve slope of the whole aircraft

$$FIKN = \frac{2\,\pi\,(0.5\;BFD)^2}{GCLW\;SWN} \tag{A388}$$

where BFD is a typical width of the fuselage ahead of the wing.

For the wing-body interference factor, FIWBW, we have

$$FIWBW = (\frac{BFD}{BW} + 1\,)^2 \tag{A389}$$

For the tail interference it is assumed a tailplane nearly at the same height from the ground with the wing and having the same airfoil section type with the wing.

Hence for the lift-curve slope of the aircraft, GCLA, we have

$$GCLA = GCLW\;(FIKN + FIWBW)\;\frac{SWN}{SW}\; +$$

$$GCLW\;FIWBW\;(1 - GDW)\;RDP\;\frac{SETN}{SW} \tag{A390}$$

where RDP is a downwash factor, GDW is given by

$$GDW = \frac{GCLW}{\pi\;AW}\;\left[\frac{LTCQM^2 + BW^2 + LTCQM\;DKW}{LTCQM\;DKW}\right] \tag{A391}$$

and DKW is given by

$$DKW = \left[\;(\frac{BW}{2}\,)^2 + LTCQM^2\;\right]^{\frac{1}{2}} \tag{A392}$$

The first term of the equation for GCLA is for the

The first term of the equation for GCLA is for the fuselage and wing-fuselage interference and the second for the tail interference.

18.   CRITICAL LIFT COEFFICIENT, DK2 FACTOR IN
        LIFT-DEPENDENT DRAG AND MAXIMUM LIFT
        COEFFICIENT READING (SUBROUTINE LIFTCO)

This subroutine linearly interpolates the available data of critical lift coefficient (CLC), DK2 factor in lift-dependent drag estimation and maximum lift coefficient (CLMAX) versus Mach number to find the values corresponding to the required Mach number.

19.   DRAG ESTIMATION (SUBROUTINE DRAG)

19. 1.   DRAG COEFFICIENT AT ZERO LIFT

The components of the drag coefficient at zero lift are estimated as functions of Mach number by separate methods valid for subsonic, transonic and supersonic speeds. Fig.A14 defines the principal components of the drag coefficient and some of the parameters associated with the estimation methods.

For Mach numbers up to 0.8 the zero-lift drag coefficient of the wing is given by

$$CDOW = CFR\ RCDW\ \frac{SWN}{SW} \tag{A393}$$

where CFR is the skin friction for flat plates, and is given by the greater of

$$CFR = 0.49\ [\log_{10}\ (RND1\ RCWCD\ CWMN)^{-0.2625} \tag{A394}$$

and

$$CFR = 0.49\ [\log_{10}\ (RND1\ RCWCD\ CWMN)^{-0.2625}$$

$$\left\{ \frac{RND1\ HTR\ [0.85\ \exp(-0.30494\ MN^2)\ +\ 0.15]\ -52}{\{5.625\ \log_{10}(RND1\ RCWCD\ CWMN\ -\ 6.075]^2} + \right.$$

$$\left. 0.936 \right\} \tag{A395}$$

In this equation HTR is the roughness height and RND1 is the Reynolds number per unit metre

$$RND1 = \frac{AH\ MN}{NU} \tag{A396}$$

where NU is the kinetic viscosity.

RCWCD is a weighting factor on the mean chord to account for the variation of Reynolds number across the span, and is defined by assuming that the skin friction varies as -1/6 power of Reynolds number.

$$RCWCD = \frac{1.18658}{(UWCN + 1)} \left[\frac{UWCN^2 - 1}{UWCN^{1.83333} - 1} \right] \qquad (A397)$$

In equation A393 RCDW is twice the form factor and is given by

$$RCDW = 2 \ (3 \ RTW \ \cos^2 \ QW2 + 1) \qquad (A398)$$

An additional allowance of 10 % of CDOW is made for the drag due to control gaps and leaks.

Similar expressions are used for the estimation of the zero-lift drag of the empennage. For the tailplane

$$CDOET = CFR \ RCDET \ \frac{SETN}{SW} \qquad (A399)$$

where CFR is obtained from eqn A395, with CWMN replaced by CETM, and RCWCD replaced by RCETD.

RCETD is found from eqn A397 with UWCN replaced by UETN. RCDET is found from eqn A398 with RTW and QW2 replaced by RTET and QET2 respectively.

For the fin

$$CDOEF = CFR \ RCDEF \ \frac{SEFN}{SW} \qquad (A400)$$

where CFR is obtained from eqn A395, with CWMN replaced by CEFM, and RCWCD replaced by RCEFD.

RCEFD is found from eqn A397 with UWCN replaced by UEFN. RCDEF is found from eqn A398 with RTW and QW2 replaced by RTEF and QEF2 respectively.

An additional allowance of 20 % of CDOET and CDOEF is made for the drag due to control gaps and leaks.

The zero-lift drag of the fuselage, up to Mach number of 0.8 is given by

$$CDOF = CFR\ RCDF\ \frac{WFX(50)\ -\ WFG3\ -\ WCWSC\ -\ WCCAN}{SW} \qquad (A401)$$

where WFX(50) is the fuselage total surface area and WCWSC and WCCAN are the surface areas of the windscreen and canopy respectively.

The footprint area of the flying surfaces, WFG3, is calculated by integrating the thickness distribution of the aerofoil(s) of the flying surfaces (eqn A195). It is given by

$$WFG3 = 0.69282\ (2\ RTW\ CWCB^2 + 2\ RTET\ CETB^2 + RTEF$$

$$CEFB^2) \qquad (A402)$$

CFR is obtained from eqn A395 with CWMN replaced by XF(50) and RCWCD replaced by RLFD.

RLFD is found from

$$RLFD = \left\{ \left[\left(1 - \frac{XF(9)}{XF(50)} \right)^{-1/6} - 1 \right] \left(\frac{2\ HII\ +\ 4\ BII}{PFX(10)} \right) \right.$$

$$\left. +\ 1 \right\}^{-6} \qquad (A403)$$

The form factor RCDF is defined as

$$RCDF = 0.9987 + 0.3378\ RDFL + 3.534\ RDFL^2 -$$

$$3.933\ RDFL^3 \qquad (A404)$$

where

$$RDFL = \frac{2}{XF(50)} \left(\frac{OFXH\ -\ OII}{\pi} \right)^{1/2} \qquad (A405)$$

and OFXH is the maximum actual cross-sectional area of the fuselage.

The zero-lift drag of the canopy, up to Mach numbers of 0.8, is given by

$$CDOC = CFR \ RCDC \ \frac{(WCWSC + WCCAN)}{SW} \tag{A406}$$

where CFR is obtained from eqn A395 with (RCWCD CWMN) replaced by the length of the canopy LCCAN. RCDC is given by

$$RCDC = \left(0.5 - \frac{XF(14)}{XF(50)} \right) \left[\frac{2.93}{\dfrac{LCCAN}{RCCANC} - 2.8} + 3.8 \right]$$

$$+ \ 1.35 \tag{A407}$$

where RCCANC is canopy radius at fuselage station C.

The drag due to the gun port is given by

$$CDGC = \frac{0.0046}{SW} \tag{A408}$$

The subsonic drag of the boundary layer diverter is given by

$$CDIV = \frac{0.25 \ OVI}{SW} \tag{A409}$$

The supersonic afterbody drag of the fuselage, which includes contributions from the boattail and base is given by

$$CDB = \left[\frac{0.05 \ (OFX(50) - OPJ)}{(OFX(38) - OPJ)} + 0.014 \right] \frac{OFX(38)}{SW} \tag{A410}$$

where OFX(38) is the actual fuselage cross-sectional area at the engine compressor inlet and OPJ is the nozzle exit area.

The drag of the undercarriage when extended, CDUT, is assumed to be

$$CDUT = 0.02 \qquad \text{(A411)}$$

An allowance of 15 % of the drag of the main components of the aircraft is made for the interference effects between components and for small excrescences and surface irregularities not included in the equivalent roughness (eqn A395). Adding the component drag coefficients and the allowance specified above, and the allowances specified for each component, a basic drag coefficient is obtained for Mach numbers less than 0.8

$$CDOV08 = 1.25\ CDOW + 1.35\ (CDOET + CDOEF) +$$
$$1.15\ CDOFG \qquad \text{(A412)}$$

where

$$CDOFG = CDOF + CDOC + CDIV + CDGC \qquad \text{(A413)}$$

The value of this drag coefficient at 0.8 Mach, CDOV08, is scaled to provide an estimate of the basic drag at higher, subsonic and supersonic, Mach numbers

$$CDOV = CDOV08\ (1.21784 - 0.300627\ MN + 0.0342234\ MN^2\ )$$
$$+ ECCDIV \qquad \text{(A414)}$$

where the additional term is an increment to the drag of the diverter to account for compressibility effects. This is defined for Mach $\leq$ 1

$$ECCDIV = 0.25\ \frac{OVI}{SW}\ (176 - 600\ MN + 675\ MN^2 - 250\ MN^3)$$

$$\text{(A415)}$$

and for Mach > 1

$$\text{ECCDIV} = 0.25 \ \frac{\text{OVI}}{\text{SW}} \tag{A416}$$

The drag due to compressibility effects at zero lift, which is added to the basic drag calculated by the methods described above, is assumed to start with a gradual, quadratic, rise defined by the Mach number, MDD, at which the drag coefficient is 0.002 above the CD0V08 value, and the gradient dCd/DMN equals one. With these assumptions it can be shown that the drag increase begins at a Mach number of (MDD - 0.04). MDD is defined by

$$\text{MDD} = 0.945 - 0.006 \left[7 - 0.01 \ \frac{\text{QW4}}{\text{RTW}} \right]^{1.8} \tag{A417}$$

for (QW4/RTW) $\leq$ 700 where QW4 is measured in degrees for this correlation, or

$$\text{MDD} = 0.945 \tag{A418}$$

for (QW4/RTW) > 700

The Mach number at which the drag rise begins will also be dependent on the lift coefficient, CL, and is found from

$$\text{MD} = \text{MDD} - \text{FMD1 (CL} - \text{CLDES)}^{1.5} + \text{FMD2} \tag{A419}$$

where CLDES is the design lift coefficient in the high subsonic/transonic regime, and FMD1 and FMD2 are constants, the later providing an allowance for improvements in aerodynamic technology. If CL < CLDES then the second term of eqn A419 is ignored.

The wave drag at higher Mach numbers is estimated by a series of curve fits to a set of charts that correlate measured supersonic drag with the major geometric parameters.

For a wing a function of the thickness to chord ratio is first defined

$$\text{RTWD} = \text{RTW} \ \{ \ [1.726 \ \exp \ (-2.25 \ \text{QW2}^2) - 0.6] \ \log_{10} \text{AWN}$$

$$+ \ 1.25 \ \cos \ \text{QW2} \ \} \tag{A420}$$

The wave drag of the wing at Mach = 1 is then

$$CDWW1 = RTWD^{1.666} \frac{SWN}{SW} \qquad \text{(A421)}$$

and at Mach = 1.3 is

if $RTWD^{2/3} \leq 0.3$

$$CDWW2 = CDWW1 \left[\frac{0.07882}{RTWD^{2/3}} + 0.84142 \right] \qquad \text{(A422)}$$

or if $RTWD^{2/3} > 0.3$

$$CDWW2 = CDWW1 \left\{ 0.5124 \left[5.318 - \left(\frac{0.3}{RTWD^{0.666}} - \right. \right. \right.$$
$$\left. \left. \left. - 2.0521 \right)^{2} \right]^{\frac{1}{2}} + 0.0526 \right\} \qquad \text{(A423)}$$

For the tailplane the function of the thickness to chord ratio, RTETD, is defined using eqn A420 with RTW replaced by RTET, QW2 replaced by QET2 and AWN replaced by AETN. Eqns A421 and A422 are then used to find the wave drag at Mach = 1 (CDTW1) and Mach = 1.3 (CDTW2) respectively. In these eqns RTWD is replaced by RTETD and SWN by SETN.

For the fin the function of the thickness to chord ratio, RTEFD, is defined using eqn A420 with RTW replaced by RTEF, QW2 replaced by QEF2 and AWN replaced by AEFN. Eqns A421 and A422 are then used to find the wave drag at Mach = 1 (CDFIW1) and Mach = 1.3 (CDFIW2) respectively. In these eqns RTWD is replaced by RTEFD and SWN by SEFN.

The wave drag of the fuselage is considered in terms of contributions from the forebody and the afterbody. The wave drag of the forebody comprises the drag of the nose section as far after as the inlet plane of the intake diffuser, which for Mach = 1 is given by

$$CDFW1 = \frac{OFX(9)}{SW} [0.89 - 0.07\ RLDFS] [0.5641 - 0.2696$$

$$RLDFS + 0.04822 \ RLDFS^2 - 0.00312 \ RLDFS^3 \ ]$$

$$(A424)$$

and for Mach = 1.3

when RLDFS > 2

$$CDFW2 = \frac{OFX(9)}{SW} \ 0.7235 \ RLDFS^{-1.7448} \qquad (A425)$$

or when RLDFS ≤ 2

$$CDFW2 = \frac{OFX(9)}{SW} \ [0.592533 - 0.188329 \ RLDFS] \qquad (A426)$$

In these equations RLDFS is the fineness ratio for the nose section

$$RLDFS = \frac{XF(9)}{\left[\dfrac{OFX(9)}{\pi} \right]^{\frac{1}{2}}} \qquad (A427)$$

The second contribution to the drag of the forebody comes from the region from the inlet intake diffuser plane back to the maximum cross-sectional area of the fuselage. A fineness ratio for this region is defined as

$$RLDFI = \frac{XFOH - XF(10)}{2 \left[\dfrac{OFXH - OFX(10)}{\pi} \right]} \qquad (A428)$$

where XFOH is the distance from the nose, at which the maximum actual fuselage cross-sectional area, OFXH, occurs. Eqns A424, A425 and A426 are used to determine the wave drag contribution at Mach = 1, CDFW3, and at Mach = 1.3, CDFW4, by replacing RLDFS by RLDFI and OFX(9)

by (OFXH - OFX(10)). If the maximum cross-sectional area occurs at the inlet plane of the intake diffuser, then these wave drag terms will be zero.

The wave drag of the afterbody is calculated in three stages. An equivalent afterbody with a pointed tail is defined first by extrapolating the area distribution curve a length ELFT rearwards. ELFT is given by

$$ELFT = \frac{EXF(47) + EXF(48) + EXF(49) + EXF(50)}{\left\{ \left[\dfrac{OFX(46)}{OFX(50)} \right]^{\frac{1}{2}} - 1 \right\}} \qquad (A429)$$

The fineness ratio of this equivalent body is then

$$RLDFT = \frac{0.5 \, [XF(50) - XFOTH + ELFT]}{\left[\dfrac{OFXTH}{\pi} \right]^{\frac{1}{2}}} \qquad (A430)$$

where OFXTH is the maximum actual fuselage cross-sectional area of the afterbody and XFOTH is the distance from the nose at which it occurs. At Mach = 1 the drag of the equivalent afterbody is found from

$$CDFW5 = \frac{OFXTH}{SW} \{0.01 + 0.219 \exp [0.6105 (1.72 - RLDFT)] \} \qquad (A431)$$

and at Mach = 1.3

$$CDFW6 = \frac{OFXTH}{SW} \{0.01 + 0.3838 \exp [-0.415 \, RLDFT] \} \qquad (A432)$$

The interference effect of the front fuselage on the drag of the afterbody is next considered. The increment in wave drag is

$$ECDFT = - \frac{OFXTH}{4\ SW\ RLDFT^2}\ \left[\left(\frac{2\ RLDFT}{XFOHS} \right) \left(\frac{OFXHS}{\pi} \right)^{\frac{1}{2}} \right.$$

$$\left\{ 1.575 - \left[0.678 + \frac{1.954\ (XFOTH - XFOHS)}{(XF(50) - XFOTH + ELFT)} \right]^{-1} \right.$$

$$\left. - 0.1 \right\} \tag{A433}$$

where OFXHS is the maximum nett fuselage cross-sectional area which occurs at a distance XFOHS from the nose. The effect of truncating the body by removing the pointed tail is estimated by applying the factor

$$RCDFT = 1.0 - 0.0155\ ROFNMA^2 - 4.160\ ROFNMA^3 +$$

$$3.175\ ROFNMA^4 \tag{A434}$$

where ROFNMA is the area ratio OFX(50)/OFXTH

Using eqns A424 to A434 the drag coefficient for the afterbody at Mach = 1, CDFW7, is given by

$$CDFW7 = RCDFT\ (CDFW5 + ECDFT) \tag{A435}$$

and at Mach = 1.3

$$CDFW8 = RCDFT\ (CDFW6 + ECDFT) \tag{A436}$$

The wave drag in the canopy is calculated as the sum of contributions from front and rear sections. The drag of the front part of the canopy at Mach = 1, CDCW1, is found from eqn A424 with OFX(9) replaced by $(0.5\ \pi\ RCCANC^2)$ and RLDS replaced by (0.28 LCCAN/RCCANC). At Mach = 1.3 the drag CDCW2 is obtained from eqn A425 with the same parameters replaced.

The drag of the rear part of the canopy at Mach = 1, CDCW3, and at Mach = 1.3, CDCW4, is found from eqns A431 and A432 with OFXTH replaced by $(0.5\ \pi\ RCCANC^2)$ and RLDFT replaced by (0.85 LCCAN/RCCANC) .

The drag coefficient of the complete canopy at Mach = 1,
CDCW5, is given by

$$CDCW5 = 2.38 \ (0.43 \ CDCW1 + CDCW3) \qquad \text{(A437)}$$

and at Mach = 1.3

$$CDCW6 = 1.1 \ (0.6 \ CDCW2 + CDCW4) \qquad \text{(A438)}$$

The constants in these equations allow for the mutual
interference effects of wave drag of the front and rear
parts of the canopy.

The total wave drag of the basic aircraft is obtained as
the sum of the components determined above. At Mach = 1

$$CDW1 = CDWW1 + CDTW1 + CDFIW1 + CDFW1 + CDFW3 + CDFW5$$
$$+ \ CDCW5 \qquad \text{(A439)}$$

$$CDW2 = CDWW2 + CDTW2 + CDFIW2 + CDFW2 + CDFW4 + CDFW6$$
$$+ \ CDCW6 \qquad \text{(A440)}$$

The wave drag coefficient of the aircraft is assumed to
remain constant for Mach numbers greater than 1.3. To
define the variation of wave drag with Mach number in the
range MD $\leq$ MN $\leq$ 1.3 some empirical factors from
measurements of aircraft drag, are used. The gradient of
the wave drag coefficient with Mach number, at Mach = 1,
is given by

$$GCDTW = 55.054 \ (CDW2 - CDW1) \qquad \text{(A441)}$$

In the range MD $\leq$ MN $\leq$ 1 a cubic variation of wave drag
with Mach number is assumed

$$CDWT = CDTK0 + CDTK1 \ MN + CDTK2 \ MN^2 + CDTK3 \ MN^3$$

$$\text{(A442)}$$

where

$$CDTK3 = \frac{(1 - MD)\ (GCDTW + 0.1) - 2\ CDTW1 - 0.002}{(1 - MD)^3}$$

<div align="right">(A443)</div>

$$CDTK2 = \frac{0.5\ (GCDTW - 0.1)}{(1 - MD)} - 1.5\ CDTK3\ (1 + MD)$$

<div align="right">(A444)</div>

$$CDTK1 = GCDTW - 2\ CDTK2 - 3\ CDTK3 \qquad (A445)$$

$$CDTK0 = CDW1 - CDTK1 - CDTK2 - CDTK3 \qquad (A446)$$

In the range $1 < MN \leq 1.3$ the variation of wave drag with Mach number is given by

$$CDWT = (CDW2 - CDW1) \left\{ \frac{1 - \left(\dfrac{1.3 - MN}{0.3}\right)^2}{1 - \left(\dfrac{1.3 - MN}{0.3}\right)^2} \right\} + CDW1$$

<div align="right">(A447)</div>

The drag at zero lift due to the spillage of airflow around the outside of the intake cowl is estimated by methods for the separation drag at subsonic speeds, and for the wave drag at supersonic speeds. In the Mach number range $1 \leq MN \leq 1.1$ contributions to drag are assumed to arise from both sources. The ratio of the intake capture area to the area of the intake stream tube at infinity is first calculated.

$$ROIID = \frac{MPA}{RO\ V\ OII}$$

<div align="right">(A448)</div>

If ROIID is greater than unity, then it is assumed that the spillage drag is zero. The spillage drag at subsonic speeds is assumed to be proportional to the pre-entry drag

$$CDS = \frac{OII\ RCDK\ CDPRE}{SW}$$

<div align="right">(A449)</div>

there CDPRE is the pre-entry drag, and RCDK is a constant
for a particular type of intake, typically in the range
0.2 to 0.6 depending on the sharpness of the intake lips.
The pre-entry drag is given by

$$\text{CDPRE} = 2 \ \text{ROIID} \left(\frac{\text{ROIID}}{\text{RRIID}} - 1 \right) + \frac{(\text{RRIID}^{1.4} - 1)}{0.7 \ \text{MN}^2} \tag{A450}$$

where RRIID is the ratio of the air density at the inlet
of the intake to the freestream air density. This may be
calculated using the following expression derived from
the energy equation

$$\text{RRIID}^{2.4} - (1 + 0.2 \ \text{MN}^2) \ \text{RRIID}^2 + 0.2 \ \text{MN}^2 \ \text{ROIID}^2 = 0 \tag{A451}$$

Newton's method, with a starting value of RRIID = 1.5,
provides a rapid method of solution that converges on the
upper root which corresponds to a decelerating flow.

The spilliage drag at supersonic speeds is calculated
using the expression

$$\text{CDS} = \frac{5 \ \text{OII}}{3 \ \text{SW}} \left[1 - \frac{1}{\text{MN}^2} \right] (1 - \text{ROIID}) \tag{A452}$$

In the Mach range $1 \le \text{MN} \le 1.1$ a composite form of eqns
A449 and A452 is used

$$\text{CDS} = \frac{\text{OII}}{\text{SW}} \left\{ 10 \ (1.1 - \text{MN}) \ \text{RCDK} \ \text{CDPRE} + \frac{5}{3} \left[1 - \frac{1}{\text{MN}^2} \right] \right.$$

$$\left. (1 - \text{ROIID}) \right\} \tag{A453}$$

19. 2.   LIFT-DEPENDENT DRAG COEFFICIENT

The lift-dependent contribution to the drag coefficient, CDV, is assumed to have a parabolic variation with the lift coefficient, CL. Two regions are defined by three parameters, K1, CLC and K2, and are joined by a cubic transition region. For $CL \leq CLC - 0.01$

$$CDV = \frac{K1\ CL^2}{\text{Đ AW}} \qquad\qquad (A454)$$

For $CLC - 0.01 < CL < CLC + 0.01$

$$CDV = \frac{1}{\text{Đ AW}}\ (CDVK0 + CDVK1\ CL^2 + CDVK2\ CL^4 +$$

$$+ CDVK3\ CL^6) \qquad\qquad (A454)$$

For $CL \geq CLC + 0.01$

$$CDV = \frac{1}{\text{Đ AW}}\ [K2\ CL^2 + (K1 - K2)\ (CLC - 0.01)^2\ ]$$

$$(A455)$$

To match equations (A453) and (A454) at (CLC - 0.01) and (CLC + 0.01) respectively, the coefficients in equation (A454) are

$$CDVK3 = \frac{(K1 - K2)}{0.32\ CLC^3} \qquad\qquad (A456)$$

$$CDVK2 = \frac{(K2 - K1)}{0.32\ CLC}\ \left(\ 7 + \frac{0.0003}{CLC^2}\ \right) \qquad\qquad (A457)$$

$$CDVK1 = K1 - 2\ CDVK2\ (CLC - 0.01)^2 - 3\ CDVK3$$

$$(CLC - 0.01)^4 \qquad\qquad (A458)$$

$$CDVK0 = (CLC - 0.01)^2 [K1 - CDVK1 - CDVK2$$

$$(CLC - 0.01)^2 - CDVK3 (CLC - 0.01)^4] \qquad (A459)$$

The parameter K1 is estimated by using a series of curve fits to a set of charts that correlate measurements of the lift-dependent drag coefficient over a range of Mach numbers, with the major geometric parameters. In the subsonic speed range, $0 < MN < 0.8$, K1 is assumed not to vary with Mach number. The constant value is defined by

$$K1 = RCDVK \; FK1D0 \qquad (A460)$$

where if $FK1SK4 \cdot 0.6159$

$$FK1D0 = \frac{1}{FK1SK4} (0.8137 + 0.767 \; FK1SK4 - 0.7542$$

$$FK1SK4^2)^{-1} \qquad (A461)$$

otherwise

$$FK1D0 = \frac{1}{FK1SK4} \qquad (A462)$$

In eqn A460 RCDVK is a factor to allow for the effect of advanced technology on the aerodynamic performance. The constant FK1SK4 is defined as

$$FK1SK4 = FK1SK3 [FK1SK1 (1 - FK1SK2) + FK1SK2] \qquad (A463)$$

where

$$FK1SK1 = 0.85 - 0.306 \; QW4 \; (1 + 0.0535 \; QW4) +$$

$$(\log_{10} AW - 0.5441) [-0.179 - 1.38 \; QW4 +$$

$$2.433 \; QW4^2 - 1.722 \; QW4^3 + 0.431 \; QW4^4] \qquad (A464)$$

$$FK1SK2 = 0.515 - 0.1 \tan^{-1} [50(0.091 - RTW)] \qquad (A465)$$

$$FK1SK3 = 0.8738 + 0.795 \; UW - 1.654 \; UW^2 + 1.145 \; UW^3$$

<div align="right">(A466)</div>

unless UW · 0.3833 when FK1SK3 = 1

In the supersonic range, MN > 1.2, K1 is assumed to vary linearly with Mach number

$$K1 = RCDVK \; [FK1D1 + GK1D1 \; (MN - 1.2)] \qquad (A467)$$

The constants FK1D1 and GK1D1 are derived using the values of K1 at MN = 1.4, FK1H1, and at MN = 2, FK1H2, calculated as shown

$$FK1D1 = FK1H1 - \frac{(FK1H2 - FK1H1)}{3} \qquad (A468)$$

$$GK1D1 = \frac{FK1H2 - FK1H1}{0.6} \qquad (A469)$$

FK1H1 and FK1H2 are found by substituting MN = 1.4 and MN = 2 respectively in the following expressions

$$FK1H = (FK1HK1 \; FK1HK2 \; FK1HK3)^{-1} \qquad (A470)$$

where

$$FK1HK1 = 0.07595 + \frac{0.05 \; RTQWT \; (3 + RTQWT)}{\left\{ 1 + \left[\dfrac{(MN - 1)^{\frac{1}{2}}}{\tan \; QWL} - 1 \right]^2 \right\}}$$

$$+ \; 1.652 \; \frac{(MN^2 - 1)^{\frac{1}{2}}}{\tan \; QWL} - 1.14 \; \frac{(MN^2 - 1)^{\frac{1}{2}}}{\tan^2 \; QWL}$$

$$+ \; 0.3492 \; \frac{(MN^2 - 1)^{3/2}}{\tan^3 \; QWL} - 0.03912 \; \frac{(MN - 1)^2}{\tan^4 \; QWL}$$

<div align="right">(A471)</div>

unless $\dfrac{(MN - 1)^{\frac{1}{2}}}{\tan\ QWL} > 3.06356$ (A472)

when

$$FK1HK1 = 0.07595 + \dfrac{0.05\ RTQWT\ (3 + RTQWT)}{\left\{ 1 + \left[\ \dfrac{(MN - 1)^{\frac{1}{2}}}{\tan\ QWL} - 1\ \right]^2\ \right\}} \qquad (A473)$$

where

$$RTQWT = \dfrac{\tan\ QWT}{\tan\ QWL} \qquad (A474)$$

$$FK1HK2 = 1.28\ [AW\ (MN^2 - 1)^{\frac{1}{2}}]^{-1.0034}\ -$$

$$[AW\ (MN^2 - 1)^{\frac{1}{2}}]^{-1.921}\ \{\ 10\ [\ -1.747$$

$$+\ 7.708\ UW\ \cos\ QW2 - 19.73\ (UW\ \cos\ QW2)^2$$

$$+\ 18.53\ (UW\ \cos\ QW2)^3\ ]\ \} \qquad (A475)$$

$$FK1HK3 = 1 - \dfrac{1.825\ 0.1\ CWMG}{LTCQM} \qquad (A476)$$

In the transonic range, 0.8 < MN < 1.2, a cubic curve is used to calculate K1

$$K1 = RCDVK\ (FK1K0 + FK1K1\ MN + FK1K2\ MN^2 + FK1K3\ MN^3)$$

$$(A477)$$

where the four constants FK1K0 to FK1K3 are obtained by matching the value and the derivative with respect to the Mach number of the eqn A477 to the corresponding

parameters at 0.8 and 1.2 Mach number given by eqns A461, A462, A467 and A469. Thus

$$FK1K3 = 6.25 \, [GK1D1 - 5 \, (FK1D1 - FK1D0)] \qquad (A478)$$

$$FK1K2 = 1.25 \, GK1D1 - 3 \, FK1K3 \qquad (A479)$$

$$FK1K1 = - \, 1.6 \, FK1K2 - 1.92 \, FK1K3 \qquad (A480)$$

$$FK1K0 = FK1D0 - 0.8 \, FK1K1 - 0.64 \, FK1K2$$
$$- \, 0.512 \, FK1K3 \qquad (A481)$$

The parameter CLC which determines the transition point between the CL regimes, equation (A454), is a function both of the technology used in the design of the high-lift system, and of the geometric variables. It is therefore not estimated within the design synthesis but supplied, in tabular form versus Mach number, as data applicable to a certain class of high lift, variable-camber system on a wing. Similarly the parameter K2, which determines the lift-dependent drag in the upper CL regime, equation (A455), is supplied as an increment, DK2, on K1, in the form of a table versus Mach number.

Thus

$$K2 = K1 + DK2 \qquad (A482)$$

For both CLC and DK2 parameters an interpolation procedure is used to determine values at intermediate values of Mach numbers to those in the tables.

20. SUSTAINED TURN RATE ESTIMATION (SUBROUTINE SSTR)

At first the maximum lift coefficient, CL4, and incidence, ALM, that may be sustained by the aircraft at the given engine power setting is determined with an identical procedure to that followed in subroutine SORTIE (first iteration of SORTIE). Then the corresponding maximum normal load factor, GNS, is given by

$$GNS = \frac{(Q\ SW\ CL4 + TPG\ \sin\ ALM)}{WT} \qquad (A483)$$

where TPG is the gross thrust and WT is the aircraft weight

$$WT = (MTT - MTTPP)\ G \qquad (A484)$$

where MTT is total aircraft take-off mass and MTTPP is the mass of the fuel consumed in the sortie legs previous to the one where manoeuvres take place.

The maximum normal load factor may be limited to that tolerable by the pilot or the structure.

Having estimated GNS the sustained turn rate, STR, is

$$STR = \frac{180\ G}{\pi\ V}\ (GNS^2 - 1)^{\frac{1}{2}} \qquad (A485)$$

21. ATTAINED TURN RATE ESTIMATION (SUBROUTINE SATR)

The maximum normal load factor that may be produced by the aerodynamic and propulsive forces, GNA, is given by

$$GNA = \frac{Q\ SW\ CLMAX + TPG\ \sin\ \dfrac{CLMAX}{GCLA}}{WT} \qquad (A486)$$

As with sustained turn rate the maximum normal load factor may be limited to that tolerable by the pilot or the structure.

The attained turn rate, ATR, follows

$$ATR = \frac{180\ G}{\pi\ V} (GNA^2 - 1)^{\frac{1}{2}} \qquad (A487)$$

22.   SPECIFIC EXCESS POWER ESTIMATION (SUBROUTINE SSEP)

Specific excess power, SEP, is calculated for a 1 g flight and is given by

$$SEP = \frac{V}{WT} [\ TPG - V\ MPA - Q\ SW\ CDTOT\ ] \qquad (A488)$$

23.   ESTIMATION OF THE MAXIMUM MACH NUMBER IN LEVEL FLIGHT (SUBROUTINE SMML)

The maximum Mach number that can be achieved in 1 g flight at a specified constant altitude is estimated by an iterative process based on the variation of the nett propulsive force with the aircraft speed. The nett propulsive force, F1, is given by

$$F1 = TPG \cos AL - Q1\ SW\ CDTOT - V1\ MPA \qquad (A489)$$

where V1 is an initial estimate for speed (Q1 is derived from V1) and

$$AL = \frac{CL}{GCLA} \qquad (A490)$$

$$= \frac{\dfrac{WT}{Q1\ SW}}{GCLA} \qquad (A491)$$

The equationfor F1 is solved with a Newton-Rapson technique to give V2.

If $|V2 - V1| < 1$ or F1 < 0.0001 TPGD (TPGD is max SL static thrust) the the iteration is complete.

Otherwise

$$V1 = V2 \qquad\qquad (A492)$$

and the iteration is resumed.

If a convergence is not reached after 20 iterations increased relaxation is used in the form of

$$V2 = V1 + [1 + \text{maximum of } (0, 0.0015 \ V2 \ ) \ ] \ (V2 - V1)$$

$$(A493)$$

24.   ACCELERATION THROUGH A MACH NUMBER
         INCREMENT (SUBROUTINE SACA)

The time needed to accelerate, at constant altitude and power setting, through an Mach number increment is calculated by assuming that, over a small interval of Mach number, aircraft acceleration varies linearly with Mach number. After careful consideration it was established that the interval of Mach number = 0.1 provides good results and therefore is used for the acceleration calculations.

The acceleration of the aircraft is given by

$$F1 = \frac{G}{WT} \ (TPG \cos AL - Q1 \ SW \ CDTOT - V1 \ MPA) \qquad (A494)$$

where V1 corresponds to the initial value of Mach number MNACA and Q1 to V1 and

$$AL = \frac{\dfrac{WT}{Q1\ SW}}{GCLA} \qquad (A495)$$

Following the specified increment in Mach number, 0.1 is added to the initial Mach number MN1 to give a new Mach number MN2.

$$MN2 = MN1 + 0.1 \qquad (A496)$$

The speed, V2, corresponding to MN2 is used to define the new acceleration F2

$$F2 = \frac{G}{WT}\ (TPG\ \cos\ AL\ -\ Q2\ SW\ CDTOT\ -\ V2\ MPA) \qquad (A497)$$

If F2 ≤ 0 then the aircraft cannot accelerate. Otherwise the time to accelerate through the specified Mach number increment, SDT, is given by

$$SDT = SSPD\ \left(\frac{MN2\ -\ MN1}{F2\ -\ F1}\right)\ \log\ \left(\frac{F2}{F1}\right) \qquad (A498)$$

where SSPD is the speed of sound.

If the acceleration in the Mach number increment (0.1) is constant (F2 = F1), then

$$SDT = SSPD\ \frac{MN2\ -\ MN1}{F1} \qquad (A499)$$

The above time is for an acceleration through a Mach number increment of 0.1. For other Mach number increment values the above time is multiplied accordingly.

25.   RIDE QUALITY FACTOR (SUBROUTINE RIDE)

The ride quality found in an aircraft is a function of the sensitivity of the aircraft to gusts, that is the rate of change in the normal acceleration of the aircraft with respect to gusts. A ride quality factor, RQF, is given as

$$RQF = \frac{RO \ V \ GCLA \ \dot{SW}}{MTT} \qquad (A500)$$

26. TAKE-OFF PERFORMANCE (SUBROUTINE TAKEOFF)

The take-off distance, TOD, is made of the ground roll distance to reach unstick speed and the subsequent airborne distance to clear a 15 metre high obstacle.

The ground roll distance, TOG, is given by

$$TOG = \frac{1.156 \ FMTSW}{RTPGW \ TRATE \ CLT} \qquad (A501)$$

where FMTSW is the wing loading,

$$\left(= \frac{MTT}{SW} \right) \qquad (A502)$$

RTPGW is the thrust-to-weight ratio,

$$\left(= \frac{TPGC}{MTT \ G} \right) \qquad (A503)$$

TRATE is the fraction of the gross thrust available and CLT is the maximum lift coefficient available

$$(= FCLT \ CLMAX) \qquad (A504)$$

FCLT being the fraction of the maximum lift coefficient.

The airborne distance travelled to clear an obstacle 15 m high, TOA, is given by

$$TOA = \frac{9.79}{(RTPGW \ TRATE)} \left(\frac{FMTSW}{CLT} \right)^{\frac{1}{2}} \qquad (A505)$$

and thus the take-off distance, TOD

$$TOD = TOG + TOA \qquad\qquad (A506)$$

27.   FUNCTION BLEND

The purpose of this function is, in the case where a function is defined in terms of the greater or lesser value of two subsidiary functions, to blend the two subsidiary functions at the point where they meet. A continuous first and second derivative is thus achieved, necessary in the optimization procedure.

Funcion BLEND is fully described in Ref.43.

28.   FIGURES

NOSE UNDERCARRIAGE BAY

INTAKE DIFFUSER

INTERNAL GUN BAY

INTERNAL WEAPONS BAY

AFTERBURNER SECTION

SIDE DUCTS

ENGINE (GAS GENERATOR)

MAIN UNDERCARRIAGE BAY

REMOTE LIFT SYSTEM DUCT
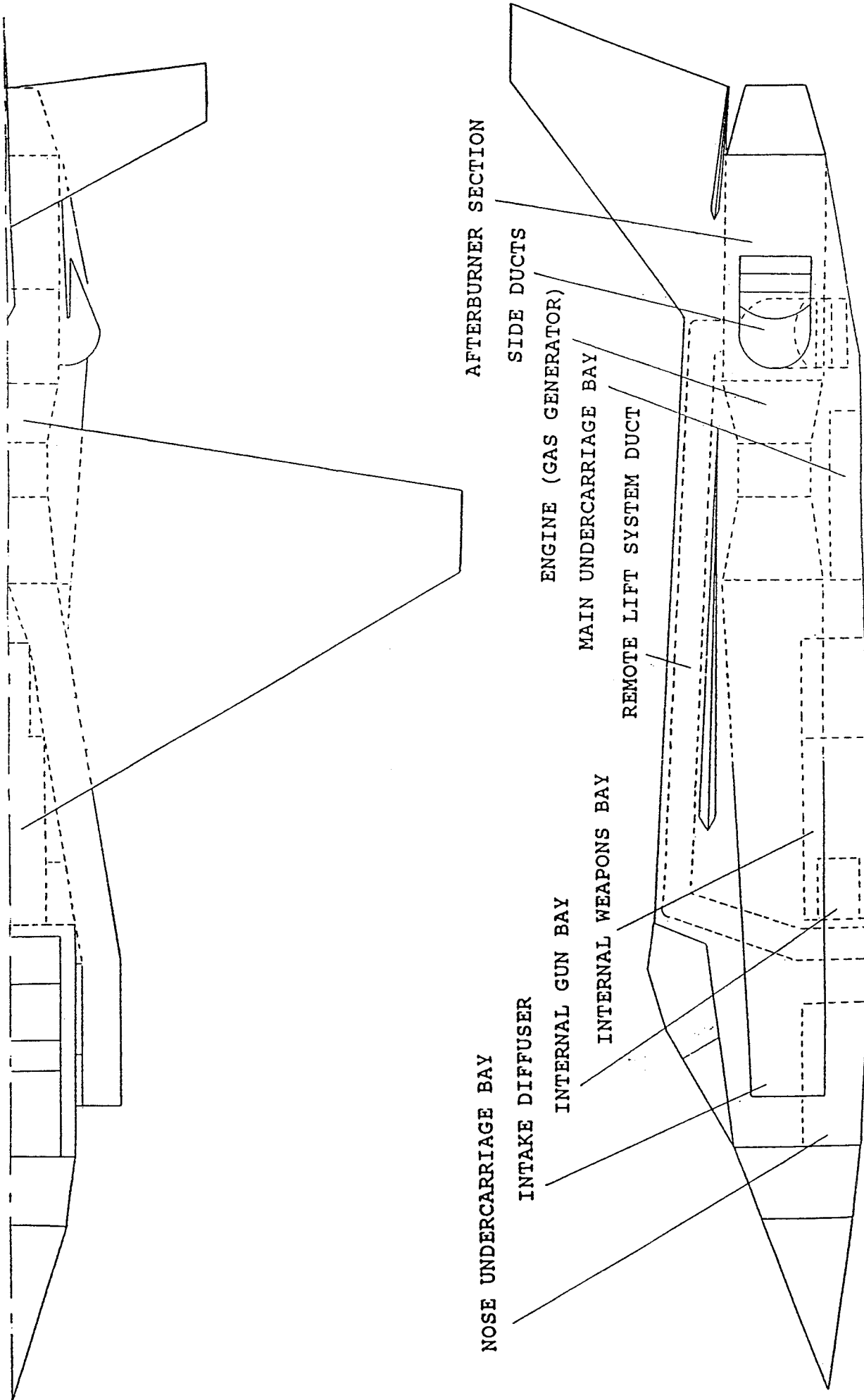
FIG.A1   AIRCRAFT BASELINE CONFIGURATION

FIG.A2   FUSELAGE STATIONS WITH CORRESPONDING SECTIONS
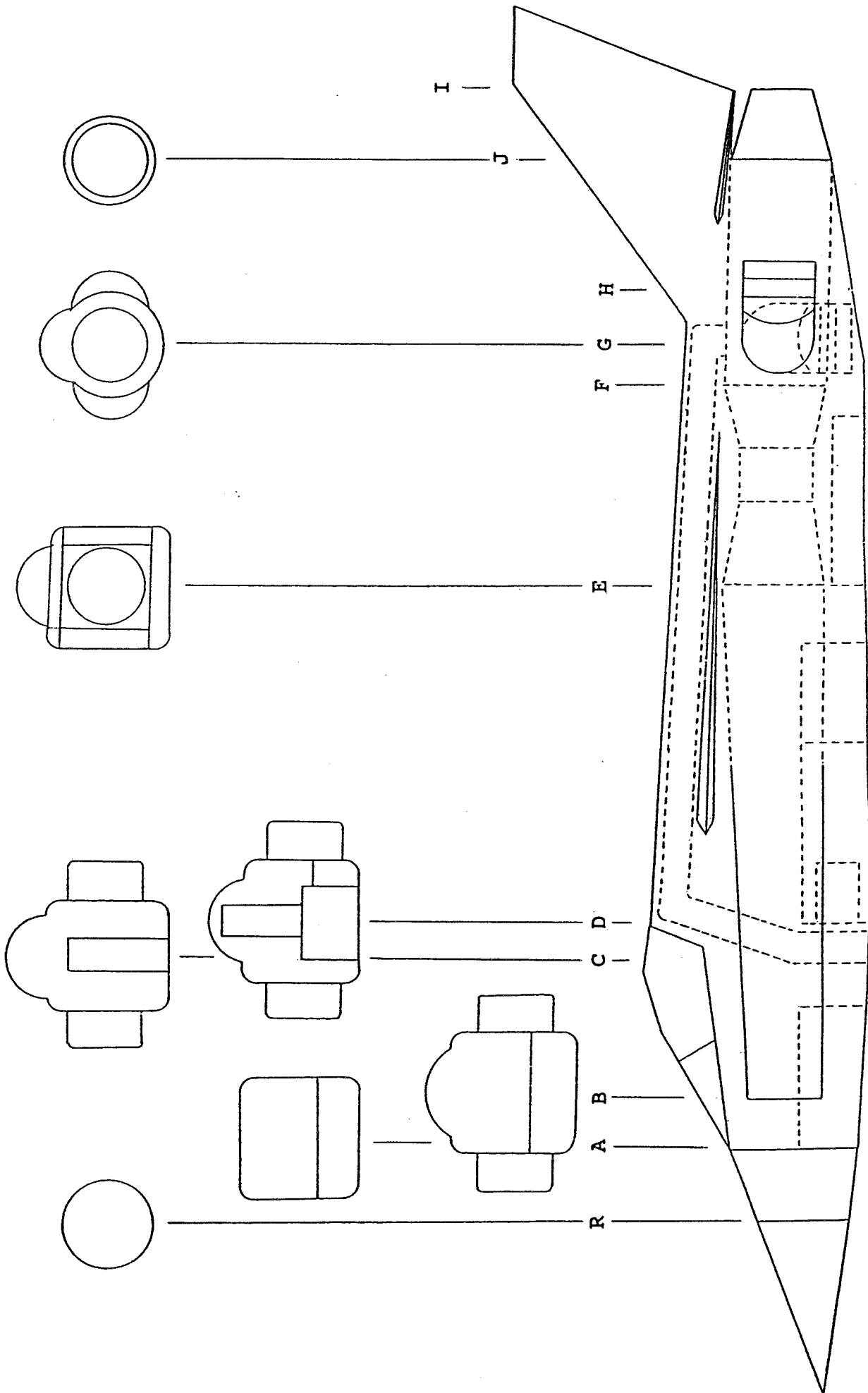
SIDE FUSELAGE FUEL TANK

CENTRAL FUSELAGE FUEL TANK
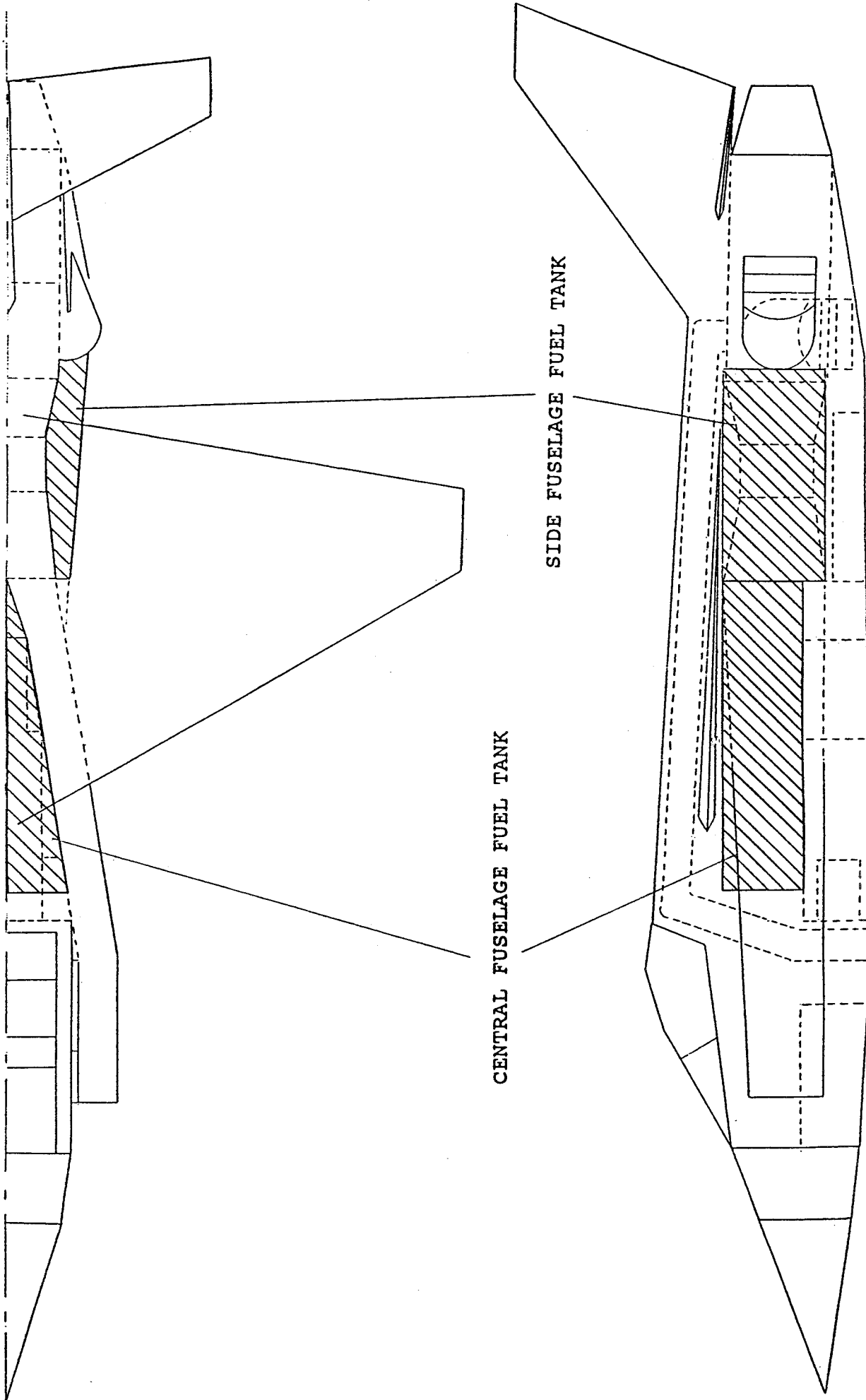
FIG.A3　FUSELAGE FUEL TANK ARRANGEMENT
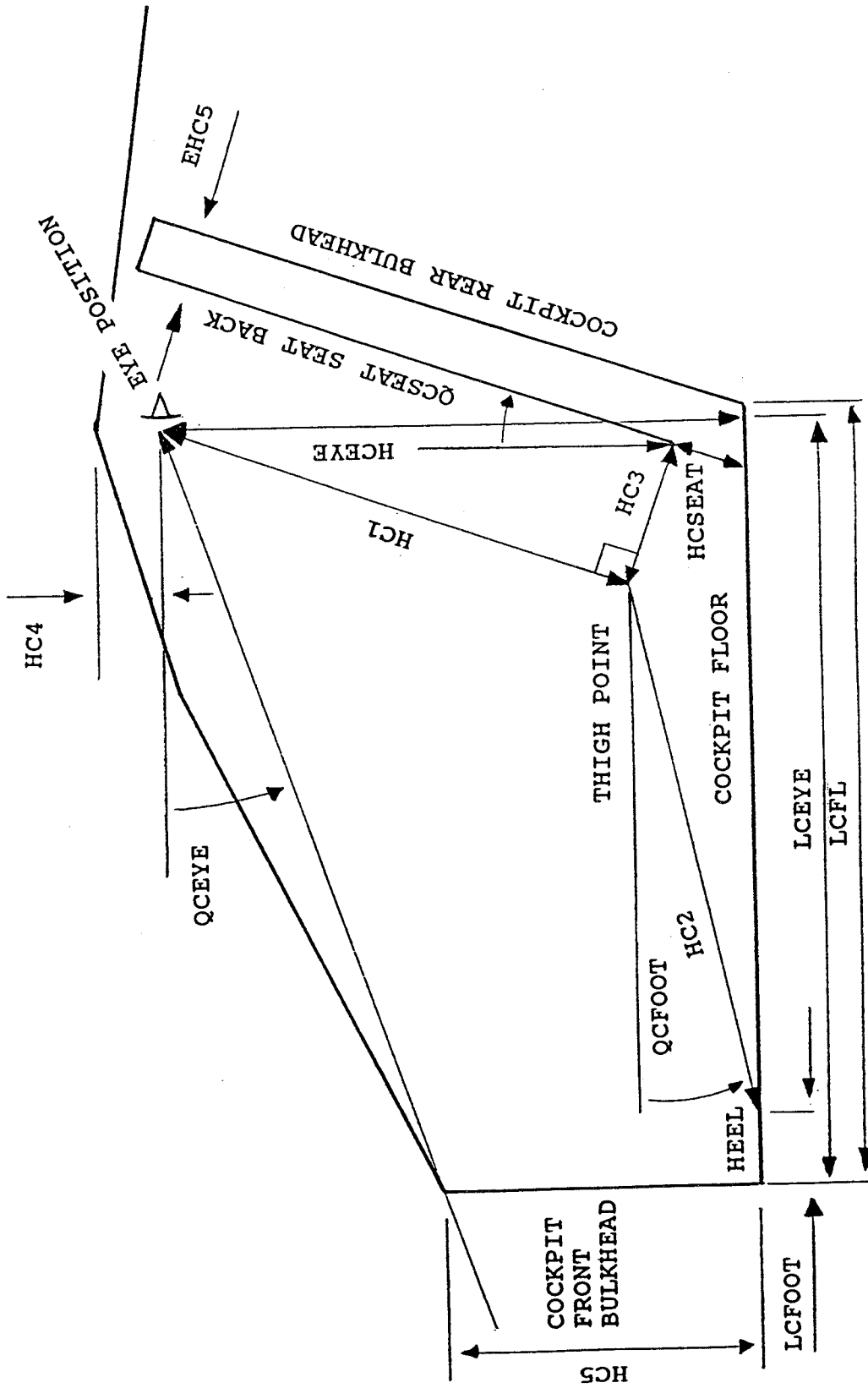
FIG.A4   COCKPIT GEOMETRY

FIG.A5   ENGINE GEOMETRY

ENGINE FACE

FUSELAGE

BFR

BII

BVI

XII = XVI

XVE

XIE
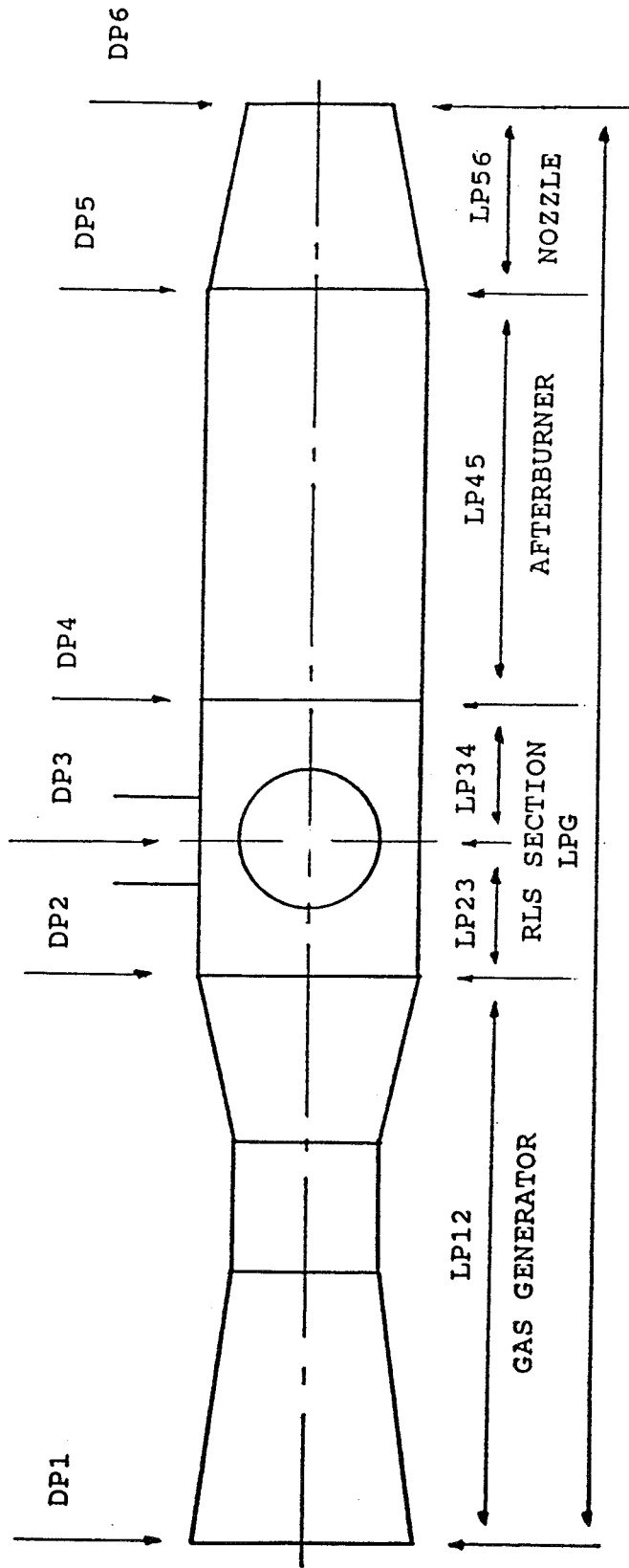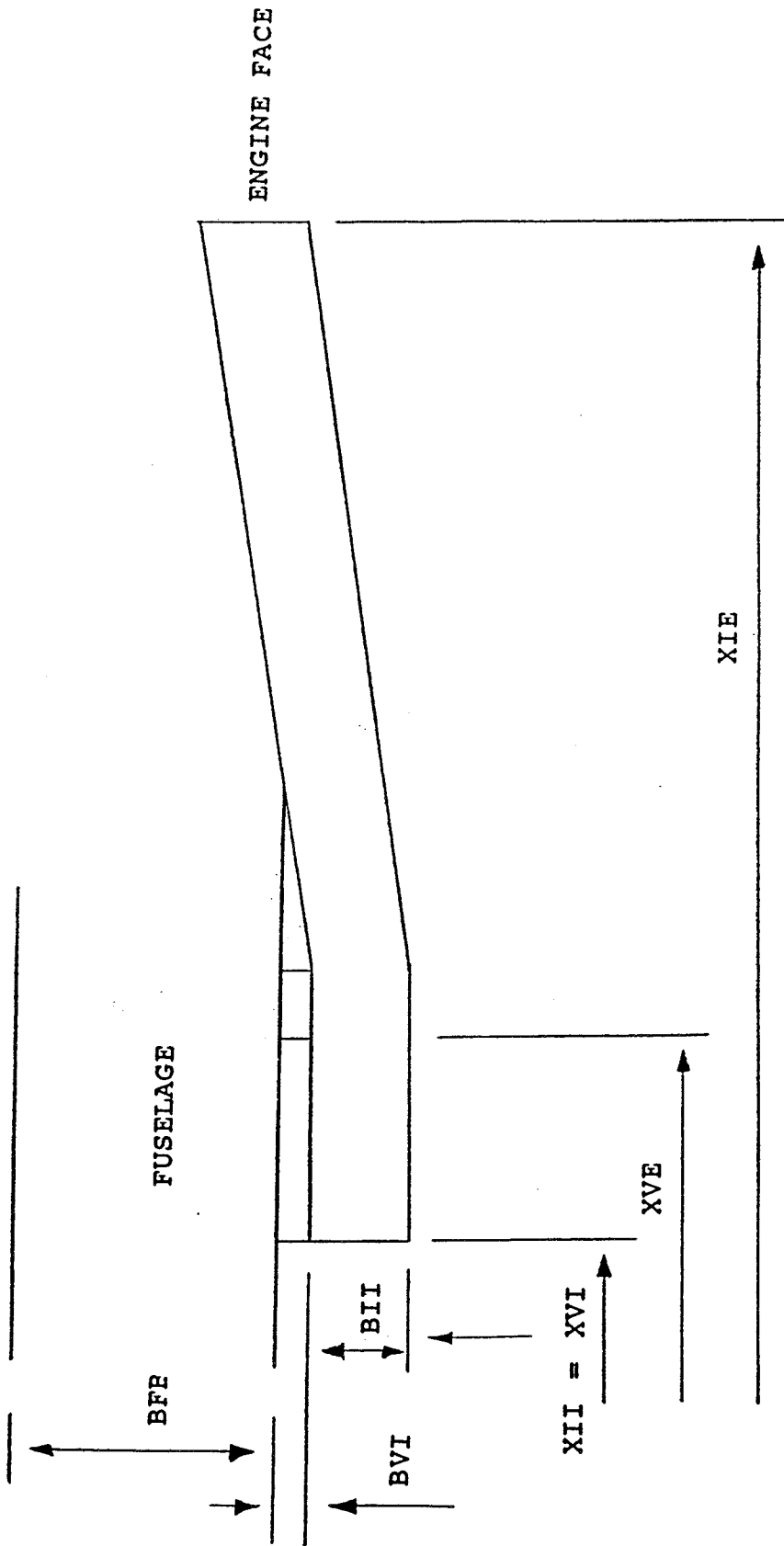
FIG.A6   INTAKE DIFFUSER AND BOUNDARY LAYER DIVERTER
         GEOMETRY
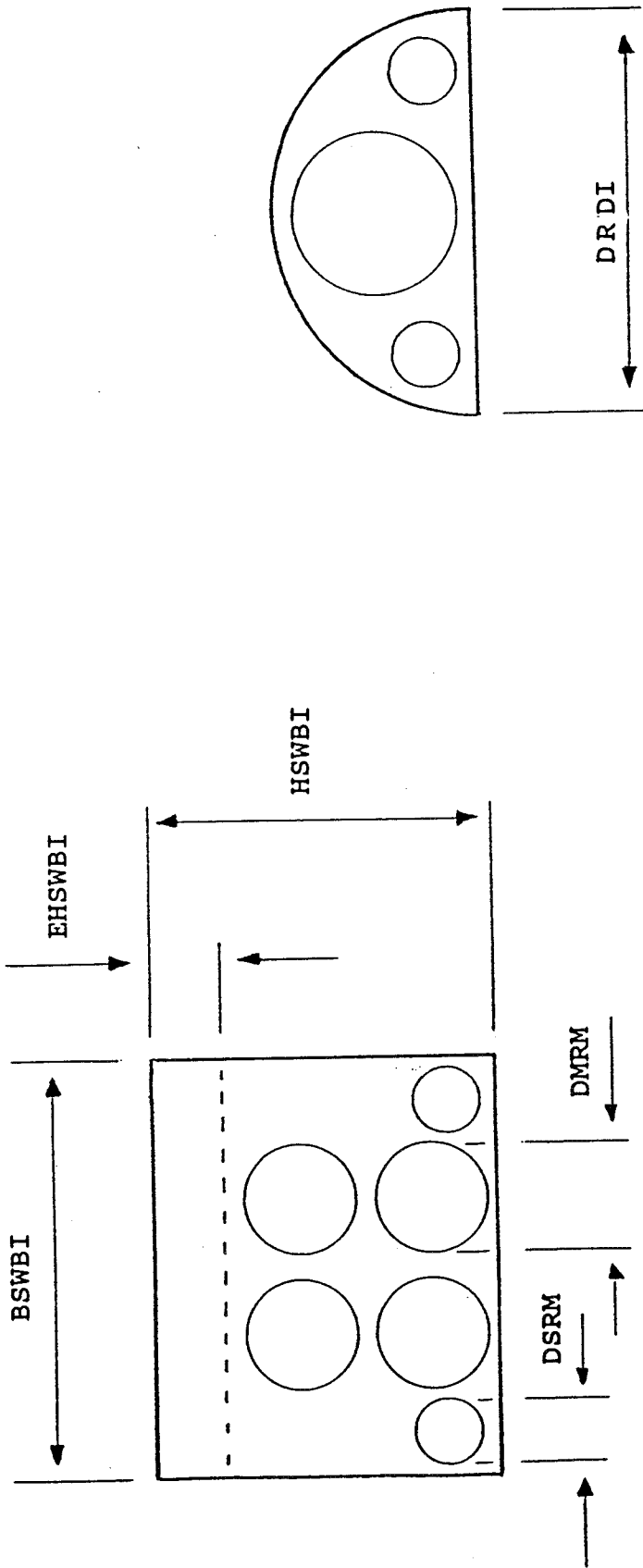
FIG.A7   WEAPONS BAY AND REMOTE LIFT SYSTEM (RLS) DUCT
CROSS-SECTIONS
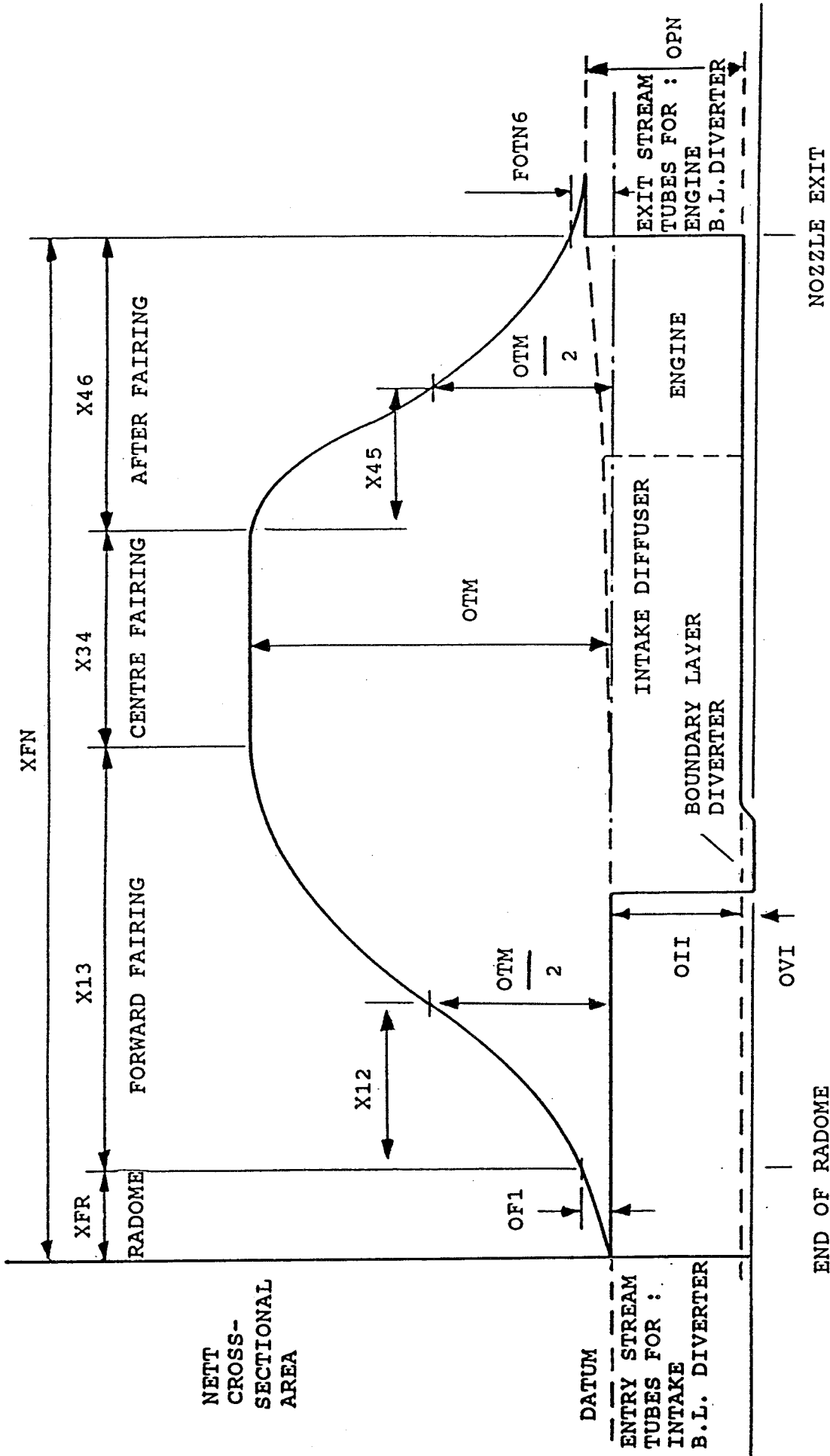
FIG.A8 FAIRING CURVE
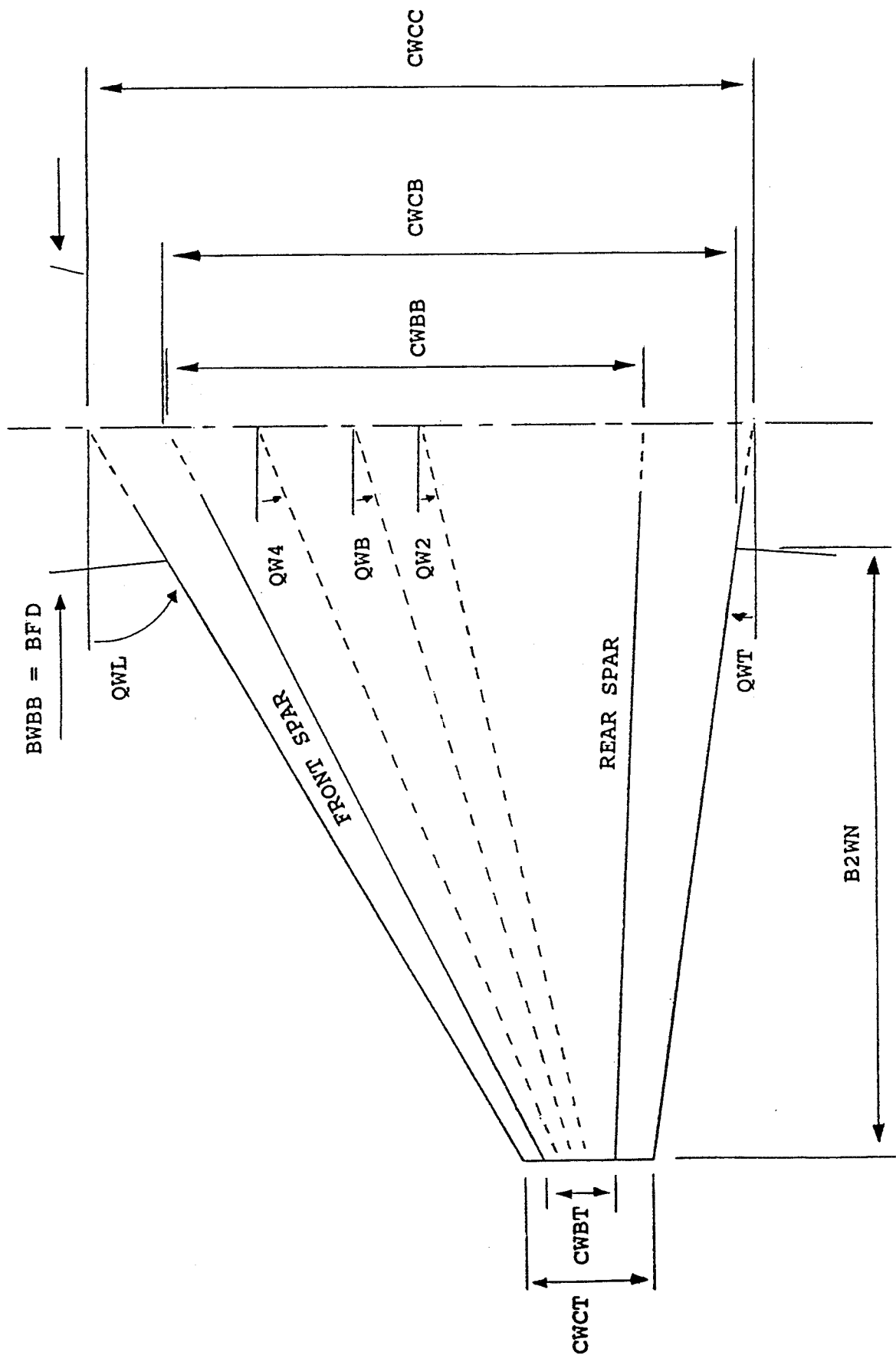
FIG.A9   WING PLANFORM
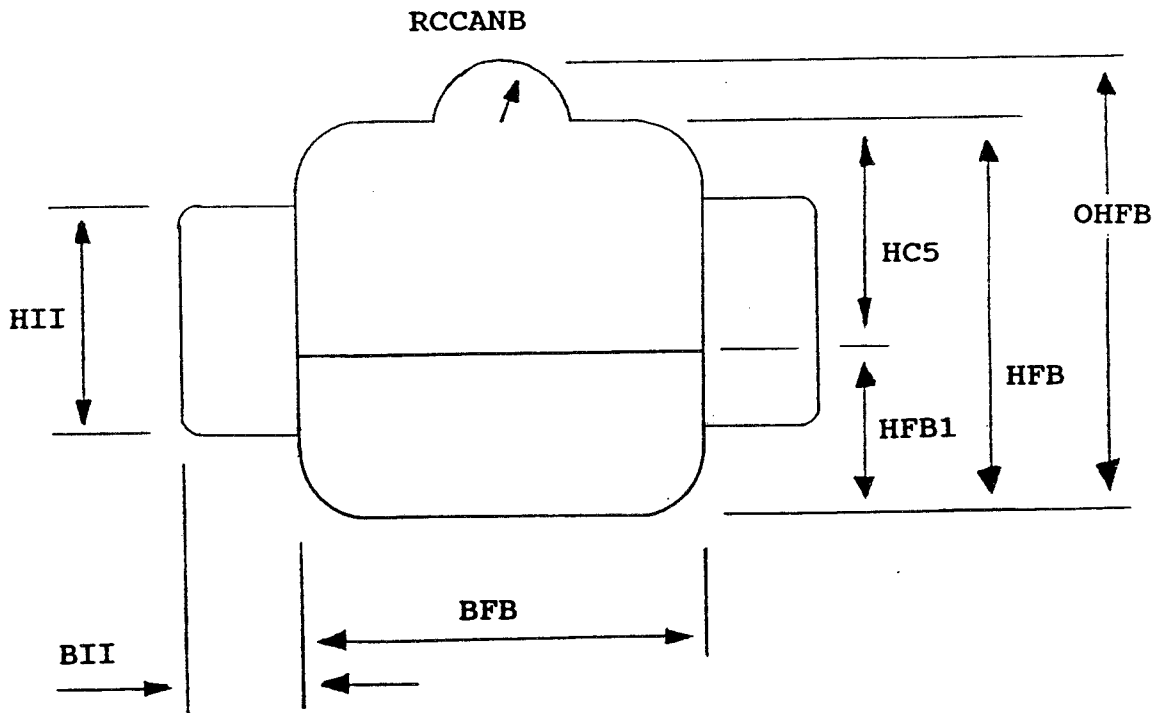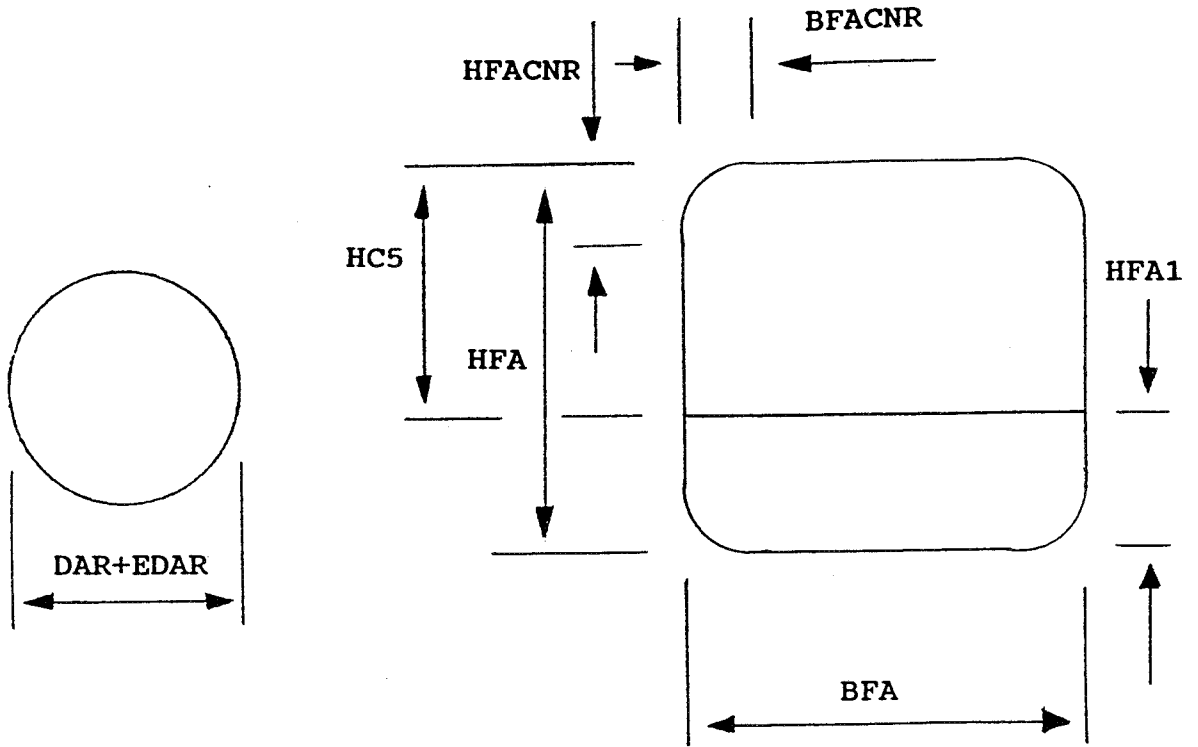
FIG.A10   CROSS-SECTIONS OF FUSELAGE STATIONS R, A AND B

RCCANC

HII

OHFC

HFC

DRDE

BFC

BII

RCCAND

HII

OHFD

HSWBI

HGABI

HFD

BSWBI

BGABI

BFD

BII
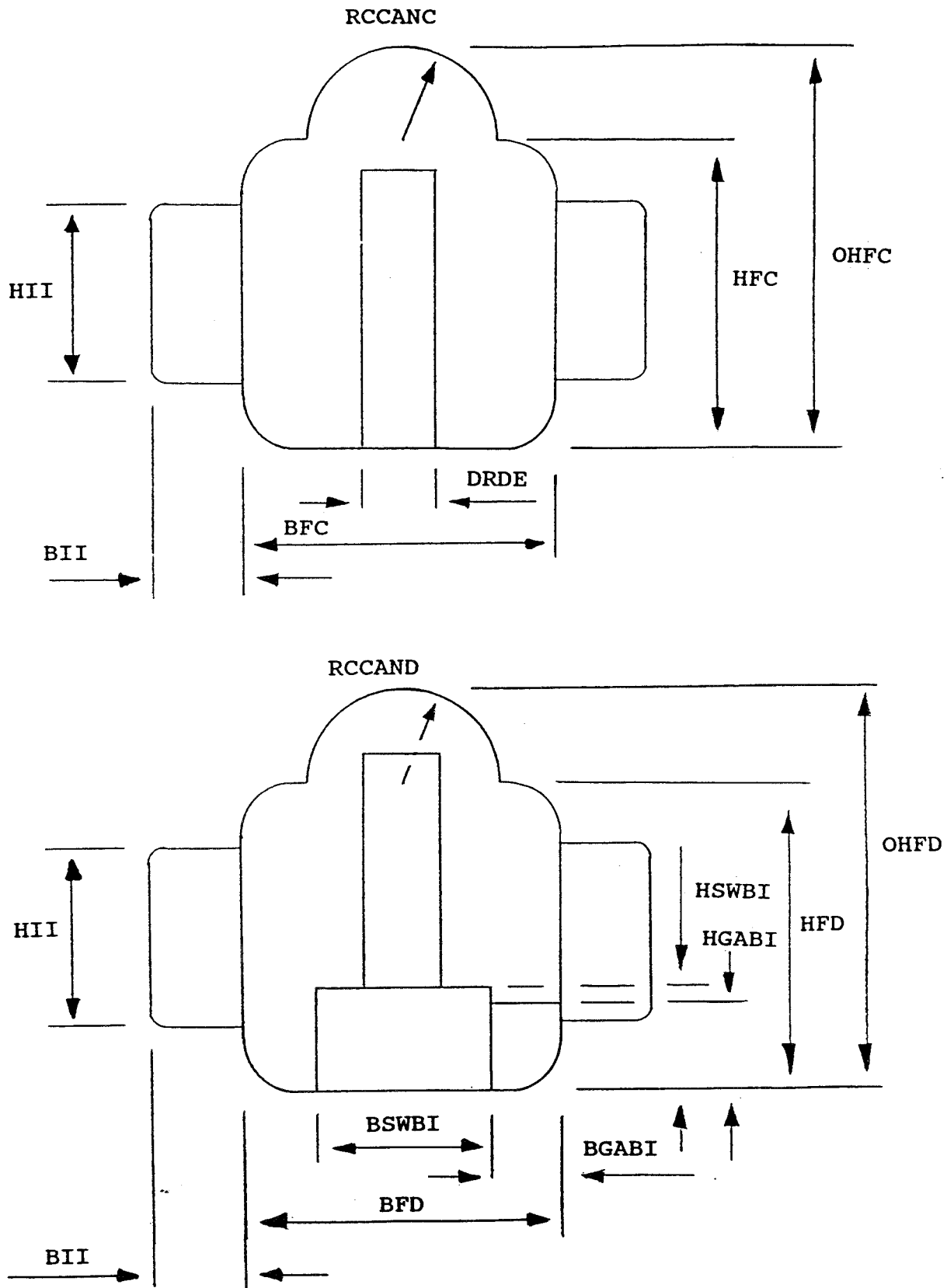
FIG.A11   CROSS-SECTIONS OF FUSELAGE STATIONS C AND D
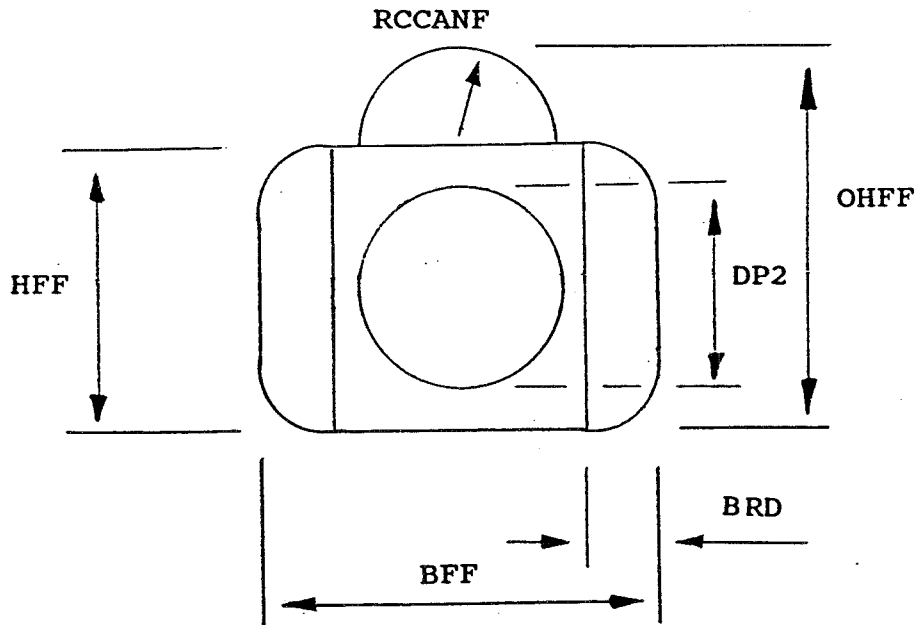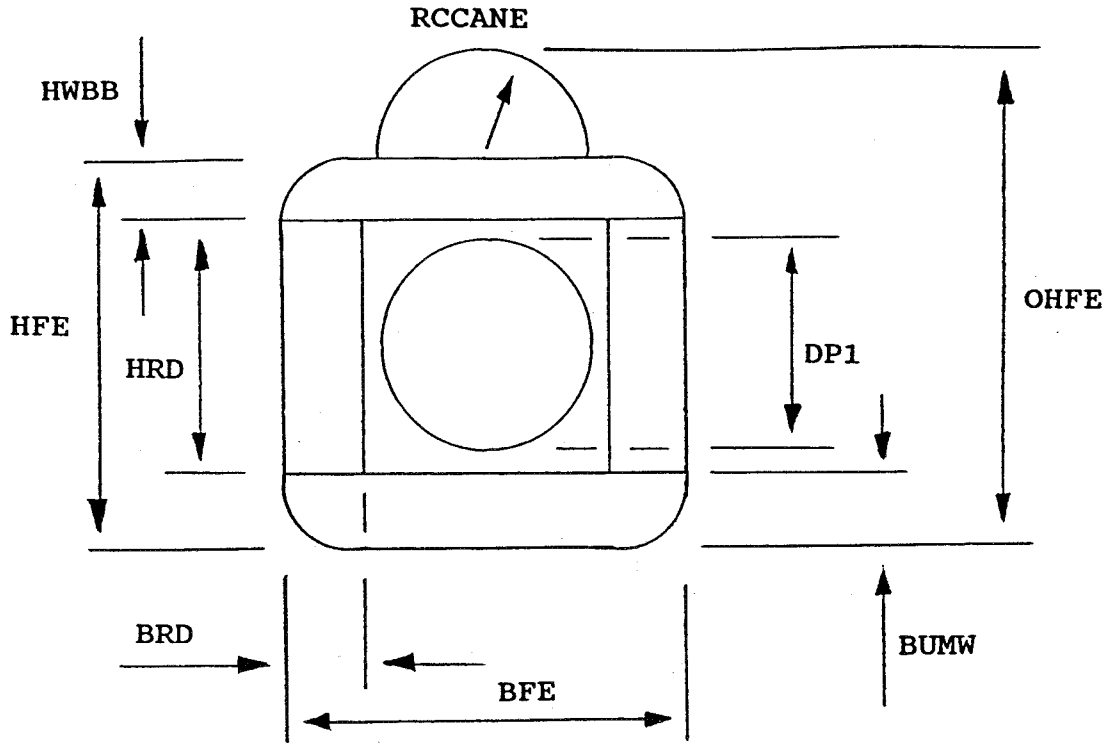
FIG.A12   CROSS-SECTIONS OF FUSELAGE STATIONS E AND F
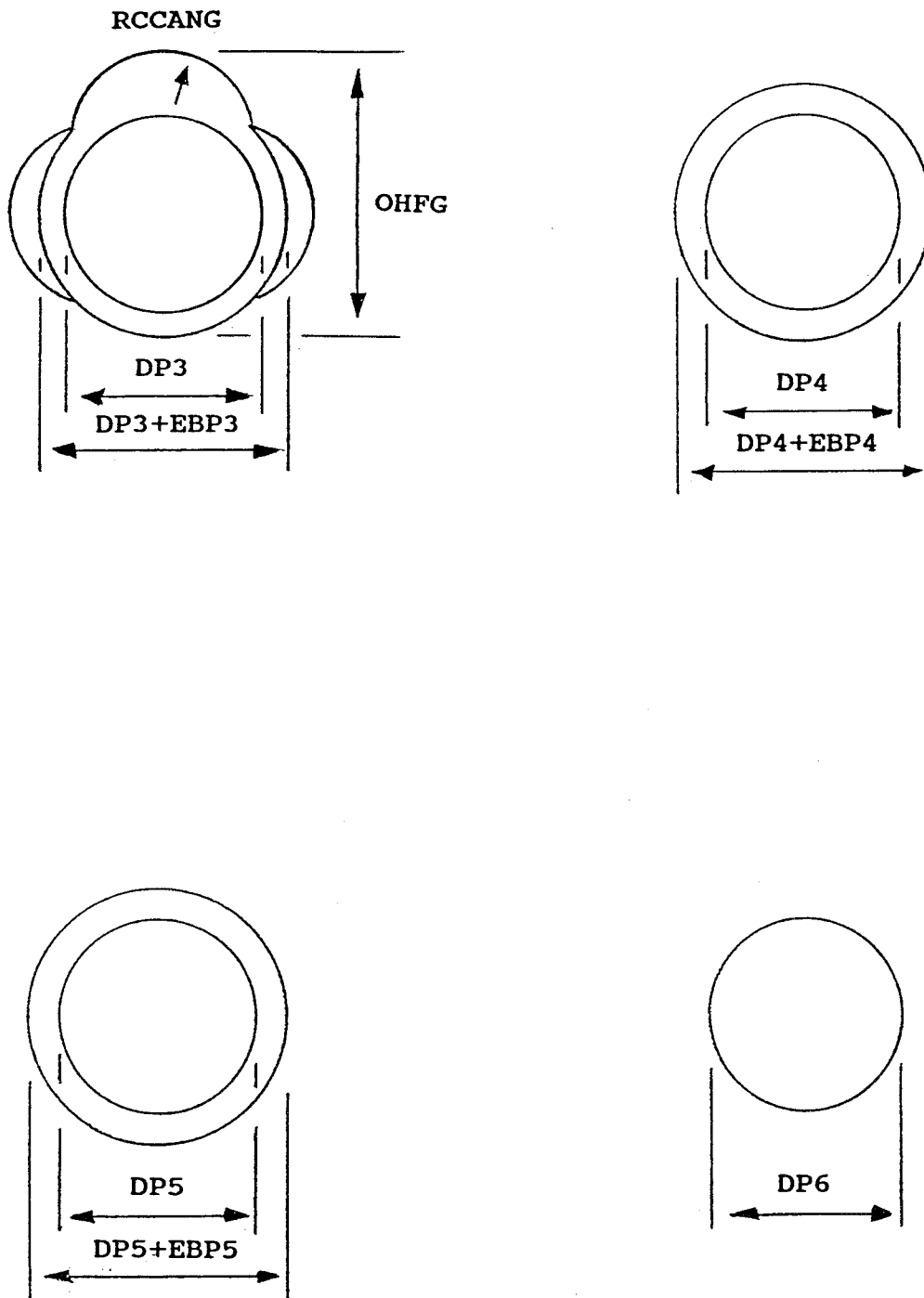
FIG.A13 CROSS-SECTIONS OF FUSELAGE STATIONS G, H, J AND I
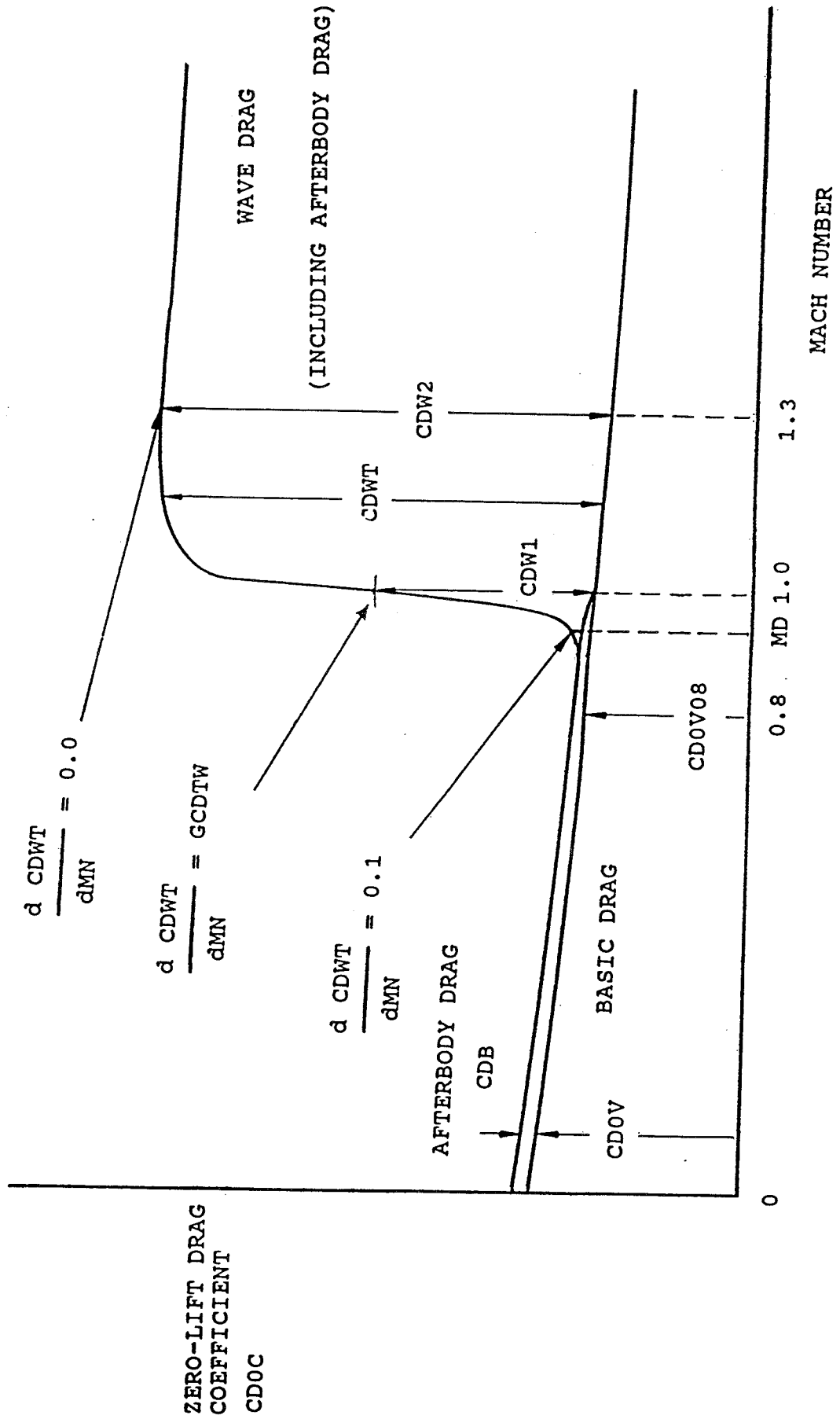
FIG.A14   DRAG AT ZERO LIFT
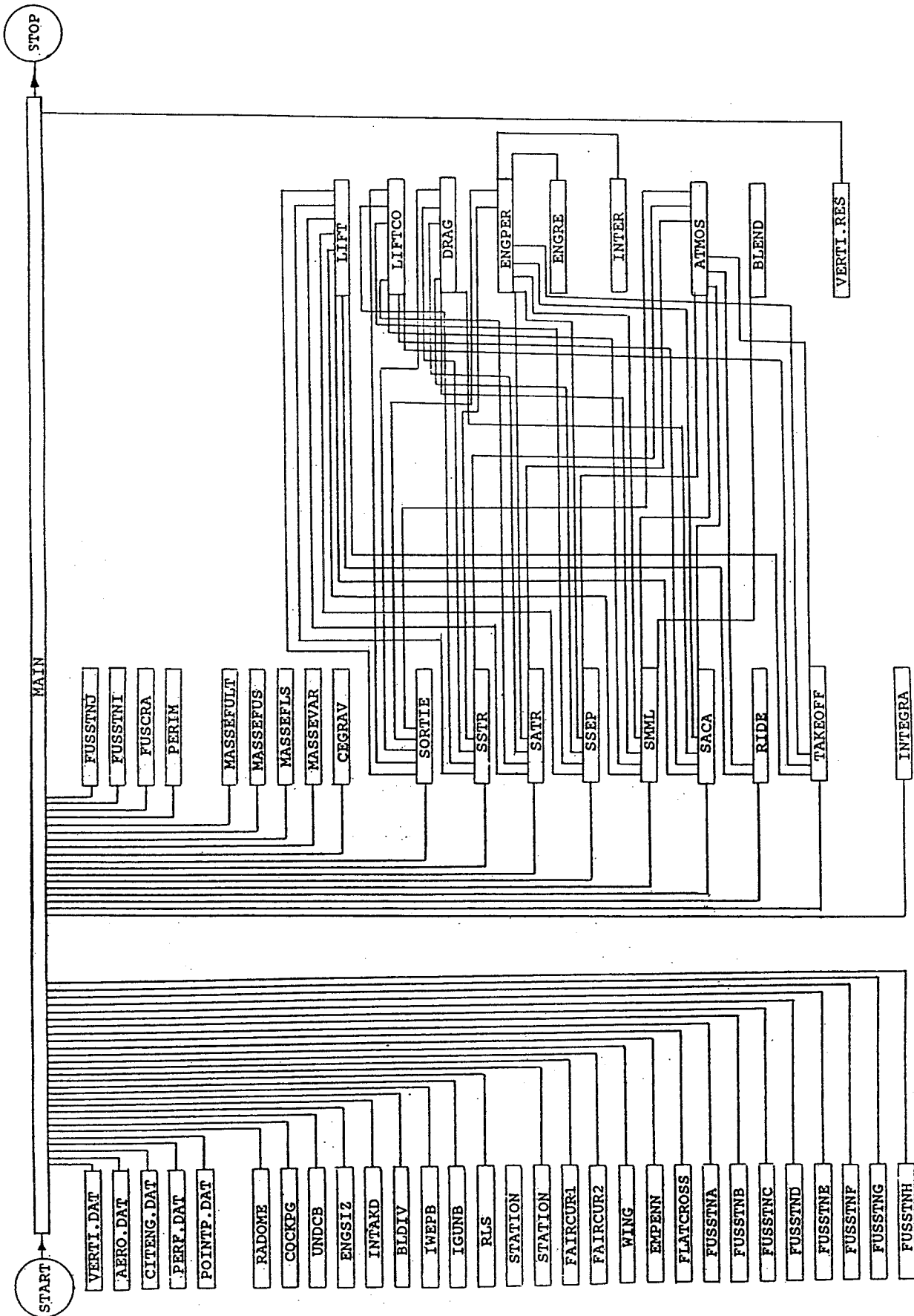
FIG.A15 SIMPLIFIED FLOWCHART FOR CODE VERTI

29.   LIST OF VARIABLES

KEY : EV   External Variable ; design constant.
--- IV   Independent Variable ; set by optimization code - given initial value.
-- Dependent Variable ; a function of external and independent variables.

Symbol	Definition	Type
AEFN	Net fin aspect ratio.	EV
AETN	Net tailplane aspect ratio.	EV
AH	Speed of sound at a given altitude.	
AII	Aspect ratio of an intake diffuser at the intake plane.	EV
AL	Aircraft incidence.	
ALF	Limit in the numerical integration.	
ALH	Maximum sustained aircraft incidence at maximum thrust.	
ALM	Maximum sustained aircraft incidence for a engine throttle setting.	
AMMX	Maximum design Mach number for the structure.	EV
ATE	Total aircraft pitching moment about nose with empty fuel tanks,no external stores, no ammunition.	
ATR	Attained turn rate.	
ATRO	Attained turn rate - output data form.	
ATROS	Attained turn rate constraint.	EV
ATT	Total aircraft pitching moment about nose with full fuel tanks,no external stores, no ammunition.	
AW	Gross wing aspect ratio.	IV
AWA	Aspect ratio of each aileron.	EV
AWB	Aspect ratio of gross wing-box.	
AWN	Net wing aspect ratio.	
AWR	Reference wing aspect ratio for wing-box mass calculation.	
AWS	Aspect ratio of each spoiler.	
AWSG	Gross aspect ratio of wing spoilers.	
B2	Semi-span.	
BCH	Width of cockpit.	EV
BEFN	Net fin span.	
BET	Limit in the numerical integration.	
BETN	Net tailplane span.	
BFA	Fuselage width at stn A.	
BFACNR	Fuselage corner width at stn A.	
BFB	Fuselage width at stn B.	
BFBS	Minimum fuselage width at stn B.	
BFC	Fuselage width at stn C.	
BFCDH	The greatest of BFC and BFD.	
BFCS	Minimum fuselage width at stn C.	

BFD	Fuselage width at stn D.	
BFE	Fuselage width at stn E.	
BFES	Minimum fuselage width at stn E.	
BFF	Fuselage width at stn F.	
BFG	Fuselage width at stn G.	
BFH	Fuselage width at stn H.	
BFI	Fuselage width at stn I.	
BFJ	Fuselage width at stn J.	
BIDD	Width of an intake diffuser at stn D.	
BII	Width of an intake diffuser at the intake plane	
BGAK	Gun ammunition bay width clearance factor	EV
BGABI	Gun ammunition bay width.	
BGM	Gun mechanism width.	EV
BGMK	Gun mechanism bay width clearance factor.	EV
BGMBI	Gun mechanism bay width.	
BMS	Wing bending moment.	
BRD	Side tank width.	IV
BSWBI	Width of the internal weapons bay.	
BSWBIK	Width clearance factor for the internal weapons bay.	EV
BUMW	Main undercarriage wheel and tyre width.	
BUMWK	Constant in correlation for main undercarriage wheel and tyre width.	EV
BUNW	Nose undercarriage wheel and tyre width.	EV
BVI	Width of the b.l.diverter stream-tube at the intake plane.	
BW	Gross wing span.	
BWA	Gross span of the ailerons.	
BWBB	Span of the center section of the wing-box.	
BWF	Gross span of trailing edge flaps.	
BWN	Net wing span.	
BWNF	Span of fuel tank in wing-box external to the fuselage.	
BWS	Gross span of all spoilers.	
C	Chord in the evaluation of the flying surfaces lateral cross-sectional area.	
CD	Drag coefficient.	
CD08	Total aircraft basic zero lift drag coefficient for M=0.8.	
CD0C	Zero lift drag coefficient of the canopy.	
CD0EF	Zero lift drag coefficient of the fin.	
CD0ET	Zero lift drag coefficient of the tail.	
CD0F	Zero lift drag coefficient of the fuselage.	
CD0FG	Zero lift drag coefficient of the gross fuselage.	
CD0T	Total zero-lift drag coefficient.	
CD0V08	Basic aircraft zero lift drag coefficient,up to M=0.8.	
CD0V	Basic aircraft zero lift drag coefficient.	
CD0W	Zero lift drag coefficient of the wing.	
CDB	Subsonic drag coefficient of the fuselage afterbody.	
CDCW1	Wave drag coefficient of the front part of the canopy for M=1.0.	
CDCW2	Wave drag coefficient of the front part of the canopy for M=1.3.	
CDCW3	Wave drag coefficient of the rear part of the canopy for M=1.0.	

CDCW4	Wave drag coefficient of the rear part of the canopy for M=1.3.
CDCW5	Wave drag coefficient of the complete canopy for M=1.0.
CDCW6	Wave drag coefficient of the complete canopy for M=1.3.
CDFIW1	Wave drag coefficient of the fin for M=1.0.
CDFIW2	Wave drag coefficient of the fin for M=1.3.
CDFW1	Wave drag coefficient of the fuselage forebody for M=1.0.
CDFW2	Wave drag coefficient of the fuselage forebody for M=1.3.
CDFW3	Wave drag coefficient of the fuselage section from the intake plane to the maximum cross-sectional area of the fuselage for M=1.0.
CDFW4	Wave drag coefficient of the fuselage section from the intake plane to the maximum cross-sectional area of the fuselage for M=1.0.
CDFW5	Wave drag coefficient of the equivalent afterbody for M=1.0.
CDFW6	Wave drag coefficient of the equivalent afterbody for M=1.3.
CDFW7	Wave drag coefficient of the afterbody for M=1.
CDFW8	Wave drag coefficient of the afterbody for M=1.3.
CDGC	Drag coefficient of the gun port.
CDIV	Subsonic drag coefficient of the b.1.diverter.
CDPRE	Intake pre-entry drag coefficient.
CDS	Intake spillage drag coefficient.
CDST	Total intake spillage drag coefficient.
CDTK0	Coefficient in cubic for interpolation of wave drag.
CDTK1	Coefficient in cubic for interpolation of wave drag.
CDTK2	Coefficient in cubic for interpolation of wave drag.
CDTK3	Coefficient in cubic for interpolation of wave drag.
CDTOT	Total aircraft drag coefficient.
CDTW1	Wave drag coefficient of the tail for M=1.0.
CDTW2	Wave drag coefficient of the tail for M=1.3
CDUT	Drag coefficient of the extended u/c.
CDV	Lift dependent drag coefficient.
CDVK0	Coefficient in cubic transition region of lift dependent drag vs CL function.
CDVK1	Coefficient in cubic transition region of lift dependent drag vs CL function.
CDVK2	Coefficient in cubic transition region of lift dependent drag vs CL function.
CDVK3	Coefficient in cubic transition region of lift dependent drag vs CL function.
CDW1	Total aircraft wave drag coefficient for M=1.0.
CDW2	Total aircraft wave drag coefficient for M=1.3.
CDWT	Total aircraft wave drag coefficient for a given Mach number.
CDWW1	Wave drag coefficient of the wing for M=1.0.
CDWW2	Wave drag coefficient of the wing for M=1.3.
CEFB	Fin root chord.

CEFM	Mean chord of the fin.	
CETM	Mean chord of the tail.	
CFR	Skin friction coefficient.	
CGV1	Term in the calculation of fuselage CG.	
CGV2	Term in the calculation of fuselage CG.	
CGV3	Term in the calculation of fuselage CG.	
CL	Lift coefficient.	
CL1	Initial estimate of maximum sustained lift coefficient used in sortie performance calculations.	EV
CL2	Actual maximum sustained lift coefficient in sortie performance calculations.	
CL3	Initial estimate of maximum sustained lift coefficient for a selected throttle setting, used in STR calculations.	EV
CL4	Actual maximum sustained lift coefficient for a selected throttle setting, in STR calculations.	
CLC	Critical lift coefficient.	EV
CLDES	Manoeuvring design lift coefficient.	EV
CLMAX	Maximum lift coefficient (trimmed) at a given mach number.	EV
CLT	Maximum lift coefficient available at take-off.	
CT	Tip chord in the evaluation of the flying surfaces lateral cross-sectional area.	
CWA	Aileron mean chord.	
CWBB	Wing-box chord at the body side.	
CWBT	Wing-box tip chord.	
CWCA2	Wing chord at mid-span of each aileron.	
CWCB	Net wing root chord.	
CWCC	Centerline chord of the gross wing.	
CWCCT	Wing chord at outboard end of T.E. flaps.	
CWCT	Wing-tip chord.	
CWFM	Mean chord of T.E. flaps.	
CWMA	Wing mean aerodynamic chord.	
CWMG	Wing mean geometric chord.	
CWMN	Mean chord of the net wing.	
CWS	Spoiler chord.	
CWY	Chord of wing at spanwise position Y.	
D1	Maximum depth of wing at the body side.	
D6	Maximum depth of the wing at the tip.	
DCLF	Lift coefficient increment due to T.E. flaps.	
DCLFH	Increment in the maximum lift coefficient due to T.E. flaps.	
DE1	Lesser of DE and D1.	
DE	Depth of the wing-box at the body side.	
DF	Flap thickness function used in the estimation of flap mass.	
DGA	Gun ammunition round diameter.	EV
DGB	Gun barrel diameter.	EV
DGBK	Gun barrel width (diameter) clearance factor.	EV
DK2	Increment on K1 to define lift dependent drag parameter K2.	EV
DM	Mach number increment.	EV
DMRM	Diameter of the medium range missile.	EV
DP1	Engine compressor inlet diameter.	
DP1R	Compressor inlet diameter of datum engine.	EV
DP2	Turbine section exit diameter.	
DP2R	Turbine section exit diameter of datum engine.	EV

DP3	RLS section diameter.	
DP3R	RLS section diameter of datum engine.	EV
DP4	RLS section exit diameter.	
DP4R	RLS section exit diameter of datum engine.	EV
DP5	Afterburner exit diameter.	
DP5R	Afterburner exit diameter of datum engine.	EV
DP6	Nozzle exit diameter.	
DP6R	Nozzle exit diameter of datum engine.	EV
DRDE	RLS duct external diameter.	
DSRM	Diameter of the short range missile.	EV
DT	Acceleration time.	
DTE	Average depth of the rear spar.	
DUMW	Main undercarriage wheel and tyre diameter.	
DUMWK	Constant in correlation for main undercarriage wheel and tyre diameter.	
DUNW	Nose undercarriage wheel and tyre diameter.	
DUNWK	Constant in correlation for nose undercarriage wheel and tyre diameter.	
DXA	Factor in the definition of subdivisions between stations.	
DXB	Factor in the definition of subdivisions between stations.	
DXC	Factor in the definition of subdivisions between stations.	
DXD	Factor in the definition of subdivisions between stations.	
DXE	Factor in the definition of subdivisions between stations.	
DXF	Factor in the definition of subdivisions between stations.	
DXG	Factor in the definition of subdivisions between stations.	
DXI	Factor in the definition of subdivisions between stations.	
EXF	Axial distance between two successive fuselage stations.	
EBP1	Engine bay width clearance at the compressor inlet.	
EBP1H	Maximum value of clearance EBP1.	EV
EBP1S	Minimum value of clearance EBP1.	EV
EBP2	Engine bay width clearance at the turbine section exit.	
EBP2H	Maximum value of clearance EBP2.	EV
EBP2S	Minimum value of clearance EBP2.	EV
EBP3	Engine bay width clearance at the RLS section centre.	
EBP3H	Maximum value of clearance EBP3.	EV
EBP3S	Minimum value of clearance EBP3.	EV
EBP4	Engine bay width clearance at the RLS section exit.	
EBP4H	Maximum value of clearance EBP4.	EV
EBP4S	Minimum value of clearance EBP4.	EV
EBP5	Engine bay width clearance at the afterburner section exit.	
EBP5H	Maximum value of clearance EBP5.	EV
EBP5S	Minimum value of clearance EBP5.	EV
EBP6	Engine bay width clearance at the nozzle exit plane.	

EBP6H	Maximum value of clearance EBP6.	EV
EBP6S	Minimum value of clearance EBP6.	EV
ECCDIV	Intake b.l.diverter drag increment due to compressibility.	
ECDFT	Afterbody wave drag increment due to interference effects of the front fuselage.	
EDAR	Radar scanner clearance.	EV
EFW	Term used for the moment arm estimation of fuselage structure.	
EFX	Term used for the moment arm estimation of fuselage skin.	
EHCS	Perpendicular distance between the seat-back and rear cockpit bulkhead.	EV
EHP1	Engine bay height clearance at the compressor inlet.	
EHP1H	Maximum value of clearance EHP1.	EV
EHP1S	Minimum value of clearance EHP1.	EV
EHP2	Engine bay height clearance at the turbine section exit.	
EHP2H	Maximum value of clearance EHP2.	EV
EHP2S	Minimum value of clearance EHP2.	EV
EHP3	Engine bay height clearance at the RLS section centre.	
EHP3H	Maximum value of clearance EHP3.	EV
EHP3S	Minimum value of clearance EHP3.	EV
EHP4	Engine bay height clearance at the RLS section exit.	
EHP4H	Maximum value of clearance EHP4.	EV
EHP4S	Minimum value of clearance EHP4.	EV
EHP5	Engine bay height clearance at the afterburner exit plane.	
EHP5H	Maximum value of clearance EHP5.	EV
EHP5S	Minimum value of clearance EHP5.	EV
EHP6	Engine bay height clearance at the nozzle exit plane.	
EHP6H	Maximum value of clearance EHP6.	EV
EHP6S	Minimum value of clearance EHP6.	EV
EHSWBI	Missile ejector mechanism height.	EV
ELFT	Rear fuselage length increment to form a complete afterbody.	
ELUP	Distance between main u/c pintle and rear of u/c bay.	EV
EMFG	Mass of miscellaneous items (e.g. gear for naval aircraft).	
EQWF	T.E. flap deflection.	EV
EQWFH	Maximum T.E. flap deflection.	EV
EQWFL	T.E. flap deflection in landing.	EV
EQWFT	T.E. flap deflection at take-off.	EV
ERR	Specified error for equality constraints.	EV
EXF	Axial distance between fuselage stations.	EV
F	Function to be integrated in the numerical integration.	
F1	First estimate of the net propulsive force.	
F2	Second estimate of the net propulsive force.	
FBP1K	Constant factor for engine bay width clearance, EBP1.	EV
FBP2K	Constant factor for engine bay width clearance, EBP2.	EV

FBP3K	Constant factor for engine bay width clearance, EBP3.	EV
FBP4K	Constant factor for engine bay width clearance, EBP4.	EV
FBWA	Total fractional span of all ailerons.	EV
FBWCF	Fractional span of the wing-box containing fuel tanks.	
FBWF	Fractional gross span of the T.E. flaps.	EV
FBWNF	Fractional span of the net wing-box containing fuel tanks.	EV
FCWD	Front spar position as a fraction of the local wing chord.	IV
FCWLFT	Chord of fixed L.E. forward of front spar as a fraction of local wing chord.	EV
FCWLHT	Distance of the T.E. of the L.E. high lift device,forward of the front spar as a fraction of the local wing chord.	EV
FCWR	Rear spar position as a fraction of the local wing chord.	IV
FCWTFT	Distance of the T.E. of the fixed section of the wing T.E. aft of the rear spar as fraction of the local wing chord.	EV
FCWTHL	Distance of the L.E. of the T.E. flaps aft of the rear spar as a fraction of the local wing chord.	EV
FDUMW	Factor to allow for main wheel diameter clearance.	EV
FDUMWK	Factor in correlation for main undercarriage wheel diameter.	EV
FDUNW	Factor to allow for nose wheel diameter clearance.	EV
FDUNWK	Factor in correlation for nose undercarriage wheel diameter.	EV
FHP1K	Constant factor for engine bay height clearance,EHP1.	EV
FHP2K	Constant factor for engine bay height clearance,EHP2.	EV
FHP3K	Constant factor for engine bay height clearance,EHP3.	EV
FHP4K	Constant factor for engine bay height clearance,EHP4.	EV
FHP5K	Constant factor for engine bay height clearance,EHP5.	EV
FHP6K	Constant factor for engine bay height clearance,EHP6.	EV
FIKN	Tail interference factor.	
FIWBW	Body interference factor.	
FK	Bending moment factor in mass estimation of the wing-box.	
FK1D0	Subsonic datum value for K1.	
FK1D1	Supersonic datum value for K1.	
FK1HK1	First factor in the expression for FK1H.	
FK1HK2	Second factor in the expression for FK1H.	
FK1HK3	Third factor in the expression for FK1H.	
FK1H	Value of K1 at supersonic speeds.	
FK1H1	Value of K1 for M=1.4.	
FK1H2	Value of K1 for M=2.0.	
FK1K0	Coefficient in cubic for the estimation of K1	

	for Mach numbers between 0.8 and 1.2.	
FK1K1	Coefficient in cubic for the estimation of K1 for Mach numbers between 0.8 and 1.2.	
FK1K2	Coefficient in cubic for the estimation of K1 for Mach numbers between 0.8 and 1.2.	
FK1K3	Coefficient in cubic for the estimation of K1 for Mach numbers between 0.8 and 1.2.	
FK1SK1	First factor for the estimation of FK1SK4.	
FK1SK2	Second factor for the estimation of FK1SK4.	
FK1SK3	Third factor for the estimation of FK1SK4.	
FK1SK4	Factor for the estimation of FK1D0.	
FLII	Distance of intake diffuser inlet from cockpit front bulkhead (station A).	EV
FLP1K	Exponent in correlation for length of engine gas generator.	EV
FLP2K	Exponent in correlation for length of engine reheat fuelling section.	EV
FLP3K	Exponent in correlation for length of engine nozzle.	EV
FLVK	Constant relating boundary layer diverter length to intake height.	EV
FMD1	First constant factor for the estimation of MD.	EV
FMD2	Second constant factor for the estimation of mD,which allows for improvements in aerodynamic technology.	EV
FMEF	Fin materials mass factor.	EV
FMET	Tail materials mass factor.	EV
FMF1	Materials mass factor for fuselage miscellania.	EV
FMF2	Materials mass factor for fuselage.	EV
FMGA	Installation factor for the internal gun ammunition bay.	EV
FMGB	Installation factor for the internal gun barrel bay.	EV
FMGM	Installation factor for the internal gun mechanism bay.	EV
FMPBK	Factor in estimation of the mass of engine gas gas generator.	EV
FMPIK	Factor in estimation of the engine installation mass.	EV
FMPRK	Exponent in estimation of mass of the engine reheat system.	EV
FMSA	Mass fraction of air systems parts other than ducts.	EV
FMSAK	Constant factor for the prediction of the air systems mass.	EV
FMSC	State-of-the-art mass factor for the flying controls.	EV
FMSCK	Constant factor for the prediction of the flying control mass.	EV
FMSEK	Constant factor for the prediction of the electrics mass.	EV
FMSFK	Constant factor for the prediction of fuel system mass.	EV
FMTLF	Factor providing the percentage of the total fuel required at landing.	EV
FMTSW	Wing mass-loading at take-off.	
FMUHK	Constant factor for the prediction of the undercarriage hydraulics mass.	EV

FMUMK	Constant factor for the prediction of the main undercarriage mass.	EV
FMUNK	Constant factor for the prediction of the nose undercarriage mass.	EV
FMWB	Materials mass factor for the wing-box.	EV
FMWBH	Factor which corrects the MWB estimates for thin wings of moderate to high aspect ratio.	
FMWL	Materials mass factor for the wing L.E.	EV
FMWT	Materials mass factor for the wing T.E.	EV
FOFB1K	Area factor (above floor) for fuselage section B.	EV
FOFB2K	Area factor (below floor) for fuselage section B.	EV
FOFCK	Area factor for fuselage section C.	EV
FOFDK	Area factor for fuselage section D.	EV
FOFEK	Area factor for fuselage section E.	EV
FOFFK	Area factor for fuselage section F.	EV
FOFGK	Area factor for fuselage section G.	EV
FOFHK	Area factor for fuselage section H.	EV
FOT6N	Increment in cross-sectional area at the nozzle exit above datum value (OII+OVI).	IV
FPS	Engine throttle setting.	
FPSED	Engine throttle setting in data input mode.	
FQWF	Factor for the estimation of the lift increment due to T.E. flaps.	
FQWT1	Factor for, for aerofoil family, relating the t.E. angle to section thickness to chord.	EV
FREEF	Factor for the Reynolds number effects on aerofoil section lift.	EV
FSUM	Partial sum in the numerical integration.	
FSUM2	Partial sum in the numerical integration.	
FSUM2	Partial sum in the numerical integration.	
FSUM3	Partial sum in the numerical integration.	
FVSTTO	Factor defining the take-off speed in terms of the stall speed.	EV
FVUMLK	Constant for the leg related volume of main undercarriage.	EV
FWLD	Non-elliptical wing loading factor.	EV
FX	Axial distance from the aircraft nose.	EV
G	Gravitational acceleration.	
GCDTW	Gradient of the wave drag coefficient with mach number at M=1.	
GCLA	Aircraft lift-curve slope.	
GCLK0	Coefficient in cubic interpolation of GCLA vs M	EV
GCLK1	Coefficient in cubic interpolation of GCLA vs M	EV
GCLK2	Coefficient in cubic interpolation of GCLA vs M	EV
GCLK3	Coefficient in cubic interpolation of GCLA vs M	EV
GCLK4	Term in expression for the estimation of GCLA.	EV
GCLW	Lift-curve slope of the wing.	
GCLWD	Lift-curve slope of the aerofoil.	
GDW	Downwash factor.	
GK1D1	Gradient of supersonic zero-lift wave drag with M.	EV
GN	Load factor.	EV
GNA	Maximum attained load factor.	
GNH	Maximum sustained load factor.	
GNS	Sustained load factor.	
GNSH	Maximum permissible value of the sustained	

GOF1	Gradient of cross-sectional area of fuselage at stn R.	
GTCPH	Maximum human G-tolerance limit.	EV
HC1	Distance between thigh point and eye point.	EV
HC2	Distance between thigh point and heel point.	EV
HC3	Distance between thigh point and NSRP.	EV
HC4	Vertical gap between eye-point and canopy.	EV
HC5	Height of the fwd cockpit bulkhead above the cockpit floor.	
HC6	Height of the raised heel-line above the cockpit floor.	
HCEYE	Height of the eye-point above the cockpit floor	
HCSEAT	Height of the NSRP above the cockpit floor measured along the seat-back line.	EV
HFA	Height of fuselage at stn A.	
HFA1	Cockpit underfloor height at stn A.	EV
HFACNR	Corner height of fuselage section A.	
HFB	Height of fuselage at stn B.	
HFB1	Cockpit underfloor height at stn B.	
HFC	Height of fuselage at stn C.	
HFCDH	The greatest of HFC and HFD.	
HFD	Height of fuselage at stn D.	
HFDS	Minimumeight of fuselage at stn D.	
HFE	Height of fuselage at stn E.	
HFF	Height of fuselage at stn F.	
HFG	Height of fuselage at stn G.	
HFH	Height of fuselage at stn H.	
HFJ	Height of fuselage at stn J.	
HFI	Height of fuselage at stn I.	
HGAK	Gun ammunition bay height clearance factor.	EV
HGABI	Gun ammunition bay height.	
HGM	Gun mechanism height.	EV
HGMK	Gun mechanism bay height clearance factor.	EV
HGMBI	Gun mechanism bay height.	
HIDD	Height of an intake diffuser at stn D.	
HIDX	Height of an intake diffuser at any stn X.	
HII	Height of an intake diffuser at the intake plane.	
HP2	Engine total height at gas generator exit.	
HP3	Engine total height at the RLS section centre.	
HP4	Engine total height at RLS section exit.	
HRD	Side tank height.	EV
HSWBI	Heigth of the internal weapons bay.	
HSWBIK	Heigth clearance factor for the internal weapons bay.	EV
HT	Flight altitude.	EV
HTACA	Altitude for the acceleration time at constant altitude.	EV
HTACAI	Altitude for the acceleration time at constant altitude - input data form.	EV
HTATR	Attained turn rate altitude.	EV
HTATRI	Attained turn rate altitude - input data form.	EV
HTEN	Altitude in engine input form.	
HTG	Geopotential height.	
HTMML	Maximum Mach number altitude.	EV
HTMMLI	Maximum Mach number altitude - input data form.	EV
HTR	Equivalent surface roughness height.	EV
HTRIDE	Ride quality factor altitude.	EV

HTRIDI	Ride quality factor altitude - input data form.	EV
HTSEP	Specific excess performance altitude.	EV
HTSEPI	Specific excess performance altitude - input data form.	EV
HTSTR	Sustained turn rate altitude.	EV
HTSTRI	Sustained turn rate altitude - input data form.	EV
HVI	Height of the b.l.diverter at the intake plane.	
HWBB	Height of the center-section of the wing-box.	
IFUN	Total sum - integration - in the numerical integration.	
K1	Lift dependent drag parameter for CL lower than CLC.	
K2	Lift dependent drag parameter for CL higher than CLC.	
KNUMI	Intermediate variable related to NNUMI.	
KY1	Intermediate variable in the evaluation of the flying surfaces lateral cross-sectional area.	
LAR	Length of the radar avionics bay.	EV
LAX1	Length of the extra avionics bay ,aft of the radar bay in section R-A.	EV
LAX2	Length of the avionics bay ,aft of the cockpit.	EV
LCCAN	Total length of canopy and windscreen.	EV
LCEYE	Horizontal distance between fwd cockpit bulkhead and eye-point.	
LCFL	Length of the cockpit floor.	
LCFOOT	Horizontal distance between fwd cockpit bulkhead and heel-point.	EV
LFCQM	Fin moment arm measured between the mean quarter chord points of the wing and fin.	
LTCQM	Tail moment arm measured between the mean quarter chord points of the wing and tail.	
LGA	Gun ammunition length.	EV
LGABI	Gun ammunition bay length.	
LGAK	Gun ammunition bay length clearance factor.	EV
LGB	Gun barrel length.	EV
LGBBI	Gun barrel bay length.	
LGBK	Gun barrel bay length clearance factor.	EV
LGM	Gun mechanism length.	EV
LGMBI	Gun mechanism bay length.	
LGMK	Gun mechanism bay length clearance factor.	EV
LIDG	Length of the intake diffuser.	
LMRM	Length of the medium range missile.	EV
LP12	Length of the gas generator of engine.	
LP12R	Length of the gas generator of datum engine.	EV
LP23	Length of the first half of the RLS section of engine.	
LP23R	Length of the first half of the RLS section of datum engine.	EV
LP34	Length of the second half of the RLS section of engine.	
LP34R	Length of the second half of the RLS section of datum engine.	EV
LP45	Length of the reheat section of engine.	
LP45R	Length of the reheat section of datum engine.	EV
LP56	Engine nozzle length.	
LP56R	Nozzle length of datum engine.	EV
LPG	Total engine length.	
LRD	Side tank length.	

LRDG	RLS duct length.	
LSRM	Length of the short range missile.	EV
LSWBI	Length of the internal weapons bay.	EV
LSWBIK	Length clearance factor for the internal weapons bay.	
LULG	Sum of lengts of all undercarriage length elements.	
LULG1K	Constant in correlation for undercarriage length.	EV
LULG1K	Constant exponent in correlation for undercarriage length.	EV
LUMB	Length of a main undercarriage bay.	
LUMN	Length of each undercarriage leg.	
LUNB	Length of the nose undercarriage bay.	
LUNS	Length of the nose undercarriage leg.	
LVG	Length of the boundary layer diverter exit.	
LWBEF	Moment arm of the center of volume of the wing fuel tanks relative to L.E. of wing-box at wing root.	
LWFK	Length of flap tracks as a fraction of the wing chord.	EV
LWTTLS	Minimum gap between Wing T.E. and tailplane l.E. at body side.	
MAR	Mass of radar avionics.	EV
MASS	Mass of the aircraft at the start of a sortie stage.	
MAX	Mass of general avionics.	EV
MCC	Mass of canopy.	
MCI	Total mass of cockpit equipment.	
MCP	Mass of crew.	EV
MCR	Critical Mach number.	
MCSEAT	Mass of ejection seat.	EV
MCTF	Central tank mass (total).	
MESTF	Side tank mass (total-each).	
MCW	Mass of the windscreen.	
MD	Drag rise Mach number.	
MDD	Drag rise Mach number at zero lift.	
MDI	Mass of the hover control system ducting.	
MEF	Total mass of fin structure.	
MEF1K	Constant in correlation for fin mass.	EV
MEF2K	Second constant in correlation for fin mass.	EV
MEF3K	Third constant in correlation for fin mass.	EV
MEF4K	Fourth constant in correlation for fin mass.	EV
MFAB	Mass of the airbrake.	
MFG	Total mass of fuselage structure.	
MFX	Mass of fuselage shell.	
MFXP	Mass of aircraft paint.	
MFW	Mass of internal fuselage structure.	
MGA	Mass of one round of gun ammunition.	EV
MGABI	Mass of the internal gun ammunition bay.	
MGB	Mass of gun barrel.	EV
MGABI	Mass of the internal gun barrel bay.	
MGM	Mass of gun mechanism.	EV
MGABI	Mass of the internal gun mechanism bay.	
MHDG	Mass per unit length for the hover control ducting.	EV
MLRD	Total RLS duct mass.	
MLRD1	RLS first duct mass.	

MRLD2	RLS second duct mass.	
MRLD3	RLS duct nozzle mass	EV
MMRM	Mass of the medium range missile.	EV
MN	Mach number.	EV
MN1	First Mach number value in calculation of acceleration time.	
MN2	Second Mach number value in calculation of acceleration time at constant altitude.	
MNACA	Mach number for the acceleration time at constant altitude.	EV
MNACAI	Mach number for the acceleration time at constant altitude - input data form.	EV
MNAR	Switch for the activation of the area-rule (subroutine flatcross).For area-rule MNAR $\geq$ 1	EV
MNATR	Attained turn rate Mach number.	EV
MNATRI	Attained turn rate Mach number - input data form.	EV
MNCR	Critical Mach number.	
MNEN	Mach number in engine input form.	
MNMAX	Maximum Mach number.	
MNMAXO	Maximum Mach number - output data form.	
MNMXOU	Maximum Mach number constraint.	EV
MNRIDE	Ride quality factor Mach number.	EV
MNRIDI	Ride quality factor Mach number - input data form.	EV
MNSEP	Specific excess performance Mach number.	EV
MNSEPI	Specific excess performance Mach number - input data form.	EV
MNSTR	Sustained turn rate Mach number.	EV
MNSTRI	Sustained turn rate Mach number - input data form.	EV
MNUMI	Intermediate variable related to NNUMI.	
MODE	Engine performance analysis mode .	
MPA	Air mass flow for the engine.	
MPAED	Air mass flow in data input mode.	
MPAC	Air mass flow at maximum gross thrust.	
MPAD	Air mass flow rate at sea-level static conds.	
MPAD1	Value of MPAD for the datum engine.	EV
MPB	Engine gas generator mass.	
MPBR	Engine gas generator reference mass.	EV
MPF	Fuel mass flow rate of the engine.	
MPFB1	Initial estimate for the mass of fuel required in a sortie leg.	EV
MPFB2	Improved estimate for the mass of fuel required in a sortie leg.	EV
MPFB2T	Total fuel mass consumed during a sortie,up to the end of the leg under consideration.	
MPFC	Fuel mass flow at maximum gross thrust.	
MPFD	Fuel mass flow at maximum gross thrust at sea level.	
MPFD1	Fuel mass flow at sea-level static conditions	EV
MPFED	Fuel mass flow in data input mode.	
MPFS1	Minimum fuel mass flow rate at sea-level static conditions.	
MPG	Total engine mass.	
MPI	Engine installation mass.	
MPL	Engine RLS section mass.	
MPLR	Engine RLS section reference mass.	EV

MPNR	Engine nozzle reference mass.	EV
MPNT	Aircraft paint.	
MPR	Engine afterburner mass.	
MPRR	Reference engine afterburner mass.	EV
MPT	Thrust reverser mass.	
MPTR	Thrust reverser reference mass.	EV
MSA	Mass of air services (airconditioning and avionics cooling systems).	
MSAK	Constant related to MSA.	EV
MSC	Mass of flying controls.	
MSCK	Constant related to the flying controls mass.	EV
MSE	Electrical system (generation & distribution) mass.	
MSEK	Constant related to MSE.	EV
MSF	Fuel system mass.	
MSG	Total mass of all aircraft systems.	
MSRM	Mass of the short range missile.	EV
MSWBI	Total mass of the internal weapons bay.	
MTCR	Stressing mass for the wing.	
MTE	Empty mass of aircraft.	
MTGFI	Total internal fuel mass.	
MTLF	Fuel mass required for landing.	EV
MTLR	Reference landing mass.	
MTOUF	Mass of oil and unused fuel.	
MTP	Total aircraft payload (fuel excluded).	
MTPR	Reference load for the definition of MTCR.	EV
MTR	Mass of fixed role equipment.	
MTT	Total aircraft take-off mass.	
MTTF	Fuel mass required for take-off.	EV
MTTPP	Fuel mass used in the point performanmce calculations.	
MTTR	Take-off reference mass.	EV
MU	Atmospheric air viscocity.	
MUH	Mass of undercarriage associated hydraulics.	
MUHK	Constant in correlation for mass of undercarriage hydraulics.	EV
MUM	Main undercarriage mass.	
MUMG	Total mass of main undercarriage including hydraulics.	
MUMK	Constant in correlation for mass of main undercarriage structure.	EV
MUN	Structure mass of nose undercarriage.	
MUNG	Total mass of nose undercarriage including hydraulics.	
MUNK	Constant in correlation for mass of nose undercarriage.	EV
MUSL	Sea-level atmospheric air viscocity.	
MWA	Total mass of ailerons.	
MWB	Total mass of the wing-box.	
MWBCF	Mass of fuel stored in the central wing-box.	
MWBEF	Mass of fuel stored in the wingbox outside the fuselage.	
MWC	Total mass of the wing.	
MWCX	Mass of miscellaneous attachments.	
MWF	Total mass of the T.E. flaps.	
MWFK	Mass of flap tracks.	
MWL	Total mass of the wing L.E.	
MWS	Total spoiler mass.	

MWT	Total mass of the fixed section of the T.E. of the wing.	
MWXF	Mass of miscellaneous fairings.	
MWXP	Mass of painting on wing.	
MXP	Mass of external pylons.	EV
MXT	Structural mass of external tanks.	EV
MXTF	Total mass of externally carried fuel.	
N1	Iteration limit variable in sortie.	
N2	Iteration limit variable in sortie.	
NACA	Number of constant acceleration constraints.	EV
NATR	Number of attained turn rate constraints.	EV
NED	Number of engine performance input data - rows of the input data table.	EV EV
NE1	Row number used in the reading of the engine performance data in table form.	
NE2	Row number used in the reading of the engine performance data in table form.	
NED1	Row number used in the reading of the engine performance data in table form.	
NED2	Row number used in the reading of the engine performance data in table form.	
NED3	Row number used in the reading of the engine performance data in table form.	
NED8	Row number used in the reading of the engine performance data in table form.	
NED14	Row number used in the reading of the engine performance data in table form.	
NED15	Row number used in the reading of the engine performance data in table form.	
NED16	Row number used in the reading of the engine performance data in table form.	
NED17	Row number used in the reading of the engine performance data in table form.	
NED18	Row number used in the reading of the engine performance data in table form.	
NED19	Row number used in the reading of the engine performance data in table form.	
NED20	Row number used in the reading of the engine performance data in table form.	
NED25	Row number used in the reading of the engine performance data in table form.	
NED26	Row number used in the reading of the engine performance data in table form.	
NED27	Row number used in the reading of the engine performance data in table form.	
NED29	Row number used in the reading of the engine performance data in table form.	
NED31	Row number used in the reading of the engine performance data in table form.	
NED32	Row number used in the reading of the engine performance data in table form.	
NEN	Number of engines in integral form.	EV
NENG	Number of engines.	EV
NGA	Number of gun ammunition rounds.	EV
NGAK	Nearest integer to the square root of NGA.	
NL1	Iteration limit variable in maximum Mach number subroutine.	
NLEG	Number of sortie stages.	EV

NMMML	Number of maximum Mach number constraints.	EV
NMRM	Number of medium range missiles.	EV
NNN1	Row number used in the reading of the engine performance data in table form.	
NNN2	Row number used in the reading of the engine performance data in table form.	
NNUMI	Number of segments in the numerical integration	
NPPERF	Number of point performance constraints.	EV
NPPER	Number of sortie performance stages fuel mass that are included in the mass estimation used in the sustained turn rate calculations.	EV
NRIDE	Number of quality ride factor constraints.	EV
NSEP	Number of specific excess performance constraints.	EV
NSRM	Number of short range missiles.	EV
NSTR	Number of sustained turn rate constraints.	EV
NU	Kinematic viscocity of atmospheric air.	
NWFK	Number of flap tracks.	EV
NWP	Number of wing pylons.	EV
NWS	Number of spoilers.	EV
NXFOH	Station number of maximum fuselage cross-sectional area.	
NXFOHS	Station number of maximum fuselage nett cross-sectional area.	
NXFOTH	Station number of maximum afterbody fuselage cross-sectional area.	
OF1	Fuselage cross-sectional area at stn R.	
OFA	Fuselage cross-sectional area at stn A.	
OFAUF	Cross-sectional area underfloor at stn A.	
OFAUFS	Minimum cross-sectional area underfloor at stn A.	
OFB	Fuselage cross-sectional area at stn B.	
OFBS	Minimum fuselage cross-sectional area at stn B.	
OFBUF	Cross-sectional area underfloor at stn B.	
OFC	Fuselage cross-sectional area at stn C.	
OFCS	Minimum fuselage cross-sectional area at stn C.	
OFD	Fuselage cross-sectional area at stn D.	
OFDS	Minimum fuselage cross-sectional area at stn D.	
OFE	Fuselage cross-sectional area at stn E.	
OFES	Minimum fuselage cross-sectional area at stn E.	
OFF1	Fuselage cross-sectional reference area at stn F.	
OFF	Fuselage cross-sectional area at stn F.	
OFFS	Minimum fuselage cross-sectional area at stn F.	
OFG1	Fuselage cross-sectional reference area at stn G.	
OFG	Fuselage cross-sectional area at stn G.	
OFGS	Minimum fuselage cross-sectional area at stn G.	
OFH	Fuselage cross-sectional area at stn H.	
OFHS	Minimum fuselage cross-sectional area at stn H.	
OFJ	Fuselage cross-sectional area at stn J.	
OFI	Fuselage cross-sectional area at stn I.	
OFX	Fuselage cross-sectional area at stn X.	
OFXH	Maximum cross-sectional area of the fuselage.	
OFXHS	Maximum net cross-sectional area of the fuselage.	
OFXTH	Maximum cross-sectional area of the afterbody.	
OGABI	Cross-sectional area of the internal gun	

	ammunition bay.
OGBBI	Cross-sectional area of the internal gun barrelbay.
OGMBI	Cross-sectional area of the internal gun mechanism bay.
OIDD	Cross-sectional area of an intake diffuser at stn D.
OIDX	Cross-sectional area of an intake diffuser at any stn X.
OIE	Total exit area of the intake diffusers.
OII	Total inlet area of the intake diffusers.
OIX	Cross-sectional area of the intake at stn X.
OP1B	Cross-sectional area of the engine at the compressor inlet.
OP2B	Cross-sectional area of the engine at the turbine section exit.
OP3B	Cross-sectional area of the engine at the middle of the RLS section.
OP4B	Cross-sectional area of the engine at the exit of the RLS section.
OP5B	Cross-sectional area of the engine at the exit of the afterburner section.
OPJ	Jet exit area at general Mach number and altitude.
OPJED	Jet exit area in data input mode.
OPJD	Jet exit area at sea-level static conditions.
OPJD1	Jet exit area at sea-level static conditions for the datum engine. EV
OPN	Total nozzle exit area.
OPX	Cross-sectional area of the engine at stn X.
ORDE	RLS duct cross-sectional area.
ORDI	RLS duct internal diameter.
OSWBI	Cross-sectional area of the weapons bay.
OT6N	Increment at cross-sectional area at nozzle, from fairing curve.
OTA1K	Coefficient in cubic for cross-sectional area of aft fairing.
OTA2K	Coefficient in cubic for cross-sectional area of aft fairing.
OTA3K	Coefficient in cubic for cross-sectional area of aft fairing.
OTA4K	Coefficient in cubic for cross-sectional area of aft fairing.
OTF1K	Coefficient in cubic for cross-sectional area of front fairing.
OTF2K	Coefficient in cubic for cross-sectional area of front fairing.
OTF3K	Coefficient in cubic for cross-sectional area of front fairing.
OTF4K	Coefficient in cubic for cross-sectional area of front fairing.
OTF4K1	First coefficient for determining OTF4K.
OTF4K2	Second coefficient for determining OTF4K.
OTF4K3	Third coefficient for determining OTF4K.
OTM	Maximum cross-sectional area of the fairing curve.
OTXN	Cross-sectional area of the fairing curve at any stn X.

OUMLB	Cross-sectional area of each main undercarriage leg bay.	
OUMWB	Cross-sectional area of each main undercarriage wheel bay.	
OUNLB	Cross-sectional area of nose undercarriage leg bay.	
OUNWB	Cross-sectional area of nose undercarriage wheel bay.	
OVI	Cross-sectional area of the boundary layer diverter at the intake plane.	
OWBB	Cross-sectional area of the centre section of the wing box.	
OX	Cross-sectional area of flying surfaces.	
OXW	Semi-lateral cross-sectional area of the wing.	
OXW2	Lateral cross-sectional area of the wing.	
OXEF	Lateral cross-sectional area of the fin.	
OXET	Semi-lateral cross-sectional area of the tailplane.	
OXET2	Lateral cross-sectional area of the tailplane.	
P	Atmospheric air pressure.	
PFX	Fuselage perimeter at stn X.	
PI	3.14	EV
Q	Dynamic pressure.	
Q1	Dynamic pressure coresponding to speed V1.	
Q2	Dynamic pressure coresponding to speed V2.	
QCCAN	Canopy centerline inclination above the horizontal.	EV
QCEYE	Pilot's forward and downward view angle measured from the eye-point.	EV
QCFOOT	Angle between the line joining the thigh-heel points and the horizontal.	
QCSEAT	Seat-back angle.	EV
QCWSC	Windscreen inclination to the horizontal.	EV
QEF2	Fin mid-chord sweep.	
QEF4	Fin quarter chord sweep.	
QEFL	Fin L.E. sweep.	EV
QEFT	Fin T.E. sweep.	EV
QET2	Tail mid-chord sweep.	
QET4	Tail quarter chord sweep.	
QETL	Tail L.E. sweep.	EV
QETT	Tail T.E. sweep.	EV
QFA	Half of angle subtended by cockpit floor at centre of section A.	
QL	L.E. sweep in the evaluation of the flying surfaces lateral cross-sectional area.	
QT	T.E. sweep in the evaluation of the flying surfaces lateral cross-sectional area.	
QW2	Mid-chord sweep of the wing.	
QW4	Quarter chord sweep of the wing.	IV
QWA	Aileron L.E. sweep.	
QWB	Wing-box centerline sweep.	
QWL	Wing leading edge sweep.	
QWT	Wing trailing edge sweep.	
R1	Engine throttle setting or gross thrust.	
R21	Function used in engine performance estimation.	
R22	Function used in engine performance estimation.	
R41	Function used in engine performance estimation.	
R42	Function used in engine performance estimation.	

RCCANB	Canopy radius at stn B.	
RCCANC	Canopy radius at stn C.	
RCCAND	Canopy radius at stn D.	
RCCANE	Canopy radius at stn E.	
RCCANF	Canopy radius at stn F.	
RCCANG	Canopy radius at stn G.	
RCDC	Form factor used in the estimation of the zero lift drag coefficient of the canopy.	
RCDEF	Form factor used in the estimation of the zero lift drag coefficient of the fin.	
RCDET	Form factor used in the estimation of the zero lift drag coefficient of the tail.	
RCDF	Form factor used in the estimation of the zero lift drag coefficient of the fuselage.	
RCDFT	Factor for truncation of pointed afterbody in wave drag calculations.	
RCDK	Sharpness parameter for intake lips in spillage drag estimation.	EV
RCDVK	Factor on K1 to allow for the effects of advanced technology.	EV
RCDW	Form factor used in the estimation of the zero lift drag coefficient of the wing.	
RCEFD	Weighting for fin mean chord for spanwise variation of Reynolds number.	
RCETD	Weighting for tail mean chord for spanwise variation of Reynolds number.	
RCSW	Foreplane volume coefficient.	EV
RCWCD	Weighting for wing mean chord for spanwise variation of Re.	
RD	Relative density of atmospheric air.	
RDFL	Equivalent fineness ratio for the fuselage used in RCDF calculations.	
RDP	Tail interference factor.	
REFFC	Fin volume ratio.	EV
RETSW	Tail volume ratio.	EV
RFCNRA	Fixed proportion of the corner radii at stn A.	EV
RFUL	Fuel density.	EV
RH	Atmospheric air density at HTH.	
RIDD	Corner radius of an intake diffuser at stn D.	
RIDX	Corner radius of an intake diffuser at any station.	
RLDFI	Fineness ratio of the fuselage section from the intake plane to the stn at which OFXH occurs.	
RLDFS	Fineness ratio of the fuselage section from the nose to the intake plane.	
RLDFT	Fineness ratio of the equivalent afterbody.	
RLFD	Weighting for fuselage length to account for reynolds number variation.	
RLTAFN	Ratio of the axial distance from the end of the center-section to the point at which the decrease in cross-sectional area is half the maximum increment to the length of the aft fairing.	IV
RLTCA	After CG position as fraction of mean aerodynamic chord, forward of mean quarter chord point.	EV
RLTCFN	Ratio of the length of the center-section to	IV

	length of the fuselage after of the forward fairing.	
RLTCL	Forward CG position as fraction of mean aerodynamic chord, forward of mean quarter chord point.	EV
RLTFFN	Ratio of the axial distance from the end of the radome to the point at which the increase in cross-sectional area is half of the maximum increment to the length of the forward fairing.	IV
RLTMFN	Ratio of the length of the forward fairing to the overall fuselage length minus the length of the radome.	IV
RLUNM	Ratio of nose to main undercarriage leg lengths	EV
RLPCW	Undercarriage CG position after of mean quarter chord point as a fraction of the mean aerodynamic chord.	EV
RWBC2	CG of central wing-box fuel tank from wing root L.E. / box chord.	
RLWCC	Wing CG position aft of mean quarter chord point as fraction MAC.	
RMLRD	RLS duct mass per unit length factor.	EV
RMPA1H	Non-dimensional maximum air mass flow rate for the engine.	
RMPF1	Non-dimensional fuel mass flow at combat dry thrust rating,at altitude.	
RMPF2	Non-dimensional fuel mass flow at combat reheat thrust rating.	
RMPF1H	Non-dimensional fuel mass flow at combat dry thrust rating,at 11000 m altitude.	
RMTLFI	Mass proportion of internal fuel remaining in tanks on landing.	EV
RND1	Reynold's number per unit metre.	
RNI	Reynold's number at the intake plane.	
RO	Atmospheric air density at a given altitude.	
ROFBNS	Scaling factor for section B.	
ROFCNS	Scaling factor for section C.	
ROFDNS	Scaling factor for section D.	
ROFENS	Scaling factor for section E.	
ROFFNS	Scaling factor for section F.	
ROFGNS	Scaling factor for section G.	
ROFHNS	Scaling factor for section H.	
ROFJNS	Scaling factor for section J.	
ROFINS	Scaling factor for section I.	
ROFNMA	Area ratio,OFK/OFXTH,used in estimation of afterbody drag.	
ROIEI	Fixed area ratio for the intake diffusers.	EV
ROIID	Ratio of the intake capture area to the area of intake stream tube at infinity.	
ROPJ1	Non-dimensional jet exit area at the combat dry thrust rating.	
ROPJ2	Non-dimensional jet exit area at the combat reheat thrust rating.	
ROSL	Atmospheric air density at sea-level.	
RP	Relative pressure of the atmospheric air.	
RPFX1K	Constant in expression of fuselage perimeter shape.	EV
RPFX2K	Constant in expression of fuselage perimeter shape.	EV

RPFX3K	Constant in expression of fuselage perimeter shape.	EV
RPFX4K	Constant in expression of fuselage perimeter shape.	EV
RQF	Aircraft ride quality factor.	
RQFO	Aircraft ride quality factor - output data form	
RQFOH	Aircraft ride quality factor constraint.	EV
RRIID	Ratio of the air density at the inlet to the freestream density.	
RRT	Square root of RT (relative temperature).	
RRTP	Square-root of RRT.	
RRTPG	Ratio of gross thrusts of the engine (=RTPG/ RTPG1).	
RSA	Air systems density.	EV
RSC	Flying control system density.	EV
RSE	Electrics density.	EV
RSF	Fuel system density.	EV
RT	Relative temperature of atmospheric air.	
RT1	Time required to fly a sortie leg.	
RTEF	Thickness to chord ratio of the fin.	EV
RTEFD	Function of the fin thickness to chord ratio used in wave drag estimation.	
RTET	Thickness to chord ratio of the tail.	EV
RTETD	Function of the tail thickness to chord ratio used in wave drag estimation.	
RTK	Relaxation constant in iteration for sortie fuel estimation.	
RTP	Engine scale factor.	IV
RTPG	Non-dimensional gross thrust of engine at general M and HT.	
RTPG1	Non-dimensional combat dry thrust.	
RTPG1H	Maximum value of RTPG1 at any altitude.	
RTPG2	Non-dimensional combat reheat thrust.	
RTPGW	Aircraft thrust to weight ratio at take-off.	
RTQWT	Ratio, TAN(QWT)/TAN(QWL) ,used in estimation of K1.	
RTW	Thickness to chord ratio of the wing.	IV
RTWD	Function of the wing thickness to chord ratio used in wave drag estimation.	
RXFCQM	Distance of the fin mean quarter chord point from the nose in terms of the aircraft length.	IV
RXTCQM	Distance of the tailplane mean quarter chord point from the nose in terms of the aircraft length.	IV
RXWCQM	Distance of wing mean quarter chord point from the nose in terms of the aircraft length XFN.	IV
SDT	Total time to accelerate over a Mach number increment at condstant altitude.	
SDTO	Total time to accelerate over a Mach number increment at condstant altitude - output data form.	
SDTOH	Total time to accelerate over a Mach number increment at condstant altitude constraint.	EV
SEFN	Nett fin area.	
SETN	Nett area of the tailplane.	
SEP	Specific excess power.	
SEPO	Specific excess power - output data form.	
SEP	Specific excess power constraint.	EV

SFAB	Total planform area of airbrakes.	EV
SLEG	Length of a sortie leg in km.	EV
SSPD	Speed of sound.	
STR	Sustained turn rate.	
STRO	Sustained turn rate - output data form.	
STROS	Sustained turn rate constraint.	EV
SW	Gross wing area.	IV
SWA	Planform area of the ailerons.	
SWB	Planform area of the wing-box.	
SWBF	Total planform area of the wing-box containing fuel tanks.	
SWF	Planform area of the T.E. flaps.	
SWL	Total planform area of the wing L.E.(fixed & movable).	
SWLF	Planform area of the fixed section of the L.E.	
SWLH	Planform area of the L.E. device (retracted).	
SWN	Net wing area.	
SWTF	Planform area of the fixed section of the wing t.E. aft of the rear spar.	
SWTG	Gross area of the wing T.E. aft of rear spar (including T.E. devices).	
T	Temperature.	
TA	Ambient temperature.	
TERM1B	First term for the estimation of the wing-box mass.	
TERM1F	First term for the estimation of the T.E. flaps mass.	
TERM1L	First term for the estimation of the wing L.E. mass.	
TERM1T	First term for the mass estimation of the fixed T.E. section of the wing.	
TERM2B	Second term for the estimation of the wing-box mass.	
TERM2F	Second term for the estimation of the T.E. flaps mass.	
TERM2L	Second term for the estimation of the wing l.E. mass.	
TERM2T	Second term for the mass estimation of the fixed T.E.section of the wing.	
TERM3B	Third term for the estimation of the wing-box mass.	
TERM3L	Third term for the estimation of the wing L.E. mass.	
TERM3T	Third term for the mass estimation of the fixed T.E. section of the wing.	
TERM4B	Fourth term for the estimation of the wing-box mass.	
TERM4L	Fourth term for the estimation of the wing l.E. mass.	
TERM5B	Fifth term for the estimation of the wing-box mass.	
TERM6B	Sixth term for the estimation of the wing-box mass.	
TERM7B	Seventh term for the estimation of the wing-box mass.	
TERM8B	Eighth term for the estimation of the wing-box mass.	
TH	Temperature above 15 degrees C.	

THETL	Lower angle limit in the calculation of the flying surfaces lateral cross-sectional area.
THETU	Upper angle limit in the calculation of the flying surfaces lateral cross-sectional area.
TOA	Airborne take-off distance to clear a 15 m screen height.
TOD	Total take-off distance (Ground + airborne).
TOG	Take-off ground roll distance.
TPDED	Engine static thrust in data input mode.
TPG	Engine gross thrust.
TPG1	Guess value of the gross thrust required along a sortie leg.
TPG2	Actual value of the gross thrust required along a sortie leg.
TPGC	Maximum gross thrust of engine.
TPGEC	Engine gross thrust in data input mode.
TPGD	Maximum sea-level static thrust of the engine with reheat.
TPGD1	Datum value of TPGD (Dry).
TPGD2	Datum value of TPGD (Reheat).
TRATE	Fraction of TPGC available for take-off.
TSL	Ambient temperature at sea-level.
TTTF	Required take-off time.
U	Taper ratio in the evaluation of the flying surfaces lateral cross-sectional area.
UEFN	Nett fin taper ratio.
UETN	Nett tailplane taper ratio.
ULTN	Ultimate load factor for structural design (1.5 x proof factor).
UOFAUF	Cross-sectional area utilization factor of underflor section A.
UW	Gross wing taper ratio.
UWB	Taper ratio of the wing-box.
UWBCF	Volume utilization factor of the center-section of the wing-box for fuel storage.
UWBEF	Exposed wing-box volume utilization factor for fuel storage.
UWCN	Net wing taper ratio.
UWCNF	Taper ratio of the wing-box fuel tank external to the fuselage.
V	Aircraft speed.
V1	First estimate of maximum speed.
V2	Second estimate of maximum speed.
V3	Maximum speed.
VAR	Radar avionics volume.
VCKPT	Cockpit volume.
VCTF	Central tank volume.
VD	Maximum design diving speed.
VESTF	Side tank volume (each).
VFGF	Central plus two side tanks volume.
VFR	Radome volume (total).
VFX	Fuselage volume from aircraft nose up to stn X.
VFXT	Volume of the entire fuselage of the aircraft.
VIDG	Total volume of one intake diffuser.
VGABI	Volume of the internal gun ammunition bay.
VGBBI	Volume of the internal gun barrel bay.

The following entries carry an "EV" / "IV" designation in the right-hand margin:

- TPG1 — EV
- TPGD1 — EV
- TPGD2 — EV
- TRATE — EV
- TTTF — EV
- UEFN — EV
- UETN — EV
- ULTN — EV
- UOFAUF — EV
- UW — IV
- UWBCF — EV
- UWBEF — EV
- VD — EV

VGMBI	Volume of the internal gun mechanism bay.	
VMMML	Maximum Mach number initial speed.	EV
VMMMLI	Maximum Mach number initial speed - input data form.	EV
VP12B	Volume of engine gas generator.	
VP24B	Volume of engine RLS section.	
VP45B	Volume of engine afterburner.	
VP56B	Volume of engine nozzle.	
VPB	Total engine volume.	
VRDG	RLS duct external volume.	
VRDI	RLS duct internal volume.	
VSA	Air systems volume.	
VSC	Flying controls volume.	
VSE	Electrics volume.	
VSF	Fuel system volume.	
VSTTO	Aircraft stall speed in the take-off configuration.	
VSWBI	Volume of the internal weapons bay.	
VUMLB	Leg related volume of each main undercarriage.	
VUMLBK	Constant term inestimation of leg related volume of each main undercarriage.	
VUMWB	Wheel related volume of each main undercarriage	
VUNLB	Leg related volume of the nose undercarriage.	
VUNWB	Wheel related volume of the nose undercarriage.	
VWBB	Volume of the center-section of the wing-box.	
VWBCF	Fuel volume in center-section of the wing-box.	
VWBEF	Fuel volume in wing-box external to the fuselage.	
WCCAN	Surface area of the canopy.	
WCWSC	Surface area of the windscreen.	
WFG1	Fuselage surface area from aircraft nose up to engine intake.	
WFG2	Fuselage surface area from aircraft nose up to engine intake.	
WFR	Total surface area of radome.	
WFX	Fuselage surface area from aircraft nose up to stn X.	
WIRD	RLS duct wall thickness.	EV
WRDG	RLS duct surface area.	
WT	Aircraft weight as used in performance estimation methods.	
X	Axial distance from the aircraft nose.	
XA	Distance of fuselage stn A from the aircraft nose.	
XB	Distance of fuselage stn B from the aircraft nose.	
XC	Distance of fuselage stn C from the aircraft nose.	
XD	Distance of fuselage stn D from the aircraft nose.	
XE	Distance of fuselage stn E from the aircraft nose.	
XEF	Intermediate variable in the fuselage cross-sectional area evaluation.	
XETCG	Moment arm of the fin in CG calculation.	
XEFLB	Distance of the L.E. of the fin root from the aircraft nose.	
XEGH	Intermediate variable in the fuselage cross-	

XEGH	Intermediate variable in the fuselage cross-sectional area evaluation.	
XET	Axial distance from the L.E. of the tail root.	
XETCG	Moment arm of the tailplane in CG calculation.	
XETLB	Distance of the L.E. of the tail root from the aircraft nose.	
XF1	Axial distance from the L.E. of the fin root.	
XF	Distance of fuselage stn F from the aircraft nose.	
XFCCG	Moment arm of the central tank in CG calculation.	
XFCG	Moment arm of the fuselage structure and skin in CG calculation.	
XFCQM	Distance of the fin mean quarter chord point from the nose.	
XFN	Distance of the nozzle exit from the aircraft nose (length of the aircraft).	IV
XFOH	Axial distance of the stn at which OFXH occurs from the aircraft nose.	
XFOHS	Axial distance of the stn at which OFXHS occurs from the aircraft nose.	
XFOTH	Axial distance of the stn at which OFXTH occurs from the aircraft nose.	
XFR	Axial distance of the rear end of the radome.	
XFSCG	Moment arm of the side tank in CG calculation. from the aircraft nose.	IV
XFXM	Centre of the surface area of the fuselage.	
XFWM	Centre of the volume of the fuselage.	
XG	Distance of fuselage stn G from the aircraft nose.	
XH	Distance of fuselage stn H from the aircraft nose.	
XII	Axial distance of the air intake plane from the aircraft nose.	
XIND	Axial distance from the intake plane.	
XRSG1	Term in the moment arm estimation of the RLS duct.	
XRSG2	Term in the moment arm estimation of the RLS duct.	
XRSG2	Term in the moment arm estimation of the RLS duct.	
XSACG	Longitudinal moment arm of the air systems.	
XSCCG	Longitudinal moment arm of the flying controls.	
XSECG	Longitudinal moment arm of the electrics.	
XSFCG	Longitudinal moment arm of the fuel system.	
XTCQM	Distance of the tailplane mean quarter chord point from the nose.	
XTECG	Distance of the aircraft CG from the nose with empty fuel tanks.	
XTTCG	Distance of the aircraft CG from the nose with full fuel tanks.	
XUMCG	Longitudinal moment arm of the main undercarriage.	
XUNCG	Longitudinal moment arm of the nose undercarriage.	
XV	Engine throttle setting,or,gross thrust.	EV
XVE	Axial distance of the b.l.diverter exit from the aircraft nose.	

	constant altitude input data form.	
XVATR :	Attained turn rate throttle setting.	EV
XVATRI :	Attained turn rate throttle setting - input data form.	EV
XVMML	Throttle setting for the maximum Mach number.	EV
XVMMLI	Throttle setting for the maximum Mach number - input data form.	EV
XVRIDE	Throttle setting for the ride quality factor.	EV
XVRIDI	Throttle setting for the ride quality factor - input data form.	EV
XW	Axial distance from the L.E. of the wing root.	
XWBCCG	Longitudinal moment arm of the fuel in the central wing-box.	
XWBECG	Longitudinal moment arm of the fuel in the wing-box external to the fuselage.	
XWCG	Longitudinal moment arm of the wing.	
XWCQM	Distance of wing mean quarter chord point from the nose.	
XWLB	Distance of the L.E. of the wing root from the aircraft nose.	
YCPG	Spanwise position of the centre of pressure of the gross wing.	
YCPX	Spanwise position of the centre of pressure of the nett wing.	
YL	Lower limit in the calculation of the lateral cross-sectional area of the flying surfaces for the area rule.	
YU	Upper limit in the calculation of the lateral cross-sectional area of the flying surfaces for the area rule.	

APPENDIX B

ASTOVL COMBAT AIRCRAFT DESIGN SYNTHESIS
AND OPTIMIZATION EXAMPLE

SUBROUTINE USERF

```
      SUBROUTINE USERF(x,func,iocode,nprob,icallf,nfe)

      integer iocode(76)
      real x(50),func(76)
```

C   Declaration of the dimensions of all array variables.
      ....
      ....

C   Declaration of all integer variables
      ....
      ....

C   Declaration of all real variables
      ....
      ....

C   Declaration of all common blocks.
      ....
      ....

C   Assignment of Independent Variable values.

```
      SW=X(1)
      AW=X(2)
      UW=X(3)
      QW4=X(4)
      RTW=X(5)
      FCWR=X(6)
      FCWD=X(7)
      RXWCQM=X(8)
      RXTCQM=X(9)
      RXFCQM=X(10)
      RTP=X(11)
      XFN=X(12)
      RLTMFN=X(13)
      RLTFFN=X(14)
      RLTCFN=X(15)
      RLTAFN=X(16)
      FOT6N=X(17)
      BRD=X(18)
```

C   Execution of the Design Synthesis subroutine.

```
      CALL VERTI8(icallf,nfe)
```

FIG.B1   SUBROUTINE USERF - EXAMPLE

```
C      Objective Function.

       FUNC(1)=(MTT-MTP-MTGFI-MTOUF-MTES)

C      Equality Constraints.

       FUNC(2)=MTGFI-MPFB2T
       FUNC(3)=(0.669*TPGD)-((11.28*MTT)-(9.03*MTGFI))

C      Inequality Constraints

       FUNC(4)=XWCQM-(RLTCA*CWMA)-XTTCG
       FUNC(5)=XTECG-(XWCQM-(RLTCL*CWMA))
       FUNC(6)=XFN-XA-LUNS-(DRDE/2.0)-LSWBI-(0.15*LIDG)-LPG
       FUNC(7)=LIDG-LIDS
       FUNC(8)=BFB-BUNW
       FUNC(9)=OFE-OP1B
       FUNC(10)=OFJ-OP5B
       FUNC(11)=STRO(1)-STROS(1)
       FUNC(12)=STRO(2)-STROS(2)
       FUNC(13)=STRO(3)-STROS(3)
       FUNC(14)=ATRO(1)-ATROS(1)
       FUNC(15)=SEPO(1)-SEPOS(1)
       FUNC(16)=SEPO(2)-SEPOS(2)
       FUNC(17)=MNMAXO(1)-MNMXOU(1)
       FUNC(18)=MNMAXO(2)-MNMXOU(2)
       FUNC(19)=SDTOH(1)-SDTO(1)
       FUNC(20)=RQFOH(1)-RQFO(1)
       FUNC(21)=TODH-TOD
       FUNC(22)=VFXT-VFXTS
       FUNC(23)=3.2-(AW*((TAND(QW4))**0.8))


       DO 13 I=2,23
       FUNC(I)=-FUNC(I)
13     CONTINUE

       RETURN
       END

→
```

FIG.B1   SUBROUTINE USERF - EXAMPLE (CONCLUDED)

INPUT DATA FILES

VERTI.DAT

```
C    MNAR,BFC
     0.6 1.8
C    PI,ERR
     3.14159 0.001
C    DAR,EDAR,GOF1,LAR,LAX1
     0.6 0.06 0.4 0.6 1.2
C    HC1,HC2,HC3,HC4,HCSEAT,LCFOOT,QCEYE,QCSEAT,EHCS
     0.745 0.694 0.33 0.254 0.222 0.127 17.0 25.0 0.3
C    MTT,MXT,MXTF,MGA1,MB1,MB2,MXP,MTPR,RMTLIF,MTGFI
     18000.0 0.0 0.0 266.0 0.0 0.0 0.0 670.0 0.2 5500.0
C    MUMK,MUNK,MUHK,FMUNK,FMUMK,FMUHK,LULG1K,LULG2K
     -0.42 6.0 4.0 0.0064 0.0468 0.0068 756.0 0.5293
C    RLUNM,FDUMWK,FBUMWK,FDUMWK,DUMWK,BUMWK,DUNWK
     0.74 0.0000329 0.0000108 0.0000196 0.419 0.107 0.318
C    FDUMW,FBUMW,FDUNW,FBUNW,BUNW,FVUMLK,VUMLBK
     1.1 1.5 1.1 1.5 0.152 0.0000045 0.31
C    NEN,LP12R,LP23R,LP34R,LP45R,LP56R,FLP1K,FLP2K,FLP3K
     1 2.275 0.617 0.526 1.473 0.8 0.5 0.5 0.5
C    DP1R,DP2R,DP3R,DP4R,DP5AR,DP5R,DP6R
     1.15 1.2 1.2 1.2 0.862 0.862 0.921
C    FMPBK,MPBR,MPLR,MPRR,MPNR,FMPRK,MPTR,FMPIK
     0.8257 1316.5 404.5 296.6 250.0 0.7965 0.0 0.125
C    TPGD1,MPFD1,MPAD1,OPJD1,MPFS1
     182572.16 9.427107 157.7646 0.581037 0.0
C    FHP1K,FBP1K,FHP2K,FBP2K,FHP3K,FBP3K,FHP4K,FBP4K
     0.6 0.6 0.4 0.4 0.4 0.4 0.4 0.4
C    FHP5K,FBP5K,FHP6K,FBP6K,EHP1S,EHP1H,EBP1S,EBP1H
     0.33 0.33 0.0 0.0 0.7 0.8 0.7 0.8
C    EHP2S,EHP2H,EBP2S,EBP2H,EHP3S,EHP3H,EBP3S,EBP3H
     0.4 0.6 0.4 0.6 0.4 0.6 0.4 0.6
C    EHP4S,EHP4H,EBP4S,EBP4H,EHP5S,EHP5H,EBP5S,EBP5H
     0.4 0.6 0.4 0.6 0.3 0.3 0.3 0.3
C    EHP6S,EHP6H,EBP6S,EBP6H
     0.0 0.0 0.0 0.0
C    FLII,ROIEI,AII,FLIDK,FBVIK,FLVK
     0.65 1.4 2.0 6.0 0.014 2.0
C    LMRM,LSRM,DMRM,DSRM,NMRM,NSRM,MMRM,MSRM
     3.65 1.55 0.178 0.075 4 2 150.0 64.0
C    LSWBIK,HSWBIK,EHSWBI
     0.18 0.035 0.25
C    LGM,LGMK,BGM,BGMK,HGM,HGMK,FMGM,MGM,NGA,LGA,LGAK
     0.8 0.008 0.25 0.003 0.25 0.003 1.6 50.0 150 0.250.003
C    DGA,BGAK,HGAK,FMGA,FMGB,MGA,MGB,DGAK
     0.025 0.003 0.003 1.1 1.6 0.5 56.0 0.003
```


FIG.B2   FILE VERTI.DAT - EXAMPLE

```
C    WIRD,RMLRD
     0.05 7.0
C    BFE,FCWLFT,FCWLHT,FBWF,FCWTFT
     1.6 0.05 0.05 0.75 0.15
C    FCWTHL,UWBCF,UWBEF,FBWNF,FBWCF,QWT
     0.15 0.9 0.9 1.0 0.0 -10.0
C    FBWS,NWS,AWS,FBWA,AWA
     0.4 2 8.0 0.2 8.0
C    RETSW,AETN,UETN,UEFN,REFFC,AEFN
     0.3 3.5 0.3 0.3 2.0 3.5
C    QETL,QETT,QEFL,QEFT,RTET,RTEF
     45.0 0.0 40.0 0.0 0.06 0.06
C    LIIWLS,LWTTLS
     0.5 0.5
C    RAHB,RFCNRA,UOFAUF
     1.0162 0.48 0.8
C    BCH,RCCANB,FOFB1K,FOFB2K,GHC
     1.1 0.1 0.95 0.9 0.577
C    RCCANC,FOFC1K,FOFC2K
     0.4 0.85 0.85
C    FOFDK
     0.85
C    FOFEK
     0.85
C    FOFFK,HRD
     0.8 0.9
C    FOFGK
     0.8
C    FOFHK
     0.85
C    RPFX1K,RPFX2K,RPFX3K,RPFX4K
     1.1 1.2 1.05 0.0
C    RFUL
     800.0
C    FMF2,WCWSC,WCCAN,VD,ULTN,AMMX,QCWSC
     1.0 1.3 1.8 400.0 12.0 2.0 30.0
C    FMWB,FMWL,FMWT,EQWFH,NWFK,LWFK,FMET
     1.0 1.0 1.0 50.0 4 0.2 1.0
C    MET1K,MET2K,MET3K,FMEF
     0.004356 1.549 0.3433 1.0
C    MEF1K,MEF2K,MEF3K,MEF4K
     0.11156 1.3 0.7812 0.2422
C    MSCK,FMSCK,MSEK,FMSEK,MSAK,FMSAK
     22.2 0.0293 29.9 0.0267 -15.9 0.011
C    FREEF,FQWT1,FWLD,XT,RDP
     0.91 1.85 0.0 5.0 0.95
C    MCP,MCI,MAR,MAX1,MAX2,MTOUF
     90.0 180.0 150.0 100.0 200.0 50.0
C    RLUPC,LGB,LGBK
     0.1 1.8 0.1
```

FIG.B2   FILE VERTI.DAT - EXAMPLE (CONTINUED)

```
C    FHTR,FMD1,FMD2,CLDES,LCCAN,RCDK,RCDVK
     0.000015 0.15 0.0 0.6 3.5 0.4 1.0
C    MTES,VFXTS,RLTCA,RLTCL,TODH,CSW
     10500.0 0.0 0.0 0.2 450.0 1
C    NLEG,TTTF,FMTLF,AL,CL1,GTCPH,MPFB1,RTK
     5 30.0 0.05 3.0 0.7 8.0 300.0 0.99
C    NPPERF,NPPER
     6 2
C    NSTR,EQWFSR,CL3
     3 0.0 0.5
C    NATR,EQWFAR
     1 0.0
C    NSEP
     2
C    NMML
     2
C    NACA
     1
C    NRIDE,NNSDT
     1 6.0
C    HTTO,EQWFT,FCLT,FVSTTO,TRATE
     0.0 30.0 0.9 1.1 0.95
C    NED,SFP
     770 100.0
```

FIG.B2   FILE VERTI.DAT - EXAMPLE (CONCLUDED)

AERO.DAT

```
C       MACH CLC DK2 CLMAX
        0.0 0.60 0.5 1.40
        0.1 0.59 0.5 1.40
        0.2 0.59 0.5 1.40
        0.3 0.59 0.5 1.30
        0.4 0.59 0.5 1.30
        0.5 0.53 0.5 1.30
        0.6 0.47 0.5 1.25
        0.7 0.43 0.6 1.20
        0.8 0.49 0.7 1.15
        0.9 0.62 0.8 1.10
        1.0 0.64 0.8 1.10
        1.1 0.62 0.8 1.10
        1.2 0.60 0.8 1.10
        1.3 0.50 0.8 1.08
        1.4 0.50 0.7 1.06
        1.5 0.30 0.6 1.04
        1.6 0.20 0.6 1.02
        1.7 0.20 0.6 1.01
        1.8 0.20 0.5 1.00
        1.9 0.20 0.5 1.00
        2.0 0.20 0.5 1.00
        2.1 0.20 0.5 1.00
        2.2 0.20 0.4 1.00
        2.3 0.20 0.4 1.00
        2.4 0.20 0.4 1.00
```

PERF.DAT

```
C    RANGE - ALT -MACH-N LOAD-JET MASS-FLAP ANG-THRUST EST
     400.0 10000.0 0.7 1.0 0.0 0.0 60000.0
     490.0 9000.0 0.6 1.1 350.0 0.0 100000.0
     5.0 9000.0 1.4 3.0 350.0 0.0 150000.0
     5.0 1000.0 0.8 8.0 210.0 0.0 200000.0
     400.0 10000.0 0.7 1.0 0.0 0.0 60000.0
```

FIG.B3   AERO.DAT AND PERF.DAT FILES - EXAMPLES

CITENG.DAT

C	ALT	MACH	POWER S	NET THR	GROSS THR	FUEL FL	NOZZLE AR	AIR FL
1	0.	0.000	1.0	19.41752	19.41752	0.497603	0.401575	62.5085
2	0.	0.000	2.0	36.77176	36.77176	0.819205	0.401566	86.4536
3	0.	0.000	3.0	62.46464	62.46464	1.333446	0.401569	113.1786
4	..	.....	...					
10	0.	0.000	10.0	182.33684	182.57216	9.427107	0.581037	157.7646
11	0.	0.200	1.0	17.82067	22.47583	0.528597	0.401548	68.2668
12	0.	0.200	2.0	34.94477	41.26301	0.874747	0.401552	92.8025
13	..	.....	...					
111	3048.	0.000	1.0	13.17810	13.17810	0.330015	0.401575	44.3300
112	3048.	0.000	2.0	25.18564	25.18564	0.542657	0.401591	61.6372
113	....	.....						

POINTP.DAT

```
C STR(3) ALTITUDE           MACH         POWER SETTING        CONSTRAINTS
         100.0 9000.0 9000.0 0.9 0.9 1.4 50.0 100.0 100.0 10.0 2.0 6.0
C ATR(3) ALTITUDE           MACH         POWER SETTING    CONSTRAINTS
         9000.0 0.0 0.0 1.4 0.0 0.0 100.0 0.0 0.0 10.4 0.0 0.0
C SEP(3) ALTITUDE           MACH         POWER SETTING     CONSTRAINTS
         100.0 9000.0 0.0 0.9 1.4 0.0 100.0 100.0 0.0 300.0 150.0 0.0
C MNMAX(3) ALTITUDE         IN SPEED     POWER SETTING        CONSTRAINTS
         100.0 11000.0 0.0 200.0 300.0 0.0 100.0 100.0 0.0 1.1 1.6 0.0
C SDT(3) ALTITUDE           MACH         POWER SETTING    CONSTRAINTS
         9000.0 0.0 0.0 0.8 0.0 0.0 100.0 0.0 0.0 60.0 0.0 0.0
C RQF(3) ALTITUDE           MACH         POWER SETTING    CONSTRAINTS
         1000.0 0.0 0.0 0.8 0.0 0.0 100.0 0.0 0.0 5.0 0.0 0.0
```

FIG.B4   CITENG.DAT AND POINTP.DAT FILES - EXAMPLES

RQPMIN.DAT

```
VARIABLES
01 1 10.0    40.000      5.000     100.000
02 1 1.0      4.000      1.500      10.000
03 1 0.1      0.300      0.250       1.000
04 1 10.0    33.000      0.000      60.000
05 1 0.01     0.050      0.020       0.200
06 1 1.0      0.600      0.300       0.800
07 1 0.1      0.150      0.050       0.300
08 1 1.0      0.760      0.000       1.000
09 1 1.0      0.930      0.600       1.000
10 1 1.0      0.950      0.600       1.000
11 1 1.0      1.600      0.700       3.000
12 1 10.0    20.000      5.000      30.000
13 1 0.1      0.400      0.000       1.000
14 1 0.1      0.300      0.000       0.500
15 1 0.1      0.100      0.000       1.000
16 1 0.1      0.800      0.500       0.990
17 1 0.1      0.300      0.200       5.000
18 1 0.1      0.350      0.100       1.000
FUNCTIONS
                 1
01 00 00 10000.0
02 01 00 100000.0
03 01 00 100000.0
04 -1 00 1.0
05 -1 00 1.0
06 -1 00 10.0
07 -1 00 10.0
08 -1 00 10.0
```

FIG.B5   FILE RQPMIN.DAT - EXAMPLE

```
09 -1 00 100.0
10 -1 00 1.0
11 -1 00 10.0
12 -1 00 10.0
13 -1 00 10.0
14 -1 00 0.1
15 -1 00 100.0
16 -1 00 100.0
17 -1 00 1.0
18 -1 00 1.0
19 -1 00 100.0
20 -1 00 10.0
21 -1 00 100.0
22 -1 00 100.0
23 -1 00 1.0
CONTROLS
XTOLU = 0.001
XTOLV = 0.001
OFROM = 1
OFREQ = 10
RFREQ = 10
NFEMAX = 16000
RUN
END
```

FIG.B5   FILE RQPMIN5.DAT - EXAMPLE (CONCLUDED)

OUTPUT FILES

VERTI.RES

STARTING POINT

ASTOVL COMBAT AIRCRAT

TAKE-OFF MASS kg 20561.70 FUEL FRACTION 0.2548
WING LOADING kg/m2 514.0 THRUST/WT 1.4482

FUSELAGE LENGTH m 20.000 ENGINE SCALE 1.60

GEOMETRY m

WING

SPAN 12.649 ROOT C 4.434 TIP C 1.460 W AREA m2 40.000
AR 4.000 TR 0.300 C/4 SWEEP deg 33.00 T/C 0.0500
MAC 3.468
NET SPAN 11.049 NET W AREA m2 32.561
MAX W BOX DEPTH 0.222

FIG.B6   FILE VERTI.RES STARTING - EXAMPLE

```
FUSELAGE
--------
LENGTH 20.000 OTM 2.5299 OTF3K -.0597 OTF4K 0.0029
OTA3K -.0090 OTA4K -.0011

STATION        XA    XB    XC    XD    XE
BREADTH      1.175 2.241 2.218 1.577 1.501
HEIGHT       1.194 1.345 1.686 1.318 1.906
NETT X-SECT A 1.069 1.362 1.812 2.477 2.406
STATION        XF    XG    XH    XJ    XI
BREADTH      1.787 1.955 1.894 1.390 1.165
HEIGHT       1.533 1.678 1.626 1.390 1.165
NETT X-SECT A 1.954 1.753 1.552 0.816 0.300

VOLUME m3 VFX(A)  2.746 VFX(D)  9.494 VFX(E)21.071 VFX(I) 31.323

ENGINE
------
LENGTH
LP12  2.878 LP24  1.446 LP45  1.863 LP56  1.012
DIAMETER
DP1 1.45 DP2 1.52 DP3 1.52 DP4 1.52 DP5 1.09 DP6 1.16

EMPENNAGE
---------
TAIL
NET SPAN  5.76 ROOT C  2.53 NET W AREA m2     9.49
NET AR  3.50 T/C 0.06 LE SWEEP deg 45.00
FIN
NET SPAN 10.88 ROOT C  4.78 NET W AREA m2    33.79
NET AR  3.50 T/C 0.06 LE SWEEP 40.00
```

FIG.B6   FILE VERTI.RES STARTING - EXAMPLE (CONTINUED)

232

CG POSITION ON MAC

FWD LIMIT 0.05 EMPTY -.08 LOADED 0.26 AFT LIMIT 0.25

MASS kg

FUSELAGE
TOTAL 3049.8 SHELL 1640.5 INTERN 890.9 WINDSCR 67.2
CANOPY 53.4

WING
TOTAL 2512.3 BOX 1760.9 LE 130.0 TE 182.3 FLAPS 331.0
AILERONS 4.8 SPOILERS 7.4 FLAPTRACKS 14.9
FAIRINGS 15.9
VARIOUS 74.9

EMPENNAGE
TAIL 409.0 FIN 1725.8

ENGINE
TOTAL 3770.6 GAS GENER 1968.7 RLS SECT 588.2
REHEAT 431.3
NOZZLE 363.5 INSTALL 419.0 RLS 228.5

U/C TOTAL 754.6 NOSE 95.6 MAIN 655.0 HYDR 4.0

FIXED ROLE EQPM TOTAL 549.6 COCKPIT 180.0
GUN 169.6
RADAR 150.0 UNUS FUEL 50.0

FIG.B6   FILE VERTI.RES STARTING - EXAMPLE (CONTINUED)

```
SYSTEMS TOTAL  1753.0  AIR COND   186.5  ELECTRIC   521.3
F CONTR    561.4  FUEL SYST   360.0  RCS    123.8

FUEL TOTAL  5240.1  W BOX CENTR   479.8  W BOX EXT  1587.6
FUSEL CENTR  726.7  FUSEL SIDE  (BOTH)   2446.1

PAYLOAD TOTAL  900.5  CREW  90.0  GUN AMMO  82.5 WEAPONS    728.0

A/C TOTAL  20561.7  EMPTY  14421.1  LANDING  15321.6
```

SORTIE PERFORMANCE

STAGE	1	2	3	4	5
ALT m	10000.0	9000.0	9000.0	1000.0	10000.0
MACH	0.700	0.600	1.400	0.800	0.700
RANGE km	400.0	490.0	5.0	5.0	400.0
LOAD FACT g	1.000	1.100	3.000	8.000	1.000
END MASS kg	19071.2	17418.1	16953.1	16638.3	15629.1
TIME s	1907.7	2687.7	11.8	18.6	1907.7
MID-MASS CL	0.3520	0.3376	0.3563	0.3718	0.3520
ALPHA deg	8.786	10.604	4.794	13.042	7.241
CD TOTAL	0.05535	0.05697	0.11570	0.11519	0.05537
THROTTLE PC	22.01	18.55	72.63	44.67	21.90
THRUST N	34552.8	30145.3	298726.2	280828.4	34394.5
FUEL kg/s	0.5317	0.4848	9.7860	5.6393	0.5290
AIR kg/s	66.874	65.513	240.048	327.165	66.716
FUEL USED kg	1014.3	1303.1	115.0	104.8	1009.2

TAKE-OFF FUEL kg 476.2 FUEL AT LANDING kg 201.1

FIG.B6   FILE VERTI.RES STARTING - EXAMPLE (CONTINUED)

234

POINT PERFORMANCE

TYPE	ACTUAL	REQUIRED	ALT	MACH	P SETTING
ACCEL .6	26.48	60.00	9000.0	0.800	100.00
M MAX	1.528	1.100	100.0		100.00
M MAX	2.137	1.600	11000.0		100.00
SUST.T.R.deg/s	0.000	10.000	100.0	0.900	50.00
SUST.T.R.	0.000	2.000	9000.0	0.900	100.00
SUST.T.R.	5.719	6.000	9000.0	1.400	100.00
ATT.T.R. deg/s	10.454	10.400	9000.0	1.400	100.00
S.E.P. m/s	203.912	300.000	100.0	0.900	100.00
S.E.P.	117.592	150.000	9000.0	1.400	100.00
RIDE Q.F.	1.980	5.000	1000.0	0.800	100.00

TAKE-OFF DISTANCE m ACTUAL 396.6 REQUIRED 450.0

FIG.B6   FILE VERTI.RES STARTING – EXAMPLE (CONCLUDED)

235

VERTI.RES

FINAL RESULTS

ASTOVL COMBAT AIRCRAT

TAKE-OFF MASS kg 18900.40 FUEL FRACTION 0.2003
WING LOADING kg/m2 470.8 THRUST/WT 1.4431

FUSELAGE LENGTH m 19.774 ENGINE SCALE 1.47

GEOMETRY m

WING

SPAN 12.624 ROOT C 4.460 TIP C 1.464 W AREA m2 40.142
AR 3.970 TR 0.299 C/4 SWEEP deg 32.94 T/C 0.0501 MAC 3.488
NET SPAN 11.024 NET W AREA m2 32.658 MAX W BOX DEPTH 0.223

FUSELAGE

LENGTH 19.774 OTM 2.4887 OTF3K -.0599 OTF4K 0.0030
OTA3K -.0092 OTA4K -.0011

FIG.B7   FILE VERTI.RES FINAL - EXAMPLE

```
STATION              XA      XB      XC      XD      XE
BREADTH            1.173   2.193   2.176   1.593   1.483
HEIGHT             1.192   1.340   1.684   1.331   1.896
NETT X-SECT A      1.067   1.358   1.809   2.453   2.343
STATION              XF      XG      XH      XJ      XI
BREADTH            1.780   1.940   1.858   1.344   1.115
HEIGHT             1.515   1.651   1.582   1.344   1.115
NETT X-SECT A      1.943   1.747   1.549   0.818   0.300

VOLUME m3 VFX(A)  2.743 VFX(D)   9.587 VFX(E)20.911 VFX(I)  30.713

ENGINE
------
LENGTH
LP12  2.754 LP24  1.384 LP45  1.783 LP56   0.968
DIAMETER
DP1 1.39 DP2 1.45 DP3 1.45 DP4 1.45 DP5 1.04 DP6 1.11

EMPENNAGE
---------
TAIL
NET SPAN  4.65 ROOT C  2.04 NET W AREA m2        6.16
NET AR  3.50 T/C  0.06 LE SWEEP deg  45.00
FIN
NET SPAN  8.23 ROOT C  3.62 NET W AREA m2       19.36
NET AR  3.50 T/C  0.06 LE SWEEP 40.00

CG POSITION ON MAC
------------------
FWD LIMIT 0.05 EMPTY 0.13 LOADED 0.25 AFT LIMIT 0.25
```

FIG.B7   FILE VERTI.RES FINAL - EXAMPLE (CONTINUED)

MASS   kg

FUSELAGE
TOTAL 3272.3 SHELL 1614.8 INTERN 1110.1 WINDSCR 67.2
CANOPY 53.4

WING
TOTAL 3501.7 BOX 2053.3 LE 130.1 TE 396.7 FLAPS 779.6
AILERONS 4.8 SPOILERS 7.4 FLAPTRACKS 16.5 FAIRINGS 15.9
VARIOUS 97.4

EMPENNAGE
TAIL 229.0 FIN 756.0

ENGINE
TOTAL 3501.2 GAS GENER 1822.6 RLS SECT 548.5 REHEAT 402.2
NOZZLE 339.0 INSTALL 389.0 RLS 213.2

U/C TOTAL 754.6 NOSE 95.6 MAIN 655.0 HYDR 4.0

FIXED ROLE EQPM TOTAL 549.6 COCKPIT 180.0 GUN 169.6
RADAR 150.0 UNUS FUEL 50.0

SYSTEMS TOTAL 1753.0 AIR COND 186.5 ELECTRIC 521.3
F CONTR 561.4 FUEL SYST 360.0 RLS 123.8

FUEL TOTAL 3786.2 W BOX CENTR 179.7 W BOX EXT 592.9
FUSEL CENTR 740.5 FUSEL SIDE (BOTH) 2273.0

FIG.B7   FILE VERTI.RES FINAL - EXAMPLE (CONTINUED)

PAYLOAD TOTAL 900.5 CREW 90.0 GUN AMMO 82.5 WEAPONS 728.0

A/C TOTAL 18900.4 EMPTY 14213.7 LANDING 15114.2

SORTIE PERFORMANCE

STAGE	1	2	3	4	5
ALT m	10000.0	9000.0	9000.0	1000.0	10000.0
MACH	0.700	0.600	1.400	0.800	0.700
RANGE km	400.0	490.0	5.0	5.0	400.0
LOAD FACT g	1.000	1.100	3.000	8.000	1.000
END MASS kg	17510.0	15970.8	15593.0	15295.5	14384.5
TIME s	1907.7	2687.7	11.8	18.6	1907.7
MID-MASS CL	0.3511	0.3368	0.3563	0.3708	0.3511
ALPHA deg	7.372	8.978	3.979	10.860	6.089
CD TOTAL	0.04874	0.05014	0.10279	0.09922	0.04875
THROTTLE PC	19.77	16.58	31.75	39.49	19.70
THRUST N	31395.3	27341.2	251339.0	246663.1	31294.3
FUEL kg/s	0.4792	0.4425	2.3636	4.7115	0.4775
AIR kg/s	63.684	62.451	179.521	304.233	63.580
FUEL USED kg	914.2	1189.2	27.8	87.5	911.0

TAKE-OFF FUEL kg 476.2 FUEL AT LANDING kg 180.3

FIG.B7   FILE VERTI.RES FINAL - EXAMPLE (CONTINUED)

POINT PERFORMANCE

TYPE	ACTUAL	REQUIRED	ALT	MACH	P SETTING
ACCEL .6	25.92	60.00	9000.0	0.800	100.00
M MAX	1.701	1.100	100.0		100.00
M MAX	2.475	1.600	11000.0		100.00
SUST.T.R.deg/s	9.998	10.000	100.0	0.900	50.00
SUST.T.R.	2.947	2.000	9000.0	0.900	100.00
SUST.T.R.	7.497	6.000	9000.0	1.400	100.00
ATT.T.R. deg/s	10.454	10.400	9000.0	1.400	100.00
S.E.P. m/s	299.154	300.000	100.0	0.900	100.00
S.E.P.	212.613	150.000	9000.0	1.400	100.00
RIDE Q.F.	2.400	5.000	1000.0	0.800	100.00

TAKE-OFF DISTANCE m ACTUAL 297.6 REQUIRED 450.0

FIG.B7   FILE VERTI.RES FINAL – EXAMPLE (CONCLUDED)

RQPMIN.RES

Program RQPMIN Version 1.0 for VAX

ANALYSIS OF INPUT FILE DATA AND CONTROL PARAMETERS

Variable data

Number of variables =   18

Index	Status	Scale	Starting value	Lower bound	Upper bound
1	1	0.1000000E+02	0.4000000E+01	0.5000000E+00	0.1000000E+02
2	1	0.1000000E+01	0.4000000E+01	0.1500000E+01	0.1000000E+02
3	1	0.1000000E+00	0.3000000E+01	0.2500000E+01	0.1000000E+02
4	1	0.1000000E+02	0.3300000E+01	0.0000000E+00	0.6000000E+01
5	1	0.1000000E-01	0.5000000E+01	0.2000000E+01	0.2000000E+02
6	1	0.1000000E+01	0.6000000E+00	0.3000000E+00	0.8000000E+00
7	1	0.1000000E+00	0.1500000E+01	0.5000000E+00	0.3000000E+01
8	1	0.1000000E+01	0.7600000E+00	0.0000000E+00	0.1000000E+01
9	1	0.1000000E+01	0.9300000E+00	0.6000000E+00	0.1000000E+01
10	1	0.1000000E+01	0.9500000E+00	0.6000000E+00	0.1000000E+01
11	1	0.1000000E+01	0.1600000E+01	0.7000000E+00	0.3000000E+01
12	1	0.1000000E+02	0.2000000E+01	0.5000000E+00	0.3000000E+01
13	1	0.1000000E+00	0.4000000E+01	0.0000000E+00	0.1000000E+02
14	1	0.1000000E+00	0.3000000E+01	0.0000000E+00	0.5000000E+01
15	1	0.1000000E+00	0.1000000E+01	0.0000000E+00	0.1000000E+02
16	1	0.1000000E+00	0.8000000E+01	0.5000000E+01	0.9900000E+01
17	1	0.1000000E+00	0.3000000E+01	0.2000000E+01	0.5000000E+02
18	1	0.1000000E+00	0.3500000E+01	0.1000000E+01	0.1000000E+02

FIG.B8   RQPMIN.RES - EXAMPLE

Problem function data

Number of constraints =   22

Index	Status	Type	Scale		Index	Status	Type	Scale
1	0	0	0.1000000E+05		2	1	0	0.1000000E+05
3	1	0	0.1000000E+06		4	-1	0	0.1000000E+01
5	-1	0	0.1000000E+01		6	-1	0	0.1000000E+02
7	-1	0	0.1000000E+02		8	-1	0	0.1000000E+02
9	-1	0	0.1000000E+03		10	-1	0	0.1000000E+01
11	-1	0	0.1000000E+02		12	-1	0	0.1000000E+02
13	-1	0	0.1000000E+02		14	-1	0	0.1000000E+00
15	-1	0	0.1000000E+03		16	-1	0	0.1000000E+03
17	-1	0	0.1000000E+01		18	-1	0	0.1000000E+01
19	-1	0	0.1000000E+03		20	-1	0	0.1000000E+02
21	-1	0	0.1000000E+03		22	-1	0	0.1000000E+03
23	-1	0	0.1000000E+01					

objective is function   1   problem number =   1

Control parameters
----

nfemax = 16000	nimax = 1000	nsmax = 20	nsetvf = 8
nsetc = 4	nsetcf = 8	nsetv = 4	rfrom = 1
ofreq = 10	ofrom = 1	rfreq = 10	

| centrl = F | fdset = F | norep = F | cheats = T | fast = T | quasi = T |
| fixrp = F | timid = F | monitr = F | nofrec = F | yesbc = F | shrnk = T | projct = T |

FIG.B8   RQPMIN.RES - EXAMPLE (CONTINUED)

```
xtol    = 0.1000000E-05     xtolu   = 0.1000000E-02     xtolv   = 0.1000000E-02     gtol    = 0.1000000E-02
rtol    = 0.1000000E+00     omegar  = 0.1000000E+00     rpmax   = 0.2000000E+00     ctol    = 0.1000000E-02
umin    = 0.1000000E-05     vminf   = 0.1000000E-02     vminc   = 0.1000000E-05     mu      = 0.1000000E-03
umax    = 0.1000000E+00     vmax    = 0.1000000E+00     omega   = 0.1000000E+00     cmax    = 0.1000000E-01
bdtol   = 0.1000000E+00     lmtol   = 0.1000000E+00     mtol    = 0.5000000E+00     diftol  = 0.5000000E-03
subtol  = 0.1000000E-02     qrtol   = 0.1000000E+02     bfstol  = 0.1000000E-05
ztol    = 0.1000000E-29
```

End of input data

Program RQPMIN Version 1.0 for VAX

STARTING POINT

free variables

```
  1  0.4000000E+01   2  0.4000000E+01   3  0.3000000E+01   4  0.3300000E+01   5  0.5000000E+01   6  0.6000000E+00
  7  0.1500000E+01
  8  0.7600000E+00   9  0.9300000E+00  10  0.9500000E+00  11  0.1600000E+00  12  0.2000000E+01  13  0.4000000E+01
 14  0.3000000E+01
 15  0.1000000E+01  16  0.1000000E+01  17  0.8000000E+01  18  0.3000000E+01
```

FIG.B8   RQPMIN.RES - EXAMPLE (CONTINUED)

objective function
----

f(x) = 0.3871068E+00

equality constraints
----

2 -0.1016441E+00 3 -0.1080766E+00

active inequality constraints
----

 4 0.3162098E-01 5 0.4570608E+00 11 0.1000000E+01 12 0.2000000E+00 13 0.2810316E-01 15 0.9608844E+00
16 0.3240771E+00

inactive inequality constraints
----

 6 -0.2952909E+00 7 -0.9496094E+00 8 -0.2089007E+00 14 -0.5443096E+00 9 0.8506336E-02 10 0.0000000E+00
17 -0.4276433E+00
18 -0.5372723E+00 19 -0.3352296E+00 20 -0.3022345E+00 21 -0.5343335E+00 22 -0.3132237E+00 23 -0.3681262E+00

Program RQPMIN Version 1.0 for VAX

FIG.B8   RQPMIN.RES - EXAMPLE (CONTINUED)

end of iteration number   1
----

end of a successful feasiblity step
number of calls made to user function so far =   392

free variables
----

   8 0.6742311E+00 11 0.1508980E+01 12 0.2041463E+01   9 0.9776771E+00   1 0.3883265E+01   2 0.4000000E+01
  18 0.3498502E+01
  17 0.3000000E+01   5 0.5000000E+01   7 0.1500000E+01   4 0.3000000E+01   3 0.3000000E+01 13 0.4000000E+01
  14 0.3000000E+01
  15 0.1000000E+01 16 0.8000000E+01

variables fixed at or near their lower bounds
----

   6 0.3000000E+00

variables fixed at or near their upper bounds
----

  10 0.1000000E+01

FIG.B8   RQPMIN.RES - EXAMPLE (CONTINUED)

objective function
----

f(x) = 0.3935423E+00

equality constraints
----

2 -0.1235107E-03 3 -0.2308938E-01

active inequality constraints
----

4 0.7015228E-02 11 0.1715565E-02

inactive inequality constraints
----

15 -0.4317688E-01 5 -0.3239393E+00 13 -0.1323803E+00 12 -0.9417369E-01 16 -0.7061415E+00 6 -0.3501351E+00
7 -0.1011848E+01
8 -0.2056513E+00 14 -0.5443096E+00 9 0.7130320E-02 10 0.0000000E+00 17 -0.6361188E+00 18 -0.9151169E+00
19 -0.3606793E+00
20 -0.2666035E+00 21 -0.1389266E+01 22 -0.3176751E+00 23 -0.3681262E+00

FIG.B8   RQPMIN.RES - EXAMPLE (CONTINUED)

Lagrange multiplier estimates
----

2 0.1308760E+01   3 0.2221137E-01   4 0.6751923E-02 11 -0.3056519E+00

Partial derivatives of Lagrangian function
----

 8 0.0000000E+00 11 0.7450581E-08 12 0.0000000E+00   9 0.1490116E-07   1 0.5532093E-01   2 0.7070982E-01
18 -0.9488447E-01
17 0.0000000E+00   5 -0.4380036E-01   7 0.1694216E+00   4 0.3151349E-01   3 0.1833036E-01 13 -0.1804036E-01
14 -0.5226777E-01
15 -0.3701131E-04 16 0.2391479E-03   6 -0.1925723E+01 10 -0.7435918E-01

Norms of active constraint gradients
----

2 0.2204726E+00   3 0.1149070E+01   4 0.1252910E+02 11 0.2396761E+01

convergence criteria
----

pdatum = 0.3923905E+00   ldatum = 0.3923905E+00   gdatum = 0.5852911E-03
nu   = 0.0000000E+00   numax = infinite
unormx = 0.2608127E-01   unormd = 0.2608127E-01   rtol   = 0.1000000E+00   xtolu = 0.1000000E-02
vnormx = 0.0000000E+00   vnorm = 0.0000000E+00   xtolv = 0.1000000E-02   grdldn = 0.1694216E+00
nde   = 0   ndef = 20   ndec = 0   ncalls = 52   nfuncs = 32

FIG.B8   RQPMIN.RES - EXAMPLE (CONTINUED)

Program RQPMIN Version 1.0 for VAX

end of iteration number   11
----

end of a successful minimization step
number of calls made to user function so far =   1030

free variables
----

 8 0.6792758E+00 11 0.1467613E+01 10 0.9914331E+00 6 0.3134658E+00 1 0.3879399E+01 2 0.3995808E+01
18 0.3485311E+01
17 0.2999997E+01 5 0.5001482E+01 7 0.1499447E+01 4 0.3294123E+01 3 0.2997784E+01 13 0.3998196E+01
14 0.2991289E+01
15 0.1000057E+01 16 0.8000157E+01 9 0.9798208E+00 12 0.2039295E+01

objective function
----

f(x) = 0.3692844E+00

equality constraints
----

 2 -0.3449707E-04 3 0.6250000E-06

FIG.B8 RQPMIN.RES - EXAMPLE (CONTINUED)

active inequality constraints
----

11 0.3328324E-04   4 0.0000000E+00

inactive inequality constraints
----

17 -0.4966396E+00   5 -0.2782698E+00 13 -0.1447302E+00 12 -0.9491148E-01 16 -0.7616248E+00   6 -0.3573953E+00
 7 -0.1019329E+01
 8 -0.2040979E+00 14 -0.5430096E+00   9 0.6798082E-02 10 0.0000000E+00 15 -0.6058899E-01 18 -0.9067427E+00
19 -0.3285713E+00
20 -0.2640511E+00 21 -0.1442437E+01 22 -0.3163921E+00 23 -0.3761737E+00

Lagrange multiplier estimates
----

 2 -0.3381015E+01   3 0.2955003E+00 11 -0.1035694E+00   4 -0.6511039E-02

Partial derivatives of Lagrangian function
----

 8 0.7450581E-08 11 0.1280569E-07 10 -0.6961636E-07   6 -0.3166497E-07   1 0.5390371E-01   2 0.6389069E-01
18 0.2200997E+00
17 0.0000000E+00   5 -0.1957817E-01   7 0.1816003E-02   4 0.8853241E-01   3 0.3336415E-01 13 0.3325305E-01
14 0.1433089E+00
15 -0.6561152E-03 16 -0.2367982E-02   9 0.5459145E-01 12 0.3410341E+00

FIG.B8   RQPMIN.RES - EXAMPLE (CONTINUED)

Norms of active constraint gradients
----

2 0.5234829E+00   3 0.1786113E+01 11 0.2965080E+01   4 0.1280450E+02

convergence criteria
----

pdatum = 0.3693977E+00   ldatum = 0.3693977E+00   gdatum = 0.2298212E-08
nu   = 0.0000000E+00   numax = infinite
unormx = 0.9951143E-04   unormd = 0.9951143E-04   rtol   = 0.1000000E-01   xtolu = 0.1000000E-02
vnormx = 0.4340118E+00   vnorm = 0.1000000E+00   xtolv = 0.1000000E+00   grdldn = 0.3410341E+00
nde   = 0   ndef = 52   ndec = 0   ncalls = 146   nfuncs = 94

Program RQPMIN Version 1.0 for VAX

end of iteration number   21
----

end of a successful minimization step
number of calls made to user function so far = 1694

free variables
----

 8 0.6838636E+00 11 0.1464769E+01 10 0.9978976E+00   6 0.3205609E+00 18 0.3426057E+01   7 0.1499220E+01
16 0.8000323E+01
17 0.3000763E+01   5 0.5004205E+01   2 0.3971060E+01   4 0.3971060E+01   3 0.2995289E+01 13 0.3996258E+01
14 0.2985314E+01
15 0.9992111E+00   1 0.3989123E+01   9 0.3989123E+01 12 0.9980076E+00   0.2054844E+01

FIG.B8   RQPMIN.RES - EXAMPLE (CONTINUED)

objective function
----

f(x) = 0.3656146E+00

equality constraints
----

2 0.6347656E-06 3 0.8906250E-05

active inequality constraints
----

11 0.4949570E-04 4 -0.6675720E-05 15 -0.2441406E-05

inactive inequality constraints
----

18 -0.9249295E+00 5 -0.2468739E+00 12 -0.9460294E-01 16 -0.7265211E+00 6 -0.3712418E+00 7 -0.1035546E+01
8 -0.2038941E+00
14 -0.5443096E+00 9 0.6789749E-02 10 0.0000000E+00 17 -0.5880709E+00 13 -0.1568619E+00 19 -0.6000000E+00
20 -0.2575126E+00
21 -0.1504873E+01 22 -0.3184378E+00 23 -0.3986375E+00

Lagrange multiplier estimates
----

2 0.1908567E+00 3 -0.1322685E+01 11 -0.1908436E+01 4 -0.6596171E-03 15 0.9248000E+00

FIG.B8   RQPMIN.RES - EXAMPLE (CONTINUED)

Partial derivatives of Lagrangian function

```
 8 -0.4768372E-06 11  0.5960464E-07 10  0.0000000E+00  6  0.1192093E-06 18 -0.7450581E-08  7 -0.5287752E-03
16 -0.1174315E-02
17 -0.7292574E-03  5  0.3455998E-02  2  0.1350289E+00  4 -0.3043809E+00  3  0.2671763E-02 13  0.2838112E-03
14  0.2159834E-02
15 -0.6232406E-03  1  0.5390055E+00  9  0.4088998E-02 12  0.4441679E-02
```

Norms of active constraint gradients

```
 2  0.5477104E+00  3  0.1695861E+01 11  0.3196909E+01  4  0.1286765E+02 15  0.6618107E+01
```

convergence criteria

```
pdatum = 0.3655062E+00     ldatum = 0.3655062E+00     gdatum = 0.2580074E-08
nu     = 0.0000000E+00     numax  = 0.5814611E+02
unormx = 0.5096373E-03     unormd = 0.5096373E-03     rtol  = 0.1000000E-01     xtolu  = 0.1000000E-02
vnormx = 0.1423888E+01     vnorm  = 0.1000000E+00     xtolv  = 0.1000000E+00     grdldn = 0.5390055E+00
nde    = 0     ndef =  84     ndec = 0     ncalls =    266     nfuncs =    182
```

Program RQPMIN Version 1.0 for VAX

FIG.B8   RQPMIN.RES - EXAMPLE (CONTINUED)

```
end of iteration number    31
-----------------------------------

end of a successful feasiblity step
number of calls made to user function so far =    2912

free variables
--------------

  8  0.6773027E+00  11  0.1485162E+01  12  0.2018675E+01  18  0.3520655E+01   7  0.1499164E+01   1  0.4006016E+01
 16  0.8006647E+01
 17  0.3001110E+01   5  0.5004749E+01   2  0.3970934E+01   4  0.3290561E+01   3  0.2995477E+01  13  0.3996674E+01
 14  0.2985703E+01
 15  0.9995601E+00

variables fixed at or near their lower bounds
---------------------------------------------

  6  0.3000000E+00

variables fixed at or near their upper bounds
---------------------------------------------

  9  0.1000000E+01  10  0.1000000E+01

objective function
------------------

f(x) =   0.3884203E+00
```

FIG.B8   RQPMIN.RES - EXAMPLE (CONTINUED)

equality constraints
----

  2   0.2746289E-02   3   0.7640625E-04

active inequality constraints
----

 15 -0.7843017E-04   4   0.4768372E-03

inactive inequality constraints
----

 18 -0.9095773E+00 11 -0.9923076E-02   5 -0.3127804E+00 12 -0.9879985E-01 16 -0.6175560E+00   6 -0.3359904E+00
  7 -0.9945985E+00
  8 -0.2047075E+00 14 -0.5443096E+00   9   0.7234266E-02 10   0.0000000E+00 17 -0.6186000E+00 13 -0.1426723E+00
 19 -0.3576093E+00
 20 -0.2598014E+00 21 -0.1484709E+01 22 -0.3135588E+00 23 -0.3968098E+00

Lagrange multiplier estimates
----

  2 -0.3682696E+00   3   0.9988662E-01 15 -0.2195863E+00   4 -0.4774231E-01

FIG.B8   RQPMIN.RES - EXAMPLE (CONTINUED)

Partial derivatives of Lagrangian function
----

8   0.5960464E-07 11   0.3445894E-07 12   0.1862645E-08 18 -0.1746230E-08   7   0.1058967E+00   1 -0.1159504E+00
16 -0.2997608E-02
17   0.0000000E+00   5 -0.3633375E-01   2   0.2989674E-01   4   0.1091263E+00   3   0.1321699E-01 13 -0.4425814E-02
14 -0.1500370E-02
15 -0.1008811E-02   6 -0.1223767E+01   9   0.1423406E+00 10   0.3133123E+00

Norms of active constraint gradients
----

2   0.2043716E+00   3   0.1142849E+01 15   0.5351947E+01   4   0.1225039E+02

convergence criteria
----

pdatum =   0.3874110E+00   ldatum =   0.3874110E+00   gdatum =   0.7781468E-05
nu   =   0.0000000E+00   numax =   infinite
unormx =   0.4805435E-01   unormd =   0.4805435E-01   rtol   =   0.1000000E-02   xtolu =   0.1000000E-02
vnormx =   0.1215237E-02   vnorm =   0.1215237E-02   xtolv =   0.1000000E-02   grdldn =   0.1159504E+00
nde   =   0   ndef =   95   ndec =   25   ncalls =   422   nfuncs =   302

Program RQPMIN Version 1.0 for VAX

end of iteration number   41
----

end of a successful feasiblity step
number of calls made to user function so far =   3300

FIG.B8   RQPMIN.RES - EXAMPLE (CONTINUED)

free variables
----

8   0.6819428E+00   10 0.9858580E+00   11 0.1462748E+01   6   0.3159353E+00   1   0.4014895E+01   7   0.1498024E+01
16 0.8001753E+01
17 0.2999441E+01   5   0.5006766E+01   2   0.3970093E+01   4   0.3293541E+01   3   0.2991575E+01   13 0.3992305E+01
14 0.2981005E+01
15 0.9992824E+00   18 0.3550712E+01   12 0.1973851E+01   9   0.9957859E+00

objective function
----

f(x) = 0.3636202E+00

equality constraints
----

2 -0.1857910E-03   3   0.3615625E-03

active inequality constraints
----

4   0.1850128E-03

FIG.B8   RQPMIN.RES - EXAMPLE (CONTINUED)

inactive inequality constraints
----

11 -0.1284885E-02 15 0.2281799E-02 18 -0.8718656E+00 5 -0.2781858E+00 12 -0.9530757E-01 16 -0.6258676E+00
 6 -0.3028465E+00
 7 -0.9550282E+00 8 -0.2039770E+00 14 -0.5443096E+00 9 0.7334673E-02 10 0.0000000E+00 17 -0.5658784E+00
13 -0.1506609E+00
19 -0.3602388E+00 20 -0.2598916E+00 21 -0.1530566E+01 22 -0.3065599E+00 23 -0.3948460E+00

Lagrange multiplier estimates
----

 2 -0.7903465E+01 3 0.1015927E+01 4 -0.1210891E-01

Partial derivatives of Lagrangian function
----

 8 -0.2980232E-07 10 -0.5308539E-07 11 -0.1629815E-08 6 0.1470608E+01 1 0.9803022E-01 7 -0.1265189E+00
16 -0.5012098E-02
17 0.0000000E+00 5 -0.3529557E-02 2 0.8029886E-01 4 0.1710619E+00 3 0.5634566E-01 13 0.6144121E-01
14 0.3218544E+00
15 -0.1647603E-02 18 0.5227668E+00 12 0.7688587E+00 9 0.9724957E-01

Norms of active constraint gradients
----

 2 0.5578982E+00 3 0.1753891E+01 4 0.1225305E+02

FIG.B8 RQPMIN.RES - EXAMPLE (CONTINUED)

convergence criteria
----

pdatum = 0.3654537E+00   ldatum = 0.3654537E+00   gdatum = 0.1994755E-06
nu   = 0.0000000E+00   numax   = 0.1312339E+04
unormx = 0.3306092E-02   unormd = 0.3306092E-02   rtol   = 0.1000000E-02   xtolu   = 0.1000000E-02
vnormx = 0.7687663E-01   vnorm   = 0.7687663E-01   xtolv   = 0.1000000E-02   grdldn = 0.1470608E+01
nde   = 0   ndef = 35   ndec = 95   ncalls = 460   nfuncs = 330

Program RQPMIN Version 1.0 for VAX

end of iteration number   51
----

end of a successful feasiblity step
number of calls made to user function so far =   3823

free variables
----

 8 0.6816662E+00 11 0.1465574E+01 10 0.9851044E+00   6 0.3147032E+00 12 0.1977431E+01   7 0.1498024E+01
16 0.8001753E+01
17 0.2999441E+01   5 0.5006766E+01   2 0.3970093E+01   4 0.3293541E+01   3 0.2991575E+01 13 0.3992305E+01
14 0.2981005E+01
15 0.9992824E+00 18 0.3550712E+01   1 0.4014203E+01   9 0.9957859E+00

objective function
----

f(x) = 0.3663713E+00

FIG.B8   RQPMIN.RES - EXAMPLE (CONTINUED)

equality constraints
----

2 0.3222656E-05 3 0.8906250E-05

active inequality constraints
----

4 0.5722046E-05 11 0.1992226E-03

inactive inequality constraints
----

15 0.8461914E-02 18 -0.8751327E+00 5 -0.2814655E+00 12 -0.9467213E-01 16 -0.6261275E+00 6 -0.3052629E+00
7 -0.9579439E+00
8 -0.2040682E+00 14 -0.5443096E+00 9 0.7346528E-02 10 0.0000000E+00 17 -0.6010240E+00 13 -0.1497215E+00
19 -0.3408323E+00
20 -0.2600980E+00 21 -0.1523792E+01 22 -0.3071268E+00 23 -0.3948460E+00

Lagrange multiplier estimates
----

2 0.1455115E+01 3 -0.1573262E+01 4 0.4001669E-02 11 0.9701430E-01

FIG.B8   RQPMIN.RES - EXAMPLE (CONTINUED)

Partial derivatives of Lagrangian function
----

8 -0.2980232E-07 11 -0.8940697E-07 10 0.4470348E-07   6 -0.1676381E-06 12 -0.1870414E+00   7 0.1045093E-03
16 0.1203557E-02
17 0.1306745E-04   5 0.1098057E-01   2 -0.3571704E-01   4 -0.4727623E-01   3 -0.1758450E-01 13 -0.1280005E-01
14 -0.7087208E-01
15 0.4404449E-03 18 -0.1133880E+00   1 -0.4081335E-01   9 -0.3180073E-01

Norms of active constraint gradients
----

2 0.1179947E+01   3 0.1770732E+01   4 0.1228019E+02 11 0.3608931E+01

convergence criteria
----

pdatum = 0.3663813E+00   ldatum = 0.3663813E+00   gdatum = 0.3981208E-07
nu   = 0.0000000E+00   numax = 0.1312339E+04
unormx = 0.1007674E-03   unormd = 0.1007674E-03   rtol   = 0.1000000E-02   xtolu = 0.1000000E-02
vnormx = 0.7687663E-01   vnorm = 0.7687663E-01   xtolv = 0.1000000E-02   grdldn = 0.1870414E+00
nde   =   0   ndef =   95   ndec =   48   ncalls =   528   nfuncs =   385

Program RQPMIN Version 1.0 for VAX

FIG.B8   RQPMIN.RES - EXAMPLE (CONTINUED)

end of iteration number   55

CONVERGENCE DETECTED   [Code B]   after 3972 calls to user routine

free variables
----

  8 0.6816662E+00 11 0.1465574E+01 10 0.9851044E+00   6 0.3147032E+00 12 0.1977431E+01   7 0.1498024E+01
 16 0.8001753E+01
 17 0.2999441E+01   5 0.5006766E+01   2 0.3970093E+01   4 0.3293541E+01   3 0.2991575E+01 13 0.3992305E+01
 14 0.2981005E+01
 15 0.9992824E+00 18 0.3550712E+01   1 0.4014203E+01   9 0.9957859E+00

objective function
----

f(x) = 0.3663713E+00

equality constraints
----

  2 0.3222656E-05   3 0.8906250E-05

active inequality constraints
----

  4 0.5722046E-05 11 0.1992226E-03

FIG.B8   RQPMIN.RES - EXAMPLE (CONTINUED)

Inactive inequality constraints
----

15 0.8461914E-02 18 -0.8751327E+00   5 -0.2814655E+00 12 -0.9472213E-01 16 -0.6261275E+00   6 -0.3052629E+00
7 -0.9579439E+00
8 -0.2040682E+00 14 -0.5443096E+00   9   0.7346528E-02 10   0.0000000E+00 17 -0.6010240E+00 13 -0.1497215E+00
19 -0.3408323E+00
20 -0.2600980E+00 21 -0.1523792E+01 22 -0.3071268E+00 23 -0.3948460E+00

Lagrange multiplier estimates
----

2   0.1455115E+01   3 -0.1573262E+01   4   0.4001669E-02 11   0.9701430E-01

Partial derivatives of Lagrangian function
----

8 -0.2980232E-07 11 -0.8940697E-07 10   0.4470348E-07   6 -0.1676381E-06 12 -0.1870414E+00   7   0.1045093E-03
16   0.1203557E-02
17   0.1306745E-04   5   0.1098057E-01   2 -0.3571704E-01   4 -0.4727623E-01   3 -0.1758450E-01 13 -0.1280005E-01
14 -0.7087208E-01
15   0.4404449E-03 18 -0.1133880E+00   1 -0.4081335E-01   9 -0.3180073E-01

Norms of active constraint gradients
----

2   0.1179947E+01   3   0.1770732E+01   4   0.1228019E+02 11   0.3608931E+01

FIG.B8   RQPMIN.RES - EXAMPLE (CONTINUED)

```
convergence criteria
--------------------

pdatum =  0.3663813E+00        ldatum =  0.3663813E+00        gdatum =  0.3981208E-07
nu     =  0.0000000E+00        numax  =  0.1312339E+04
unormx =  0.1007674E-03        unormd =  0.1007674E-03        rtol   =  0.1000000E-02        xtolu  =  0.1000000E-02
vnormx =  0.1870414E+00        vnorm  =  0.1000000E+00        xtolv  =  0.1000000E+00        grdldn =  0.1870414E+00
nde    =     0    ndef =          95    ndec =    52        ncalls =  537    nfuncs =          390
```

FIG.B8   RQPMIN.RES - EXAMPLE (CONCLUDED)

APPENDIX C

AIRCRAFT LIFT-CURVE SLOPE EVALUATION
WITH REFERENCE TO INTERFERENCE

The aircraft lift-curve slope $\partial Cl/\partial\alpha$ (Ref.3) is given by

$$\left[\frac{\partial Cl}{\partial\alpha}\right]_{a/c} = \left[\frac{\partial Cl}{\partial\alpha}\right]_W [KN + KB(W) + KW(B)] \left[\frac{S_n}{S}\right]_W$$

$$+ \left[\frac{\partial Cl}{\partial\alpha}\right]_t [KW(B) + KB(W)] \left[1 - \frac{\partial\epsilon}{\partial\alpha}\right]$$

$$\frac{\Delta q}{q} \left[\frac{S_n}{S}\right]_t \frac{S_t}{S_W} \qquad\qquad (C1)$$

where

KN   is the interference factor due to the aircraft forebody

KB(W)   is the interference factor due to the interaction of the aircraft body with the wing

KW(B)   is the interference factor due to the interaction of the wing with the aircraft body

$\dfrac{\partial\epsilon}{\partial\alpha}$ is the downwash gradient

$\dfrac{\Delta q}{q}$ is the dynamic pressure ratio

For the forebody interference factor KN, we have from slender body theory for the forebody lift, L_{fb}

$$L_{fb} = 2 \qquad\qquad\qquad\qquad (C2)$$

Transformong the lift in factor form to be used in Eqn C1

$$KN = \frac{2\pi \left[\dfrac{d}{2}\right]^2}{\left[\dfrac{\partial Cl}{\partial \alpha}\right]_W S_W} \tag{C3}$$

where d is the diameter of the forebody and S_W is the surface area of the wing.

The wing-body interaction interference factors KB(W) and KW(B), are provided in a graph in Ref.3 as functions of the ratio of the body diameter over the flying surface span.

To find an analytical expression, a polynomial is assumed of the form

$$KB(W) = a1 \left(\frac{d}{b}\right)^2 + a2 \left(\frac{d}{b}\right) + a3 \tag{C4}$$

Substituting values from the graph of Ref.3 we find that

$$KB(W) = 0.8 \left(\frac{d}{b}\right)^2 + 1.2 \left(\frac{d}{b}\right) \tag{C5}$$

Similarly for KW(B) we have

$$KW(B) = 0.2 \left(\frac{d}{b}\right)^2 + 0.8 \left(\frac{d}{b}\right) + 1 \tag{C6}$$

The sum of the two factors is given by

$$KB(W) + KW(B) = \left(\frac{d}{b}\right)^2 + 2 \left(\frac{d}{b}\right) + 1 \tag{C7}$$

$$= \left(\frac{d}{b} + 1 \right)^2 \qquad\qquad (C8)$$

For the downwash finite wing theory is used and a tailplane position at the same height with the wing is assumed.

The velocity, w_{inf}, induced by the wing's infinite vortex is given by

$$w_{inf} = \frac{\Gamma_o}{2b} (\cos \beta + 1) \qquad\qquad (C9)$$

where

$$\Gamma_o = \frac{2 V_\infty S_w C1}{b \pi} \qquad\qquad (C10)$$

β is the angle formed between a wing vortex element and a tailplane surface element, Γ_o is the circulation at the origin of the wing vortex system and b the wing span.

Therefore the corresponding downwash angle, ϵ_{inf}, is

$$\epsilon_{inf} = \frac{w_{inf}}{V_\infty} = \frac{2 V_\infty S C1}{b \pi 2 b} (\cos \beta + 1) \frac{1}{V_\infty} \qquad\qquad (C11)$$

$$= \frac{C1}{AR} (\cos \beta + 1) \qquad\qquad (C12)$$

where AR is the aspect ratio.

The velocity, w_{bound}, induced by the wing's bound vortices is

$$w_{bound} = \frac{\Gamma_o}{x_T} \sin \beta \qquad\qquad (C13)$$

Therefore

$$\epsilon_{bound} = \frac{w_{bound}}{x_\tau} = \frac{2\ V_\infty\ S_w\ Cl}{b\ \pi}\ (\sin\ \beta)\ \frac{1}{V_\infty} \qquad (C14)$$

$$= \frac{Cl}{\pi\ AR}\ \frac{2b}{x_\tau}\ \sin\ \beta \qquad (C15)$$

The total downwash is the sum of the two, thus the downwash gradient, $\partial\epsilon/\partial\alpha$, is given by

$$\frac{\partial\epsilon}{\partial\alpha} = \frac{\partial Cl}{\partial\alpha}\ \frac{1}{\pi\ AR}\ \left\{ \frac{x_\tau^2 + b^2 + x_\tau\ [\ (0.5\ b)^2 + x\tau^2\ ]^{\frac{1}{2}}}{x_\tau\ [\ (0.5\ b)^2 + x_\tau\ ]^{\frac{1}{2}}} \right\}$$

$$(C16)$$

The dynamic pressure ratio, $\Delta q/q$, is given as input data.